LASE 2006

Lasers and Applications in Science and Engineering

2006 Symposium Chairs

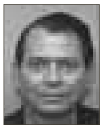

L. N. Durvasula
DARPA

Jan J. Dubowski
Université de Sherbrooke (Canada)

2006 Symposium Cochairs

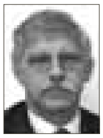

Friedrich G. Bachmann
ROFIN-SINAR Laser GmbH (Germany)

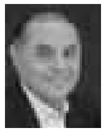

Henry Helvajian
The Aerospace Corp.

Laser Source Engineering

Program Chair: **Gregory Quarles,** VLOC

6100 **Solid State Lasers XV: Technology and Devices** *(Hoffman, Shori)*
6101A **Laser Resonators and Beam Control IX** *(Kudryashov, Ilchenko, Paxton)*
6101B **8th International Workshop on Laser Beam and Optics Characterization** *(Giesen, Nickel)*
6101C **High Energy/Average Power Lasers and Intense Beam Applications** *(Davis, Heaven, Schriempf)*
6102 **Fiber Lasers III: Technology, Systems, and Applications** *(Brown, Nilsson)*

Nonlinear Optics

Program Chair: **Peter Powers,** Univ. of Dayton

6103 **Nonlinear Frequency Generation and Conversion: Materials, Devices, and Applications V** *(Powers)*

Semiconductor Lasers and LEDs

Program Chair: **Daniel Johnstone,** Virginia Commonwealth Univ.

6104 **High-Power Diode Laser Technology and Applications IV** *(Zediker)*
6132 **Vertical-Cavity Surface-Emitting Lasers X** *(Lei, Choquette)*
6133 **Novel In-Plane Semiconductor Lasers V** *(Mermelstein, Bour)*
6134 **Light-Emitting Diodes: Research, Manufacturing, and Applications X** *(Streubel, Yao, Schubert)*

Laser Communication and Propagation

Program Chair: **G. Stephen Mecherle,** fSona Communications Corp.

6105 **Free-Space Laser Communication Technologies XVIII** *(Mecherle)*

Laser Micro-/Nanoengineering and Applications

Program Chairs: **Henry Helvajian,** The Aerospace Corp.; **James S. Horwitz,** U.S. Department of Energy

6106A **Laser Applications in Microelectronic and Optoelectronic Manufacturing XI** *(Arnold, Holmes, Meunier, Okada)*
6106B **Synthesis and Photonics of Nanoscale Materials IV** *(Dubowski, Geohegan, Träger)*
6107 **Laser-Based Micro-Packaging** *(Bachmann, Hoving, Lu, Washio)*
6108 **Commercial and Biomedical Applications of Ultrafast Lasers VI** *(Heisterkamp, Neev, Nolte, Schaffer)*

PLEASE NOTE: Abstract publication does not guarantee manuscript publication.

Conference 6100: Solid State Lasers XV: Technology and Devices

Monday-Thursday 23-26 January 2006

Proceedings of SPIE Vol. 6100

6100-01, Session 1

Size-scaling of TEM_{00} mode optically-pumped semiconductor lasers

L. E. Hunziker, C. Ihli, D. S. Steingrube, E. J. Reed, N. Hodgson, Coherent, Inc.

We show that TEM_{00} mode optically-pumped semiconductor lasers (OPSL) can be scaled to footprints < 10 cm without affecting performance. In particular, we have demonstrated up to 10 W TEM_{00} mode output at 488 and 532 nm with resonator footprints as small as 1 cm. Performance metrics critical to manufacturability such as resonator misalignment sensitivity and stability range maintain acceptable values down to this scale.

6100-02, Session 1

Optically pumped semiconductor lasers at 505-nm in the power range above 100 mW

W. R. Seelert, Coherent Luebeck (Germany); S. Kubasiak, Coherent Luebeck; J. Negendank, Coherent Luebeck (Germany); J. Chilla, H. Zhou, E. S. Weiss, Coherent, Inc.

Lasers based on optically pumped semiconductors (OPS) offer unique capabilities in both wavelength tailoring and power scaling compared to traditional solid-state lasers. In particular, these lasers can be designed in wavelength to realize for instance 505nm, which enables excitation of two fluorescent dye chemistry sets originally established by 488 and 514 nm legacy argon lasers. Highly efficient intra cavity frequency doubling of an 1010nm OPS yields over 100 mW of output power at 505 nm. In this paper we will present a brief background on OPS technology. We will then discuss specifics of the 505 nm laser and present both performance and reliability data for this laser.

6100-03, Session 1

Continuous-wave visible laser by intracavity-doubled fiber laser

T. Shinozaki, Y. Kaneda, Y. Urata, S. Wada, Megaopto RIKEN (Japan)

A novel continuous-wave blue-green laser was developed by utilizing the second-harmonic of the emission from Yb doped gain fiber. The laser cavity consists of an FBG, a gain fiber, an aspheric lens, a dichroic mirror for output coupling of second harmonic, a periodically-poled $LiNbO3$ (PPLN), and a high reflector. The gain fiber was pumped by a 580-mW, fiber pigtailed laser diode at 974 nm through the FBG. The Yb laser emission from the fiber end was focused onto the high reflector, providing optical feedback and forming the resonator. The PPLN was placed near the end mirror in order to increase the fundamental intensity. The emission wavelength can be selected by changing the FBG within the bandwidth of the gain fiber.. FBG for 1016 nm was selected for the experiment. Circulating power of the fundamental wave in the cavity was measured to be 1500 mW when a 5 % output coupler was placed in stead of high-reflecting end mirror. Stable output in excess of 30 mW at 508 nm was obtained. The optical-optical efficiency from LD to the visible output was about 5%. The fluctuation of the laser output power was less than 0.5% for more than 2 hours without a power feedback loop. The optical noise was lower than 2%rms for the frequency between 10 Hz and 1 MHz. The M2 value was measured to be 1.2. This wavelength-selectable laser will be a useful light source for applications including biological imaging, flow cytometry, spectroscopic analysis.

6100-04, Session 2

Ceramic Yb:YAG microchip laser

E. P. Ostby, J. Huie, Raytheon Space and Airborne Systems; R. L. Gentilman, R. A. Ackerman, Raytheon Co.

A CW ceramic Yb:YAG microchip laser is presented with 1 W output power and 20% optical slope efficiency. The ceramic material was fabricated by Raytheon's Advanced Materials Laboratory. Results are presented for 1% and 5% atm. Yb:YAG.

6100-05, Session 2

Microchip laser operating at 1338-nm

J. Sulc, H. Jelinkova, Czech Technical Univ. in Prague (Czech Republic); K. Nejezchleb, V. Skoda, Crytur, Ltd. (Czech Republic)

Q-switched microchip laser emitting radiation at wavelength 1338nm was designed and realized. This laser was based on monolith crystal which combines in one piece a cooling undoped part (undoped YAG crystal, 4mm long), active laser part (YAG crystal doped with Nd^{3+} ions, 12mm long) and saturable absorber (YAG crystal doped with V^{3+} ions, 0.7mm long). The diameter of the diffusion bounded monolith was 5mm. The initial transmission of the V:YAG part was 85%. The microchip resonator consists of dielectric mirrors directly deposited on the monolith surfaces. The pump mirror (HT for pump radiation, HR for generated radiation) was placed on the undoped YAG part. The output coupler with reflection 90% for the generated wavelength was placed on the V^{3+}-doped part. Q-switched microchip laser was tested under pulsed, and CW diode pumping. The pulse length it was the same for all regimes equal to 6.2ns. The wavelength of linearly polarized laser emission was fixed to 1338nm. The pulse energy depends on the mean pump power. For pulsed pumping the output pulse energy was stable up to mean pump power 1W and it was equal to 135μJ, which corresponds to peak power 22kW. In CW regime for pumping up to 14W the pulse energy was stabilized to 37μJ (peak power 6kW). The mean output power increased up to 0.4W only by increase of the generated pulse repetition rate (11kHz for mean pump power 14W).

6100-06, Session 2

Subnanosecond tunable dye laser pumped by a Nd:YAG microchip laser

A. M. Jones, O. F. Swenson, North Dakota State Univ.

We have demonstrated a narrowband Littman configuration dye laser longitudinally pumped by the second harmonic of a 250 Hz pulse repetition frequency microchip laser with up to 50 microjoule pulse energies at 532 nm. Rhodamine 6G dye in methanol with a 3 cm cavity length produced 9 microjoule pulses with a slope efficiency of 20% at the peak intensity. The dye laser can be tuned from 550 to 575 nm. A 532 nm pump threshold below 4 microjoules was observed. Adding tunability to compact, economical microchip lasers with a spectrally narrow pulsed dye laser provides ideal characteristics for biotechnological applications.

6100-07, Session 2

Highly efficient ultra-low threshold microchip cerium fluoride lasers generating sub-nanosecond pulses at 287-nm and 310-nm

H. Liu, D. Spence, D. Coutts, Macquarie Univ. (Australia)

We present an all-solid-state pumped microchip Ce:LiLuF laser. The pump source was a miniature Ce:LiCAF laser pumped in turn by a microchip Nd:VYO4 laser. Cerium doped fluoride lasers are only solid-state laser sources operating in the ultraviolet regime, covering the range 280 to 335 nm. They have attracted broad interest for biophotonics applications, particularly in fluorescence sensing. Our robust and compact solid-state cerium laser sources, are a promising route for generating inexpensive tunable UV sources for these applications.

We have demonstrated the use of miniature cavities for Ce:LiLuF and Ce:LiCAF producing ultra-low threshold and high efficiency operation, allowing the use of a low cost frequency-quadrupled microchip Nd:YVO4 pump laser producing 10 μJ pulses at 1 kHz and 266 nm. This was used to pump a 2.5 mm long Ce,Na:LiCAF crystal contained in a 4 mm long cavity, generating 3.5 μJ pulses at 287 nm with a slope efficiency of 45%, and with a pulse duration of under 500 ps.

The output of the Ce:LiCAF laser was used to pump an ultra-low threshold Ce:LiLuF laser that used a 1.25 mm long crystal in a 2.5 mm long cavity. We have obtained ~450 ps, 650 nJ pulses at 310nm from the Ce:LiLuF laser, with slope efficiency of 40%. The lowest pump threshold measured was ~800 nJ, using an output coupler with 90% reflectivity. The pump polarisation induced color center loss effect of Ce:LiLuF crystal was minimised due to an extremely fast cavity build up time.

We will present results demonstrating wavelength tuning for these ultra-low threshold miniature cavities.

6100-08, Session 2

Low-cost 355-nm CW milliWatt-scale diode-pumped intra-cavity frequency tripled microchip assembly

T. Georges, A. Nicolas, C. Chauzat, OXXIUS (France); P. Féron, École Nationale Supérieure des Sciences Appliquées et de Technologie (France)

Low noise CW milliWatt scale UV lasers are needed for many analysis applications in the semiconductor and the biological fields. Intracavity tripling has been widely used to improve the UV output power of Q-switched or modelocked lasers, but no efficient diode-pumped CW UV laser was ever reported.

One of the key to success is the use of a monolithic laser structure which both eliminates the birefringence interference issue and facilitates the single frequency operation. The monolithic structure is obtained by optically contacting crystals. It does not require any alignment, reduces the manufacturing cost and improves reliability.

The optimization of the amplifying medium and doubling and tripling crystals involves as many parameters as pump absorption, thermal lens, cavity length, 1064 nm mode size, walk-off, acceptance angles, polarizations, phases. The interplay between these parameters will be discussed.

Finally, several amplifying media (Nd:YAG and Nd:YVO4), doubling crystals (KTP, KNbO3, BBO, BiBO and LBO) and tripling crystals (BBO, BiBO, LBO) were tested. With a 4W 808 nm diode pump, several configurations have led to low noise 355 nm single frequency operation exceeding several milliWatts. We believe that this power can still be improved.

6100-09, Session 3

Recent progress in eye-safe solid-state laser with resonant, ultra-low- photon-defect, diode pumping

M. A. Dubinskii, Army Research Lab.

The most promising today's technologies for high power solid-state lasers are hinging upon wavelengths near one micron (1-μm). For various military scenarios in urban areas it is very important to minimize the ocular hazard zone around the laser by using the DEW in the 1.5-1.8-mm 'eye-safe' band. 1-μm laser wavelength shifting via stimulated Raman scattering is possible, but at the sacrifice of the overall laser system efficiency and significant additional heat removal complications.

Direct resonant pumping of Er:YAG, due to its ultra-low-photon-defect nature, provides the most efficient eye-safe laser source with absolutely minimal pump-induced beam distortions - which is critical for high power applications. In fact, with the correctly engineered 'pump-lase' scheme photon defect of practical resonantly pumped Er:YAG laser can be almost 2 times lower than that of diode-pumped Yb:YAG laser. Even historically-first Er-doped crystalline solid-state laser at 1645 nm with Er-glass laser excitation around 1540 nm has proven to be efficient, even though quite impractical, eye-safe source.

This presentation provides comprehensive analysis of recent progress in eye-safe bulk solid-state laser development based on resonant, ultra-low-photon-defect pumping. The most efficient and most powerful Er:YAG laser systems based on narrow-band fiber laser pumping as well as on direct wide-band long-wavelength (state-of-the art InP) diode pumping are compared. Specifics associated with relatively low-cross-section and spectrally-narrow absorption features of 4I15/2 → 4I13/2 transitions of Er3+ ion as well as concentration dependent parasitic up-conversions are discussed. Approach to using 1470-nm versus 1530-nm absorption line groups along with analysis of cryogenically-cooled Er:YAG laser is also presented.

6100-10, Session 3

High-power fiber-bulk hybrid lasers

W. A. Clarkson, D. Y. Shen, J. K. Sahu, Univ. of Southampton (United Kingdom)

Cladding-pumped fiber lasers are becoming increasingly attractive for high power generation due to their high efficiency and immunity from thermal effects. However, due their small core size and long device length, pulse energies are rather limited. In contrast, conventional 'bulk' solid-state lasers offer the prospect of much higher pulse energies, but suffer from detrimental thermal effects which can degrade beam quality and efficiency. An alternative strategy for scaling output power and pulse energy, which is attracting growing interest, is to use a hybrid laser scheme. In this approach, the fiber laser is used as a high-brightness source for in-band pumping of a bulk solid-state laser. One of the main attractions of the fiber-bulk hybrid laser scheme is that most of the heat generated via quantum defect heating is deposited in the fiber, and thermal effects in the bulk laser are dramatically reduced leading to the prospect of much improved efficiency, beam quality, higher average output power and higher pulse energy. This approach has already been successfully applied to a number of different solid-state lasers operating in the eyesafe wavelength regimes around 1.6μm and 2μm. In this paper, we describe recent progress in the development of high-power Er fiber pump sources for hybrid erbium lasers, and we will report on recent developments in power scaling of hybrid erbium lasers in cw and pulsed modes of operation.

6100-11, Session 3

100-megawatt power Q-switched Er:glass laser

J. Taboada, J. M. Taboada, Taboada Researsch Instruments, Inc.; D. J. Stolarski, J. Zohner, L. Chavey, Northrop Grumman Corp.

A very high energy Q-switch Er:glass low repetition rate laser is reported. By incorporating a rotating resonant reflector, very high shutter speeds of the cavity Q were achieved of an Er:glass laser designed for 75J, 600 microsecond long pulse operation. Reproducible 3.75J, 33 nanosecond, 1533 nm laser pulses were obtained with less than 1 minute period.

6100-12, Session 4

Progress in hybrid fiber/bulk solid state lasers

P. F. Moulton, A. Y. Dergachev, Q-Peak, Inc.

Fiber lasers are capable of efficiently generating high-beam-quality, high cw powers. Bulk lasers have excellent energy-storage characteristics for production of high-peak-power, energetic pulses. The combination of fiber lasers as pump sources for bulk solid state lasers provides a unique, effective laser system. We describe our recent work in the use of >100 W-power Tm:fiber lasers to pump high-energy, Q-switched, 2050-nm Ho:YLF lasers.

6100-13, Session 4

3.9-4.8 μm gain-switched lasing of Fe:ZnSe at room temperature

V. V. Fedorov, J. Kernal, A. Gallian, The Univ. of Alabama at Birmingham; V. V. Badikov, Kuban State Univ.; S. B. Mirov, The Univ. of Alabama at Birmingham

Absorption and luminescence properties of Fe:ZnSe and Fe:Cr:ZnSe crystals in the middle infrared spectral range were studied at room and low temperatures. The undoped polycrystalline samples were grown by chemical vapor deposition and doping of the 1 mm thick ZnSe polycrystalline wafers was performed by after growth thermal diffusion of Fe and Cr. Room temperature emission cross section of 5T2-5E transition of iron ions was estimated from spectroscopic measurements. Middle infrared emission of Fe2+ in ZnSe was studied under three different regimes of excitation: ordinary optical (2.92 um) excitation of 5T2 first excited state of Fe2+; excitation via 5E level of Cr co-dopant (1.56 um); and excitation via photo-ionization transition of Fe2+ (0.532 um). For the first time the energy transfer from Cr2+ (5E level) to Fe2+ (5T2 level) under 1.56μm wavelength excitation was observed and resulted in simultaneous room temperature emission of Fe:Cr:ZnSe crystal over ultra-broadband spectral range of 2-3 and 3.5-5 um. We also report the first observation of middle infrared emission at 3.5-5 um induced by 2+-3+-2+ ionization transitions of iron ions in Fe2+:ZnSe. The obtained result is essential for optical pumping of Fe:ZnSe by easily available and efficient visible lasers, and, most importantly, open a pathway for Fe:ZnSe broadband middle-infrared lasing under direct injection of free electrons and holes. A first room temperature gain-switched lasing of Fe:ZnSe crystal at 4.4 um was demonstrated in nonselective cavity under 2.92 um excitation with pulse duration of 5ns. The 2.92 um excitation was realized with a H2 Raman cell (2nd Stokes) pumped in a backscattering geometry by a Q-switched Nd:YAG laser operating at 1.064 um. Selective cavity experiments were performed in a Littrow mount configuration. Room temperature tunable oscillation of Fe:ZnSe crystal over 3.9-4.8 um spectral range has been demonstrated.

6100-14, Session 5

Future trends and applications of ultrafast laser technology

J. M. Eichenholz, M. Li, I. A. Read, S. Marzenell, P. Feru, R. D. Boggy, J. D. Kafka, Spectra-Physics

In this talk we will present an overview of recent development of ultrafast lasers sources and their applications. This talk will highlight some recent state of the art ultrafast pulse results from Ti:Sapphire and Ytterbium based laser systems. There are significant advantages in being able to directly diode pump Ytterbium materials resulting in more compact bulk solid state and fiber based laser systems. Several newly emerging technologies such as Optical Parametric Chirped Pulse Amplification, Supercontinuum Generation and Carrier Envelope Phase Stabilization have generated great excitement in recent years. The evolution of more compact and user friendly ultrafast laser systems has enabled completely new fields that take advantage of the extremely high peak powers and very short time duration of ultrafast laser pulses. Recent results in the fields of multiphoton microscopy, micromachining, 3-D fabrication, and spectroscopy will be discussed.

6100-15, Session 5

High energy, 40 fs compact diode-pumped femtosecond laser for nanostructuring applications

C. Hoenninger, R. Bello Doua, E. P. Mottay, Amplitude Systemes (France); F. Salin, Univ. Bordeaux 1 (France)

High peak power femtosecond oscillators exhibit great potential for many applications such as micro- and nano-machining and structuring, waveguide writing in glass, nonlinear frequency conversion or seeding of ultrafast fiber and bulk amplifiers. Ultrashort pulse durations below 50 fs are routinely produced by Ti:sapphire lasers. However, due to the need for a green pump laser, Ti:Sapphire lasers suffer from a greater complexity. Diode-pumped Ytterbium femtosecond lasers on the other hand are compact and reliable lasers, but, because of the limited amplification bandwidth, typically exhibit pulse duration greater than 60 fs.

We present a directly diode-pumped 40-fs laser source with pulse energies higher than 120 nJ, more than 2 MW peak power, and a pulse repetition rate of 9 MHz. The laser setup is compact and fits in a 60 x 40 cm footprint. The laser source consists of a passively mode-locked femtosecond oscillator and fiber-based post-compression module. The oscillator operates at 9 MHz pulse repetition rate and produces pulse energies up to 300 nJ at 370 fs pulse duration. The oscillator is then focused into a standard single mode fiber in order to broaden the pulse spectrum to about 60 nm bandwidth. Owing to the high initial pulse energy the used fiber is as short as 1.5mm. After collimation it was sufficient to reflect the beam 8 times on 2 parallel chirped mirrors having -250 fs≤ each. The overall transmission of this pulse compression module was about 80% resulting in 120 nJ transmitted pulse energy in 40-fs pulses.

6100-16, Session 5

Diode-pumped Yb3+:CaGdAlO4 femtosecond laser

Y. Zaouter, Univ. Paris-Sud II (France) and Amplitude Systemes (France); F. P. Druon, P. M. Georges, Univ. Paris-Sud II (France); J. Petit, P. Golner, B. Viana, École Nationale Supérieure de Chimie de Paris (France)

We report the first experimental demonstration of a directly diode-pumped passively mode-locked femtosecond laser based on an ytterbium-doped CaGdAlO4 (Yb:CALGO) single crystal. This uniaxal crystal was grown by use of a Czochralski technique and has a tetragonal structure (I4/mmm) in which Yb3+ ions substitute both Gd3+ and Ca2+ ions. The thermal conductivity is of interest as it reaches Ka = 6.9 W/m/K and Kc = 6.3 W/m/K, respectively along the a and c axes. To produce ultra-short pulses, we used a high brightness fiber-coupled diode (5W with a fiber core-diameter of 50μm) as a pump module, compensated the intra-cavity positive dispersion mainly introduced by the gain medium with a pair of SF10 prisms, and initiated and stabilized the mode-locking process using a semiconductor saturable absorber mirror (SESAM). Furthermore, we compensated the extra-cavity spatial dispersion and set up a post compression module to reach the Fourier transform-limited duration. With a 2.5mm long Yb3+:CaGdAlO4 crystal weakly doped at 2-at.%, we demonstrated the generation of femtosecond pulses as short as 47 fs with an emission spectrum of 24.7 nm and with an average power of 48 mW at a repetition rate of 109 Mhz. This is, to our knowledge, the shortest pulses ever produced from an oscillator based on an ytterbium-doped bulk material.

6100-17, Session 5

Generation of 13.5-fs pulses from a diode-pumped Kerr-lens mode-locked prismless Cr:LiSGaF laser

P. Russbueldt, D. Hoffmann, R. Poprawe, Fraunhofer-Institut für Lasertechnik (Germany)

Since the appearance of fs-lasers users are demanding for affordable fs-sources. Diode-pumped colquiriite fs-oscillators are promising, but did not match the requirements yet. With diode-pumped Cr:LiSAF and Cr:LiSGaF KLM oscillators $\Delta \lambda$=60 125nm bandwidth, τ=13.5 20fs pulse-width, P=80 157mW average power are simultaneously achieved for the first time. A plug and play functionality and a sealed 480x165x128mm3 package eases industrial applications.

Planar folding mirrors between laser crystal and curved mirrors of a Z-fold cavity eliminate aberrations of the pump radiation and are the key for high output power, stable modelocking and a compact set-up. Consideration of the saturation of self-amplitude modulation (SAM) by gain-saturation, pump-geometry and diffraction crucially improves soft aperture KLM. Calculations and experiments indicate, that the SAM saturates for high peak-powers, while SPM continuously increases. In a Z-fold cavity the location of the laser crystal, the radius of curvature (ROC) of the folding mirrors and the length of resonator determines SAM and mode matching, while the ROC of the terminating mirrors and the path-difference of the cavity arms control the saturation of the SAM.

The weak non-linear pulse-formation in colquiriite KLM oscillators requires exact dispersion management, accomplished by well characterized dispersive mirrors. Raman shifts the mode-locked spectrum to longer wavelength, which is counteracted by negative TOD and a variable reflective output coupler. With an Cr:LiSGaF oscillator pumped by two broad emitter laser diodes (P=252+372mW, λ=672nm) τ=13,5fs pulse-width, $\delta;\lambda$=110nm bandwidth ($\tau\delta\upsilon$=0,59) and 102mW mean power at 93MHz repetition rate are achieved without any maintenance over a period of several weeks.

6100-18, Session 5

Cryogenically cooled Ti:sapphire amplifiers

A. Fry, Coherent, Inc; S. Fournier, J. Heritier, S. Edstrom, J. MacKay, Coherent, Inc.

Power scaling in laser systems is fundamentally constrained by detrimental effects of absorbed heat in the lasing medium. Cryogenic cooling is well known technique for improving thermal performance in solid state laser materials. In particular the dramatic increase in the thermal conductivity of Ti:sapphire at cryogenic temperatures has enabled a new class of commercial high-average-power femtosecond Ti:sapphire amplifiers. We report on recent developments in this technology.

6100-19, Session 5

Temporal characterization of ultrashort laser pulses based on the third-order cross-correlation function

A. J. Carson, C. C. Barnes, Del Mar Photonics, Inc.; B. R. Campbell, The Pennsylvania State Univ.; N. V. Didenko, S. E. Egorov, A. V. Konyashchenko, Del Mar Photonics, Inc.

High contrast temporal characterization of the output pulse profile of ultrafast laser amplifiers is important in a variety of applications. For example, in high intensity laser-target interactions high contrast in excess of 10 billion is often required. A new design of pulse contrast measuring correlator based on the third order cross-correlation function is presented. We discuss optical layout that uses two nonlinear crystals to generate second harmonic (SH) and third harmonic (TH) light. The third order cross-correlation function is obtained by measuring the TH signal as a function of the optical delay between the fundamental and SH pulses. The device demonstrates the ability to measure a wide array of output parameters including: contrast ratio, pulse pedestal, pre- and post-pulses, and amplified spontaneous emission. It also provides information about the third-order cross-correlation function of pulse intensity on a femtosecond temporal scale and can be used for alignment of high power femtosecond lasers. We discuss the results of using third-order cross-correlation technique to characterize the temporal pulse shape of ultrashort laser pulses from Ti:Sapphire regenerative and multipass amplifiers as well as for Cr:Forsterite regenerative amplifier.

6100-20, Session 6

High performance, widely tunable Ti:Sapphire laser with nanosecond pulses

B. Jungbluth, J. Wueppen, J. Geiger, B. Bach-Zelewski, D. Hoffmann, P. Loosen, R. Poprawe, Fraunhofer-Institut für Lasertechnik (Germany)

Design, theoretical modeling and experimental characterization of a widely tunable Ti:Sapphire laser with nanosecond pulses and high pulse peak power is presented. The laser provides a continuous tuning range of more than 675 nm to 1025 nm with no exchange of optics required. At a pulse rate of one kilohertz it reaches pulse energies of up to 2.5 mJ, pulse durations of around 20 ns, a spectral bandwidth of 10 GHz and an almost diffraction-limited beam quality of M2 < 1.2 with a smooth characteristic of these parameters over the full wavelength range. This clearly exceeds the performance data published so far with our previous designs. Effects, which tend to have provoked spectral gaps in the past, have been totally understood and definitely suppressed by a modified resonator design. Thanks to its high pulse peak power and excellent beam quality, this laser is well suited for frequency conversion and can serve as a basic module of an all-solid-state laser system thatis tunable from less than 200 nm to more than 1000 nm. The presentation contains a detailed description and discussion of all performance-determining design aspects, i.e. pump scheme and pump beam shaping, resonator design and the comparison of different tuning elements. As a main prerequisite of an appropriate resonator design, thermal lensing in Ti:Sapphire crystals is discussed on the basis of experimental and theoretical results. This includes the wavelength dependency of the focal length, the astigmatism in end-pumped Ti:Sapphire crystals with Brewster-cut endfaces, the influence of the pump-light distribution and different cooling schemes.

6100-21, Session 6

High efficiency CW green pumped Alexandrite lasers

J. W. Kuper, D. C. Brown, Snake Creek Lasers, LLC

The use of a laser to pump alexandrite has been demonstrated in the past using for example, a 647 nm Argon CW laser with tunable operation obtained over the range of 726-802 nm and a maximum output of 600 mW at the peak of the gain curve. However, even with the high (\>50%) slope efficiency reported in these experiments, such an approach was not considered commercially viable because of the low (< 0.1%) efficiency of ion lasers. On the other hand, using red diodes to directly pump alexandrite could provide higher overall efficiency but due to low diode brightness, power outputs are limited. To date, the maximum CW output power demonstrated with diode pumping was only about 200 mW at the fundamental wavelength [2]. We have recently suggested [3] that the commercial availability of efficient diode pumped high brightness 532 nm lasers with outputs powers scalable to well over 10 W, can provide an alternative pump laser source for alexandrite that would be superior to either dye, ion or diode lasers. Here we report over 1.4 W stable CW output achieved in experiments using a 5 W high beam quality Nd:YVO4 532 nm Millenia laser (from Spectra-physics) to end-pump an alexandrite laser rod. This output corresponds to a free running mode centered at 767 nm. Further improvements in the slope efficiency to over 50% are projected based on optimized pump and mode spot sizes. Preliminary second harmonic con-

version experiments were also conducted, which are in the process of being scaled to over 100 mW of tunable output around 375 nm. Future work will extend the spectral range to the third harmonic near 250 nm. With pump powers of over 15 W already available, we believe that a green laser pumped alexandrite provides a highly promising approach for producing efficient, power scalable tunable laser systems operating in the near infrared (around 750 nm), and the ultraviolet (near 375 and 250 nm) spectral regions.

REFERENCES

1. R. Scheps, J. Myers, T. Glesne, and H. Serrese, "Monochromatic End-Pumped Operation of an Alexandrite Laser," Opt. Comm., 97, pp. 363-366 (1993)

2. Light Age, Inc. Somerset, NJ, www.light-age.com.

3. J. W. Kuper and D. C. Brown, Proceedings of SPIE Vol. 5707, Edit. H. J. Hoffman, R. K. Shori, pp. 265-270, 2004

6100-22, Session 6

Characterization of cobalt doped ZnSe and ZnS crystals as saturable absorbers for alexandrite lasers

R. A. Sims, J. Kernal, V. V. Fedorov, S. B. Mirov, The Univ. of Alabama at Birmingham

Cobalt doped ZnSe and ZnS crystals have been studied to determine their effectiveness for passive Q-switching for 700-800nm spectral range (Alexandrite laser). Samples were prepared using Bridgeman technique for single-step growth of Co doped crystals as well as after growth thermal diffusion of Co in undoped crystals. ZnS:Co:Cr crystals, which have been produced using the Bridgeman technique, show maximum initial absorption coefficients of 17 cm-1 at 725nm.

Experimental results are reported on effective thermal diffusion of Co2+ in ZnSe and ZnS polycrystals and thermal diffusion constants of cobalt ions in ZnSe and ZnS was estimated. The nonlinear saturation properties of cobalt doped ZnSe and ZnS crystals have been investigated experimentally. The induced transparency measurements were performed using electro-optically Q-switched, alexandrite laser radiation at 731, 741, and 778 nm with a pulse duration of about 70 ns. The induced transmission measurements were analyzed using a four-level absorber model and the absorption cross sections have been estimated at both 731nm and 741nm to be 9.5x10^-18 cm2 and 8.2X10^-18 cm2, respectively. Absorption cross sections calculated from saturation measurements at 4A2-4T1(4P) transition are in agreement with results earlier reported for mid-infrared spectral region at 4A2-4T2 transition of Co2+ ions. The described Co-doped crystals are very promising as passive Q-switches for alexandrite laser resonators. Co2+ centers feature high cross section of saturation and their absorption bands are nicely matched to the spectral emission of the tunable alexandrite laser. An efficient passive Q-switching of the alexandrite laser cavity was realized.

6100-23, Session 6

Construction and characterization of a Ti:Sapphire CW laser system with kHz linewidth

S. Hadrich, P. Jauernik, Sirah Laser und Plasmatechnik GmbH (Germany); S. Schmid, G. Sommerer, Spectra-Physics GmbH (Germany); L. McCrumb, Spectra-Physics Lasers

Tunable, frequency stabilized lasers are essential for numerous precision measurements and experiments such as laser cooling. We report the construction of a Ti:Sapphire laser system that is designed to be stable to 10-8 in 1 sec averaging. This level of accuracy is obtained by the use of a unique mechanical design, careful choice of optical components and a state-of-the-art active control. The system is comprised of a ring cavity, an intra-cavity electro-optical modulator, a digital signal processor based control unit and an external reference cavity. Optionally, one can frequency double the output to extend the accessible wavelength range. We present data of the output energy achieved, tuning curves, beam parameters, doubling efficiency, amplitude noise, and spectral noise.

6100-72, Session 6

Power scaling and extended tunability of mode-locked Titanium doped sapphire lasers

S. Marzenell, R. Boggy, I. A. Read, D. E. Spence, J. D. Kafka, Spectra-Physics

We show the historical development of commercially available mode-locked lasers based on titanium doped sapphire. We will show experimental and theoretical data on the limits of these lasers, especially average output power and tuning range. The latest one-box systems offer an average power of more than 2.9W at 800nm, which corresponds to more than 350kW peak power at 800nm. In addition, the systems are tunable from 700nm to 1020nm using only one optics set. These achievements enable further advancements of certain applications. Micromachining applications are demanding the increased peak power whereas multi-photon microscopy is looking for more tunability and higher average power.

6100-24, Session 7

Fluoride laser crystals: old and new

H. P. Jenssen, College of Optics and Photonics/Univ. of Central Florida and AC Materials, Inc.; A. Cassanho, AC Materials, Inc.

Since the beginning, oxide and fluoride materials have competed to become gain materials of choice for solid state lasers, from early materials such as Calcium Fluoride and Calcium Tungstate crystals to the now ubiquitous Nd hosts YLF, YAG and Vanadate. Among Tunable laser materials, MgF2 - an early favorite, gave way to superior oxides such as Alexandrite and Ti:Sapphire only to be followed by development of still newer tunable fluoride media, notably, fluoride colquiriites such as Cr-doped LiSAF and LiCaF. As laser engineering progressed, and with the advent of practical diode pumping configurations, the requirements on material properties have undergone some key changes as well. This includes a renewed emphasis on crystal quality to allow consistently reliable operation for OEM applications, improved material characterization techniques, tailoring of absorption properties to match available diode wavelengths, and the ability to utilize new transitions amenable to resonant pumping, including quasi-three level transitions. While oxides such as YAG, Vanadates and Ti:sapphire have seen major quality improvements in the past decade, fluoride crystal improvements did not lag far behind. Thus, improvements in preparation, crystal growth and fabrication techniques now allow large YLF crystals of excellent quality to be consistently produced. At the same time, ongoing efforts in growing and optimizing new fluoride crystals identified a number of attractive laser materials, with Barium Yttrium Fluoride BaY2 F8 (BYF), KY3F10 (KYF) and the tunable Cr doped LiCaGaF6 as notable recent examples.

In this talk we will review developments in hydrofluorination and crystal growth techniques which allowed growth of for high quality large size BYF crystals, that are optically scatter free and as easy to fabricate as YLF. Characterization and spectroscopic studies showed that Nd-doped BYF, in particular, has properties that make them a potentially better match for diode pumped lasers than the more common Nd:YLF. In addition, the longer lifetimes of excited state transitions showed that Ho-doped BYF crystals may be superior to other fluorides for generating longer wavelengths, especially in the mid-IR, where long lifetimes are often correlated with higher overall laser efficiencies. Other fluoride crystals benefited from application of improvements realized for BYF, including the recently developed KYF and LiCaGaF6. Key advantages of these new crystals will be discussed and several fluoride crystal based laser schemes will be presented. These include the demonstration of scalable outputs from a 4μm Ho:BYF laser and some recent results from a 1μm Nd doped BYF and the tunable Cr doped LiCaGaF6.

6100-25, Session 7

Modeling of time-dependent thermal effects in Cr2+-doped zinc selenide thin disks

P. A. Berry, K. L. Schepler, Air Force Research Lab.

The mid-IR wavelength range is important for both military and scientific applications. While Cr2+-doped zinc selenide laser materials have shown great promise with multi-watt operation at room temperature with broad tunability in the 2-3 ∝m spectrum[1,2], their development has been hampered by their susceptibility to thermal effects. The high thermo-optic coefficient of zinc selenide gives rise to thermally-induced phase gradients when pumped by non-uniformly distributed beam profiles. The resulting thermal lens, along with increased non-radiative transitions due to increased temperature, cause laser instability and decreased power output.

These materials are often pumped with pulsed lasers of varying pulse repetition frequencies (PRFs). Understanding the thermal response of the material in the time domain is important to characterizing and mitigating the overall thermal effects present in the laser. Finite element modeling was used to create time-dependent models in which the PRF of the pump beam could be varied and the accompanying thermal lensing and temperature rise quantified. Initial results show that there are optimal PRFs that can be used to combat both thermal lensing and temperature rise producing maximum average output power. These results are also compared to experimental measurements of laser performance at kHz to cw PRF settings. Experiment and model are in reasonable agreement.

References

1 J. B. McKay, W. B. Roh, and K. L. Schepler, "4.2 W Cr2+:ZnSe face cooled disk laser," in OSA Trends in Optics and Photonics, Conference on Lasers and Electro-Optics, (Optical Society of America, Washington DC 2002) pp. 119-120.

2 W. J. Alford, G. J. Wagner, A. C. Sullivan, J. A. Keene, and T. J. Carrig, "High-power and Q-switched Cr:ZnSe lasers," in OSA Trends in Optics and Photonics vol. 83, Advanced Solid State Photonics, J. J. Zayhowski, Editor. (Optical Society of America, Washington DC 2003), pp. 13-17.

6100-26, Session 7

Middle-infrared electroluminescence of n-type Cr doped ZnSe crystals

L. Luke, V. V. Fedorov, I. S. Moskalev, A. Gallian, S. B. Mirov, The Univ. of Alabama at Birmingham

We report the study of middle-infrared electroluminescence of Cr doped bulk ZnSe and ZnS crystals. ZnS samples were prepared using Bridgman technique for single-step growth of Cr doped crystals with Al, Ag or Au co-doping. Comparative spectroscopic studies of Cr:ZnS and Cr-Al, Cr-Ag, and Cr-Au co-doped ZnS crystals show that absorption, emission spectra and kinetics of fluorescence of Cr in these crystals are identical. However, the Bridgman technique does not provide good electrical conductivity of ZnS crystals. n-type Cr-doped ZnSe samples were prepared in three stages. At the first stage the undoped polycrystalline ZnSe samples were grown by chemical vapor deposition. At the second stage doping of the 1 mm thick ZnSe polycrystalline wafers was performed by after growth thermal diffusion of Cr. At the third stage, Cr-doped ZnSe wafers were annealed with Al2Se3 and Zn powders in sealed vacuumed ampoules at 950 C for 96 hours. Comparison of the absorption spectra of the crystals before and after thermal diffusion indicates the preservation of the desired Cr2+ ions. Ohmic contacts were formed by wetting the surface of the crystals with In. The best crystals demonstrated conductivity of up to 10-100 ohm*cm. The electroluminescence measurements were taken using synchronous detection methods with an InSb detector. A pulse generator (100V at 5 kHz) and a lock-in amplifier were used to distinguish luminescence signals from blackbody radiation. We report the first observation of middle-infrared (2-3um) electroluminescence of n-type Cr doped bulk ZnSe crystals.

6100-27, Session 7

Mid-infrared (3-5 μm) emission from rare earth doped KPb2Br5

U. Hommerich, E. Nyein, P. Amedzake, Hampton Univ.; S. B. Trivedi, Brimrose Corp. of America; J. M. Zavada, U.S. Army Research Office

Solid-state lasers operating in the MIR wavelength region (3-5 um) are of great technological interest for applications as eye-safe lasers, medical lasers, remote sensing of chemical and biological agents, as well as military countermeasures. The development of MIR solid-state lasers based on traditional oxide and fluoride laser hosts is limited by non-radiative decay through multi-phonon relaxations. On the contrary, rare earth doped crystals with low maximum phonon energies can exhibit efficient MIR emission at room temperature. In this paper, we present initial results of the material synthesis and optical properties of rare earth (Pr, Nd, Dy, Er, Tm) doped potassium lead bromide (KPb2Br5). KPb2Br5 is moisture resistant and can be handled under ambient atmospheric conditions. Moreover, KPb2Br5 has a maximum phonon energy of only ~140 cm-1, which leads to small non-radiative rates and efficient MIR emission. The 3-5 um emission properties of several rare earth doped KPB crystals will be presented at the conference.

6100-28, Session 8

Spatial mapping of fluorescence and Raman spectra across grain boundaries in a transparent Nd-YAG ceramic laser material

V. Gopalan, W. B. White, J. P. Stitt, G. L. Messing, The Pennsylvania State Univ.

Recently, dramatic improvements have been made in transparent ceramic lasers that offer high output powers and low losses that are competitive with the best single crystal laser technology today. To understand this, it is necessary to obtain a very detailed characterization of the influence of grain boundaries in the ceramic host material. This talk will present results on spatial mapping of fluorescence and Raman spectra across grains and grain boundaries in a transparent Nd-YAG laser material with 5% Nd- doping using confocal and near-field scanning optical microscopies. The Raman signal from the host YAG material does not show any significant spectral shifts, but only intensity and lineshape changes between grains and grain boundaries. The fluorescence spectrum near 1064nm wavelength relating to Nd-doping does show differences in the sidebands, indicating changes in the Nd-energy levels between grain and grain boundaries. These will be discussed.

6100-29, Session 8

Development of Neodymium doped ceramic Yttria

N. S. Prasad, NASA Langley Research Ctr.; S. B. Trivedi, S. Kutcher, C. Wang, G. V. Jagannathan, Brimrose Corp. of America; U. Hommerich, Hampton Univ.; V. Shukla, R. Sadangi, B. Kear, Rutgers Univ.

Significant progress is being made in the development of polycrystalline ceramic material based solid-state lasers. Advancements made in the development of Nd doped Ceramic YAG material has facilitated it to be used in high average output power applications. Another material development that is rapidly advancing is the neodymium doped Yttria (Nd:Y2O3). Recently, we reported on the development of Nd:Y2O3 material with good emission properties but was translucent in nature. In further studies, transparent Nd:Yttria ceramic material was successfully prepared using improved material processing techniques. Using a proprietary scalable production method, spherical non agglomerated and monodisperse ceramic powders of Nd:Y2O3 were utilized to fabricate polycrystalline ceramic material samples with sintered grain size in a suitable

range. In this paper, we present our initial results on the material, optical, and spectroscopic properties of a highly transparent (Nd:Y2O3).

Polycrystalline ceramic lasers have enormous potential commercial applications, which include remote sensing, chemical detection and space exploration research. Furthermore, the cost to produce ceramic laser materials is potentially much lower than that for single crystal materials because of the shorter time it takes to fabricate the material and also because of the possibility of mass production. The polycrystalline ceramic material that we have produced has been characterized for its suitability as a diode pumped solid state laser. Potential laser designs will be discussed including end-pumping schemes and the thin-disk laser configuration.

6100-30, Session 8

Laser properties of mixed Nd:YxGd1-x VO4 crystals with different crystal compositions

Y. Tang, X. Wang, S. Tang, Crystal Research, Inc.; N. C. Fernelius, Air Force Research Lab.

With Gd ions replacing a fraction of Y ions in Nd:YVO4 crystal, a new class of mixed gadolinium yttrium vanadate crystals Nd:YxGd1-xVO4 is formed with adjustable laser parameters. As a result, a new laser crystal may be produced with optimized stimulated cross-section and fluorescence lifetime. In this paper, important laser parameters, such as laser slope efficiency, thermal properties, and overall optical-to-optical efficiency, of new mixed vanadate crystals Nd:YxGd1-xVO4 were investigated with different Nd doping levels as well as different yttrium and gadolinium composition ratios. Comparative studies will be presented in reference to better known laser crystals like Nd:YVO4 and Nd:GdVO4 crystals.

6100-31, Session 8

Compositional influence on spectroscopy properties of Yb3+ doped tellurite glasses

M. A. Alencar, R. F. Souza, M. V. Vermelho, M. T. de Araujo, J. M. Hickmann, Univ. Federal de Estado de Alagoas (Brazil); L. R. Kassab, R. Kobayashi, Univ. Estadula de Sao Paulo (Brazil)

Optical glasses based on TeO2 are promising materials for photonics and optoelectronics. They are transparent in the visible, near and middle infrared region. In comparison with silica glasses, they present larger refraction index (~2.0) and smaller phonon energies are obtained. In relation to fluoride glasses, which also have various photonic applications, they offer the advantage of better chemical durability. Yb3+ ions are important in the development of ultra-short pulse lasers and as an energy transfer sensitizer in infrared to visible upconversion lasers. In this work, we investigate the variation of the spectroscopic properties with chemical composition of Yb3+ doped tellurite glasses pursuing applications regarding optical fibers, nucleation of nanoparticles and thin films. The different host glass compositions are prepared using adequate temperatures for melting and annealing. The position of the visible and IR cut-off wavelength varies with the composition. In the visible region the shortest cut-off wavelength is around 300 nm; in the middle infrared region the cut-off wavelength is situated around 7000 nm. We investigate the influence of the composition in the emission and absorption cross-sections and effective linewidth. Moreover, fluorescence lifetimes ranging from 0.7 ms to 1.0 ms were measured. The minimum pump intensity is evaluated for each case in order to investigate a possible laser action using these materials and the obtained values are excellent compared to fluorophosphates laser glasses, Yb:YAG and Yb:YAP laser crystals.

6100-32, Session 8

From 20 Hz to hundreds of electron volts: rare Earth materials for high-bandwidth optical signal processing, lasers, and phosphors

R. L. Cone, C. W. Thiel, P. B. Sellin, Montana State Univ./Bozeman; T. Bˆttger, Univ. of San Francisco; Y. Sun, Montana State Univ./Bozeman; R. M. Macfarlane, IBM Almaden Research Ctr.

Material and device studies span many application areas:

Inhomogenous broadening of infrared rare earth 4f-4f transitions at low temperatures provides time-coherent spectral storage in 105-108 frequency bins for device applications that include real-time holographic signal processing with sub-MHz spectral resolution and bandwidths of tens to hundreds of GHz. Compact vibration-insensitive frequency references for stabilizing diode lasers to 20Hz linewidths over 10ms for signal processing, spectroscopy, quantum information demonstrations, and interferometry are provided by homogeneous linewidths often less than 1kHz. Our Tm3+- and Er3+-doped materials have been used to integrate both memory and high-bandwidth signal processing capabilities into a processor for high-resolution high-bandwidth range-Doppler radar called S2CHIP - “Spatial Spectral Coherent Holographic Integrating Processor” - without requiring high bandwidth analog-to-digital converters. Spatial-spectral holography is a synthesis of holography and spectral hole burning.

To accelerate development of materials for lasers, phosphors, and spectral hole burning and spatial-spectral holography applications, energies of rare-earth ion 4fN states relative to crystal band states have been measured for important optical host materials. Combining valence band maxima and 4f electron binding energies measured by photoemission with 4fN to 4fN-15d transition energies, we accurately describe 4fN and 4fN-15d binding energies across the entire series of rare-earth ions. Measurements on two different ions in a host are now sufficient to predict binding energies of all rare-earth ions in that host. These results provide insight into electron transfer transitions, luminescence quenching, and valence stability.

Research supported by Air Force Research Laboratory and Montana Board of Research and Commercialization Technology.

6100-33, Session 9

MOPA with kW average power and multi MW peak power: experimental results, theoretical modeling and scaling limits

K. Nicklaus, M. Hoefer, H. D. Hoffmann, J. Luttmann, R. Wester, R. Poprawe, Fraunhofer-Institut für Lasertechnik (Germany)

A Master-Oscillator-Power-Amplifier design combining rod and slab laser technology for high pulse energy, high average power and near diffraction limited beam quality for industrial use has been developed. To achieve the good beam quality at high average and high pulse power, an advanced birefringence compensation scheme, which allows for high mode overlap while simultaneously minimizing the power densities on optical surfaces, has been developed and applied.

The prototypes deliver an average power of up to 860 W with M2 < 2 or 1.3 kW with M2 < 12 at 10 kHz repetition rate and 5-16 ns pulse duration. At 1 kHz and 5 ns up to 420 mJ pulse energy can be achieved. The prototypes are fully computer controlled and can be operated from 0 to 100 % output power and single shot to 10 kHz. They are currently operated for plasma creation in a laboratory surrounding and have run for more than one thousand hours without failure up to now.

An analytical solution of thermally induced refractive index profile in dependency of the pump light distribution including the effect of thermally induced birefringence, temperature dependency of the thermal conductivity and the thermal dependency of the refractive (d2n/dT2) has been derived, allowing a fast calculation of thermally induced aberrations without the use of FEA. Experimental results are compared to predictions from analytical and FEA modeling. Based on experimental and theoretical results, scaling limits of rod based MOPAs are predicted.

6100-34, Session 9

Power-scaling in re-imaging waveguide lasers

I. T. McKinnie, Coherent Technologies, Inc.; B. Callicoatt, National Institute of Standards and Technology; C. S. Wood, J. Koroshetz, J. R. Unternahrer, M. Tartaglia, S. Christensen, O. Koski, M. Hinckley, M. J. Bellanca, E. Schneider, D. D. Smith, Coherent Technologies, Inc.

Bulk rod, slab and disk solid-state lasers have gained widespread acceptance for use in a broad range of applications in industry, scientific research, medicine and engineering. However the size, weight and prime power requirements of these lasers preclude their use on many mobile air, sea and space-borne platforms. Fiber lasers have potential to address some of these applications, but the geometry of the fiber gain medium severely limits power-scaling for pulsed formats and for narrowband operation.

Re-Imaging (or self-imaging) waveguide (WG) technology offers the high efficiency and brightness of a fiber laser, combined with the higher pulse energies available from bulk laser. The large aperture of the waveguide is typically 10000x the entrance aperture of a fiber and length is much shorter, enabling considerable single-frequency power-scaling and pulse-energy scaling potentially to >200 mJ per WG. The re-imaging process - analogous to free-space Talbot Imaging - retains diffraction-limited beam quality despite the large aperture. Additional advantages include: a thermally robust geometry with highly effective cooling through two large-area surfaces, leading to a 1-D temperature profile with minimal stress birefringence; polarization-maintenance; and a very simple and efficient pumping scheme. The WG architecture also has the advantage of being generic and flexible for a variety of different gain media.

The paper will report on our recent demonstrations of: single-frequency average power-scaling to ~ 200W and peak power-scaling to ~ 40MW in 1ns-class pulses. Further power-scaling to multi-kW lasers and phased arrays will be discussed.

6100-35, Session 9

Improving the beam quality of a high power Yb:YAG rod laser

D. G. Harris, F. Patel, C. Turner, Jr., The Boeing Co.

An approach to improving the beam quality (BQ) of rod lasers configured with a stable resonator is described. The objective has been to understand the issues relating resonator mode size, laser rod diameter and materials to obtain good beam quality at high powers. A diffractive optics model of the bare cavity was developed which allowed insight into beam quality considerations. Additionally, a demonstration of mode control to improve laser performance was also an objective.

An investigation has been made of scaling issues of a kilowatt class Yb:YAG rod laser which is of a robust and compact design. It is of interest to understand the issues and limitations which will allow this architecture to scale to high powers while retaining good beam quality. Diode Pumped Solid State Lasers (DPSSLs) offer compact efficient high power sources of laser radiation, but have been limited to power levels of a few hundred watts with good (M2 ~ 2) beam quality. To date in order to obtain good beam quality at higher powers has required nonlinear optical techniques such as SBS phase conjugation. An approach that will provide good beam quality with an uncomplicated design is very appealing.

It is desired to keep the resonator design simple, effective and in concert with the robust yet simple philosophy of the architecture, and without requiring complex additions to the architecture. Yb:YAG was chosen because of its low quantum defect translating to higher quantum efficiency and less heat deposited into the host as compared to Nd:YAG. The quasi three level nature of Yb does, however, require high pump rates to achieve transparency of the medium.

The laser is an end pumped Yb3+:YAG system that has been described elsewhere1. The thermally induced birefringence compensation is achieved using a dual rod stable cavity configuration with a quartz optical rotator located between the rods2. The rotator has the effect of changing the polarization and making the resonator symmetrical. The rods are end pumped by diode arrays. The diode pumping radiation is transferred to the rods by hollow lensducts; at the entrance to the lensduct is a focusing lens which focuses most of the radiation into the laser rod. The lensduct captures that pumping radiation escaping from the optical system and redirects it into the rod. Once the pumping rays enter the 2mm diameter Yb:YAG rod, they uniformly fill the cross section and propagate down the 5 cm length by total internal reflection.

Interferometric measurements of the medium during lasing conditions determined that aberrations limitations to BQ. The experiments measured the severity of the aberrations and the Zernike coefficients were determined. A simple model provided some insight into the operation of the laser.

A larger mode volume and more extraction of laser power while retaining good beam quality can be achieved with a super-Gaussian mode. The super-Gaussian mode will also reduce the aberrations associated with mode-medium induced aberrations by extracting with a more uniform flat top lasing mode. The approach chosen is to have the resonator mode in the rod be nearly a super-Gaussian, and then determine the mirror specifications.

The designs for the mirror profiles were developed using a diffractive optics model. The approach is to use phase conjugating elements, reflective rather than transmissive, to define the preferred mode (one with the lowest losses), in a resonator. In practice, a super-Gaussian beam was propagated from the center of the cavity to a resonator mirror, where the conjugate phase was then calculated. From here the mode was propagated back to the center of the cavity and using a Fox-Li analysis; it was verified to be a low order eigenmode of the resonator. Inputs to the code consist of optical schematic element parameters, distances, focal lengths, indices of refraction (n0 and n2-focusing), initial mode (intensity, phase, wavelength and polarization) and flags for controlling the number round trip iterations, parametric sensitivities, and plots. The code outputs include plots/tables of the fields at designated locations, the radial phase profile of the phase conjugating elements and iteration histories (power loss, fill factors and phase Strehl).

The mirrors were fabricated and tested. A brightness improvement of more than 2 was measured.

We wish to acknowledgement the support of the Boeing Company as well as the Joint Technology Office.

REFERENCES

[1] R.J. Beach, E.C. Honea, S.B. Sutton, C.M. Bibeau, J.A. Skidmore, M.A. Emanuel, S.A. Payne, P.V. Avizonis, R.S. Monroe, and D.G. Harris, "High-Average-Power Diode-Pumped Yb:YAG Lasers," in Proc. SPIE, Vol. 3889, p 246, (1999).

[2] W.C. Scott, M. deWit, " Birefringence Compensation and TEM00 Mode Enhancement in a Nd:YAG Laser," Appl. Phys. Lett. 18, 3, (1971).

6100-36, Session 10

High power Q-switched TEM00 mode diode-pumped solid state lasers with > 30W output power at 355-nm

C. X. Wang, G. Y. Wang, A. V. Hicks, D. R. Dudley, Y. H. Pang, N. Hodgson, Coherent, Inc.

Since their first commercial introduction in 1997, diode-pumped Q-switched Vanadate and YAG lasers with 355 nm output have advanced in power level and reliability and are now qualified in many industrial processes, such as via hole drilling, stereo lithography, wafer scribing and dicing. At present, average 355nm output powers of up to 20W are commercially available with pulse energies of several 100 micro-Joules and repetition rates of up to 150 kHz.

In this paper, we report reliable high power UV generation with TEM00 mode output powers in excess of 30W in Q-switched, end-pumped Nd:YVO4 and side-pumped Nd:YAG lasers using extra-cavity sum frequency generation in LBO. With a sidepumped dual-rod Nd:YAG rod os-

cillator and extra-cavity tripling, 32W of 355nm TEM00 mode output have been achieved at a repetition rate of 50 kHz. With an end-pumped Vanadate MOPA configuration, similar 355nm power levels were realized at repetition rates around 100 kHz. Lifetest results are presented and the scaling to higher power is discussed.

6100-37, Session 10

High power second and third harmonics generation of a two stage partially diode end-pumped Nd:YAG INNOSLAB MOPA System

M. Höfer, J. Löhring, S. Röhrig, J. Luttmann, K. Nicklaus, R. Wester, D. Hoffmann, R. Poprawe, Fraunhofer-Institut für Lasertechnik (Germany)

We report a partially diode end-pumped INNOSLAB based MOPA system, consisting of an A/O q-switched Nd:YAG oscillator with a stable-unstable hybrid resonator design and one amplifier stage. The system can be operated from 5 to 30 kHz. At 10 kHz the oscillator delivers 60 W output power. The amplifier is set up in a folded single pass configuration. It delivers a linear polarised output power of 120 W @ 10 kHz with M < 1.5 and a pulse length of 30 ns. By using a 20 mm LBO crystal, a second harmonic power of 65 W @ 532 nm with near diffraction limited beam quality of M < 1.3 is achieved. With an optimised setup for third harmonics generation the system provides a power of 36 W @ 355 nm at 100 W fundamental power. An excellent beam quality of M < 1.5 was measured over the whole power range. A comprehensive comparison of the evaluated experimental data with a developed numerical model for frequency conversion is presented. Beside aspects like diffraction, walk-off, time and space depended pulse shape the model considers thermal effects like thermal dephasing due to absorptions during the conversion process by using FEA modelling. Temperature distributions are calculated and compared with experimental data. Applying the numerical model an improvement of conversion efficiency and further power scaling to the hundred watt level of the third harmonic is currently under investigation.

6100-38, Session 10

Advances in high power harmonic generation

L. A. Eyres, J. Gregg, J. Morehead, D. J. Richard, W. M. Grossman, JDS Uniphase Corp.

We report next-generation Q-switched, intracavity-frequency-converted, diode-side-pumped, Nd:YAG lasers with output powers of > 30 W at 355 nm and > 40 W at 532 nm. In particular, we will discuss design and performance of a 532 nm laser having a variable pulse width externally adjustable over the range of 40 ns to 300 ns. The laser can also be operated to generate substantially constant output power at fixed pulsewidth over a wide range of pulse repetition rates.

6100-39, Session 11

Generation of THz and IR Radiation in DAST crystals

P. Günter, ETH Zürich (Switzerland)

Abstract not available.

6100-40, Session 11

100 Terawatt laser based on optical parametric amplification in DKDP crystal

E. A. Khazanov, V. V. Lozhkarev, V. Ginzburg, E. Katin, A. Kirsanov, G. Luchinin, A. Mal'shakov, M. Martyanov, O. V. Palashov, A. K. Poteomkin, A. M. Sergeev, G. I. Freidman, A. Shaikin, I. V. Yakovlev, Institute of Applied Physics (Russia)

The problem of creating optical parametric chirped pulse amplifiers (OPCPA) up to the multiterawatt and petawatt level has been discussed in literature. Erlier we suggested using non-degenerate parametric amplification in DKDP crystal and showed that in the DKDP crystal a ultra-broadband phase matching at the central wavelength of signal radiation of 910 nm can be achieved, thus making it possible to amplify 10-15 fs pulses. In this paper we describe the 100-terawatt laser system based on this architecture.

The system consists of the femtosecond Cr:forsterite master oscillator (45 fs pulses with 2 nJ energy at central wavelength of 1250 nm), original stretcher that comprises two prisms besides the standard diffraction gratings; three DKDP crystal OPCPA pumped by the second harmonic of Nd:YLF and Nd:glass lasers and vacuum compressor based on two diffraction gratings and one corner reflector (clear aperture of 110 mm, transmission coefficient 65%.). Energy efficiency of optical parametric amplifier was 27%. Maximum energy of compressed pulses was 10J at 910nm wave length. Autocorrelation function corresponds to a 72 fs Lorenz pulse at FWHM. Thus, peak power at the output was 130TW. This value 8 times exceeds the record level achieved in other OPCPA lasers.

Calculations show that one more optical parametric amplifier with an aperture of 200-300mm and pump pulse energy of 1-2 kJ at 527 nm is needed to have the multipetawatt power. Currently work is being done to create a multipetawatt laser source.

6100-41, Session 11

New wavelengths generated by BaWO4 or KGW intracavity Raman laser

H. Jelnkova, J. Šulc, M. Nemec, Czech Technical Univ. in Prague (Czech Republic); J. K. Jabczynski, W. Zendzian, Wojskowa Akademia Techniczna (Poland)

We report on the generation of the new infrared laser wavelengths (1175 nm, 1196 nm, and 1199 nm) based on the intracavity Raman conversion of the Nd:YAP laser radiation (1079.6 nm). Barium tungstate (BaWO4) and potassium gadolinium tungstate (KGW) crystals were used as solid state Raman converters. The laser was based on three mirror linear cavity forming resonator for fundamental (resonator lengths 126 mm) and Raman (resonator lengths 35 mm) radiation generation. As a active laser crystal Nd:YAP in the form of Brewster angle trigonal slab was used. This shape of the active medium allows constructing the simple linear laser cavity. For pumping of this crystal the QCW fast-axis collimated laser diode was used. To obtain high peak power in fundamental radiation the Cr3+:YAG crystal was used for Q-switching. Raman laser was optimised for maximal output energy at the first Stokes wavelength. The stable output was reached for both Raman crystals. In the case of BaWO4 crystal the output pulse (energy ~165 uJ, length of pulse 1.7 ns) with the wavelength 1199 nm was generated. The Raman generated wavelengths in the case of KGW crystal were 1175.6 nm and 1195.7 nm, depending on the orientation of the crystal inside the resonator. The output energy in generated pulse with the length ~1 ns (FWHM) was ~90 uJ for both orientations. The beam output structure was close to fundamental mode with the divergence ~ 3 mrad. The efficient second harmonic generation giving possibility of new wavelengths generation in visible region was demonstrated.

6100-42, Session 11

Characterization of RTP crystals for electro-optic and non-linear applications

H. Albrecht, M. A. Herrmann, D. Lupinski, Cristal Laser SA (France)

The aim of this work is to introduce the RTP material (a KTP isotype) and point out its main fields of application for solid-state lasers.

First, we'll address its use as an electro-optical modulator (for Q-switches or pulse-picking applications). A set of measurements performed in house (transmission, extinction ratio, half-wave voltage, damage threshold, lifetime) along with the comparison with other relevant data of other E-O

materials show that RTP crystals offer the best compromise in most cases.

Then, in order to give a full scope of RTP's possible applications in solid-state lasers, we'll also present an overview of non-linear interactions achieved with RTP up to date. The described experiments include: frequency-doubling at 1064 and 1123 nm, frequency mixing resulting in a 628-nm wavelength, and an eye-safe OPO pumped at 1064 nm. The study reviews performance figures of adequately cut RTP crystals (efficiency, tolerances, walk-off, damage threshold) and compares them with other suitable non-linear materials.

In addition, we'll present precise bulk RTP absorption data obtained thanks to the Photothermal Common-path Interferometer. These measurements are performed for various crystallographic orientations and are of interest for both electro-optical and non-linear applications.

All our data will be summarized in an easy-to-read table to help the user make the best choice.

6100-43, Session 12

Review of solid-state lasers for space applications (Tutorial)

R. S. Afzal, Spectra Systems Corp.

The development history of solid-state lasers for space applications will be reviewed. Examples of flight lasers will be discussed with an emphasis on the evolution of design and performance.

6100-45, Session 12

Space qualification issues in AcoustoOptic Tunable Filter (AOTF) based spectrometers

S. B. Trivedi, J. I. Soos, F. Jin, S. Kutcher, Brimrose Corp. of America; N. S. Prasad, NASA Langley Research Ctr.

For space qualificaiton, an AOTF-based spectrometer must be capable of withstanding extended operation while enduring environmental extremes. Such extremes include the presence of vibration and g-forces, temperatures ranging from cryogenic to 120+oC, temperature cycling, and radiation exposure. The AOTF consists of mechanical fixtures and opto-mechanical parts (transducer bonding and AOTF crystal), electronic components (RF driver, impedance matching circuit, and detection system) and optical components (crystals, lenses, transmission and receiving optics). In space, the mechanical components of a system are vulnerable to high g-forces and temperature effects (i.e. dimensional changes); while both the electrical and optical components are subject to temperature and radiation effects. Based on our experience in the development of AOTF-based instrumentation and exposure to space qualification issues, we will discuss the manufacturing and packaging issues for the AOTF spectrometer as they relate to space qualification.

AOTF spectrometers have several advantages over traditional grating-based spectrometers. An AOTF is an all solid-state tunable filter with no moving parts and is therefore immune to orientation changes or even severe mechanical shock and vibrations. The AOTF is a high throughput and high speed programmable device capable of randomly accessing thousands of precise wavelengths in less than a second, making it an excellent tool for in-situ NIR spectroscopy. Brimrose has recently developed a novel transducer mounting technique that enables the AOTF spectrometer to operate at cryogenic temperature and under temperature cycling conditions. Thus, AOTF spectrometers are well suited for applications involving space exploration due to their ruggedness, tunability and absence of moving parts.

6100-46, Session 12

Qualification of the laser transmitter for the CALIPSO aerosol lidar mission

F. E. Hovis, Fibertek, Inc.

Space-based missions impose a unique set of requirements on laser designs. We will review the issues encountered and lessons learned during the qualification of the laser transmitter for the CALIPSO aerosol lidar mission. From our experience during the design, build, and qualification of the laser we developed a set of guidelines for designing and building future space-based lasers. These guidelines are listed and briefly described below.

1. Use mature laser technologies - It is always tempting to insert the newest laser technology into space-based lidar missions. Unfortunately, the cost and schedule constraints of a space-based lidar mission coupled with the logistic complications of any "routine" space mission provide ample opportunities for failure without even introducing a significant technology risk component.

2. Use validated contamination control procedures - The evolution of contaminants in an optical compartment is one of the major long term failure mechanisms in space-based lasers. It is critical to first identify materials that have a higher risk of causing contamination induced optical damage and then to develop processes that eliminate these contaminants.

3. Operate all optical components at appropriately de-rated levels - Derating guidelines for the electrical and mechanical components of space hardware are well established. Similar guidelines for the derating of optical components of lasers are not available. We made a first attempt at establishing such guidelines based on our CALIPSO laser transmitter experience. The laser diodes used to pump the Nd:YAG gain medium were run at peak optical powers de-rated by ~25% of their design values. The power density in the Nd:YAG slab is 1/3 the damage threshold. For all other optics the average fluence/damage threshold ratio is <1/4.

4) Use alignment insensitive resonator designs - The raw boresight requirement for the laser in the CALIPSO mission was >100 μrad. For many traditional laser resonators, a 100 μrad misalignment would cause a significant power drop. By using a laser resonator design that tolerates misalignments over 100 μrad, we reduced the risk of failure due to unexpected launch events.

5) Budget properly for the space-qualification of the electronics and software - Although the design and qualification of the required electronics is in principle straight forward, the implementation of those designs in space-qualified versions can take mush longer and be much more expensive than even ground based military systems. The development and qualification of software for use in space can be a surprisingly long and costly process.

6100-70, Session 12

Qualification and issues with space flight laser systems and components

M. N. Ott, D. B. Coyle, NASA Goddard Space Flight Ctr.; J. S. Canham, Swales Aerospace; H. W. Leidecker, Jr., NASA Goddard Space Flight Ctr.

Issues for developing flight quality solid state laser systems are still numerous, 34 years after the Apollo 15 flashlamp pumped Ruby Lunar Lander laser altimeter. The largest issue currently is the limited supply of high power diode arrays. Since Spectra Diode Labs ended their involvement in the pulsed array business in the late 1990's, there has been a flurry of activity from other manufacturers, but nothing focused on flight quality production. The focus now, inevitably, is on the usage of commercial parts to enable space flight designs.

System level issues such as power cycling, operational derating, duty cycle, and contamination risks to other laser components are among the issues that must be pursued for increased laser transmitter reliability. Designs and processes can be formulated for the system and the components (including thorough modeling) to mitigate risk based on the known failures modes and lessons learned that GSFC has collected over the past ten years of space flight operation of lasers.

In addition, knowledge of the potential failure modes related to the system and the components themselves can allow the qualification testing to be done in an efficient yet, effective manner. Careful designs of test plans with physics of failure knowledge, will enable cost effect qualification of commercial technology. Presented here will be lessons learned from space flight experience, knowledge of potential failure modes, mitigation techniques, and testing options to best test a system for these failure modes from the system level to the component level.

6100-73, Session 12

Qualification of fiber lasers for space applications

S. T. Hendow, S. E. Falvey, B. E. Nelson, Northrop Grumman Corp.

There are many applications where fibers are employed in space, such as fiber gyros and fiber sensors. Fiber lasers are becoming increasingly attractive for space for similar reasons, which are lightweight, small size and low power consumption. The majority of components used in such systems are commercial off-the-shelf parts that have been developed using technologies similar to those used in the development of parts for the fiber telecom market. Space however has environmental conditions that require further hardening of these parts. Accordingly, a generic qualification protocol is suggested for qualifying generic parts for space flight. This protocol is based on merging the qualification requirements for telecom, such as those by Telcordia, with the qualification for spaceflight, such as by NASA. A set of components (at 1064 nm) is chosen for testing the protocol. These include doped fibers, combiners, sources, pumps, isolators and fiber Bragg gratings. The scope of the vibration, thermal and radiation tests used to validate the protocol is limited to the environmental conditions of lower Earth orbit satellites, 100 to 1000km orbital altitude and up to 60 degrees inclination. Also presented in this paper is a summary of a thorough survey conducted for publications related to space qualification of fibers and lasers for space.

This project is sponsored by the USAF Materiel Command, AFRL, Kirtland AFB with Jackson and Tull as the Prime Contractor, under contract number F29601-01-D-0078.

6100-48, Session 13

Stable, tunable solid-state laser sources for airborne and space-based laser radar applications

C. P. Hale, J. W. Hobbs, E. C. Andrews, M. W. Phillips, Coherent Technologies, Inc.

In recent years as laser remote sensing technologies have matured and operating environment demands have accelerated, the design and development of more environmentally robust laser sources has increased in importance. In many instances (e.g. coherent laser radar), single frequency operation in the presence of severe vibration, shock, and temperature change is necessary, as is small size, low power draw, and in many applications, eyesafe operating wavelength. Often such architectures utilize injection-seeding techniques to actively control the spectra of larger and higher power pulsed transmitter lasers, and special servos are required for operation in these harsh environments. In certain airborne and space-based coherent-detection applications, very large (multi-GHz) platform-induced Doppler shifts must be compensated for in order to lower the detection bandwidth of the instrument to practical values; robust techniques must be developed for actively offset-locking of individual master and local oscillator sources to produce the proper compensation. Other techniques under development require extraordinarily high frequency stability and very fast frequency tuning capability, combined in the same laser source. In this paper we review Coherent Technologie's efforts in these areas over the past decade and provide some insight into our approaches to solving these difficult laser and laser remote sensing problems. We will describe the environmentally-hardened METEOR laser and associated tests that we have subjected these lasers to, as well as space-qualifiable active offset-locking of two eyesafe METEORs to multi-GHz offsets and sub-kHz accuracy. We will summarize our current activities in these areas and likely future requirements.

Acknowledgements: Many agencies and sponsors have supported these efforts over the past decade. Specifically, the authors acknowledge the support of M.J. Kavaya (NASA Langley and previously, NASA Marshall), R. Richmond and M. Dierking (AFRL), and R. Menzies (NASA JPL).

6100-49, Session 13

Performance of the GLAS laser transmitter

R. S. Afzal, Spectra Systems Corp.

The design and operating performance of the GLAS laser transmitters currently orbiting on the ICESat satellite will be presented. The laser performance in the context of an integral component in laser altimeter and LIDAR will be discussed.

6100-50, Session 13

Flight hardening of laser systems

K. Dinndorff, BAE Systems

Laser failure mechanisms and flight hardening techniques will be discussed. Practical examples will be presented.

6100-71, Session 13

High efficiency, passively Q-switched Nd:YAG MOPA for spaceborne laser-altimetry

D. Kracht, S. Hahn, J. Neumann, R. Wilhelm, M. Frede, Laser Zentrum Hannover eV (Germany); P. Peuser, European Aeronautic Defence and Space Co. (Germany)

For the spaceborne laser-altimeter (BELA) of ESA's BepiColombo mission a master-oscillator-power-amplifier system (MOPA) is presented. The specified system-requirement is a pulsed laser source with a nearly diffraction limited beam (M < 1.6) that combines high pulse energy of about 50 mJ at less than 10 ns pulsewidth and up to 20 Hz pulse repetition rate with the stringent environmental conditions at space missions. A low-mass (< 1.3 kg) and high optical-to-optical efficiency (> 15 %) laser setup is required. Stable operation at a temperature range of at least 25 K for the MOPA system and 15 K for the pump diodes has to be guaranteed.

Both oscillator and amplifiers are longitudinally pumped by fiber coupled QCW laser diodes. The performance of a longitudinal pumped system is, because of the longer absorption path, less sensitive to pump wavelength variations due to temperature changes of the laser pump diodes. The pump-pulse duration of 200 μs represents as a trade-off between output energy and efficiency of the whole system.

The Nd:YAG oscillator was passively Q-switched with Cr4+:YAG crystal as a saturable absorber. With 100 W of peak pump power a nearly diffraction limited (M *1.2) laser pulse with a duration of 2.8 ns and a pulse energy of 2.4 mJ was generated. The output beam of the oscillator was amplified in a two stage amplifier. A maximum of 62 mJ pulse energy was achieved by pumping each crystal with a peak pump power of 600 W.

6100-51, Session 14

High-power solid-state sodium laser guidestar for the Gemini North Observatory

A. J. Tracy, A. K. Hankla, C. A. Lopez, D. C. Sadighi, I. T. McKinnie, Coherent Technologies, Inc.; C. d'Orgeville, M. P. Sheehan, Gemini Observatory; D. J. Bamford, Physical Sciences, Inc.; S. J. Sharpe, D. J. Cook, Physical Sciences Inc.

We report on the first commercial solid-state sodium laser guidestar system (LGS). The LGS developed at CTI was recently delivered to Gemini. The laser is a single beacon system that implements a novel laser architecture and represents a critical step towards addressing the need of the astronomy and military adaptive optics (AO) communities for a robust turn-key commercial LGS. The laser was installed on the center section of the 8 m Gemini North telescope, with the output beam relayed to a launch telescope located behind the 1m diameter secondary mirror. The laser routinely generates 12 W average power with M2 < 1.2. A wavelength locking system maintains lock to the D2 line at +/- 100 MHz.

The laser architecture is based on cw mode-locked solid-state lasers. The mode-locked format enables more efficient SFG conversion, and dispenses with complex resonant intensity enhancement systems and injection-locking electronics. The linearly-polarized, near-diffraction-limited, modelocked 1319 nm and 1064 nm pulses are generated in separate dual-head diode-pumped resonators. The two IR pulses are input into a single-stage, 20 mm PPSLT sum-frequency generation (SFG) crystal provided by Physical Science, Inc. Visible (589 nm) power of >16 W have been generated, representing a conversion efficiency of 40%.

6100-52, Session 14

Optical extraction from Nd:YAG lasers with ASE gain depumping losses

D. A. Copeland, The Boeing Co.

Optical extraction characteristics of cw solid-state lasers with amplified spontaneous emission (ASE) gain depumping losses are solved exactly and using first-order perturbation theory. The model includes gain depumping losses by ASE and saturation with pump rate and assumes that the medium is homogeneously-broadened. The rate equations describing the spatial growth of the intracavity intensities for a stable optical resonator are summarized, the threshold lasing condition is derived, and the optical extraction efficiency determined for medium parameters appropriate to high gain Nd:YAG lasers. Comparisons with the simple, uniform intracavity intensity model show the latter is not always a good approximation. The well-established empirical critera that the gain-length product satisfy gL < 2-4 to limit ASE power losses is shown to be a consequence of a constraint arising to ensure the validity of a perturbation solution of the stable resonator model and its upper limit is shown to be determined by the spectroscopic and lifetime parameters of the gain media.

6100-53, Session 14

Comparative performance of passively Q-switched diode-pumped Yb:GGG, Yb:YAG, and Yb-doped tungstates lasers using Cr4+ -doped garnets

Y. Y. Kalisky, Nuclear Research Ctr. Negev (Israel); G. Boulon, Univ. Claude Bernard Lyon 1 (France); O. Kalisky, Jerusalem College of Technology (Israel)

We investigated the CW free-running and repetitive modulation in the kHz frequency domain of a passively Q-switched, diode-pumped Yb:YAG, Yb:GGG and Yb:KYW lasers, by using Cr4+:YAG as a saturable absorber. The results presented here are focused towards the design of a passively Q-switched Yb doped garnets or Yb doped tungstates microlaser. The free-running performance of Yb:YAG, Yb:GGG , Yb:KGW and Yb:KYW were characterized, and experimental parameters such as gain and loss were evaluated. We carried out a fit between our experimental results and an existing numerical model, which relates the experimental and the physical parameters of the ytterbium diode-pumped system to the minimal threshold pumping power. The best performance among the laser crystals was obtained for Yb:YAG laser. A maximum peak power of 4.5-kW, at an average output power of 1.32-W, were extracted with of 25 % extraction efficiency.

6100-54, Session 14

High-power Q-switched rotary disk lasers

S. Basu, Sparkle Optics Corp.

Rotary disk laser™ has a very efficient thermal management approach that uses physical motion of the gain medium in a diode-pumped solid state laser. The benefits of rotary disk lasers over conventional bulk solid state lasers are high efficiency, power scalability and high peak power pulsed operation in a single-mode output beam. In the first test, we have generated 28.2 W of Q-switched power at 109.4 kHz in 65 ns pulses with 1.05 times diffraction limited beam quality. We will present power scaling results of the Q-switched rotary disk laser.

6100-55, Session 14

Tailoring the performance of solid state lasers: why and how

S. Geiger, Bavarian Photonics GmbH (Germany)

Diode-pumped q-switched lasers now enable a very diverse array of precision materials-processing applications. An important key to the ongoing market growth and applications diversification is the development of lasers whose performance is optimally tailored to meet the needs of specific applications. For example, long output pulses are preferable for soft wafer marking, whereas short pulses are desirable for solar cell scribing and creating gray-scale pictures for passports and other personal identity applications.

The pulsewidth and overall output power are interdependent performance characteristics determined by laser design parameters such as resonator length, repetition rate, and pumping intensity. This interdependence leads to trade-offs when optimizing the laser performance. These trade-offs can be somewhat mitigated by selecting a laser material with higher or lower emission cross-section. In this articles we compare and contrast the performance and design of a Nd:YAG laser optimized for long pulse output and a Nd:YVO4 laser optimized for short pulse output and high pulse repetition rates. This performance comparison is discussed in the context of specific applications for these lasers.

6100-74, Session 14

Diode pumped pulsed solid state MOPA-systems with high brilliance for remote sensing applications

M. Ostermeyer, Univ. Potsdam (Germany)

We are in the process of realizing a diode pumped solid state laser system emitting ns-pulses with duration between 10-100 ns delivering 400 W of average output power at 1 μm wavelength. Laser heads for side pumped and side cooled rods are used. As a first step on this path a Nd:YAG MOPA system delivering 100W with pulse energies of up to 0.5 J and an M2 < 2.1 was realized. This system was running single frequency and was frequency stabilized with a Pound-Drever-Hall related scheme with 2 MHz stability.

In the process of reaching our final specifications different options for the laser material are evaluated. Core doped Nd:YAG ceramic rods offer interesting options for side pumped lasers. Double pass MOPA arrangements utilizing these rods with and without phase conjugation have been realized and investigated.

Also we have been evaluating Yb:YAG as material for high power high energy ns-pulsed laser systems. The ramifications are discussed.

6100-77, Session 14

Saturable absorbed Er:YAG Q-switched laser with short pulse

V. Leyva, K. Spariosu, R. D. Stultz, Raytheon Co.

We demonstrate a passively Q switched Er:YAG laser with 5nsec pulse widths using Cr2+:ZnSe as a saturable absorber. Over 1 Watt of output power is achieved with multi kilohertz pulse repetition rates. The laser is resonantly pumped with a 1534nm fiber laser and uses a micro slab design which allows for efficient all solid state cooling and efficient laser operation of the 2% erbium doped YAG material.

6100-56, Poster Session

Modeling a diode pumped Nd: YAG rod laser

H. Shu, Y. Chen, M. A. Bass, College of Optics and Photonics/ Univ. of Central Florida; M. A. Acharekar, Sensors World, Inc.

We calculated the performance potential of a diode pumped Nd: YAG rod laser, including the absorbed pump distribution, optical distortions in the rod such as the pump induced thermal lensing, gain medium surface distortion and birefringence, the laser beam propagation in the optically distorted Nd: YAG rod and the free space part of the cavity, and eventually the output laser beam. The absorbed pump distribution was calculated using ASAP, the pump induced thermal lensing and change of dielectric tensor were calculated using FEMLAB, the laser beam propagation was calculated with a computational scheme we developed which employs the beam propagation method combined with sparse matrix technology. We propose a special cavity design, which can select the spatial eigen mode shape of a laser cavity and simultaneously compensate the pump induced thermal lensing, gain medium surface distortion and birefringence. We applied this special cavity design to the considered Nd: YAG rod laser, and the converged solutions calculated with our computational model give both high extraction efficiency and good beam quality for the output. We also analyzed the sensitivity of the output beam to mirror tilt, thermal induced mirror distortion, and some errors in the cavity length or the optical distortions in the rod. : The computational model was developed with sponsorship from DARPA Contract No. HR 00110410002 and AFOSR Contract No. FA9550051005.

6100-59, Poster Session

Cryogenic Faraday isolator for high average power lasers

D. S. Zheleznov, I. B. Mukhin, O. V. Palashov, A. V. Voitovich, E. A. Khazanov, Institute of Applied Physics (Russia)

Reducing of thermal effects in magneto-optical elements of the Faraday isolators is an actual problem nowadays. These effects caused by the beam absorption are depolarization and wavefront distortions (thermal lens). In this paper we discuss the possibility to decrease such perversion by cooling the Faraday isolator to nitric temperature. It is known that Verde constant and the magnetic field of permanent magnets rise with the cooling. This effect permits to shorten the magneto-optical medium, with the value of Faraday angle conservation, so that geometrically the element will be a thin disk, which offers a number of advantages over a cylinder. Moreover, we have shown that thermo-optical property of Terbium Gallium Garnet (TGG) crystal and magneto-optical glasses are much better at cryogenic temperatures.

Experimental dependences of depolarization, thermal lens, Verde constant and magnetic field on temperature were measured. Depolarization ratio decreased by a factor of 8, thermal lens optical power - 2.7, Verde constant and the magnetic field rised correspondingly by a factor of 3.5 and 1.14. Changing geometry of the magneto-active element to the thin disk, when disk-thickness-to-beam-radius ratio is 0.3, with cooling through the ends by sapphire window gives 6-fold depolarization lessening. Thus, experimental results obtained at 91 K allow to rise the laser power by a factor of 28 with the same isolation ratio. It is expected, that at 77 K temperature the laser power will increase by a factor of 47 providing an effective isolation at average powers of tens of kilowatts. A design of the cryogenic Faraday isolator prototype is discussed.

6100-60, Poster Session

Diode-end-pumped actively and passively Q-switched Nd:GdVO4 lasers at 1.34 mm

C. Du, S. Ruan, Y. Yu, Shenzhen Univ. (China)

High-power diode-pumped solid-state lasers (DPSSL) operating in the 1.3-mm spectral region have wide applications in the fields of medical treatment, optical fiber communication, and efficient production of red radiation by frequency doubling. Recently, we report a 13.3-W laser-diode-array end-pumped 0.3 at.% Nd:GdVO4 continuous-wave laser operating at 1.34 mm.

Short-pulse lasers at 1.3 mm have many important applications such as fiber sensing, efficient generation of red laser, and intracavity Raman conversion to the 1.5-mm eye-safe spectral region. So in this paper, we report short-pulse generation at 1.34 mm with diode-end-pumped actively and passively Q-switched Nd:GdVO4 lasers.

For acousto-optical Q-switched operation in a plano-concave resonator, when the transmission of output coupler was 17.1%, the maximum average output power, the highest pulse energy, the shortest pulse width and the highest peak power were obtained to be 4.54 W, 223 mJ, 19 ns and 11.75 kW, respectively.

For passively Q-switched operation with an uncoated 0.5at.% Co:LaMgAl11O19 crystal as the saturable absorber in a three-mirror-folded resonator, the maximum average output power, the highest pulse energy, the shortest pulse width and the highest peak power were obtained to be 500 mW, 25.5 mJ, 160 ns and 150 W, respectively. We believe that the pulsed laser performance can be improved significantly with the AR coated Co:LaMgAl11O19 crystal and optimum laser resonator in future experiments.

6100-61, Poster Session

Novel laser range finding algorithms

J. Chen, Chung-Hua Univ. (Taiwan)

Novel laser range finding algorithms of single modulation frequency, twofold modulation frequencies, multiple modulation frequencies as well as arbitrary modulation frequencies have been developed. The laser range finders are capable of measure up to hundred meters in distance, with accuracy of 1 mm.

We have developed series of laser range finding algorithms that are single modulation frequency, twofold modulation frequencies, multiple modulation frequencies as well as arbitrary modulation frequencies.

In the single modulation frequency ranging, the dynamic range is limited by the phase resolution, and it is difficult to increase to the high value practically. A fixed twofold modulation frequencies ranging can use the low frequency to generate longer ranging distance while simultaneously use high frequency to obtain high resolution. Yet, the variable multiple modulation frequencies can enhance us to meet better ranging distance and most suitable resolution. Moreover, the arbitrary modulation frequencies ranging can give us much better design flexibility and cheaper hardware cost.

We will present the theories, analysis, and the verifications of all the above algorithms.

6100-62, Poster Session

Improvement of output power dynamic range of unsymmetric Nd:YAG laser with unstable laser mirror configuration

H. S. Kim III, Chosun Univ. (South Korea)

We numerically investigate the characteristic of single Nd:YAG rod laser for the various resonator parameters in order to get the best condition for the wide output power dynamic range with a good beam quality and a high power. The beam quality is analyzed with ABCD matrixes including the thermal characteristic of Nd:YAG rod. The analysis is focused on stability, M^2, beam waist and mode-volume of laser beam inside resonator. We find that the best conditions are obtained when the resonator mirrors are configured to the unstable resonator type such as convex-plan resonator. For the convex-plan resonator, the optimum configuration is obtained when a laser rod is set at near the curved laser mirror. And the results show that the dynamic range can be shifted toward the high output power region without any reduction of the range width by varying the laser mirror curvature of the convex-plan resonator

6100-63, Poster Session

Investigation of the characteristic of InGaAs single quantum well semiconductor saturable absorber mirror for passive mode-locking for Yb:YAG laser

H. S. Kim, J. Kim, J. Park, Chosun Univ. (South Korea)

We numerically investigate InGaAs single quantum well semiconductor saturable absorber mirror (SESAM) for a passive mode-locking for Yb:YAG laser. Investigated SESAM has the structure consisting of single quantum well and Bragg layers and protection layers against optical damage. To determine the design parameters, we calculate the field distribution inside SESAM and As-ion implantation energy for the various conditions. We choose In_(x)Ga_(1-x)As as a material of SQW of which band gap energy can be near lasing wavelength of Yb:YAG laser. And to determine the In-fraction of In_(x)Ga_(1-x)As, we do the simple estimation. The results show that In-fraction of the fabricated SQW is approximately 0.24 ~0.28. SESAM grown by MOCVD should be implanted by As ion to have short recovery times. Hence we calculate As-ion implantation energy with which the ion concentration can maximize at the position of SQW. With the help of the numerical results, we design and fabricate InGaAs single quantum well semiconductor saturable absorber mirror (SESAM) for Yb:YAG laser.

6100-64, Poster Session

Side-pumped Neodymium slab lasers Q-switched by V:YAG on 1.3 μm

J. K. Jabczyński, W. Zendzian, J. Kwiatkowski, Wojskowa Akademia Techniczna (Poland); J. Sulc, M. Nemec, H. Jelínkov, Czech Technical Univ. in Prague (Czech Republic)

Nd:YAG and Nd:YAP crystals in form of triangle which makes possible to realize a slab side-pumped configuration with one total internal reflection were tested as an active medium for diode-pumped laser. The resonator arrangements for Q-switched regime were prepared for the emission corresponding to Nd^{3+} ion transition $^4F_{3/2} \rightarrow {}^4I_{13/2}$ referring to each crystal (λ = 1318 nm Nd:YAG and λ = 1342 nm Nd:YAP). Optical pumping was accomplished by a fast axis collimated quasi-cw diode DILAS E7Y1-808.3-600Q-H175V with peak power 600 W. Pumping radiation was focused by two plan-convex lenses into an active medium. The parameters of the pumping radiation were: wavelength 808 nm, maximum pumping energy was 150 mJ, pulse length 250 μs, repetition rate up to 14 Hz. In free running regime the maximum reached energy was 24 mJ and 27.5 mJ for Nd:YAG and Nd:YAP, respectively. The corresponding obtained slope efficiency was 19.9 % and 23.7 % for Nd:YAG and Nd:YAP laser oscillator, respectively. Proper Q-switching for 1.3 μm was realized with saturable absorber V:YAG which initial transmission was optimized for shortest possible pulse length. For that obtained pulses were 6 ns with the energies 740 μJ and 432 μJ for Nd:YAG and Nd:YAP, respectively. This results correspond to peak power reached 125 kW (Nd:YAG), and 77 kW (Nd:YAP) in fundamental TEM_{00} mode which allows this laser to be used as an efficient source for further nonlinear conversion or other applications.

6100-65, Poster Session

Lasing properties of new Nd^{3+}-doped tungstate, molybdate, and fluoride materials under selective optical pumping

J. Šulc, H. Jelínkov, Czech Technical Univ. in Prague (Czech Republic); T. T. Basiev, M. E. Doroschenko, L. I. Ivleva, V. V. Osiko, P. G. Zverev, General Physics Institute (Russia)

The purpose of this work was to determine the relative efficiencies of new Nd^{3+} -doped laser active/Raman - tungstate, molybdate, and fluoride - materials ($SrWO_4$, $PbWO_4$, $BaWO_4$, $SrMoO_4$, $PbMoO_4$, SrF_2, and LaF_3) under selective longitudinal optical pumping by the alexandrite (~ 750 nm), or diode (~ 800 nm) laser.

Crystals with various length, orientations and active ions concentrations were tested. To optimize the output of the tested lasers a set of input dichroic and output dielectric mirrors with different reflectivities were used. For realized lasers operating at pulsed free-running regime, threshold energy, slope efficiency, emission wavelength, and radiation polarization were determined. For each crystal, fluorescence lifetime and absorption coefficient under given pumping were established. The slope efficiency in case of Nd^{3+}:$PbMoO_4$ laser at wavelength 1054 nm was measured to be 54.3% with total efficiency of 46% which is the best result obtained for all new tested crystals. For Nd^{3+} doped $SrWO_4$, $PbWO_4$, and $BaWO_4$ crystals simultaneous laser and self-Raman emission were demonstrated in Q-switched regime. Thus newly proposed laser Raman crystals demonstrate high efficiency for Nd^{3+} laser oscillations comparable with well known and widely used KGW:Nd^{3+} crystal. Further improvement in the quality of tungstate and molybdate type crystals should result in further increase in lasing efficiency at 1.06 μm wavelength. Self Raman frequency conversion of Nd^{3+} laser oscillations in these crystals should result in high efficient pulse shortening, high peak power and new wavelengths in 1.2-1.5 μm wavelength region.

6100-66, Poster Session

Experimental method research on kHz, ns pulsed Nd:YAG laser with diode-end-pumped, acousto-optic and Cr:YAG passive Q-switched

H. Zhao, The North China Research Institute of Electro-Optics (China)

We describe experimental research on Kilohertz, ns pulsed Nd:YAG laser with diode-end-pumped, acousto-optic Q-switched and Cr:YAG passive Q-switched. Under the condition of 3W diode 2.5kHz pulsed pumped, 7.5ns, 80μJ laser output with A-O Q-switched and 4.6ns, 30μJ with Cr:YAG Q-switched are obtained. Taking into account various parameter such as distribution of pump power, intracavity photon density, cavity length, turn-off time of A-O Q-switch, and absorption cross section of Cr:YAG passive Q-switch, we set up a power-scaling model to optimize and design a kHz repetition rate, ns pulse width Nd:YAG laser. In experiment, we also found that the laser beam quality under the condition of Cr:YAG Q-switched is batter than that of A-O Q-switched, the reason are discussed.

6100-67, Poster Session

Enhancement of blue thulium emission on Nd:Yb:Tm doped YLF crystals

L. C. Courrol, Faculdade de Tecnologia de São Paulo (Brazil); I. M. Ranieri, L. Gomes, S. L. Baldochi, N. D. Vieira, Jr., Instituto de Pesquisas Energéticas e Nucleares (Brazil)

Nowadays laser research is widely focused in the development of visible compact sources. Particularly, blue laser are important in the compact disc industry, optical storage systems, color displays and in new medical and dermatological applications (such as tattoo and permanent hair re-

moval) and in atmospheric and physics research. Solid state lasers are attractive for most applications because they are rugged, relatively simple and easy to use. Thulium-doped materials generate blue laser radiation through the nonlinear conversion of radiation from the infrared into visible range. The dynamics of up-conversion is explained by taking into account various cross-relaxation (CR) and excited state absorption (ESA and ETU) processes. The emissions at 480nm and 450nm can be observed after pumping thulium ions with two or three red or infrared photons. YLiF4 (YLF) crystals doped with thulium and also co-doped with ytterbium are well-known as active media that generate stimulated radiation on a number of lines over a wide spectral range from 450nm to 2350nm, upon selective laser and flash lamp pumping. In this work we studied the optical properties of YLF:Nd:Yb:Tm crystals. YLF crystals were grown by Czochralski technique and three samples of diferent portions of crystals were orientated, cut and polished with 2mm thickness. The absorption spectra at room temperature of the samples in the range 200nm-1200nm were measured. The emission spectra were obtained by exciting the samples, with laser diode at 797nm and were analyzed with a 0.5 m monochromator and a photomultiplier tube. The signal was amplifed with a lock-in and processed by a computer. A time resolved luminescence spectroscopy technique was employed to measure the luminescence decays induced by ultrashort laser excitation to determine the mechanism involved in the energy transfer processes. The results are shown and importance of the presence of neodymium ions for enhencement of blue emission in the samples is described.

6100-68, Poster Session

Acousto-optically Q-switched and mode locked diode pumped Nd:YVO4 laser

J. K. Jabczynski, W. Zendzian, J. Kwiatkowski, Wojskowa Akademia Techniczna (Poland)

Compact picosecond, high power lasers are needed in several areas such as micromachining, ophthalmology, metrology etc. A promising method enabling generation of picosecond pulses trains with energies of a few microJoules each in a simple resonator involves simultaneous Q-Switching and Mode Locking (QML). We have demonstrated efficient operation in the QML regime using an acousto-optic modulator applied in double role as both an active Q-switch and a mode locker. The pumping beam, emitted by 20-W laser diode bar equipped with a beam shaper forms the caustics of 0.8-mm width inside a 0.3-at.% Nd3+ doped 10-mm-long YVO4 crystal located in close vicinity to the rear flat mirror of the first arm of a Z-type resonator. The acousto-optic Q-switch with 40.7 MHz radiofrequency was located near a flat output coupler. The two folding mirrors were mounted on the translation stages to enable matching the resonance frequency of the cavity to the modulation frequency of acousto-optic cell. Due to weak prelasing at 40.7 MHz frequency, the Q-switched pulse train starts to build up from ordered mode locked radiation. The QML pulses with envelope durations of 100-150 ns and with near 100% modulation depth were observed for wide range of pump powers and repetition rates. Above 3 W of output average power, 0.130 mJ of the envelope energy were achieved, having approximately 5-8 mode locked pulses. The maximum energy of a single mode locked pulse was about 0.03 mJ with pulse durations well below 1 ns.

6100-69, Poster Session

Mode locked Nd:YVO4 laser with intracavity synchronously pumped optical parametric oscillator

A. Zavadilova, V. Kubecek, M. Cech, P. Hirsl, H. Jelinkova, Czech Technical Univ. in Prague (Czech Republic); J. M. Diels, The Univ. of New Mexico

The motivation of this work is the development of laser sensor and gyroscope based on short pulse solid state ring laser. In comparison with regular ring laser containing the gain medium and saturable absorber where counterpropagating pulses overlap, a ring synchronously pumped optical parametric oscillator in which the pulse crossing point is controlled externally by the time of arrival of the pump pulses is the ideal source for short pulse laser sensor. The optimum configuration is a parametric oscillator synchronously pumped inside the optical resonator of the diode pumped mode-locked solid state laser.

We are developing a such system and as a first step we have demonstrated operation of a diode pumped Nd:YVO4 laser passively mode-locked using semiconductor saturable absorber with synchronously pumped intracavity optical parametric oscillator in linear configuration. The repetition rate of the pump laser was 133 MHz and pulse duration of 15 ps. Parametric oscillator was based on 20 mm long Brewster cut single grating (with poling periode of 30.3 um) periodically poled magnesium doped lithium niobate (MgO:PPLN) crystal. The temperature tuning of parametric luminescence from the crystal with peak wavelength at 1537 nm - 1550 nm for temperature variation from 30 C to 57 C was observed. The detailed parameters of the parametric generator will be presented.

6100-75, Poster Session

Optimization of a femtosecond Ti:Sapphire amplifier using an acousto-optic programmable dispersive filter, SPIDER and a genetic algorithm

O. Korovyanko, R. Rey-de-Castro, C. Elles, Y. Li, R. A. Crowell, Argonne National Lab.

An acousto-optic programmable dispersive filter has been used in combination with a genetic algorithm to optimize the output of a Ti:Sapphire CPA laser. We applied genetic algorithm for second harmonic optimization and recorded the evolution of spectral phase, amplitude and temporal pulse profile is at each step of our algorithm. The prospect of adaptive control of terawatt laser pulses for ultrafast laser-plasma electron accelerator is discussed.

6100-76, Poster Session

Power scaling 1617-nm Er:YAG operation using narrow bandwidth output coupler

V. Leyva, K. Spariosu, Raytheon Co.

We demonstrate low quantum defect operation with over 6W output power in an Er:YAG laser operating at 1617nm while pumped with a 1534nm fiber laser. A narrow bandwidth Volume Bragg Grating (VBG) centered at 1617nm is used as an output coupler. The use of a VBG output coupler resulted in improved mode spectra and beam quality as compared to operation at 1645nm without wavelength stabilization. The efficiency and thermal load of the 1617nm operation is investigated.

Conference 6101A: Laser Resonators and Beam Control IX

Wednesday-Thursday 25-26 January 2006

Proceedings of SPIE Vol. 6101A

6101A-01, Session 1

Study of dark line resonances with mode-locked lasers and its applications

L. Arissian, J. M. Diels, The Univ. of New Mexico

Abstract not available.

6101A-04, Session 1

About some new possibilities of increasing the intrinsic output power of the photon beam: for definite laser active media

C. I. Isarie, I. V. Isarie, State Univ. of Sibiu (Romania); A. M. Voineag, Inspectoratul de Invatamant (Romania); D. V. Muntean, SC. Satroagro SRL Bucuresti (Romania)

Producers and users of laser beam equipment have some wishes as: to have economic machines, the machines must be as small and light as possible, the power supply must be also very light and small.

All mentioned desires - and other related with them - may be accomplished by an adequate efficiency of laser beam process.

As we know, the first laser began with 2% efficiency. In the process of time, the efficiency increased progressive, and in this way was possible after the year 2000 to have laser weapons mounted on jet planes, including the power supply.

In a laser system, there are many points where photons are lost. To reduce this losses, we must treat with the utmost care all points of the "chain" where photons could be lost. We mention: the resonance cavity - inside -, the exit from the resonance cavity, the mirrors and lenses and also other related factors. Each improvement in one of the mentioned points could contribute to the general raising of the laser machine efficiency.

Authors were concerned first with some possibilities of increasing the intrinsic output of the photon beam, for definite laser active media, by applying some fields inside the resonance cavity. Such fields, characterized by nature, energy, frequency and other parameters could influence positive the efficiency of the photon beam emission.

6101A-10, Session 1

Spinning-disk lasers, computer simulation

A. H. Paxton, Air Force Research Lab.

Abstract not available.

6101A-14, Session 1

Three-mirror laser resonators: revisited

J. R. Leger, Z. Yang, Univ. of Minnesota

Abstract not available.

6101A-78, Session 1

Optical manipulation using extended light fields

P. Reece, V. G. Garcés-Chávez, M. P. MacDonald, K. Dholakia, Univ. of St. Andrews (United Kingdom)

The single-beam gradient-force optical trap, produced by focusing a laser to a diffraction-limited spot, has long been established as the quintessential tool for optical manipulation. From the atomic to the microscopic scale optical traps have been used extensively where precise, targeted and non-invasive control of mesoscopic objects is required. Extended area optical manipulation using patterned light fields, is an emerging field. It demonstrates the potential for expanding the applications of optical manipulation and creates an "optical potential energy landscape" in two and three dimensions. The ability to tailor such an optical landscape can be used to simultaneously manipulate multiple particles and study both the dynamics of particles in the optical potential as well as inter particle interactions. In the following presentation I will discuss some of our recent work on extended area optical manipulation for aggregating, trapping, ordering and sorting with micro-particles[1-4].

REFERENCES

1. MacDonald, M.P., G.C. Spalding, and K. Dholakia, Microfluidic sorting in an optical lattice. Nature, 2003. 426(6965): p. 421-424.

2. Paterson, L., et al., Light-induced cell separation in a tailored optical landscape. Applied Physics Letters, 2005. 87(12) 123901

3. Garces-Chavez, V., K. Dholakia, and G.C. Spalding, Extended-area optically induced organization of microparticies on a surface. Applied Physics Letters, 2005. 86(3) 031106

4. Cizmar, T., et al., Optical conveyor belt for delivery of submicron objects. Applied Physics Letters, 2005. 86(17) 174101

6101A-05, Session 2

Dispersion compensation in optical parametric chirped-pulse amplification systems

C. Wang, Y. Leng, X. Liang, B. Zhao, Z. Xu, Shanghai Institute of Optics and Fine Mechanics (China)

Optical Parametric Chirped-pulse Amplification (OPCPA) Systems are hybrid systems of optical parametric amplification (OPA) and chirped-pulse amplification (CPA), which is the dominant technic in ultrashort pulse amplification. An OPCPA system has a different mechanism from common CPA systems. It depends on the OPA process to get the pre-amplification and Ti:Sapphire laser amplification to get the following amplification. Therefore it has different inner dispersion from common CPA systems. The second- and third-order dispersion formula of OPA are presented to depict the physics picture and simplify analysis. OPCPA system needs a grating expander to stretch ultrashort pulses and a conjugated grating compressor to recompress the amplified pulses. The combine of grating expander and compressor also introduces phase dispersion to the system due to optical aberration. All these phase dispersion hinder our effort to recompress the amplified pulses to the shortest duration. The compensation of system dispersion depends on the design of the expander and the compressor. We design such a system to eliminate the dispersion up to 4th-order phase. This design is based on our practical OPCPA system and will give benefit to its optimization. It's the first time that the phase dispersion in OPCPA is discussed to our knowledge.

6101A-06, Session 2

Assigning error to an ISO 11146 M2 measurement

T. S. Ross, Air Force Research Lab.

The ISO 11146:1999 standard has been published for 6 years and set forth the proper way to measure the M2 parameter. In spite of the strong experimental guidance given by this standard and the many commercial devices based upon ISO 11146, it is still the custom to quote M2 mea-

surements without any reference to significant figures or error estimation. To the author's knowledge, no commercial M2 measurement device includes error estimation. There exists, perhaps, a false belief that M2 numbers are high precision and of insignificant error. This paradigm causes program managers and purchasers to over-specify a beam quality parameter and researchers not to question the accuracy and precision of their M2 measurements. This paper will examine the experimental sources of error in an M2 measurement including discretization error, CCD noise, discrete filter sets, noise equivalent aperture estimation, laser fluctuation and curve fitting error. These sources of error will be explained in their experimental context and convenient formula given to properly estimate error in a given M2 measurement. This work is the result of the author's inability to find error estimation and disclosure of methods in commercial beam quality measurement devices and building an ISO 11146 compliant computer automated M2 measurement device and the resulting lessons learned and concepts developed.

6101A-08, Session 2

Recent developments in real-time, intracavity, adaptive correction of a multi-kilowatt, solid-state, heat-capacity laser

K. N. LaFortune, R. L. Hurd, S. S. Olivier, J. M. Brase, R. M. Yamamoto, Lawrence Livermore National Lab.

The Solid-State, Heat-Capacity Laser (SSHCL) program at Lawrence Livermore National Laboratory is a multi-generation laser development effort scalable to the megawatt power levels. Current operating power levels are in the tens of kilowatts. A key feature of a heat-capacity laser is its ability to produce hundreds of kilojoules of energy in a short period and at a moments notice. As soon as the laser is turned on, it can deliver its peak performance. It does not need to "warm up" before it is fully operational. This is achieved by tracking the changes in the system that occur during the laser's operation. An intracavity adaptive optics system with over 100 degrees of freedom is used to track and correct for both the static and dynamic aberrations present within the oscillator. Despite the simplicity of the design, many challenges are encountered in the implementation of such a system. An overview of these and their resolution are discussed. The overall system design, measurement techniques and correction algorithms along with the most recent experimental results will be presented.

* Supported by U.S. Army Space and Missile Defense Command.

This work was performed under the auspices of the U.S. Department of Energy by University of California, Lawrence Livermore National Laboratory under Contract W-7405-Eng-48. UCRL-ABS-213485

6101A-79, Session 2

Progress on the national ignition facility

E. I. Moses, Lawrence Livermore National Lab.

Abstract not available.

6101A-80, Session 2

Adaptive systems for single pulse lasers

A. V. Kudryashov, Moscow State Open Univ. (Russia) and Adopt Ltd. (Russia); A. Alexandrov, V. V. Samarkin, Moscow State Open Univ. (Russia)

Abstract not available.

6101A-07, Session 3

Thermo-optically driven adaptive mirror

F. Reinert, W. A. Lüthy, Univ. Bern (Switzerland)

The ideal adaptive optical mirror combines large aperture with high spatial and temporal resolution and a phase shift of at least 2pi. Further, a simple low-cost solution is preferred. No adaptive system can fulfill all these requirements. We present a system that has the potential to reach this goal with the exception of high temporal resolution. But even with a moderate temporal resolution of one second such a system can find practical applications. For example as a laser resonator mirror that allows to modify the intensity distribution of the emission, or to correct slowly varying aberrations of optical systems. Our thermo-optically driven adaptive mirror is based on the thermal expansion of a thin layer of Sylgard with a gold coated front side. The surface modification is induced by selectively heating different areas of this Sylgard film. Heating is achieved by imaging a pattern onto the rear side of this thin film. We present a preparation method to produce thin films of Sylgard on sapphire. Sapphire is used as an efficient heat sink. The thermo-optically induced modifications of the surface are analyzed with an interferometer operated at 632nm. Without heating, the mirror surface of 24mm diameter has an optical quality of about a quarter wavelength. Upon heating, surface modulations of up to 350nm and slopes of 240nm/mm are measured. The irradiated intensity was only 370mW/cm2. Contrast of about 30% is reached with a resolution of 1.6 line-pairs per millimeter. The temporal resolution is better than one second.

6101A-11, Session 3

Intracavity self-frequency conversion in periodically poled active nonlinear Nd:Mg:LiNbO3 crystal

A. A. Novikov, G. D. Laptev, I. V. Shutov, M.V. Lomonosov Moscow State Univ. (Russia)

The combination of laser oscillation of active ions with nonlinear optical properties of the host material offers an opportunity for production lasers with self-frequency conversion. The crystals with self-frequency conversion properties act like laser in which the active medium serves itself and furthermore as a nonlinear medium. The up-to-date progress in this field associated with using periodically poled active nonlinear crystals, which essentially expand the number of realizing nonlinear processes. Recently the processes of self-frequency doubling, self-frequency summing and self-optical parametric oscillation have been realized in periodically poled active nonlinear crystals in cw and Q-switched regimes.

In this paper the processes of Q-switched self-frequency conversion have been investigated experimentally and theoretically. We have experimentally studied energy and temporal characteristics of radiation in the Q-switched processes of self-frequency doubling and self-frequency summing in periodically poled Nd:Mg:LiNbO3 crystal which was located in hemispherical cavity and end-pumped by laser diode.

The study of such system is fulfilled by means of equations describing evolution of interacting waves and inverse population in active nonlinear crystal. The dynamics of intensity of radiations and its pulse characteristics have been investigated by numerical method. The influence of parameters of Q-switching, cavity, crystal and pump on laser dynamics and generation characteristics are analyzed. It has been established that there exist optimal parameters of analyzed system, which correspond the maximum efficiency of processes of self-frequency conversion. It has been shown that the average power of radiation in Q-switched regime of self-frequency conversion may be higher that in the cw one. The theoretical results are in a good accordance with obtained experimental data.

6101A-13, Session 3

Adaptive wavelets applied to distortion correction in laser diode arrays

K. J. Jones, Rice Univ.

Laser diode arrays can produce great amounts of optical power. Unfortunately, these lasers tend to oscillate in multiple spatial and longitudinal modes. The spatial modes were investigated by the author (1999, 2000) in the first use of wavelet analysis on the perpendicular profiles of laser diode arrays. The first efforts to study phase distortion on laser diode arrays using wavelets was carried out by the author in 2004. Adaptive optics is the field dedicated to automatic compensation for wavefront distortion. A number of approaches are available to achieve spatial spectral control of high power diode laers using phase conjugate mirrors: high-finesse etalon in external cavity or a grating inserted in a phase conjugate cavity. The method being developed here is to determine phase (and hence phase distortion) using wavelet ridge extraction. An adaptive wavelet system will be developed to cancel distortion. Adaptive systems are important when the signals are changing with time. For phase distortion, an adaptive system similar to echo cancelation is proposed.

In a previous paper (2004), the 1-D perpendicular profiles of a diode array were plotted. The 10 stripe phase coupled array of the perpendicular profile displays spatial instabilities between the stripes (spatial-temporal pulsations in the index/gain-guided laser arrays). The Morlet wavelet transform of the 1-D profile is made and plotted as a spectrogram. The local maxima is also plotted. The ridge of the wavelet transfrom is the point where the frequency of the signal is equal to the frequency of the analyzing signal. It is possible to recover phase and hence distortion in the perpendicular profiles.

In a previous paper (2004), wavelet-based phase extraction was applied to laser diode arrays to correct distortion in spatial modes. In this paper, an adaptive wavelet system will be developed to actively correct phase distortion in spatial modes of laser diode arrays.

6101A-81, Session 3

Correction of the radiation of 1 kW CW diode pumped glass laser

J. V. Sheldakova, V. V. Samarkin, Moscow State Open Univ. (Russia)

Abstract not available.

6101A-86, Session 3

Aberration correction in a telescope with a membrane primary mirror

S. A. Dimakov, S.I. Vavilov State Optical Institute (Russia)

Abstract not available.

6101A-02, Session 4

One-color operation of the RF pulse excited slab-waveguide CO2 laser

E. F. Plinski, J. S. Witkowski, D. A. Wojaczek, Politechnika Wroclawska (Poland)

The paper gives an algorithm for elaboration of the RF excited slab-waveguide CO2 laser working on one chosen emission line in a pulse regime. The solution of the problem bases on an RF transversal excitation in a slab-waveguide laser structure and laser signature phenomenon. The structure gives a homogeneous distribution of the excited laser plasma along the electrodes. The plasma in the structure is stable and reproducible from the pulse to pulse comparing to conventional tube lasers, and particularly, to flow dynamic lasers. On the other hand, the applied unstable kind optical resonator produces a single-mode operation by definition. It suppresses higher modes in the laser cavity. The only problem are parasitic “hooting modes” created along the waveguide direction - between electrodes. But usually they do not bring too much perturbations to a spectral contents of the laser output radiation. The problem of the one-color operation of the laser can be solved by careful selection of the laser signature. The paper shows the results of the experiments, and gives the methodology to design the CO2 laser in a pulse regime operating on one chosen emission line. Controlled two-color and multi-color pulsed operations are also considered. The results can be applied to design lasers for the trace gas analysis around of 10 or 9 μm or other spectral devices. It can be also applied for material processing of the media sensitive for the wavelength.

6101A-09, Session 4

Laser Doppler velocimetry using photacoustic effect of RF-excited CO2 laser

J. Choi, Honam Univ. (South Korea)

A laser Doppler velocimeter employing a CO2 laser has been developed by using its photoacoustic effect. A change in the pressure of a discharge, induced by mixing of a returned wave with an originally existing wave inside the cavity, is employed to detect the Doppler frequency shift. We found that a Doppler frequency shift as small as 50kHz was detected, and also a good linear relationship between the velocity and the Doppler frequency shift was obtained.

6101A-03, Session 5

Hybrid ECL/DBR wavelength and spectrum stabilized lasers demonstrate high power and narrow spectral linewidth

S. Rudder, Innovative Photonic Solutions; G. J. Steckman, Ondax, Inc.

The use of LiNbO3 based Volume Holographic Gratings (VHGs) to provide spectrally filtered feedback to a semiconductor laser diode was demonstrated in the mid 1980s, however issues with long term stability had left this technology on the sidelines. Photo-sensitive glass based VHGs do not exhibit long term aging or thermal/photo bleaching effects, and therefore have enabled a new type of External Cavity Laser (ECL). This highly manufacturable “hybrid ECL/DBR” (HED) laser utilizes precision VHGs and has been used to create high performance lasers with spectrally tailored output. Lasers with fiber coupled output powers in excess of 1.2 W and spectral line widths of less than 0.15 nm have been demonstrated. Additionally, multi-mode lasers have been developed for High Resolution Raman Spectroscopy that exhibit spectral line widths below 0.06 nm (i.e. < 1 wavenumber) with fiber coupled output power in excess of 350 mW. The use of glass based VHGs provides HED laser wavelength stabilization of better than 0.01 nm/oC, and allows the production of lasers at virtually any wavelength between 650 nm - 2400 nm.

6101A-82, Session 5

Bending insensitive, highly Yb-Doped LMA triple-clad fiber for nearly diffraction-limited laser output

A. Croteau, C. Paré, H. Zheng, P. Laperle, Y. Taillon, Institut National d’Optique (Canada)

Abstract not available.

6101A-83, Session 5

Generation mechansims of white light laser radiation in tapered fibers

R. Zhang, J. Teipel, D. Tuerke, H. W. Giessen, Univ. Bonn (Germany)

Abstract not available.

6101A-84, Session 5

Method of fabrication of 1D and 2D gratings

D. Stepanov, S. Surve, Bandwidth Foundry Pty Ltd. (Australia)

Abstract not available.

6101A-12, Session 6

Laser resonators formed by two nanoparticles

X. Wu, W. Fang, A. Yamilov, A. A. Chabanov, H. Cao, Northwestern Univ.

We realized laser action in an unstable resonator formed by two nanopartilcles in a dye solution. The subwavelength particles act as Mie scatterers and provide coherent feedback. Although the cavity formed by two particles is very unstable and leaky, laser action was realized under intense optical pumping. The lasing modes were equally spaced in frequency, and laser output was directional. We experimented with several kinds of particles: titanium dioxide particles, zinc oxide particles, and silica nanospheres. A small amount of these particles are suspended in Rhodamine 640 solutions. The scattering mean free path is on the order of 1mm. The solution was pumped by a focused laser beam from a pulsed Nd:YAG laser (532nm, 20ps, 10Hz). At low particle density, the pumped volume is a cylindrical strip. Below the lasing threshold, the emission spectrum exhibited a broad spontaneous emission band peaked at 620nm with a shoulder at 660nm. Above the threshold, equally-spaced sharp peaks emerged between 605nm and 615nm. The width of individual peaks was less than 0.16nm. The laser output was parallel to the pump strip. Calculation shows the lasing peaks originate from the unstable resonators formed by two particles close to both ends of the pump strip. The large gain coefficient at intense pumping compensated the cavity loss, and lasing threshold was reached. With increasing particle concentration, thus decreasing the mean free path, lasing threshold is increased due to enhanced scattering loss caused by additional particles in between the two. Eventually, lasing action stops above certain particle density.

6101A-61, Session 6

Radiation-pressure-driven micro-mechanical oscillator

K. J. Vahala, California Institute of Technology

Radiation confined within a vessel will exert a pressure upon its walls. If the vessel is a high-Q micro-cavity, then a weak power level, coupled to the cavity, can build to a substantial circulating power and thereby exert a resonantly-enhanced pressure on the internal micro-cavity walls. If great enough, such a pressure will deform the cavity structure and change the resonant condition. Such a mechanism has been theoretically proposed by Braginsky to produce a parametric instability leading to mechanical oscillation of the microcavity structure. The mechanism has also been considered as a possible limitation in the next generation LIGO interferometer system. And yet, in a third area, it has been proposed that such a radiation pressure mechanism could provide a path to study the quantum entanglement of radiation with macroscopic motion. We have recently observed the radiation pressure driven parametric oscillation for the first time. In this paper, we describe the micro-cavity system used to generate mechanical oscillations at RF rates as well as the detailed measurements of threshold power, spectral linewidth variation, as well as both mechanical and optical Q dependences of important system parameters.

6101A-62, Session 6

Heavy photon states in photonic chains of resonantly coupled size-matched microsphres

M. Kuwata-Gonokami, The Univ. of Tokyo (Japan)

The manipulation of light at a micrometer length scale has recently attracted considerable attention both from the fundamental and the applications points of view. The micro-manipulation of light can be achieved by light confinement at a scale comparable to the wavelength. Light propagates through a system of such units due to the coupling between nearest neighbors. Such a tight binding photon approach to the micro-manipulation of light allows to guide light by connecting units, which can be referred to as photonic atoms, in arbitrarily shaped microstructures (photonic molecules). Using microspheres is the most natural choice to use as units of a tight binding photon device. It is well known that a dielectric sphere acts as an optical microcavity that has very long photon storage time within a small mode volume. In order to explore the feasibility of light micro-manipulation, one has to confirm the existence of coherent coupling between spheres of a size equivalent to few times the optical wavelength.

We propose and demonstrate a bottom upapproach to construct photonic structures for efficient control of speed of light. Super-mono-dispersive polymer micro spheres of 4 to 5 micron in diameter are used as building blocks and a size uniformity better than 0.05% could be obtained by sorting the spheres using spectroscopic methods. The spheres are positioned in a V-groove on a silicon substrate and from a photonic chain with resonant coupling of the optical whispering gallery modes. Photonic band modes are clearly observed in fluorescence and resonant scattering spectra, and an excellent agreement with a tight binding model calculation is found. Group index as high as 40 is obtained. Based on these result, we will discuss prospects for the further reduction of the group velocity and control of group velocity dispersion with such structures.

REFERENCES

1. T. Mukaiyama et al. Phys. Rev. Lett. 82, 4623 (1999).
2. M. Kuwata-Gonokami, Proc. SPIE 3930, 175 (2000).
3. Y. Hara et al. Optics Letters, 28, 2473 (2003).
4. Y. Hara et al. Phys. Rev. Lett. 94, 203905 (2005).

6101A-64, Session 6

Whispering gallery modes excitation in borosilicate glass microspheres by K+ ion-exchanged channel waveguide coupler

K. Grujic, Univ. of Tromso (Norway); J. P. Hole, Univ. of Southampton (United Kingdom); O. G. Helleso, Univ. of Tromso (Norway); J. S. Wilkinson, Univ. of Southampton (United Kingdom)

Optical microsphere resonators, with their exceptionally low optical losses and high Q-factors, are attracting a lot of interest in integrated optics and related fields. Not being accessible by free-space beams, modes of a microsphere resonator require near-field coupler devices. Efficient evanescent coupling has been demonstrated previously by using fragile or large devices, impractical for integrated optics, such as thin tapered fibres, fibre half-block couplers, angle-polished fibres and bulk prisms. A straightforward extension would be the use of integrated optics waveguides. However, not many waveguide coupling schemes are currently present in the literature. In this work, we demonstrate whispering gallery modes (WGM) excitation in borosilicate glass microspheres. Light from a tunable Ti: sapphire laser was coupled into a single mode K+ ion-exchanged channel waveguide formed in BK7 glass substrate. The microspheres, 7.9μm ± 0.8μm in diameter, were dispersed on the sub-

strate surface. The particles sitting on the waveguide surface were observed through a microscope and the laser light scattered by the particles was recorded with a CCD camera. Successful WGM excitation was observed with Q-factors of about 400.

6101A-67, Session 6

Silicon microspheres

A. Serpengüzel, Koç Univ. (Turkey)

Silicon microspheres are superb optical resonators. We have characterizaed the elastic light scattering characteristics of these silicon spheres in the near-infrared communication wavelenght of 1300 nm. The excitation beam is coupled with the use of optical fiber. Optical channel dropping in the near-infrared communication wavelenghts of 1300 nm has also been performed. The observed morphology dependent resonances of the silicon spheres have quality factors of 100000. The measured quality factors are limited by the sensitivity of the experimental setup. These optical resonances provide the necessary narrow linewidths, that are needed for high resolution wavelenght division multiplexing applications. In addition to channel dropping, detection, and switching applications of this optoelectronic system is possible. The silicon microsphere shows promise as a building block for CMOS based silicon microphotonics.

6101A-70, Session 6

Crystalline micro-resonators: status and applications

I. S. Grudinin, California Institute of Technology

We report on the fabrication technique of ultra high Q optical crystalline whispering gallery mode microresonators and discuss their properties. The technique is suitable for the majority of available optical crystals and for production of the resonators with small size. To validate the method, we made CaF_2 resonators with Q factors exceeding 10^8 and diameter as small as 80 micron. Possible utilization of these new resonators in quantum optics is discussed.

6101A-63, Session 16

Ultra-low threshold quantum dot microdisk laser

Z. G. Xie, S. Goetzinger, Stanford Univ.; W. Fang, Northwestern Univ.; Y. Yamamoto, Stanford Univ.; H. Cao, Northwestern Univ.; G. S. Solomon, Stanford Univ.

Ultra-low threshold lasers have applications in low-power communications. These lasers are also of fundamental interest, where a full understanding of lasing based on a few discrete emitters is evolving. This is especially true in solid-state systems, for instance those with a quantum dot (QD) gain medium, where a typical spectrum of discrete emission lines observed at lower pump power is often highly modified under higher pump powers.

Here we discuss a microcavity laser containing a dilute QD gain medium that has an ultra low, sub-microwatt CW lasing threshold. The structure is based on a high-quality factor microdisk cavity of GaAs with a low density of InAs-based QDs embedded in the microdisk. We estimate 250 QDs in the 1.8 μm diameter microdisk under investigation. Of these QDs approximately 60 are spatially located within the modal region of the disk, which extends inwards approximately 250 nm from the disk edge. Only a small portion of these QDs couple to the narrow cavity modes, which have a free spectral range of 45 nm and an initial linewidth of 0.06-0.07 nm. Despite the small number of QDs it is unlikely from our estimates the system lases from a single QD state. Linewidth narrowing and lifetime reduction with increasing pump are both observed.

6101A-65, Session 16

Silica polygonal micropillar resonators: Fano lineshapes tuning by using a Mach-Zehnder interferometer

K. Y. Hon, A. W. Poon, The Hong Kong Univ. of Science and Technology (Hong Kong China)

We report our recent experimental demonstration of silica hexagonal and octagonal micropillar resonators using angle-resolved prism coupling. These micropillar resonators are large-sized (~125 mm ~175 mm) polygonal fused-silica fibers with rounded corners. The polygonal microresonators have the key merit of flat cavity sidewalls, enabling a relatively long lateral interaction length for the evanescent coupling to wavefront-matched N-bounce ray orbits. Our experimental setup reveals (i) singlemode resonances (Q ~ 1.5 x104) in hexagonal micropillar resonators that are selectively input and output coupled near 60o light ray angles (favor 6-bounce ray orbits), and (ii) singlemode resonances (Q ~ 1.2 x 104) in octagonal micropillar resonators that are selectively input and output coupled near 67 on light ray angles (favor 8-bounce ray orbits).

The sharp resonance lineshapes observed in the reflection field are characteristically asymmetric, known as Fano lineshapes. Our angle-resolved measurements show that the Fano lineshapes continuously evolve for exceeding 2p phase change (dip-to-peak-to-dip) within a sub-degree range of reflection angles. These Fano lineshapes are given by the interference between a Lorentzian resonance field and a coherent continuum field.

Guided by this interpretation, we are currently experimenting with resonance lineshapes tuning by means of a Mach-Zehnder interferometer. One of the interferometer arms is coupled to a fixed singlemode prism-coupled polygonal micropillar resonator, whereas the other is coupled to a tunable delay line with an amplitude control. Initial results suggest that the Fano resonance lineshapes can be tuned by using the interferometer setup, when the resonance field amplitude and the coherent background field amplitude are comparable. Potential applications of Fano lineshapes tuning in optical filters, switches, and sensing will be discussed.

6101A-66, Session 16

Edge roughness in microresonators: optimum design strategies

J. E. Heebner, E. Chang, J. S. Kallman, T. C. Bond, M. E. Lowry, Lawrence Livermore National Lab.

Using the volume current method, we present an analytic formulation that can be written in normalized fashion to organize the treatment of scattering losses due to edge roughness in microdisk and microring resonators.

Close agreement with literature studies is found.

The formulation is intended to be implemented as a tool for strategic microresonator design.

6101A-68, Session 16

Spontaneous emission lifetime modification using high quality factor oxide apertured micropillars

N. Stoltz, M. Rakher, S. Strauf, A. Badolato, Univ. of California/ Santa Barbara; D. D. Lofgreen, Raytheon Vision Systems; P. M. Petroff, L. A. Coldren, D. Bouwmeester, Univ. of California/ Santa Barbara

An oxide aperture is used to confine optical modes in a micropillar structure. This method overcomes the limitations due to sidewall scattering loss typical in semiconductor etched micropillars. High cavity quality factors (Q) up to 48 000 are determined by external Fabry-Perot cavity scanning measurements, a significantly higher value than prior work in III-V

etched micropillars. Measured Q values and estimated mode volumes correspond to a maximum Purcell factor figure of merit value of 72. Experimental time correlated photon counting measurements show resolution limited quantum dot lifetimes of less than 200 picoseconds.

6101A-69, Session 16

Calligraphic poling for WGM resonators

M. Mohageg, Jet Propulsion Lab.

We demonstrate a novel technique to form arbitrary-shaped domain patterns in lithium niobate, including circular and radial periodical structures suitable for modal quasi-phase-matching in nonlinear experiments with whispering-gallery modes. Fabrication of continuous domains as narrow as 2 μm across and hexagonal patterns of the same order accompanied by real time visualization of the poling process are presented.

6101A-71, Session 16

Geometric optics of whispering gallery modes

M. L. Gorodetsky, A. E. Fomin, M.V. Lomonosov Moscow State Univ. (Russia)

Quasiclassical approach allows to obtain rather precise analytical approximations for the eigenfrequencies and quality factors of whispering gallery modes in convex axisymmetric bodies. We obtain practical formulas for the calculation of eigenfrequencies in dielectrical spheroid and torus and compare them with the known solutions for the particular cases and with numerical calculations.

6101A-72, Session 16

Recent advances in organic electro-optic materials for ring micro-resonators and optical modulation

A. Akelaitis, L. R. Dalton, Univ. of Washington

Recently developed organic electro-optic materials have demonstrated large increases in activity creating a drive towards utilizing organics in ring micro-resonators and modulators. These materials allow for extremely low drive voltages and fundamental response times within the terahertz region. Present synthetic efforts have efficiently incorporated molecules with large first molecular hyperpolarizabilities, into macromolecular systems producing unprecedented electro-optic coefficients, r33. Previously, incorporation of these large molecules into macromolecular systems proved difficult due to phase separation or molecular aggregation within the processed films. Therefore, integration into workable devices was inconsistent and difficult. The new material systems however, have shown considerably enhanced film qualities, leading to improved device incorporation and fabrication. This talk will focus on current organic materials strategies and their incorporation into current ring micro-resonator devices and results.

6101A-76, Session 16

Influence of a controllable scatterer on the high-Q modes of a microsphere resonator

A. Mazzei, H. Krauter, L. de Souza Menezes, S. Götzinger, Humboldt-Univ. zu Berlin (Germany); V. Sandoghdar, ETH Zürich (Switzerland); O. Benson, Humboldt-Univ. zu Berlin (Germany)

The high-Q Whispering Gallery Modes (WGM) of a microsphere resonator represent an optimal environment to observe non-linear optical processes. Q-factors of the order of 10^8 combined with mode volumes of only few μm^3 guarantee extremely high circulating power in the cavity modes on one hand, and very high Purcell factors on the other hand. One of the dominating losses mechanism is given by Rayleigh scatterers in the modes. In this experiment the glass fiber tip of a Scanning near Field Optical Microscope is used as a controllable scatterer with two different scopes[1]. First we use the scatterer to influence the intramodal coupling between a clockwise and a counter-clockwise propagating WGM of a microsphere resonator, and to point out the role of the Purcell factor in this process. Second we investigate the role of the scattering mechanism in non-linear optical processes such as Stimulated Raman Scattering in a microcavity[2].

REFERENCES

[1] S. Gotzinger, O.Benson, V. Sandoghdar, Opt. Lett. 27, 80-82 (2002);

[2] S. M. Spillane, T. J. Kippenberg, K. J. Vahala, Nature 415, 621-623 (07 Feb 2002) Letters to Editor.

6101A-85, Session 16

Nonlinear optics in ray-chaotic resonators

E. E. Narimanov, J. Zubin, Princeton Univ.

Abstract not available.

6101A-15, Poster Session

Modern laser technologies used for cutting textile materials

C. I. Isarie, A. Dragan, State Univ. of Sibiu (Romania); L. G. Isarie, SC SibDress SA (Romania)

With modern laser technologies we can cut multiple layers at once, yielding high production levels and short setup times between cutting runs.

One example could be the operation of cutting the material named Nylon 66, used to manufacture automobile airbags. With laser, up to seven layers of Nylon 66 can be cut in one pass, that means high production rates on a single machine.

Airbags must be precisely crafted piece of critical safety equipment that is built to very high levels of precision in a mass production environment. Of course, synthetic material, used for airbags, can be cut also by a conventional fixed blade system, but for a high production rates and a long term low-maintenance, laser cutting is most suitable.

Most systems, are equipped with two material handling systems, which can cut on one half of he table while the finished product is being removed from the other half and the new stock material laid out.

The laser system is reliable and adaptable to any flatbed-cutting task. Computer controlled industrial cutting and plotting machines are the latest offerings from a well established and experienced industrial engineering company that is dedicated to reduce cutting costs and boosting productivity in today's competitive industrial machine tool market. In this way, just one machine can carry out a multitude of production tasks.

Authors have studied the cutting parameters for different textile materials, to reach the maximum output of the process.

6101A-16, Poster Session

Noise reduction of violet laser diodes by selection of feedback light polarization

H. Konishi, W. Sasaki, H. Yashiro, K. Takegami, Doshisha Univ. (Japan); A. Ikeda, Y. Kamioka, K. Nagashima, Funai Electric Co., Ltd. (Japan)

We have demonstrated an optical feedback noise reduction of 45mW type 408 nm GaN violet laser diodes by selecting the polarization of the feedback light in a typical optical disk pick-up system. The polarization of the feedback light is selected by means of rotatable quarter-wave plate. In this method, we have attained certain noise reduction without superposition of a high frequency component on driving current, which makes the pick-up system simple and inexpensive. As a result of our experiment, by adjusting the rotation angle of quarter-wave plate, we could

suppress the optical output fluctuations to less than 25% of peak-to-peak values in our violet laser diodes caused by the external cavity length variations. In addition, we also measured noise reduction effect by the method of high frequency superposition. As a consequence, our present method could be a new approach for practical and simplified industrial fabrications of inexpensive, substantially low noise optical disk pick-up systems for high power violet laser diodes.

6101A-18, Poster Session

Spatial structure of radiation at self-frequency conversion in active nonlinear crystals

A. A. Novikov, G. D. Laptev, A. S. Chirkin, M.V. Lomonosov Moscow State Univ. (Russia)

Active nonlinear crystals combine the properties of laser (active) and nonlinear media. Such combination opens wide possibilities for laser with self-frequency conversion, when the laser generation at fixed frequency and nonlinear frequency conversion takes simultaneously place in the same crystal.

In this paper the results of study of spatial characteristics of radiation in the processes of self-frequency doubling, self-frequency mixing and self-optical parametric oscillation are presented. The scheme under consideration is a periodically poled active nonlinear crystal located into the cavity, which is formed by two spherical mirrors with finite aperture. The crystal is end-pumped by CW laser radiation. Our theoretical approach takes into account many experimental features of self-frequency conversion processes, for instance diffraction due to finite aperture of mirrors and propagation of radiation between the mirrors. The numerical calculations are used for analysis. The influence of various parameters of system (pump power, pump focusing, cavity length, size, reflection and curvature of mirrors) on spatial structure of generated radiation has been analyzed. It has been shown that the nonlinear frequency conversion (due to quadratic nonlinear coefficient) has weak effect on spatial field structure of fundamental radiation. The dependences of energy characteristics of radiation at self-frequency conversion on various parameters of the scheme under consideration are also studied. It has been shown that there are optimal parameters for maximal frequency conversion efficiency. All calculations are carried out for periodically poled Nd:Mg:LiNbO3 active nonlinear crystal.

6101A-19, Poster Session

Modal analysis of 'non-Gaussian' Gaussian laser beams

T. S. Ross, Air Force Research Lab.

It is possible to construct summations of Laguerre-Gaussian modes which have the appearance of a zero order fundamental Gaussian but which, in fact, have no zero order content. These examples have circulated informally as a warning against trusting a single beam profile measurement as to the indication of the modal content of a given beam. These 'non-Gaussian' Gaussian beams also turn out to be extremely revealing of the fundamental assumptions upon which all modal decompositions and modal-based beam quality measures are based upon. Due to the contrived nature of these beams, they are also subject to some very subtle but important theoretical errors. This paper will rigorously examine a 'non-Gaussian', Gaussian beam in terms of its amplitude and phase characteristics, propagation behavior, M2 and what it reveals about modal decompositions and modal beam quality measures in general.

6101A-20, Poster Session

Development of a lamp-pumped Cr:LiSAF laser operating at 20Hz for a Terawatt CPA system

R. E. Samad, G. E. C. Nogueira, S. L. Baldochi, N. D. Vieira, Jr., Instituto de Pesquisas Energéticas e Nucleares (Brazil)

Cr:LiSAF is a laser crystal with three absorption bands in the visible range, and a wide emission band extending from 700nm to 1000nm, low nonlinear refractive index and a high saturation fluence that allows efficient energy storage, and a long lifetime of the upper laser transition level (67μs at room temperature) that makes this material suitable for flashlamp pumping. Terawatt CPA systems are traditionally assembled using Ti:Sapphire as both seeder and amplifying medium, though this requires costly high power doubled Neodymium lasers to pump the short lived (3μs) Ti:Sapphire upper laser level, that has a moderately low energy storage capacity. Alternatively, due to the emission overlap that Cr:LiSAF and Ti:Sapphire exhibit, many Terawatt hybrid CPA systems were developed based on Ti:Sapphire oscillators as seeder and flashlamp pumped Cr:LiSAF crystals as amplifying medium due to its comparatively low cost and good energy storage capacity. Flashlamp pumped Cr:LiSAF lasers and amplifiers have been limited to a few Hertz (1-10) repetition rates due to the host low thermal conductivity and steep dependence of the Chromium laser level lifetime with the temperature. At high repetition rates, this dependence can conduct the system to a catastrophic heat generation regime that decreases the laser efficiency, and can ultimately lead to the breaking of the laser medium.

We report here the development, construction and characterization of a flashlamp pumped Cr:LiSAF laser resonator emitting pulses around at 845nm, that can be operated at 20Hz under 100J of electrical pumping. The pumping cavity has two Xenon lamps, each one fed by its own power supply to a maximum energy of 50J per pulse. The power supplies can be operated from single pulse up to 20Hz. The pumping cavity is water cooled, has a ceramic reflector insert, and was developed to minimize the heat load on the Cr:LiSAF rod. A compact and stable (g1°g2=0.57) resonator was designed for lasers tests and gain medium characterization. When operating this resonator with a 10% transmission output coupler, pulses with 0.6J of energy and 60μs were obtained under 100J electrical pumping at 20Hz, resulting in 10kW peak power pulses with 12W of mean power. With this output coupler, under 100J pumping, the overall laser efficiency is 0.6%, and the slope efficiency is 0.8%. This pumping cavity will be part of a multipass amplifier in a hybrid Ti:Sapphire/Cr:LiSAF CPA system, aiming the extraction of ~1TW, 60fs pulses at a maximum repetition rate of 20Hz.

6101A-73, Poster Session

Fano resonance in transmission spectra of a tapered optical fiber coupled with a microsphere

H. Fujiwara, A. Chiba, J. Hotta, S. Takeuchi, K. Sasaki, Hokkaido Univ. (Japan)

Abstract not available.

6101A-74, Poster Session

Photorefractivity in WGM resonators

A. B. Matsko, Jet Propulsion Lab.

We report on the study of photorefractive properties of as-grown nominally pure lithium niobate and tantalate crystals using high-Q whispering gallery mode resonators. The photorefractive effect manifests itself as a peculiar dynamic modification of the spectrum of the resonator and is observed in near (780 nm) as well as in the far (1550 nm) infrared. Our experiments support the conclusion that the photorefractivity does not have a distinct red threshold. We show that the maximum saturated refractive index change in the infrared is of the same order of magnitude as in the visible light.

6101A-75, Poster Session

Axial systems of small contrast

A. A. Savchenkov, Jet Propulsion Lab.

The technological revolution brought about by silicon micro-circuits is in part fueled by the ability to engineer electronic density of states. This same capability has been the subject of pursuit by researchers that strive to develop photonic circuits that replace the electron with the photon.

Manipulation of photon density of states allows one to modify linear, nonlinear, and quantum properties of light-matter interactions. In this work we demonstrate tailoring the photon density of states in whispering gallery mode resonators to an extent that has not been previously achieved. Using a similarity between morphologies of an optical planar waveguide and a whispering gallery axial-symmetric solid state resonator, we theoretically propose and experimentally demonstrate a novel dimensional ring-like macroscopic optical circuit element. This circuit element is characterized by high finesse and small mode volume. This approach may result in novel photonic devices with unprecedented features.

Conference 6101B: 8th International Workshop on Laser Beam and Optics Characterization

Sunday 22 January 2006

Proceedings of SPIE Vol. 6101B

6101B-22, Session 8

Measuring the chirp of an ultrashort laser pulse at the noise floor

D. Bender, M. P. Hasselbeck, M. Sheik-Bahae, The Univ. of New Mexico

We extract the chirp of an ultrashort laser pulse accurately in real-time using a simple modified auto-interferometric correlation (MOSAIC) technique. Through the use of our newly developed time-domain algorithm, chirp information is accessible in low signal-to-noise conditions. We exhibit results revealing high sensitivity to chirp with signal-to-noise levels approaching unity. Corrective algorithms have been developed to accommodate signal distortions due to bandwidth limitations, autocorrelator misalignment, and non-quadratic detector response.

In our original implementation of MOSAIC published in 2002, traces were generated by spectrally filtering a second-order IAC waveform. This spectral filtering scheme yielded a fringe-resolved MOSAIC trace. We report a new implementation of MOSAIC that uses a combination of a homodyne technique and low pass filtering to acquire the fringe-free envelope of the MOSAIC trace. The smooth envelope can be averaged yielding temporal features sensitive to the order of chirp. This new technique allows for considerable enhancement of sensitivity and utility in the following ways: 1) accurate chirp measurement is possible with signals close to the noise level, 2) bandwidth-limited detection and non-quadratic response are automatically corrected, 3) the order of the chirp can be determined, and 4) algorithm efficiency is improved by more than a factor of two.

Time-domain MOSAIC is particularly useful for characterizing ultrashort pulses deep in the ultraviolet or far-infrared where second-order signals are often weak, distorted, and noisy. In-situ pulse monitoring is also possible because a relatively small amount of power needs to be diverted to the autocorrelator.

6101B-23, Session 8

Characterization of general astigmatic beams

A. Letsch, A. Giesen, Univ. Stuttgart (Germany)

The well tested and accepted ISO standard 11146 provides the measurement procedures to characterize the propagation properties of stigmatic and simple astigmatic laser beams which are intrinsically symmetric. The beam diameters are defined by the second order moments of the power density distribution which can be measured e.g. with a CCD-camera. In this standard the second order moments are used since the knowledge of these second order moments allows the calculation of the beam properties behind aberration-free optical systems with the well known ABCD-matrices. The new ISO/FDIS 11146-2 provides a new measurement procedure to characterize general astigmatic beams which are characterized by ten independent second order moments of their Wigner distribution. We present experimental results of the characterization of such a general astigmatic beam. In this experiment a well characterized simple astigmatic beam is propagated through a cylindrical lens which is tilted with respect to the symmetry axis of the beam so that the simple astigmatic beam is transformed into a general astigmatic beam. This general astigmatic beam is characterized according to the new ISO standard. According to ISO 11146 the twist parameter is measured by acquiring two power density distributions in the focal plane of a cylindrical lens which is orientated in horizontally and vertically focusing orientation. The twist parameter is given by the difference of the measured mixed spatial moment (xy) divided by the focal length. In general, the twist parameter is given by the difference of the mixed spatial second order moments multiplied by the focal length of the cylindrical lens and a parabolic dependency on the distance of the cylindrical lens. Therefore, the measurement of the twist parameter can be improved by measuring the mixed spatial second order moments in vertically and horizontally focusing direction and by fitting a parabola to the difference of these moments. The measured data and the derived beam properties are presented with a detailed error analysis of the data.

6101B-24, Session 8

Correlation between geometrical and intrinsic classification of general astigmatic laser beams

G. Nemes, ASTiGMAT

Geometrical and intrinsic classification of laser beams is based on the structure of the beam matrix (of second-order moments) and on the value of the two independent beam invariants, respectively. Recently the ISO 11146 Standard was expanded to include the characterization and measurement of the spatial properties of general astigmatic (GA) beams in addition to that of stigmatic (ST) and simple astigmatic (SA) beams. Any beam belongs to one of these three categories according to geometrical classification, and appropriate optics (of ABCD-type, made by lenses and free spaces) can transform, to some extent, one category of beams into another. The intrinsic classification helps to better assess the possibility of such transformations, by dividing all beams in two classes, intrinsic stigmatic (IS) and intrinsic astigmatic (IA), using the beam invariant named “intrinsic astigmatism parameter”, a. IS beams (a = 0) are intrinsically equivalent to (can be transformed into or are generated from) ST beams, that are the simplest beams within the geometrical classification. They have also rotational symmetry everywhere in free space. IA beams (a \> 0) cannot be transformed into ST beams by ABCD-optics. They can, however, be transformed at most into aligned SA beams, representing the next to simplest category of beams in geometrical classification. Aligned SA beams have orthogonal symmetry everywhere in free space and through aligned cylindrical optics.

This paper analyses the intrinsic properties of the SA and GA beams. For SA beams, in the aligned case, the calculation of the beam propagation ratio invariants Mx2 and My2 is straightforward, and the equality of inequality of these two numbers discriminates between the IS and the IA case, respectively. For the rotated SA case, the beam matrix should be first transformed by an appropriate rotation into an aligned SA matrix, and then the above simple calculation can be performed. The GA beam matrices pose the challenging problem: there are 10 apparently different matrix structures representing GA beams and determining by direct calculation the intrinsic astigmatism parameter for all of them is not straightforward. We solve all cases in three steps: First, we look at the “free-space equivalence” between the 10 different GA matrices and determine that only 8 of them are independent (two cases representing the same beam at different locations in free space). Second, we compute directly from the beam matrix the intrinsic astigmatism parameter and assess its value - this is possible in 6 out of the 8 cases. Third, for the remaining two cases we compute the intrinsic astigmatism parameter from the gaussian-Schell-model of the beam, that is formally equivalent to second-order moments model. As a result, it is possible now to determine the IS or IA character of a GA beam (or its intrinsic signature) just by looking at its matrix. The surprising result is that out of 8 independent and different beam matrices describing GA beams, the simplest 7 matrices are always IA, while the most complete one can be either IS or IA. The main application is the beam identification after measurement.

6101B-25, Session 8

Comparison of laser beams quality criteria

E. A. Khazanov, E. Perevezentsev, A. K. Poteomkin, Institute of Applied Physics (Russia)

Nowadays the power of lasers with diffraction beam quality is on significant rise. But it's not easy to archive ideal quality because of severe undesired distortion. Under different forms of distortion the beam shows different behavior. Under any form of distortion there is the need to qualitatively characterize the beam quality. Three various qualitative criteria are most commonly used for this purpose, each of them describing the beam with one ratio: overlapping integral, Strehl ratio, and M^2 parameter. All these criteria are well-known and frequently used in the literature, though the problem of their interrelation has never been discussed.

In this paper we have analyzed the above mentioned criteria and have researched of their interrelations in three most common types of beam quality degradation: thermal lens, electronic self-focusing, and spherical aberration. Thus, using various criteria it could become possible to compare different results. It is also analyzed if the criteria are flexible enough or interchangeable. Approximate analytical expressions for all three criteria and three types of beam distortion are derived for Gaussian and super-gaussian intensity shapes. The formulae we get correspond well with the numerical calculations. The efficiency of characterizing those beams by various criteria is discussed.

6101B-26, Session 8

Comparison of different beam diameter definitions to characterise thermal damage of the eye

K. Schulmeister, R. Gilber, F. Edthofer, B. Seiser, Austrian Research Ctrs. GmbH - Seibersdorf (Austria)

A computer model for the laser induced heating of an absorbing layer was used to calculate damage thresholds for the primate retina. Thresholds in terms of retinal radiant exposure per pulse were calculated for a range of laser pulse durations (from 1 μs to 1 s), laser spot sizes (from 30 μm to 3 mm) and beam profiles (e.g. top hat, Gaussian, near and far field of instable resonator, oblong).

For laser safety, where the exposure limit for the eye is stated as a function of what could be referred to as the 'thermal beam diameter', a diameter criterion is needed that yields, for an arbitrary size and shape of the beam profile at the retina, a correct value of the 'thermal beam diameter'. The analysis shows that 'traditional' beam diameter definitions including the second moment diameter in many cases yield incorrect results, especially for beams of instable resonators and multiple sources. A procedure is proposed that can be applied to determine a 'thermal damage parameter' for a given beam profile. It is also discussed that the power that passes through an aperture (such as the pupil of the eye) is not always correctly predicted for non-Gauflian beams, depending on the beam diameter definition.

6101B-27, Session 8

Characterization device for measuring beam parameter product and beam quality of collimated and uncollimated diode lasers

M. Roehner, C. Scholz, K. M. Boucke, R. Poprawe, Fraunhofer-Institut für Lasertechnik (Germany)

Diode laser systems have been established for material processing and pumping solid state lasers in the recent years, due to flexibility, efficiency and lifetime. In the meantime, diode laser bars with an output power of more than 120W are available, with an efficiency of above 50%. For material processing like hardening metal surfaces or welding thin blanks/plates the output power has to be increased, so that several diode laser bars are arranged vertically and/or horizontally. Depending on the application, e. g. pumping solid state lasers or fiber coupling, a special intensity profile of these diode laser systems is required. Therefore, the optical system has to be adapted. In order to design optical systems, beam characteristics (beam parameter product, intensity profile and wavelength) have to be well known. Due to low divergence angle and large rayleigh-length (about 0.5 m) of collimated diode lasers, beam parameter product is mostly measured by using a focusing lens. Depending on numerical aperture, the lens system increases aberations, which lead to a worser beam parameter product. Instead of using a lens in order to measure the beam parameter product, moving a slit or turning the diode laser around fast- and slow-axis is an alternative. By measuring the divergence angle in different positions along propagation axis (near- and farfield) the beam parameter product of collimated and uncollimated diode lasers can be calculated.

During the presentation, basic principles of measuring beam parameter product and beam quality of diode laser stacks are shown. Based on these principles different measuring methods are compared. Their advantages are discussed and measuring errors are estimated. Finally, a complete automated characterization device for measuring beam parameter product and beam quality of collimated and uncollimated diode lasers is presented.

6101B-28, Session 8

ETALONs for pure and composite transversal modes

M. R. Duparré, B. Luedge, Friedrich-Schiller-Univ. Jena (Germany); S. Schroeter, Institut für Physikalische Hochtechnologie e.V. (Germany)

This day and age in the laser community we find a couple of coexisting and simultaneously competing approaches for the characterization of spatial laser beam properties. Around the well-established Method of Second Order Moments, described in full detail in the ISO-Standard 11146/1-2-3, such methods are arranged like determination of Wigner Distribution Function, Hartmann-Shack wavefront sensor or decomposition of the beam into its transversal modal components. Each of mentioned methods has its own amenities, depending on specific demands and boundary conditions.

To compare these approaches with each other with very high accuracy, it would be extremely helpful to have access to a set of ETALONs for different pure or composite transversal modes.

Diffractive Optical Elements (DOEs) open a promising possibility to generate and to establish such ETALONs working later in different labs and under different conditions in a very reliable and reproducible manner.

We present first results of designing, manufacturing and testing ETALONs for pure and for composite Gauss-Hermite modes.

6101B-29, Session 9

Spot size dependence of LIDT in the ns regime

M. Jupé, L. S. Jensen, K. Starke, D. Ristau, Laser Zentrum Hannover e.V. (Germany); Y. Lien, D. Wernham, European Space Agency (Netherlands)

During the last decade, laser systems found their way into space born measurement techniques. Typical applications are the analysis of the atmosphere or the precise topographic suveying of the earth and other planets. In all these satellite based measurement devices, the lifetime of the laser and its optical opical systems is of crucial importance. Especially, systems based on lasers with high pulse energies have to be assured in respect to their power handling capability. Damage of a single component in the beamline or in the laser would jeopardize the success of the entire mission. Consequently, a very detailed characterization background is necessary for the preparation of space born measurement systems. In the framework of these considerations lifetime investigations concerning spotsize and pulse duration have to be performed. The present report summarises results of such measurements with different lasers at a wavelength of 1.064μm in a pulse duration range from 8 ns to 200 ns. The spot size was varied from a few microns up to some tenths of millimeters in order to investigate in the spot size dependence of the LIDT for different coated optics.

6101B-30, Session 9

Scattering analysis of optical components in the DUV

S. Schröder, Fraunhofer Institut für Angewandte Optik und Feinmechanik (Germany); S. Gliech, A. Duparré, Fraunhofer-Institut für Angewandte Optik und Feinmechanik (Germany)

The increasing demands on optical components especially for DUV lithography applications at the excimer laser wavelengths necessitate at-wavelength characterization tools. Losses resulting from light scattering play a critical role in this wavelength range. A system for the measurement of total and angle resolved scattering at 193 nm and 157 nm has been developed at the Fraunhofer Institute in Jena which allows total and angle resolved measurements at both wavelengths for backscattering as well as forward scattering. The main parts of the system were developed in the framework of the Eureka project EU-2359: Instruments and Standard Test Procedures for Laser Beam and Optics Characterization. The TS measurements follow the directions of the international standard ISO 13696, and for ARS measurements a new ISO standard is being developed. Extremely low background scattering levels of 10-6 for the TS measurements and more than 11 orders of magnitude dynamic range for ARS have been accomplished. Examples are presented for dielectric multilayer mirrors, which comprise scattering and reflectance measurements for different designs and coating materials.

6101B-33, Session 9

Two-dimensional optical thickness mapping technique based on nonlinear phase modulation of a focused laser beam

N. V. Tabiryan, S. R. Nersisyan, BEAM Engineering for Advanced Measurements Co.

We tested a new approach to measuring the optical depth and characterizing the quality of transparent optical materials such as glass. The technique is based on detecting the signal of laser beam intensity on the axis of the beam in the far field zone. The material being characterized is positioned in the focal region of the beam. The registered signal is then highly sensitive to the variations in nonlinear phase modulation. Scanning the substrate across the beam (x-scan) then results in variations of the self-phase modulation signal according to the optical thickness variations of the material. Thus, three-dimensional profiles of optical thickness of different substrates can be mapped. This process allows revealing defects and singularities on the substrates providing a measure of the optical quality of the substrate.

We will also report about using highly sensitive nonlinear optical technique for measuring absorption coefficients of highly transparent optical materials. Fundamentally, as low absorption coefficients as 10-5 cm-1 can be easily measured by scanning a substrate of a transparent optical material in the focal region of a lens along the propagation direction of the beam (z-scan).

The sensitivity of this technique proved to be large enough to reveal strong variation between the absorption coefficients of optical windows made of the same material BK7 by different manufaturers.

6101B-34, Session 9

Automated test station for laser-induced damage threshold measurements according ISO 11254-2 standard

A. Melninkaitis, D. Miksys, T. Balciunas, T. Rakickas, R. Grigonis, V. Sirutkaitis, Vilnius Univ. (Lithuania)

All laser components have some limit to the intensity of optical radiation, which they can withstand, and the measurement of laser-induced damage thresholds (LIDT) is required. In the case of repetitive pulses the LIDT measurements must be performed according ISO 11254-2 standard and this procedure requires the long time and large human resorces. In order to speed up the LIDT measurements with minimal human resources we developed the automated station for LIDT measurements according ISO-11254-2 standard. In this presentation we overwiev the main parts of this automated station and present the results of LIDT measurements with repetetive nanosecond and femtosecond pulses. In order to control the LIDT measurements the software based on the programming package LabView was created. The LIDT software controls the experimental sample positioning in X and Y directions, laser pulse energy attenuation, and shutter, as well as automates damage detection and performs statistical analysis. The program is able to recognize damage when it occurs by the change in scattered light. The input of the technical parameters of the sample and laser beam is required to start the measurements. The minimal distance between test sites on the sample surface is calculated automatically, and the surface area is divided in hexagonal matrix. The program also chooses the energy for each laser pulse train incident on the separate surface area sites. The program allows fast damage inspection by moving the sample under the Nomarski microscope. After completion of measurement and damage inspection, the program automatically generates the measurement report document.

6101B-35, Session 9

Absorptance and scattering losses measurements in IR range by high average power tunable radiation of optical parametric oscillator based on a periodically poled lithium niobate

O. Balachninaite, M. Maciulevicius, A. Melninkaitis, M. Sinkevicius, R. Grigonis, V. Sirutkaitis, Vilnius Univ. (Lithuania); R. Eckardt, Cleveland Crystals Inc.

Radiation of optical parametric oscillator (OPO) based on a periodically poled lithium niobate (PPLN) tunable in IR range was successfully used for reflection and transmission and scattering measurements in our previous experiments. However the available average power of this laser system was in range 20-100 mW and was not enough for absorptance measurements of low absorption materials in IR. In this report we present the results on development of OPO on PPLN with average power of tunable radiation in range of 200-1000 mW and its applications for absorptance and scattering losses measurements in nonlinear crystals and optical coatings in range 1.4-4.5 um. As maximal energy per pulse in OPO on PPLN is limted by laser-induced damage threshold of PPLN surface at the level 0.9 mJ for 200 um diameter beam the real way for average power increasing is to use laser with energy per pulse in range of 0.5 mJ and repetition rate in range 5-20 kHz. We developed such system using TEM00 mode diode-pumped Nd:YAG laser with repetition rate up to 40 kHz. PPLN OPO based on 12 different gratings provided tuneable coherent output in the 1.4-um to 4.5-um spectral range. Absorptance and scattering losses measurements in wide IR range were performed on few traditional and new nonlinear crystals and coatings designed for IR.

6101B-36, Session 9

Detection of laser optic damage using gradient direction sensitive matching

B. Chen, J. Tzeng, L. M. Kegelmeyer, J. Liebman, S. Azevedo, D. W. Paglieroni, Lawrence Livermore National Lab.

Large and energetic pulsed laser systems, such as the National Ignition Facility (NIF), can cause damage to optical elements in the beamlines. In-line camera-based inspection systems are employed to image the optics between shots and automatically locate and measure potential damage sites for refurbishment or optic replacement. For some damage sites, diffraction ring evidence from alternate focal-plane images can improve detection reliability. This paper presents the application of a robust pattern matching algorithm based on the gradient direction information of individual pixels for finding diffraction ring patterns in out-of-focus images of features. This algorithm, Gradient Direction Sensitive Matching, finds candidate ring centers by computing the similarity of the gradient direction of a ring pattern to that of a luminance disk. These initial candidates are further refined to reduce false alarms. Finally, we fit a theoretical ring pattern equation to the candidate ring patterns for the estimation of the size and location of the site. Detection results on images from simulated and real features demonstrate the potential effectiveness of our approach, showing improved true positive detections with fewer false alarms.

This work was performed under the auspices of the U.S. Department of Energy by University of California, Lawrence Livermore National Laboratory under Contract W-7405-Eng-48.

6101B-37, Poster Session

On the characterization of the rotation of the irradiance profile of partially coherent beams

R. Martínez-Herrero, P. M. Mejías, Univ. Complutense de Madrid (Spain)

On the basis of the intensity moments formalism, four matrices, Mi, i = 0, 1, 2, 3, are proposed, whose elements, defined for any partially coherent field, are closely related with the second-order measurable parameters used in the ISO standard 11146.[1] The determinants of the matrices have invariance properties along certain first-order optical systems. Matrix M0 concerns the beam size, the far-field divergence and the beam quality. The rotation of the principal axes of the beam around its propagation axis can be inferred from matrices M1 and M2. Finally, it can be obtained from matrix M3 the extrinsic or orbital part of the angular momentum. In addition, a new parameter is introduced in terms of these matrices, which is invariant through rotationally-symmetric first-order optical systems. Such measurable quantity provides information about the rotation capability of the beam irradiance profile under free propagation.

This work has been supported by the Ministerio de Educación y Ciencia of Spain, under project FIS2004-1900, within the framework of EUREKA Project EU-2359.

1. ISO 11146, Lasers and laser-related equipment - Test methods for laser beam widths, divergence angles and beam propagation ratios, Parts 1, 2 and 3 (2005).

6101B-38, Poster Session

Characterization of non-uniformly totally polarized beams

R. Martinez-Herrero, P. M. Mejías, G. Piquero, Univ. Complutense de Madrid (Spain)

Several parameters are introduced to characterize the linear (or circular) polarization content of a non-uniformly totally polarized beam over the regions of the wavefront where the intensity is significant. These figures of merit can be calculated and measured from the values of the Stokes parameters integrated throughout the beam profile. In practice, this kind of average can reduce the influence of the tales of the beam profile, thus decreasing certain experimental harmful effects. The present parameters can be considered, in a sense, as complementary to the so-called weighted degree of polarization, introduced some years ago.[1] The physical meaning of the above parameters is tested by computing some numerical examples, and their measurability is checked by considering non-uniformly totally polarized beams generated after propagation through uniaxial anisotropic materials.

This work has been supported by the Ministerio de Educación y Ciencia of Spain, under project FIS2004-1900, within the framework of EUREKA Project EU-2359.

[1] See, for example, P. M. Mejías, R. Martínez-Herrero, G. Piquero and J. M. Movilla, “Parametric characterization of the spatial structure of non-uniformly polarized laser beams,” Prog. Quantum Electron, 26, 65-130 (2002).

6101B-39, Poster Session

Spatial characterization of laser beams modified by interferences

J. Serna, Univ. Complutense de Madrid (Spain)

The great versatility of laser makes them useful in many different applications. To maintain this variety of uses it very important to have an appropriate spatial characterization of the beams emitted by laser sources. Fortunately now we have adequate tools for this spatial characterization, both in the theoretical field and in the experimental field.

In the case of laser sources coherence property, a natural characteristic of beams produced by them, could give rise to the appearance of interference fringes. A dust particle, or a partial reflection at an interface can produce secondary beams that interfere with the principal beam producing the above-cited fringes. As extreme cases we can find the beams produced by interferometers such as Michelson or Fabry-Perot interferometers. Abundance of this type of effects makes it useful to study how interferences modify the spatial parameters that characterize laser beams, including beam width, beam divergence and beam propagation ratio.

Conference 6101C: High Energy/Average Power Lasers and Intense Beam Applications

Monday 23 January 2006

Proceedings of SPIE Vol. 6101C

6101C-40, Session 11

Electra: repetitively pulsed 700 J, 100 ns electron beam pumped KrF laser

M. F. Wolford, Science Applications International Corp.; M. C. Myers, J. L. Giuliani, Jr., J. D. Sethian, Naval Research Lab.; F. Hegeler, Commonwealth Technology Inc.

Electra is a repetitively pulsed, electron beam pumped Krypton Fluoride (KrF) laser at the Naval Research Laboratory that is developing the technologies that can meet the Inertial Fusion Energy (IFE) requirements for durability, efficiency, and cost. The technologies developed on Electra should be directly scalable to a full size fusion power plant beam line.

The pump source for the laser is formed by two pulsed power systems, 30x100 cm2 cathodes, pressure foil support structures (hibachi); a double sided electron beams exciting the KrF laser medium with a volume of 90 liters. The counter-propagating electron beams have a diode voltage of 500 keV, current of 90 kA, and with a 100 ns flat-top pulse. A 9000 liter gas recirculator is used to provide fresh gas for every shot and allow convection cooling of the foil. A plano-parallel resonator is formed with a dielectric high reflector and fused silica blank. Single sided anti-reflection coated fused silica is used to enclose the Kr, Ar and F2 gas used in the laser. The laser beam aperture is 900 cm2.

Electra in oscillator mode has demonstrated single shot and rep-rate laser energies exceeding 700 J with 100 ns pulsewidth at 248 nm. Continuous operation of the KrF laser has lasted for 2.5 hours without failure at 1 Hz. Successful operation at 5 Hz has lasted in bursts of 100 seconds. We have measure uniform near field throughout the whole aperture in amplifier mode.

Work supported by U.S. Department of Energy, NNSA/DP

6101C-41, Session 11

High power and short pulse RF-excited CO2 laser MOPA system for LLP EUV light source

T. Ariga, H. Hoshino, T. Miura, A. Endo, Extreme Ultraviolet Lithography System Development Association (Japan)

Laser produced plasma (LPP) EUV (Extreme Ultraviolet) light source is the candidate for a high quality, 115 W (13.5 nm, 2 % bandwidth) EUV light source in the next generation microlithography. Cost effective laser driver is the key requirement for the realization of the concept to meet to the industrial schedule. A CO2 laser driven LPP system, with a Xenon droplet target, is therefore a promising light source alternative for the EUV. As a first step, we are developing a high power and high repetition rate CO2 laser system to achieve 10 W EUV power at the intermediate focus. The CO2 laser system for the 115 W EUV power is under development.

This paper describes on the development of a CO2 laser MOPA (Master Oscillator Power Amplifier) system with a short pulse length less than 15 ns, an average power of a few kW, and a repetition rate of 100 kHz based on RF-excited, axial flow CO2 laser modules. Various issues are reported on the laser system design, namely tunable 100 W seeder, parasitic oscillation suppression, small signal gain and saturation energy, and beam quality. Additional approach is discussed to increase the amplification efficiency futher.

Acknowledgement: This work was supported by NEDO.

6101C-42, Session 11

Super power avalanches discharge and its application for the excitation of gas lasers

V. F. Tarasenko, Institute of High Current Electronics (Russia); S. I. Yakovlenko, General Physics Institute (Russia)

Volume discharges under elevated pressure of atomic and molecular gases are usually formed with preliminary ionization of discharge gap by different sources of ionizing radiation, and plasma formed with such discharges is widely used in pulsed laser. It is also known about possible formation of such discharges without preliminary gas ionization by non-uniform electric field and nanosecond excitation pulses. In this case, the discharge gap is applied with short voltage pulse. The pulsed nanosecond discharge formed under high pressure of atomic and molecular gases in non-uniform electric field where the electrode with small curvature radius plays the role of cathode, may have volume form with high specific power energy input, possesses the number of unique properties, and may find different applications in various fields. In particular, such a discharge may be used for pre-ionization in high-pressure lasers and formation of subnanosecond e-beams in gas diodes [1]. Properties of plasma produced in volume nanosecond high-pressure discharge and its formation conditions under elevated pressure in air, nitrogen, krypton, argon, neon, helium, and gas mixtures Ar-N2, Ar-Xe, CO2-N2-He in the gap with the cathode having small curvature radius have been investigated. Time-amplitude characteristics and radiation spectra of plasma in different gases in the range of 230-600 nm were defined. Lasing in the gas mixture Ar-Xe has been achieved by excitation through volume nanosecond high-pressure discharge.

Comparison of spectral radiation in nitrogen, krypton, argon, and neon under pumping of mentioned gases by volume discharge in non-uniform electric field (super power avalanches discharge), by nanosecond e-beam, and by volume pulsed discharge in the uniform electric field with high initial voltage was made. Very important is that the volumetric character of the discharge remained at an essential (more than one order) electric field decrease in the gap. In order to decrease electric field a metallic ball with a diameter of 40 mm was used as a potential electrode. In such conditions the spark channels were not observed at positive and negative polarity of a voltage pulse. The bright spots were seen on the potential electrode only.

A non-local criterion for a runaway electron generation is proposed. This criterion results in the universal two-valued dependence of critical voltage Ucr on pd for a certain gas (p is a pressure, d is an interelectrode distance). This dependence subdivides a plane (Ucr, pd) onto the area of the efficient electron multiplication and the area where the electrons leave the gas gap without multiplication.

[1] V.F. Tarasenko, and S.I. Yakovlenko. UFN, 174, No.9, 953-971 (2004).

6101C-43, Session 11

Non-chain HF and DF lasers pumping self-sustained discharge

V. F. Tarasenko, A. N. Panchenko, V. M. Orlovskii, Institute of High Current Electronics (Russia)

Effect of different experimental parameters on the output of non-chain discharge HF (DF) laser was studied. Mixtures of SF6 with H2, D2 and C5H12 were under study. The lasers were pumped by an inductive or LC-generator with primary capacitor C=13=360 nF providing current pulse duration 100-300 ns and specific input energy up to 100 J/l.

The following factors affecting the laser parameters were found:

1.Electric field uniformity in the laser gap. Distortion of the uniformity resulted in discharge constriction and low laser efficiency.

2.UV- illumination of the laser volume significantly improves the laser output from mixtures of SF6 with H2 or D2. Appreciable effect of illumination in mixtures with C5H12 was revealed only at high gas pressure.

3. The current pulse duration should be relatively short. Increase of the energy deposition duration from 100 to 250 ns resulted in two-fold decrease of the laser output.

4.The gas mixture composition and specific energy deposition. In the case of violation of conditions of discharge formation the use of hydrocarbons improves the laser energy. However, in the optimal experimental conditions maximal performance of the non-chain lasers was realised in H2(D2)-based mixtures. Maximal intrinsic efficiency of HF-laser approached ultimate one and was as high as 9-10% at specific input energy 30-70 J/l which corresponds specific output of 3-7 J/l. Therewith electric efficiency was as high as 6%. In the case of DF-laser intrinsic and electrical efficiencies were as high as 7% and 5%, respectively. The laser energy in both cases exceeds 1 J.

Further increase of the input energy decreased the laser efficiency due to hydrogen donor burning and increase of absorption of the laser radiation due to build up of concentration of HF (DF) molecules in ground state in the active volume.

It was found that much more lines are observed in output spectra of the efficient HF and DF-lasers. In the case of HF-laser, transitions from three vibrational levels of excited HF molecules were observed. The number of lines in each transition increases to 8-11, and total number of radiation lines can be as high as 30 and strong cascade lasing on a number of vibrational-rotational lines is observed. Emission on four vibrational bands of DF molecules was observed in the SF6-D2 mixtures while the number of the radiation lines was about 40. The radiation spectra of the efficient non-chain lasers are very similar to those obtained with e-beam excitation which provides uniform energy deposition, high efficiency and eliminates problems with development of discharge non-uniformities.To our opinion, high discharge uniformity, the use of H2(D2) based mixtures increasing the rate of fluorine atom formation in the laser active volume and intense cascade laser action improving the energy extraction from the active media can explain high efficiency of the discharge HF(DF)-lasers obtained in our experiments.

6101C-44, Session 12

Development of thermally controlled diode-pumped solid-state laser

O. Matsumoto, R. Yasuhara, T. Kurita, Osaka Univ. (Japan) and Hamamatsu Photonics K.K. (Japan); T. Ikegawa, Osaka Univ. (Japan) and Hamamatsu Photonics K.K. (Kenya); T. Sekine, T. Kawashima, Osaka Univ. (Japan) and Hamamatsu Photonics K.K. (Japan); J. Kawanaka, T. Norimatsu, N. Miyanaga, Y. Izawa, M. Nakatsuka, Osaka Univ. (Japan); M. Miyamoto, H. Kan, Hamamatsu Photonics K.K. (Japan); H. Furukawa, S. Motokoshi, Osaka Univ. (Japan)

A high average-power diode-pumped solid-state laser (DPSSL) has been developed for industrial and scientific applications. In the development of a DPSSL, we successfully obtained output energy of 10.6 J at rep. rate of 1 Hz and 8.4 J at 10 Hz. Our final target of the DPSSL is output energy of 100 J at 10 Hz. The new system of a DPSSL is designed to demonstrate the scalability to 100-J output energy. The system of the DPSSL is composed with dual water-cooled Nd:glass slab amplifier modules. The laser slab geometry with zig-zag optical path was designed for attaining the current goal of 20-J output energy with the scalability to 100 J. Laser diode (LD) modules pump the laser medium with the peak power density of 2.5 kW/cm2. Twin LD modules totally generate the pump energy of 80 J with electrical to optical conversion efficiency over 50%. Suppression of a parasitic oscillation and reduction of thermal effects are very important problems to a high average-power DPSSL. Cladding glasses were adopted for the solution of these problems. Generation of heat by absorption of amplified spontaneous emission was simulated with cladding glasses arranged at the upper and lower sides of the laser slab. It turned out to be effective in the improvement of the temperature distribution in the laser glass. The whole system has been successfully designed, and the performance of the system is examined in late 2005. This work is partly supported by NEDO (New Energy and Industrial Technology Development Organization) under the Ministry of Economy, Trade and Industry in Japan.

6101C-46, Session 12

A 100-kHz thin disk Yb:YAG regenerative amplifier

T. Miura, A. Endo, Extreme Ultraviolet Lithography System Development Association (Japan)

Laser-produced plasma using highly-energized picosecond pulse is required for micromachining and efficient generation of extreme ultraviolet (EUV) light. To realize high productivity in the industrial applications, high repetition rate and high average power laser sources are preferable. We are developing a 100-kHz picosecond Yb:YAG regenerative amplifier with 500-W average power.

At high average power operation in rod based solid state lasers, thermally induced birefringence inside the laser rod could infringe on the predetermined polarization. Therefore, we first assembled a CW Yb:YAG laser based on the thin disk laser module with a thin film polarizer and an quarter waveplate. We obtained linearly polarized CW output over 900 W without any compensation optics of the birefringence error. The polarization extinction ratio at 900-W operation was approximately 70:1.

Since the regenerative amplification requires single transverse mode operation, we evaluated the deformation of the thin disk. A commercial M2-meter was employed to measure the M2 values and the divergences of the output beam at various pumping powers. Then we estimated the radius of the curvature of the thin disk, and we optimized the cavity configuration of our laser. After the cavity optimization, we reduced the M2 value from 14 to below 4 at the output power of 500 W. We have constructed a multi-kilohertz regenerative amplifier. The seed pulse was stretched by a single mode fiber and injected into the amplifier cavity. The seed pulse was successfully amplified at 10-kHz repetition rate under the low power pumping configuration.

6101C-47, Session 13

Multiple applications for the 10kW fiber laser at the electro-optics center

D. J. Sames, T. M. Lehecka, The Pennsylvania State Univ.

The Penn State Electro-Optics Center will be installing a 10kW fiber laser at its Northpointe, PA facility in Fall 2005. This presentation will discuss the facility's capabilities and introduce three planned experiments that will utilize the high power near 1μm. The first experiment will be in the area of laser charring effects with semi-transparent composite materials. Previous work had been limited due to spot size requirements and limited available power. The new laser will enable effects testing up to levels of several hundred W/cm2. The second application will be damage testing of optical coatings. Coating damage continues to be a major obstacle in the development of HEL systems. The new facility at the EOC will allow us to test optical coating damage at fluences relevant to HEL systems. A third planned application is demonstration of a low-cost, incoherent beam combiner for short ranges. The combiner design will be discussed with preliminary results and plans for range testing at an underground mine location

6101C-48, Session 13

Concrete cutting using high-power fiber laser

K. Tei, Tokai Univ. (Japan)

We have demonstrated the measurements of attenuation constant of a multi-mode fiber (300μm core diameter and 1km length) at 1315nm. The

observed attenuation constant was below 0.7dB/km for 1315nm. The high-power (1-5 kW) laser beam coupling at 1315nm(iodine laser) and 1070nm(fiber laser) into the fiber was conducted. The laser power of 5kW was coupled into the 1km fiber at 1070nm. The overall transmittance was 85 %. We observed the first Raman stokes in the transmitted laser spectrum.

We demonstrated concrete cutting with two different modes using a 5kW fiber laser at 1070nm. The demonstrated slab thickness was 100mm. One of modes provides us the dross-free technique. This technique can be extended to thick concrete slabs more than 1m without laser power increasing.

6101C-49, Session 13

Laser-driven acoustic waves in back-irradiated thin solid foils

A. Zinovev, W. F. Calaway, Jr., J. F. Moore, M. J. Pellin, I. Veryovkin, Argonne National Lab.

Acoustic waves, generated in solids by irradiation of a surface with powerful laser pulses, are widely used to study mechanical, thermal and elastic properties of materials. Application of this technique to MEMS technology will open new insights into fabrication and characterization but will require understanding of acoustic wave generation in small-sized objects. To that end, acoustic wave generation was studied in thin (10-50 μm) metal and semiconductor foils (including Mo, Si, W, Ta, Ni, Au) backside irradiated by nanosecond IR and UV laser pulses over a range of peak intensities. Both interferometric techniques and capacitance transducers were employed for detection of surface displacements in the foils. By varying the peak laser power over a wide range of intensities (1-500 MW/cm2) detection of the transition from a thermoelastic to a laser-plasma driven shock-wave mechanism for acoustic wave generation was possible. Measurements show that this transition is accompanied by a dramatic change in the waveform of the generated shock-wave and that this waveform differs for various materials and foil thicknesses. Since thin foils were studied, the longitudinal and shear waves were experimentally indistinguishable, making the observed waveform very complex. Moreover, at higher peak laser powers, mechanical vibrations at resonance frequencies of the thin foils can occur and further complicate the analysis. Nevertheless, the observed phenomena can be described in the framework of a simplified theoretical model and can be used for materials testing in MEMS applications.

This work is supported by the U.S. Department of Energy, BES-Materials Sciences, under Contract W-31-109-ENG-38.

6101C-51, Session 14

The electric oxygen-iodine laser: chemical kinetics of O_2 ($a^1\Delta$) production and I ($^2P1/2$) excitation in microwave discharge systems

W. T. Rawlins, S. Lee, W. J. Kessler, D. B. Oakes, L. G. Piper, S. J. Davis, Physical Sciences Inc.

Generation of singlet oxygen metastables, O2($a^1\Delta$), in an electric discharge plasma offers the potential for development of compact electric oxygen-iodine laser (EOIL) systems using a recyclable, all-gas-phase medium. The primary technical challenge for this concept is to develop a high-power, scalable electric discharge configuration that can produce high yields and flow rates of O2(a) to support I(2P1/2→2P3/2) lasing at high output power. This paper discusses the chemical kinetics of the generation of O2(a) and the excitation of I(2P1/2) in discharge-flow reactors using microwave discharges at low power, 40-120 W, and moderate power, 1-2 kW. The relatively high E/N of the microwave discharge, coupled with the dilution of O2 with Ar and/or He, leads to increased O2(a) production rates, resulting in O2(a) yields in the range 20-40%. At elevated power, the optimum O2(a) yield occurs at higher total flow rates, resulting in O2(a) flow rates as large as 1 mmole/s (~100 W of O2(a) in the flow) for 1 kW discharge power. We perform the reacting flow measurements using a comprehensive suite of optical emission and absorption diagnostics to monitor the absolute concentrations of O2(a), O2(b), O(3P), I2, I(2P3/2), I(2P1/2), small-signal gain, and temperature. These measurements constrain the kinetics model of the system, and reveal the existence of new chemical loss mechanisms related to atomic oxygen. The results for O2(a) production at 1 kW have intriguing implications for the scaling of EOIL systems to high power.

6101C-52, Session 14

Singlet delta oxygen production in self-sustained and non-self-sustained slab discharges

A. A. Ionin, M. P. Frolov, P.N. Lebedev Physical Institute (Russia); I. V. Kochetov, A. P. Napartovich, Troitsk Institute for Innovation and Fusion Research (Russia); V. N. Ochkin, Y. P. Podmar'kov, P.N. Lebedev Physical Institute (Russia); O. A. Rulev, Troitsk Institute for Innovation and Fusion Research (Russia); S. Y. Savinov, L. V. Seleznev, D. V. Sinitsyn, N. P. Vagin, N. N. Yuryshev, P.N. Lebedev Physical Institute (Russia)

Singlet delta oxygen (SDO) production in slab discharges ignited in oxygen gas mixtures was experimentally studied. In slab self-sustained RF discharge experimental SDO yield was about 10%. It was demonstrated that the choice of electrodes material is very important. Experiments on SDO production in slab non-self-sustained discharge with external ionization by repeated high-voltage pulses were carried out. SDO concentration was measured by the method of intracavity laser spectroscopy. The measured concentration of SDO was about E-16 cm-3, with SDO yield being of ~7%.

6101C-53, Session 14

Quenching I(2P1/2) by O3

V. N. Azyazov, S. Ruffner, M. C. Heaven, Emory Univ.

Oxygen-iodine lasers that utilize electrical or microwave discharges to produce singlet oxygen are currently being investigated. Development of these devices is currently limited by our poor understanding of the post-discharge reactions and energy transfer processes. The role of oxygen atoms, ozone, nitrogen oxides and iodine oxides in the formation of active medium is not clear.

Ozone is present in the output from discharge singlet oxygen generator and this is source of potential complications. The ozone concentration could be comparable with that of iodine. O3 reacts with both I(2P1/2) and I(2P3/2) atoms forming IO molecules which are highly reactivity. During IO self-reactions the iodine oxides IO2 and I2O2 are produced. This is undesirable because these processes consume iodine atoms. The goal of our study was the measurement of rate constant for removal of I(2P1/2) by O3.

The rate constant for quenching of I(2P1/2) by O3 was studied by pulsed laser photolysis of I2/O3/Ar mixtures at 490 nm. Excited iodine atoms was formed by direct photodissociation of I2.

The dependence of the intensity of the atomic iodine emission at 1315 nm as a function of time and O3 pressure defines the rate constant for removal of I(2P1/2) by ozone. Molecular iodine vapor was entrained by flowing Ar carrier gas over iodine crystals. The ozone was collected on silica gel cooled to - 100 C. Ozone was generated using a commercial discharge ozonator. Once a sufficient sample has been collected, the O3 was eluted from the silica gel by a slow flow of Ar.

The 490 nm photolysis light is produced by an Nd/YAG pumped dye laser. The pulse energies used was chosen to photodissociate of about 10 % of the iodine molecules and a negligible fraction of the ozone. Iodine atomic emission, separated by a long-pass filter, was recorded by a high speed Ge photodetector (ADC 403HS). It was found that the rate constant for removal of I(2P1/2) by O3 measured by this method is 2.6x10-12 cm3/s.

6101C-54, Session 14

COIL power extraction enhanced by reducing/ eliminating iodine clusters in a high mach number nozzle

J. A. Marshall, K. P. Healey, B. Croker, Air Force Research Lab.; K. R. Kendrick, Air Force Research Lab; T. T. Yang, Advanced Photonic Sciences; Y. Hsia, The Boeing Co.; R. A. Dickerson, L. Forman, Consultant

In 1999, a nitrogen-based high Mach number COIL was designed and tested. Power of up to 20 kilowatts was achieved. It was noted that during testing, more than twice the expected iodine flow was required. Extensive modeling led to the conclusion that iodine dissociation cannot overcome iodine cluster formation, leading to a higher iodine flow rate requirement.

The original tests revealed a tendency for the cavity flow to thermally choke with larger than normal quantities of iodine flow. Therefore, a relief angle of the laser cavity was made in order to study higher iodine flow-rates.

Baseline testing with a 1.5o divergent cavity was not successful. The need for significantly higher iodine flow-rates for achieving power levels, similar to those of constant area, further confirmed the existence of iodine clusters.

The power saturation with a 1.5o cavity was also measured. The saturation data was clearly disappointing, showing only about 4 Kw at 15 % out-coupling, as compared to 12 Kw at 3 % out-coupling.

A solution envisioned to overcome the cluster formation is to use a “cluster buster”. The high temperature induced by cluster buster vaporizes the clusters, making iodine from them available for participation in the chemical kinetic processes.

The cluster busters were tested extensively. With an 85 % reflectivity mirror, the power reached about 13 Kw. This was almost three times higher than that obtained without cluster busters.

In summary, COIL power extraction efficiency has been improved significantly by effectively breaking-up iodine clusters formed under a high expansion nozzle.

6101C-55, Session 14

The auto-decomposition of NCl3 as a source of NCl(a)

W. E. McDermott, Univ. of Denver; B. Nizamov, Directed Energy Solutions; R. D. Coombe, J. Gilbert, Univ. of Denver

The NCl-I laser has been demonstrated using HN3 as a fuel. We have shown the auto decomposition of NCl3 can be initiated by modest heating of the NCl3 flow producing chlorine atoms and NCl2. We have also shown that when H2 is added to this flow, both NCl(a) and NCl(b) are produced. This reaction sequence has the potential to produce enough NCl(a) to create an inversion in the iodine atom through the fast energy transfer reaction between NCl(a) and ground state iodine atoms. In this paper we will discuss the auto decomposition kinetics of NCl3 and describe some recent experiments we have done to elucidate this mechanism.

6101C-56, Session 14

Novel concepts for advanced iodine lasers

W. J. Kessler, S. Lee, K. Galbally, W. T. Rawlins, D. B. Oakes, A. J. Bauer, S. J. Davis, Physical Sciences Inc.

This talk will describe recent research to develop new atomic iodine lasers based upon energy transfer from metastable species including O2(a) and NCl(a). The oxygen-based work will present efforts to pre-mix the singlet oxygen with an iodine donor. The iodine donor is photolyzed to produce atomic iodine nearly instantaneously in the presence of the singlet oxygen. Optical gain/loss measurements will be described. The NCl(a) donor work includes measurements of optical transparency on the iodine atom transition where the NCl(a) was produced from the NCl2 + H reaction.

6101C-57, Session 14

Highly efficient cesium vapor laser

T. Ehrenreich, B. Zhdanov, R. J. Knize, U.S. Air Force Academy

A slope efficiency of 66% and an overall efficiency of 60% have been achieved in an end-pumped Cesium vapor laser. The laser output power was 480 mW and was only limited by the pump power level.

A three-level pump scheme is used to create population inversion on the D1 transition in Cs vapors (6P1/2 to 6S1/2,). A narrowband laser pumps the atoms to the 6P3/2 state (D2 line) which is then rapidly quenched to the 6P1/2 state by an Ethane buffer gas. This creates a population inversion between the 6P1/2 and 6S1/2 states and lasing [1].

The laser cavity consists of two concave mirrors with a 20 cm radius. The high reflector has ~ 99% reflectivity at 894 nm (lasing wavelength) and ~ 90% transmission at 852 nm (pump). The output coupler has ~ 30% reflectivity at 894 nm and ~ 90% reflectivity at 852 nm .The optical length of the cavity is 16 cm. The 2 cm long Cs vapor cell is positioned in the center of the cavity. It is filed with a visual amount of metallic Cesium, 500 Torr of Ethane and has AR-coated optical quality windows. The optimal operating temperature was (88 ± 2)°C.

A Coherent MBR-100 Ti:Sapphire laser was used as a pump source for the Cs laser. It had an output power of 800 mW @ 852 with a linewidth less than 1 MHz (FWHM).

We acknowledge support from the Air Force Office of Scientific Research and the National Science Foundation under Grant No. 0355202

[1] Ehrenreich et al. Electronics Letters, 41, 415-416 (March 2005)

6101C-59, Session 14

Recent advances in German tactical COIL-efforts

W. L. Bohn, DLR (Germany)

Current COIL research is aimed at the feasibility of a future mobile COIL system for tactical applications. Chemical efficiency, beam quality and compactness of the device are hereby of primary importance. For the first time we present results obtained with a medium power containerized COIL facility. In order to realize a mobile system further optimization of major laser components are necessary. Therefore we address novel oxygen generator concepts and resonator designs with respect to their impact on the overall performance of the laser system. In addition, we demonstrate efficient BHP storage using commercially available deep freezer technology

6101C-60, Session 14

Negative branch hybrid resonator for COIL

J. Handke, T. Hall, F. R. Duschek, K. M. Grünewald, DLR (Germany)

A rectangular negative branch off-axis hybrid resonator was coupled to a 10-kW class Chemical Oxygen-Iodine Laser (COIL). Various schemes of geometrical coupling between resonator and gain medium were investigated. The extracted power was 6.6 kW and reached about 70% of the output power for the COIL device in an optimized conventional stable resonator configuration. Experimentally measured margins for the sensitivity of resonator setup and alignment were found in close agreement with numerical calculations. Power density distributions were measured in the near field and in the far field. The divergence of the emitted laser beam in the unstable direction was lower than 2 times diffraction limited.

6101C-77, Session 14

Effects of mixing on post-discharge modeling of ElectricOIL experiments

A. D. Palla, D. L. Carroll, J. T. Verdeyen, CU Aerospace LLC; W. C. Solomon, Univ. of Illinois at Urbana-Champaign

In an electric discharge Oxygen-Iodine laser (ElectricOIL), laser action at 1315 nm on the I(2P1/2) →I(2P3/2) transition of atomic iodine has been obtained by a near resonant energy transfer from O2(a1δ) which is produced using a low-pressure electric discharge. The discharge production of atomic oxygen, ozone, and other excited species adds higher levels of complexity to the post-discharge kinetics which are not encountered in a classic purely chemical O2(a1δ) generation system. Mixing effects are also present. In this paper we present post-discharge modeling results obtained using a modified version of the Blaze-II gas laser code. A 28 specie, 105 reaction chemical kinetic reaction set for the post-discharge kinetics is presented. Calculations were performed to ascertain the impact of a two stream mixing mechanism on the numerical model and to study gain as a function of reactant mass flow rates. The calculations were compared with experimental data. Agreement with experimental data was improved with the addition of new kinetics and the mixing mechanism.

Conference 6102: Fiber Lasers III: Technology, Systems, and Applications

Monday-Thursday 23-26 January 2006

Proceedings of SPIE Vol. 6102

6102-01, Session 1

Ultrashort pulse micromachining with the 10-μJ FCPA fiber laser

A. Y. Arai, J. Bovatsek, F. Yoshino, Y. Uehara, IMRA America, Inc.

IMRA's ultrashort pulse fiber laser products continue to evolve and expand the application scope. The latest prototype FCPA uJewel produces pulses with less than 500-fs pulse duration at a 50-kHz repetition rate. At the fundamental wavelength of 1045 nm, the pulse energy is greater than 10 uJ. With second harmonic generation using an LBO crystal, greater than 4-uJ pulses can be produced. The increase in pulse energy over the standard FCPA uJewel permits greater flexibility in the focusing conditions applicable for micromachining, enabling a wider variety of laser-machined structures and profiles. This paper describes the latest micromachining application areas being studied with this new laser.

6102-02, Session 1

Addressing challenging micro-processing applications and materials with fiber lasers

A. P. Hoult, SPI Optics

Fiber-integrated high power fiber lasers are becoming the technology of choice for a diverse range of micro-materials processing applications due to their efficiency, operational stability and reliability. It is now clear that a much wider range of laser parameters are available when fiber lasers are compared to conventional solid-state lasers. Add to this the lack of additional variables associated with thermal lensing and process development is greatly simplified. Of even more importance, this parameter flexibility enables these lasers to perform well beyond the state-of-the-art in certain established applications where performance expectations are already very high. Similarly, due to its low M2, the laser is shown here to perform well in applications and on materials that might not be immediately considered suitable for this type of continuous-wave modulated laser. Novel results on difficult-to-cut materials are presented along with a semi-quantitative analysis of processing with the fiber laser.

6102-03, Session 2

New milestone in development of super high power fiber lasers

V. P. Gapontsev, IPG Laser GmbH (Germany)

New technology platform for the next generation of super high power fiber lasers, developed by IPG during 2005, would be discussed. It includes darkening-free, side-pumped, highly-ytterbium-doped LMA fibers, extra high brightness single emitter diodes; perfect beam combiners, feeding and processing fibers, fiber couplers, and high-speed multi-channel beam switches, holding multiple ten kilowatt beams of optical power. These components were used for the development of truly single-mode, all-fiber format, 3.5kW CW fiber laser with a single mode fiber delivery, 20kW fiber laser with Beam Parameter Product (BPP) ~ 4 mm x mrad and 50kW output optical power system providing BPP ~ 10 mm x mrad. Unique diode lifetime and active fiber aging test results, as well as fast growing statistics of fiber laser deployment in industry production environment would be discussed.

6102-04, Session 2

Kilowatt fiber lasers and beyond

D. N. Payne, Univ. of Southampton (United Kingdom)

Born out of the telecom revolution, the supreme attributes of rare-earth doped fibers has allowed Yb-doped fiber lasers to be power-scaled from 0.1 to several kW's in only a few years. Remarkably, we still see fiber lasers being limited by the diodes rather than the fibers themselves, even as output powers have continued to rise well into the multi-kW regime. Despite these impressive results, high-power fiber laser development is still in its infancy with a high rate of progress. Limited investment rather than the fundamentals of the technology is the biggest hurdle to the 10 kW-level from a single-emitter diffraction-limited fiber source. Looking to the future, fiber sources are also extremely attractive for beam combining for power-scaling to perhaps 100's of kW. Of particular interest here is the astounding single-frequency powers that have been obtained, also now approaching 1 kW.

Numerous fiber laser pulse schemes are also available, giving pulses from the femtosecond to the microsecond regime with peak power (compressed) in the multi MW's . With large core designs, pulse energies up to 0.1 J can be obtained. Wavelengths from 800 nm to 2100 nm and beyond are seamlessly available through appropriate choice of rare-earth dopant or through Raman shifting. Moreover, these characteristics can be realized with exceptional control of the output stability and beam profile. The key to this is the ability of fibers to combine high power and high efficiency with high broadband gain and excellent beam quality in sophisticated master oscillator - power amplifier configurations.

This presentation will discuss progress and prospects for high-power fiber sources, treating "simple" power-scaling as well as more sophisticated single-frequency and pulsed sources at different wavelengths. Adding the attributes of small size, maintenance-free operation, and high thermal and electrical efficiency, we see that fiber lasers have the potential to change every industry and discipline they encounter and challenge currently held views on how to make things, how to repair things, and how to destroy things.

6102-05, Session 2

High power, narrow linewidth fiber lasers

D. T. Walton, S. Gray, J. Wang, M. Li, X. Chen, A. B. Ruffin, J. DeMeritt, L. A. Zenteno, Corning Inc.

In 2002, Corning Incorporated started research work on high power fiber lasers funded in part by DARPA. As a result of this work, Corning demonstrated 100 W single-polarization all-fiber laser oscillators and fibers designed for the suppression of stimulated Raman scattering (SRS). Currently, work involves the research and development of kW-level, single-mode, narrow linewidth fiber amplifiers. We will discuss our latest results in the areas of stimulated Brillouin scattering mitigation and advanced packaging concepts.

In high power fiber oscillators, the resulting linewidths can be as broad as a few tens of nanometers. Sub-nanometer linewidths can be achieved through the use of spectral filters such as fiber Bragg gratings. In order to reach high power levels with narrow spectral linewidths, master-oscillator, power amplifier configurations are preferred. When configured as a high power amplifier for narrow linewidth signals, fibers are plagued with stimulated Brillouin scattering (SBS). Typically, such nonlinear impairments as SBS are addressed through the use of large mode area (LMA) fibers. Achieving kW-level power operation approaches the limits of LMA fiber performance. In the current work we will detail our techniques of engineering the core refractive index profile and dopant distribution in order to mitigate SBS. Reduction of SBS by as much as 3 dB has been demonstrated.

Another consideration in the design of high power fiber laser devices is the development of appropriate packaging for operation in adverse conditions. We will discuss packaging concepts for kW-class laser systems with system-level optical nonlinearity and thermal abatement.

6102-06, Session 3

New development in high power eye-safe LMA fibers

K. Tankala, B. N. Samson, A. L. Carter, J. Farroni, D. P. Machewirth, N. Jacobson, Nufern; A. Galvanauskas, Univ. of Michigan; W. E. Torruellas, Fibertek, Inc.

The advent of double-clad fiber technology has made high power lasers and amplifiers possible. Furthermore, various techniques to achieve single mode operation in multimode fibers resulted in rapid development and optimization of ytterbium-doped large-mode area (LMA) fibers. As a result of this development, kW level (1-2 kW) continuous wave outputs and mega-watt level peak powers with sub-nanosecond pulses have been demonstrated. However, development of LMA fibers has largely been restricted to ytterbium based fibers for use at 1.06 um and minimal effort has gone into development of LMA fibers for at eye-safe wavelengths using Er/Yb co-doped (1.55 um) and Tm doped fibers (2.0 um).

In this paper we will present the advances made in the development and fabrication of highly efficient, large-mode area fibers for eye-safe wavelengths. LMA Er/Yb co-doped and Tm doped fibers, with 25 um core and 250 to 300 um clad diameters, suitable for nanosecond pulsed amplification in lidar applications and high power CW amplification are presented. The development of non-PM and PM-LMA fibers for eye-safe applications is expected to spur rapid progress in power scaling at these wavelengths similar to that witnessed by the industry at 1.06 um.

6102-07, Session 3

High pulse energy extraction with high peak power from short-pulse, eye safe all-fiber laser system

M. P. Savage-Leuchs, E. C. Eisenberg, A. Liu, J. Henrie, M. S. Bowers, Aculight Corp.

All-fiber contained laser systems play a key role, in the development of rugged, compact, and highly efficient eye safe laser sources that can generate high peak and average powers and short (<5 ns) pulses. Application of such laser systems include spectroscopy, LIDAR, free-space communications, materials processing and nonlinear optics.

In this paper we present further improvement on a novel high power all-fiber-based master oscillator power amplifier (MOPA) laser system operating in the C-band with 5 ns pulses and a repetition rate range of 6kHz - 200kHz. With this system, pulse energies of > 200 micro-Joules and peak powers of 38kW were generated using custom designed Er:Yb co-doped double-clad fibers. The spectral output of the amplified pulses shows no spectral broadening due to Four-Wave-Mixing or Stimulated Raman scattering. Additionally, a beam quality M2<2.5 was achieved. The physical performance parameters or the all-fiber laser system make it very suitable for a variety of applications. Experimental results of the all-fiber contained laser system will be presented.

6102-08, Session 4

Power scalable and efficient 790-nm pumped Tm3+-doped fiber lasers

G. P. Frith, D. G. Lancaster, Defence Science and Technology Organisation (Australia)

Tm3+-doped fibre lasers pumped at 793nm have gained significant interest as a highly efficient means of generating emission in the 1.9 to 2μm region. In this paper we describe some of the latest developments in the design and operation of high average power Tm3+-doped double-clad fibres, running in both single and multi- transverse mode. The emphasis of this presentation will be the power scaling potential of these fibre lasers, wavelength tuning and narrowing of the spectral output, and operation of the fibre as an amplifier.

To date we have demonstrated up to 85W1 from a multi-mode fibre (M2~4) with an efficiency of 51% relative to launched pump power. We have also demonstrated fibre Bragg grating tuned wavelength operation down to 1892nm.

The high efficiencies of the fibres are attributed to the cross-relaxation (CR) process2, which leads to the two-for-one phenomenon giving the laser a maximum theoretical quantum efficiency of 200%. The optimum fibre performance is achieved by using Tm3+ concentrations of up to 3(wt.)% whilst limiting clustering in the glass host by incorporation of Al3+ to maximise CR while limiting energy transfer upconversion losses3.

The quasi three-level nature of the 3F4→3H6 transition implies reabsorption of the laser, primarily in under-pumped regions of the fibre. Accordingly, for high efficiency operation, a short fibre is desirable, and the core to cladding ratio must be optimised for the fibre dopant concentration to ensure strong pump light absorption. We have found however, that using a short fibre for high power operation requires developing best practice in thermal management of the fibre.

For amplifier applications the available gain is largely limited by the relatively short life time of the 3H4 upper state. The highest gain we have demonstrated was 6dB at 1.9μm however the multimode system had a high conversion efficiency of 64.4% (relative to absorbed pump) indicating that such fibres may be useful for high power multistage amplifiers.

REFERNCES

[1] G.P. Frith, D.G. Lancaster and S.D. Jackson, Electronics Letters 41 687-8 (2005).

[2] B.M. Antipenko, Bull. Acad. Sci. USSR Phys. Ser. 48, 1562-1563 (1986)

[3] S.D. Jackson and S. Mossman, Applied Optics 42 2702-7 (2003).

6102-09, Session 4

Multi-component glass fiber lasers

S. Jiang, NP Photonics, Inc.

This talk will present NP's new development in high power singe frequency phosphate glass fiber lasers near 1.55 micron and 1 micron with spectral linewidth of 2 kHz, highly efficient Brillouin fiber laser with spectral linewidth of 200Hz, and highly efficient 2 micron single frequency and high power germanate glass fiber lasers.

6102-10, Session 4

Mid-IR supercontinuum generation in non-silica glass fibers

J. H. V. Price, Univ. of Southampton (United Kingdom); T. M. Monro, H. Ebendorff-Heidepriem, The Univ. of Adelaide (Australia); J. Y. Leong, P. Petropoulos, G. Brambilla, V. Finazzi, X. Feng, D. J. Richardson, Univ. of Southampton (United Kingdom)

Abstract not available.

6102-11, Session 5

High-power photonic crystal fibers

K. P. Hansen, J. Broeng, A. Petersson, P. M. W. Skovgaard, M. D. Nielsen, C. Jakobsen, H. R. Simonsen, Crystal Fibre A/S (Denmark)

Fiber lasers deliver excellent beam-quality and high efficiency in a robust and largely maintenance-free format, and are now able to do so with out-

put powers in the kilowatt regime. Consequently, fiber lasers have become an attractive alternative to solid-state and gas lasers for e.g. material processing like welding, cutting and marking.

The all-glass air-clad photonic crystal fibers (PCFs) combine large mode-field diameters (currently up to 40 μm), high numerical aperture (typically in the 0.6-0.65 range), high pump absorption (30 dB/m demonstrated in ytterbium) and excellent high-power handling (kW CW and mJ pulses demonstrated). These properties have made this fiber type one of the most promising candidates for the future high-power fiber laser and amplifier systems that are expected to replace many of the traditional systems in use today.

To utilize the high numerical aperture and large mode-field diameters of the air-clad PCFs, special care must be taken in the system integration. In this paper, we will show examples of how these fibers can be integrated in laser and amplifier sub-assemblies with standard fiber pump-interfaces for use with single-emitter diodes or diode-bar pump sources. Moreover, we report on the most recent advances in fiber design including rod-type fibers and broadband polarizing ytterbium-doped large-mode-area air-clad fibers. Finally, we will review the latest results on PCF-based amplifier and laser configurations with special focus on high-power CW systems and high-energy pulsed configurations.

6102-12, Session 5

Design and high power operation of a stress-induced single-polarization single-transverse mode LMA Yb-doped photonic crystal fiber

T. Schreiber, F. Röser, O. Schmidt, J. Limpert, A. Tünnermann, R. Iliew, Friedrich-Schiller-Univ. Jena (Germany); A. Petersson, C. Jacobsen, K. P. Hansen, J. Broeng, Crystal Fibre A/S (Denmark)

Many experiments have proven the potential of power scaling when using rare earth doped fibers as a gain medium in lasers and amplifiers [1]. Recently, photonic crystal fibers (PCF) pushed the output parameters of solid-state laser systems not only in continuous wave operation, but especially in ultra-short pulse systems. In order to simplify the laser setup in terms of polarization control there is a great interest in combining large mode area micro-structured fibers and polarization maintaining elements. To achieve a polarization maintaining fiber sufficient birefringence has to be introduced in the core. For large cores this can only be done by material anisotropy. Thus, stress-applying elements are usually placed inside the fiber to induce differential stress, which translates into birefringence due to the photo-elastic effect. Here we report on a new design of a single-polarization single-transverse mode photonic crystal fiber. The design is based on combining stress applying elements and the inner photonic cladding by index matching. In this way, a passive single-polarization fiber with a mode field area of ~700μm≤ is achieved exceeding values that can be obtained from step index fibers. Additionally, the largest single polarization bandwidth of Dl/lC>0.5 ever reported is observed. This design was then used to fabricate an Yb-doped single polarization fiber with low nonlinearity. Because no stress elements are placed outside the inner cladding, a high overlap of the pump cladding with the large mode core could be obtained resulting in a pump light absorption of ~14 dB/m. In a primary experiment, a highly polarized laser with no additional polarizing elements inside the cavity was built with an extinction ratio of 15.5 dB and an output power of 25 W. In a second experiment ultra-short pulses are amplified in 1.2 m of this fiber to an average power of 29 W. The degree of polarization after the amplifier characterizes the polarization holding of this single-polarization fiber and is measured to be above 23 dB for all output powers.

[1] A. Tünnermann, T. Schreiber, F. Røser, A. Liem, S. Hófer, H. Zellmer, S. Nolte, J. Limpert, "The renaissance and bright future of fibre lasers," J. Phys. B: At. Mol. Opt. Phys. 38, 681-693 (2005).

6102-13, Session 5

Very-large-core, single-mode Yb-doped photonic crystal fiber for multi-MW peak power generation

F. Di Teodoro, C. Brooks, Aculight Corp.

Generating high peak powers in pulsed rare-earth-doped fiber sources has been traditionally very challenging due to the onset of nonlinear optical effects including stimulated Raman and Brillouin scattering, nonlinear phase modulation, and four-wave mixing, all of which strongly degrade the spectral brightness. An additional limiting factor is fiber facet and bulk optical damages.

Very recently, significant progress has been reported in scaling the in-fiber peak power beyond the MW level, while retaining high spatial and spectral quality1. In this work, a single-mode, 40-μm, Yb-doped photonic crystal fiber (PCF) was used to generate peak power > 1.1 MW with M2 ~ 1 and spectral linewidth ~10 GHz.

In this paper, we report on the development of a new, intrinsically single-mode Yb-doped PCF featuring a core diameter >60μm, the largest for a single-mode fiber to date. The PCF is optimized for generation of multi-MW peak-power, diffraction-limited pulses exhibiting minimal optical nonlinearities, and is used as the final stage in a master-oscillator/fiber-amplifier system generating multi-kHz repetition-rate, sub-ns pulses at 1.06μm wavelength.

References

[1] F. Di Teodoro and C. D. Brooks, "1.1-MW peak-power, high-spectral-brightness, diffraction-limited sub-ns pulses from an Yb-doped photonic crystal fiber amplifier," Solid-State and Diode Laser Technology Review (SSDLTR 2005), Los Angeles, CA, 7-9 June 2005. Fiber-6.

6102-14, Session 5

Are hollow-core fibers attractive for high-power fiber lasers?

K. Hougaard, J. Laegsgaard, Danmarks Tekniske Univ. (Denmark); J. Broeng, Crystal Fibre A/S (Denmark); A. O. Bjarklev, Danmarks Tekniske Univ.

Silica-based hollow-core photonic bandgap (HC-PBG) fibers are of interest for high-power laser applications, due to the possibility of guiding the majority of the optical power in air, thus suppressing nonlinearities and the limitations set by the breakdown treshold of silica. In this contribution, we study numerically the laser-induced damage treshold in HC-PBG fibers as function of core size and cladding air-filling fraction, and compare to a typical silica-core large-mode area (LMA) fiber. Remarkably, the HC-PBG fibers studied yield no significant improvement over the LMA reference, indicating that radically new design ideas may be needed for HC-PBG fibers to be competitive as active components in a high-power laser system.

6102-15, Session 5

Amplification in doped hollow core photonic crystal fibers

P. J. Roberts, Univ. of Bath (United Kingdom); K. P. Hansen, J. Broeng, Crystal Fibre A/S (Denmark)

The goal of achieving high peak powers in fiber amplifiers before nonlinear effects degrade the signal pulse has been extensively explored in connection with solid core photonic crystal fibers (PCFs). Here the relatively large mode area achievable within single mode operation is exploited to reduce peak field intensity for a given signal power. Ultimately macro- and micro- bend loss constraints limit the mode area that is practical. Hollow core PCF offer the possibility of higher powers being tolerated before the onset of nonlinear effects since most of the light in the signal mode resides within the air core. These fibers have been used to

post-compress pulses which have been pre-chirped and passed through a conventional fiber amplifier. A simpler solution, which requires less interfacing and hence reduced reflections, is to use the hollow core PCF itself as an amplifier. The gain medium can either be an appropriate gas which is introduced into the core, or can be a rare-earth species introduced as a dopant to the glass which surrounds the core. The latter solid-state option is preferable due to ease of handling and because a higher intrinsic gain coefficient can be attained, but suffers from a small overlap of the guided signal mode with the active region. The prospect for doped hollow core PCF amplifiers will be reviewed, with particular emphasis on the impact of higher order core modes and core interface modes which compete for gain with the signal mode. Since the unwanted modes have a higher overlap with the gain medium than the signal mode, they must be rendered sufficiently lossy to prevent their amplification. To some extent this is provided by the inevitable roughness which exists at the glass / air interfaces within the fiber, but by careful design of the fiber to minimise the number of unwanted modes and to increase the loss of any of these modes which remain, the doped hollow core fiber has the potential to become a viable all-in-one high-power fiber amplifier.

6102-16, Session 5

Depressed clad hollow optical fiber with fundamental LP01 mode cut-off

J. Kim, P. Dupriez, D. B. S. Soh, C. A. Codemard, S. Yoo, Y. Jeong, J. Nilsson, J. K. Sahu, Univ. of Southampton (United Kingdom)

We propose and demonstrate a depressed-clad hollow optical fiber (DCHOF) for fiber laser applications, especially three-level lasers. The DCHOF consists of a ring-shaped core around an air hole in the centre and a depressed clad. According to our numerical model, such fibers provide a fundamental LP01 mode cut-off at a finite wavelength, which is useful to suppress unwanted laser transitions. In addition, the ring-shaped core can provide a relatively large pump absorption in cladding-pumped configurations. First, we demonstrated a cladding-pumped Nd-doped DCHOF laser operating at 930 nm. It generated a cw output power of 3.3 W at a slope efficiency of 41% with respect to the launched pump power with a diffraction limited beam (M2 of 1.05 with the output end of the fiber collapsed). When Q-switched, it reached 133 μJ of energy and 770 W of peak power at a repetition rate of 5 kHz. This is a record energy to the best of our knowledge. Secondly, a cladding-pumped Yb-doped DCHOF laser operating at 980 nm generated cw 7.5 W output power with M2 value of 2.7. Finally, a Yb-doped DCHOF generated an output power of 59 W at 1046 nm with a slope efficiency 81% with respect to the launched pump power when the fundamental LP01 mode cut-off was set at ~1060 nm. DCHOFs shows efficient laser performance on three-level transitions, which require efficient pump absorption and the suppression of unwanted four-level transitions. This has been enabled by the ring-shaped core and the LP01 mode cut-off characteristics of the DCHOF. Moreover, with such fiber geometry it is should be possible to reach kW-level output power from a Yb-doped fiber laser operating at shorter wavelengths, such as 1040 nm compared to the conventional 1100 nm, with high efficiency.

6102-18, Session 6

Super continuum generation for real time ultrahigh resolution optical coherence tomography

N. Nishizawa, Nagoya Univ. (Japan); A. D. Aguirre, J. G. Fujimoto, Massachusetts Institute of Technology

Optical coherence tomography (OCT) is an emerging technology for micrometer-scale, cross-sectional imaging of biological tissue and materials. One of the key limitations to achieving ultrahigh-resolution OCT imaging outside the laboratory setting has been the lack of compact, high-performance broadband light sources with sufficient power and stability to allow practical real-time imaging.

Compact, broad-bandwidth supercontinuum (SC) sources were recently demonstrated with femtosecond fiber lasers in combination with nonlinear fibers. Fiber lasers can provide a more compact and robust approach to ultrahigh resolution imaging when compared with bulk solid-state lasers.

In this paper, we describe recent studies on practical SC generation for ultrahigh-resolution OCT. SC generation is first analyzed both numerically and experimentally in terms of OCT and optimized conditions for generation are discussed. Supercontinua generated by use of highly nonlinear fiber which have a zero-dispersion wavelength near the pump wavelength, generally result in severe spectral modulation and fluctuating fine structure in the spectra. This spectral modulation produces sidelobes and reduced contrast in the interferometric point-spread function. In contrast, normally dispersive, highly nonlinear fibers (ND-HNFs) can generate smooth and Gaussian shaped supercontinua by the combination of self-phase modulation and normal dispersion. Low noise and wideband SC generation is demonstrated using ND-HNFs. Two colored SC generation is also demonstrated using photonic crystal fiber which has two close zero dispersion wavelengths. The numerical results agree with the experiments.

All fiber, low noise SC generation is demonstrated based on an ultrashort pulse fiber laser. Wideband, low noise, near Gaussian shaped, high power SC is generated in the 1.55 μm wavelength region. In vivo, high-speed OCT imaging of human skin with ~5.5 μm resolution and 99 dB sensitivity is demonstrated. Recent progress in SC generation and ultrahigh resolution OCT imaging is also reported.

6102-19, Session 6

Fiber optic applications in biomedical metrology and microscopy

S. A. Yun, Harvard Medical School and Massachusetts General Hospital

Fiber optics has undergone rapid developments over the last decade driven by the expansion of telecommunications. The tremendous advances in optical components, specialty fibers, and high-power fiber lasers are now being rapidly adapted for use in non-telecom applications. In this talk, I will review the recent progress in biomedical instrumentations using the advanced fiber optic technologies. The new instruments include in vivo confocal and multiphoton microendoscopy, optical coherence tomography, and 3-dimensional endoscopy. New technical challenges and potential solutions will be discussed.

6102-20, Session 6

Advances in femtosecond fiber lasers for THz applications

G. D. Sucha, G. Imeshev, M. L. Stock, IMRA America, Inc.

Terahertz spectroscopy and imaging are gaining importance in application areas such as security and product inspection. The ability to "look" through common materials, and to identify signatures of various chemicals such as explosives, illegal drugs, and pharmaceuticals has attracted a great deal of attention, and shows promise in areas such as portal security, for example. The vast majority of pulsed THz systems in research labs are driven by modelocked Ti:sapphire lasers which are rather large, complex, and require water cooling. Although they are well-tailored toward their specific applications, current versions of commercial pulsed THz systems have not advanced much beyond the research versions in terms of the laser source, and are thus limited in the degree to which they can be made compact, portable, and practical. The future of THz applications will hinge upon the use of compact, lightweight, and easy-to-use THz systems. This, in turn, depends critically on the availability of truly practical femtosecond laser sources. Key attributes of a laser source for THz systems include higher power, small size, portability, ease of operation, room temperature operation, environmental stability, and no water cooling. This talk will present recent advances made in the development of a variety of compact femtosecond fiber lasers which address these

points. Performance characteristics of THz systems driven by compact fiber lasers will also be described. Additionally, these Erbium:fiber based laser sources provide pulses at 800 nm (to drive conventional THz emitter & receivers) as well as 1600 nm, which can drive new types of long-wavelength THz transceivers based on new materials. This enhances the possibility of fiber-delivery, making the systems even more convenient. These new fiber lasers are well-suited to drive the portable, convenient THz systems of the future.

6102-21, Session 7

MW peak-power, mJ pulse energy, multi-kHz repetition rate pulses from Yb-doped fiber amplifiers

F. Di Teodoro, C. Brooks, Aculight Corp.

Despite the impressive progress in power scaling CW and quasi-CW optical fiber sources, fewer high-power results are available in the “Q-switch” pulsed regime characterized by pulse durations of a few ns or less and multi-kHz pulse repetition rates. A challenge for fiber amplifiers operating in this regime is the generation of high peak power with minimal nonlinear effects. Additional challenges include containment of inter-pulse amplified spontaneous emission and avoidance of optical damages. In this paper, we demonstrate the potential of fibers to generate high peak powers in pulses of excellent spectral/spatial quality.

In the first setup, a 1-ns pulse, Q-switched microchip laser (1062nm) operating at ~10-kHz pulse repetition rate (PRR) seeded a dual-stage amplifier featuring a 40-μm-core Yb-doped photonic-crystal fiber (PCF) as the power amplifier. From this amplifier, we obtained diffraction-limited (M2 = 1.05), ~1ns pulses of 1.1mJ energy, ~1.1MW peak power, ~10.2W average-power, spectral linewidth ~9GHz, negligible nonlinearities, and slope efficiency >73%. To our knowledge, these values amount to the best combined performance from a multi-kHz fiber source.

In the second setup, we replaced the seed source with a shorter-pulse (<500ps) microchip laser (1064nm) of PRR ~ 13.4 kHz and obtained diffraction-limited (M2=1.05), ~450ps pulses of energy \>0.7mJ, peak power in excess of 1.5 MW (the highest from a diffraction-limited fiber source), average power ~9.5W, spectral linewidth <35 GHz. To show further power scaling, these pulses were amplified in a 140-μm-core Yb-doped fiber, which yielded multimode (M2 ~ 9), 2.2mJ-energy, 30-W average-power pulses of peak power in excess of 4.5MW, the highest ever obtained in an optical fiber source.

6102-22, Session 7

High-peak-power (>1.2 MW) pulsed fiber amplifier

R. L. Farrow, D. A. V. Kliner, A. Hoops, J. P. Koplow, Sandia National Labs.

Bend-loss-induced mode filtering has allowed pulsed fiber lasers to be scaled to mJ pulse energies and MW peak powers while maintaining diffraction-limited beam quality, making these sources competitive with more traditional diode-pumped, solid-state lasers. We report recent results from Yb-doped fiber amplifiers seeded with a variety of pulsed seed sources.

The apparatus consisted of a Yb-doped, double-clad fiber that was end-pumped by a fiber-coupled diode bar and seeded by a passively Q-switched, Nd:YAG microchip laser. We used two different Yb-doped fibers; each fiber had a core diameter of ~30 microns, core numerical aperture (NA) of ~0.07, inner-cladding diameter of 250 microns, and inner-cladding NA of ~0.46. High Yb-doping levels provided a large pump-absorption coefficient (>15 dB/m at 976 nm), allowing the use of relatively short fibers (1-2 m). The double-clad fiber had a V-number of ~6 (at 1064 nm wavelength) but was coiled on two orthogonal spools of ~7 cm diameter to suppress high-order modes. The pump laser provided up to 50 W of power at ~976 nm from a fiber with a core diameter of 200 microns and NA of 0.22. The output of the pump fiber was imaged onto the input face of the double-clad fiber with a 1:1 telescope, providing a net coupling efficiency of 91%. Several commercial or home-built Nd:YAG (1064 nm) microchip lasers were used as seed sources; these lasers had pulse durations of 0.38-2.3 ns FWHM, pulse energies of 0.02-0.07 mJ, and repetition rates of 1.0-33 kHz, allowing us to investigate the trade-offs among peak power, pulse energy, and average power. The seed pulse was launched counter-propagating to the pump beam. The output of the fiber amplifier was characterized temporally (with 25 ps resolution), spectrally (with 0.017 nm resolution), and spatially (using a CCD camera).

When seeded with 0.38 ns pulses at 1.0 kHz and pumped with 11 W, the first fiber provided output pulses with a peak power of >1.2 MW and pulse energy of 0.57 mJ. This fiber did not support single-transverse-mode operation, but coiling the fiber provided an output beam with M2 = 2.1 (measured using Siegman’s second-moment method). The pulses exhibited spectral and temporal distortion caused by self-phase modulation (SPM), but we observed no evidence of stimulated Raman scattering. The peak irradiance in the core was >200 GW/cm2, but no optical damage was observed. The effects of SPM were reduced when using a seed pulse duration of 0.63 ns. The second fiber provided a diffraction-limited output beam (M2 = 1.1) and a pulse energy of up to 0.63 mJ.

6102-23, Session 7

Development of an efficient fiber-laser-produced plasma source of EUV radiation

A. Mordovanaki, K. Hou, J. A. Nees, B. X. Hou, A. M. Maksimchuk, G. Mourou, A. Galvanauskas, Univ. of Michigan

Over the last few years development of large core fibers has led to the demonstration of MW peak power nanosecond-long pulses in multimode as well as diffraction-limited beams. Significance of these achievements is that, for the first time, fiber lasers became capable of high-intensity plasma generation. Here we report fiber-laser driven EUV/soft X-ray radiation generation in the 10-nm to 20-nm spectral range. We achieved efficient (~1%) generation in 2% BW at λ=13.5nm, thus demonstrating the potential for fiber-laser based compact high-power light sources for the next generation lithography instruments.

We demonstrated efficient generation of EUV light from solid Tin (Sn) target using a Ytterbium-doped all-fiber system operating at 1064-nm. It is seeded with an electric pulse driven scheme that offers full control of the pulse shape and duration and allows the intentional introduction of a pre-pulse for controllable plasma pre-heating. The seed pulses are then amplified in a four-stage amplifier system to multi-mJ energies. These amplified 3 - 5-ns pulses are directed to irradiate the target at 45o incidence in a vacuum environment. A grazing incidence spectrometer was used to characterize the radiation emitted in the range 6-30nm. A specially designed diode was used to measure the conversion efficiency from laser light into a 2% bandwidth around 13.5-nm as a function of the input pulse energy, pulse shape and the intensity on target. EUV spatial distribution in the table plane was also measured.

A discussion on the merits of our fiber-based approach will be included with regard to multi-kW power scalability and migration toward sub-nanosecond regimes.

6102-24, Session 7

High peak power ytterbium doped fiber amplifiers

W. E. Torruellas, Y. Chen, B. McIntosh, Fibertek, Inc.; J. Faroni, K. Tankala, Nufern; S. Webster, D. J. Hagan, M. J. Soileau, College of Optics and Photonics/Univ. of Central Florida

Ytterbium doped optical fibers have shown remarkable optical efficiencies, CW powers in excess of 1kW while maintaining good optical beam quality. However, significant challenges remain in the power scaling of short pulse (~ns duration), lower repetition-rate fiber laser systems. In this regime, the value of the laser system comes from the higher peak power and significant pulse energy but management of phenomena such as Amplified Spontaneous Emission (ASE), Stimulated Raman Scattering

(SRS) Self-Focusing (SF) and primarily optically induced damage become paramount.

To date Fibertek has delivered near diffraction limited, M2<1.15, peak powers in excess of 1.75MW in engineered double-cladding Ytterbium doped silica fibers and stable operation over days. We believe this represents the highest peak power reported in such fibers with 1ns pulses. While we are operating below the self-focusing limit, interestingly, the energy fluence is comparable to the reported value for single pulse optical damage in pure fused silica. At the conference we will report on our progress towards achieving even higher peak powers for 1 nanosecond pulses and our testing and current understanding on the limitation of optical damage in these fibers.

6102-25, Session 8

10 mJ pulse energy and 200 W average power Yb-doped fiber laser

S. Maryashin, A. O. Unt, V. P. Gapontsev, IPG Laser GmbH (Germany)

We report on the 10 mJ energy per pulse and 200 W average power pulsed Yb fiber laser. MOPFA configuration with 65 um core multi-clad powerful amplifier allows to provide 300 ns optical pulses in wide frequency range of 1 - 50 kHz. Master oscillator is based on first relaxation peak all-fiber generator. Wall plug efficiency of 25% and 10 m long delivery output with isolated head are essential features for industrial product. More details and results would be discussed.

6102-26, Session 8

Pulsed high peak power amplifiers in a monolithically integrated all-fiber configuration

M. L. Jäger, S. Caplette, P. Verville, C. A. Delisle, A. Wetter, F. Séguin, F. Gonthier, ITF Optical Technologies, Inc. (Canada)

With the recent improvements in fiber design and manufacturing combined with the advent of fiber-coupled high-brightness pump diodes, fiber lasers and amplifiers have become prime candidates for applications where high power and excellent beam quality are required. While the tight confinement is advantageous for achieving high gain, it also lowers the threshold power for nonlinear optical effects and optical damage. Power scaling is therefore a matter of increasing the effective area of the core, which will increase the saturation energy and therefore the extractable energy. However, quasi-single-transverse-mode operation should be maintained at the same time for good beam quality.

Large-mode-area (LMA) fibers are currently the best choice for high power all-fiber based lasers and amplifiers; however, preservation of the fundamental LP01 mode in these few-moded fibers is critical.

We report on amplification experiments with all-fiber power amplifiers with fiber core diameters of 20μm and 30μm, which significantly reduces the onset of nonlinear optical effects as well as the damage threshold. In excess of 0.5mJ of output energy has been achieved while maintaining excellent beam quality. A directly modulated diode laser followed by two single-mode fiber amplification stages was used to seed the power amplifier. This MOPA design provides maximum flexibility in varying the pulse width, repetition rate and the seed energy. We will also present results on polarization-maintaining amplifiers and high power reliability data. The complete system is monolithically integrated in an all-fiber configuration with the exception of the isolators.

6102-27, Session 8

High peak power, high rep rate pulsed fiber laser for marking applications

M. Zervas, M. Durkin, K. Vysniauskas, A. Gillooly, F. Ghiringhelli, L. Hickey, P. Turner, B. Kao, Southampton Photonics, Inc. (United Kingdom); T. Hoult, Southampton Photonics, Inc.

Fibre pulsed lasers are increasingly adopted as the laser of choice in a number of industrial applications, such as micromachining, drilling and marking. In peak power driven applications, such as marking, it is essential to retain high peak powers (in excess of 2.5 to 10 kW) at high repetition rates which translates into faster character marking and increased throughput.

Conventional single-stage Q-switched lasers, although very efficient in storing energy, are characterised by variable average power and substantial peak-power drop as the repetition rate is increased. In most cases, the peak power can drop below the process (e.g. marking) threshold with an adverse effect on speed and throughput. MOPA configurations, on the other hand, can offer more controllability over the pulse characteristics and power performance of the pulsed laser and extend the operation space of a marking unit to higher repetition rates offering increased marking speed.

In this presentation, we report for the first time on a pulsed fibre MOPA configuration, which maintains the peak power over a 5 - 10kW level for rep rates in excess of 200kHz. The MOPA configuration comprises a directly modulated 1080nm laser diode seed, followed by a two-stage all-fibre amplification unit and an additional delivery fibre. The average power is in excess of 12W, the pulse energy lies in the 0.1-0.5mJ range, the pulse duration varies between 10ns and 200ns, while the peak power remains constant at about the 5kW or 10kW level for rep rates in the range 10kHz to >200kHz. To the best of our knowledge, this is the first time that such a pulsed laser performance is reported and it is expected to have a big impact in the industrial applications arena, such as the development of efficient and very fast marking machines.

6102-66, Session 8

Evaluation of a high power Q-switched Tm3+ doped silica fiber laser operating near 2um

A. F. El-Sherif, Military Technical College (Egypt)

The performance of operations and characteristics of three different modulation techniques of Q-switched Tm3+ doped silica fibre laser operating near 2 um are described. Various Q-switched regimes are observed for a range of modulation frequencies and fibre lengths when the fibre is end-pumped with a high power Nd: YAG laser operating at 1.319 um in a linear bidirectional cavity. A larger multimode core of 17 mm diameter is used to increase the laser gain volume and achieve higher pulse energy. Experimentally this laser produced pulses with a peak power of 18.5 W, at higher repetition rate of approximately 20 kHz, a single Q-switched pulse of duration 300-ns at full width at half-maximum (FWHM), and 5.5 mJ are observed by using optical (mechanical) chopper. A peak power of ~ 3.3 kW and pulse duration at FWHM of 320 ns at low repetition rate of 50-70 Hz and highest pulse energy up to 2.3 mJ by using an electro-optic modulator (EOM) is obtained. This peak power is enhanced to be 4.1 kW and shortest pulse duration at FWHM of 150 ns at low repetition rate of 100-500 Hz by using acousto-optic modulator (AOM) is obtained. The results presented show that Q-switching is currently limited by the performance of the intracavity modulator. In this paper, an evaluation of the high performance of active Q-switched Tm3+ doped fibre laser with various techniques are discussed and some reasons for the difference in performance and some potential routes to improvements are presented.

6102-28, Session 9

Scaling fiber lasers beyond kW power levels by spectral beam combining

T. H. Loftus, C. E. Hamilton, P. R. Hoffman, A. Thomas, Aculight Corp.

We report on our efforts to extend Yb fiber lasers beyond 1 kW by a scalable architecture that maintains near-diffraction-limited beam quality. For this work, power scaling is performed at two levels. The first uses a diffraction grating to spectrally beam combine (SBC) several master-oscillator power-amplifier (MOPA) fiber lasers to achieve a single combined output. The second involves scaling the individual MOPA outputs to \>

200 W, thereby reducing the number of lasers required to achieve the \>1 kW SBC power goal. As a step in this direction, we have used 59 W from a 1055 nm MOPA and 51 W from a 1065 nm MOPA to obtain a combined beam with 102 W of power with near-diffraction-limited beam quality. Experiments have demonstrated that the SBC diffraction grating can achieve irradiances > 1 kW/cm2 with minimal optical distortion. Each power amplifier is a double-clad, polarization maintaining, large mode area fiber pumped at 976 nm with up to 400 W of power. Each amplifier is seeded by a tunable, single frequency, master oscillator followed by a series of fiber pre-amplifiers. To suppress stimulated Brillouin scattering in the power amplifier, the seed source is modulated to produce 5 ns pulses at a 10 MHz repetition rate. Recently, we have demonstrated up to 208 W from a single MOPA, maintaining narrow linewidth and polarized output. We will describe our results on increasing individual MOPA power, increasing the number of MOPAs in the SBC system, and progress towards our ultimate goal of \>1 kW output.

6102-29, Session 9

Spectral combining of fiber lasers

F. Røser, A. Liem, T. Schreiber, S. Höfer, J. Limpert, Friedrich-Schiller-Univ. Jena (Germany); T. Peschel, R. Eberhardt, Fraunhofer-Institut für Angewandte Optik und Feinmechanik (Germany); A. Tünnermann, Friedrich-Schiller-Univ. Jena (Germany) and Fraunhofer-Institut für Angewandte Optik und Feinmechanik (Germany)

That rare-earth-doped fiber laser constitute a power-scalable solid-state laser concept has been proven by several demonstration of kW-class continuous-wave fiber laser systems with excellent beam quality. Nevertheless, there are restrictions due to nonlinearity, thermo-optical behavior and fiber damage. Thus, besides pushing the limits of single fiber emission, a promising way for further power scaling is combining of many fiber lasers. Several approaches have been discussed so far. They can be divided into two classes: coherent and incoherent combining. Both are possible in laser and amplifier configuration and have certainly different requirements and limitations.

In this contribution, we report on spectral (incoherent) combining of several fiber lasers to a power level well above 100 W with close to diffraction-limited beam quality. Furthermore, we will discuss the scaling potential which is given by the amplification bandwidth and possible wavelength separation of the emission of single fiber lasers. Beyond that the power handling capabilities of the combining elements will be a key issue if the real potential of the approach wants to be used. Optimized setups, regarding damage, thermo-optical and thermo-mechanical properties, will be discussed.

6102-30, Session 9

Coherently coupled high power fiber arrays

M. G. Wickham, Northrop Grumman Corp.

The status of our coherently combined, high power fiber array will be presented. We have recently coherently combined 470W of power from a 4-element fiber array. A description of the architecture and a presentation of the results obtained to date will be presented. This effort represents the results of a multi-year effort to achieve high power for a single element fiber amplifier and to understand the important issues involved in coherently combining many individual elements to obtain weapons class optical power for directed energy weapons. We will also discuss our vision on the next steps for this technology. Northrop Grumman Corporation and the High Energy Laser Joint Technology Office jointly sponsored this work.

6102-31, Session 9

Self-referenced locking of optical coherence by single-detector electronic-frequency tagging

T. M. Shay, V. N. Benham, J. B. Spring, B. G. Ward, F. Ghebremichael, M. A. Culpepper, A. D. Sanchez, Air Force Research Lab.; J. T. Baker, The Boeing Co.; D. E. Pilkington, R. W. Berdine, Air Force Research Lab.

We report a novel coherent beam combining technique. This is the first electronically phase locked optical fiber array that eliminates the need for a separate reference beam. In addition, only a single photodetector is required. The far-field central spot of the array is imaged onto the photodetector to produce the phase control loop signals. Each leg of the fiber array is phase modulated with a separate RF frequency, thus tagging the optical phase shift for each leg by a separate RF frequency. The optical phase errors for the individual array legs are separated in the electronic domain. In contrast with the previous electronic phase locking techniques, in our system the reference beam is spatially overlapped with all the RF modulated beams fiber leg beams onto a single detector. The phase shift between the optical wave in the reference leg and in the RF modulated legs are measured separately in the electronic domain and the phase error signal is feed back to the LiNbO3 phase modulator for that leg to minimize the phase error for that leg relative to the reference leg. The advantages of this technique are 1) the elimination of the reference beam and beam combination optics and 2) the electronic separation of the phase error signals without any degradation of the phase locking accuracy. We will present the first theoretical model for self-referenced LOCSET and preliminary experimental results.

6102-32, Session 9

Multi-core photonic crystal fibers for high power laser and amplifiers

L. F. Michaille, C. R. Bennett, D. M. Taylor, T. J. Shepherd, QinetiQ Ltd. (United Kingdom)

The intensity of the laser field is the main limitation of fibre lasers/amplifiers operating in pulsed operations. Enlarging the core area is one method to reduce the intensity therefore enhancing the damage threshold and increasing the total output energy. Using multicore Photonic Crystal Fibre (PCF) is another technique to scale up the modal area. Previous results using 6 and 7 core PCF have shown single mode laser action with a mode field diameter of more than 40μm and slope efficiency larger than 50% up to the 100W output power level. In order to assess the scalability of this technique, we will present the phase locking and the modal properties of a novel 18-core PCF (having a mode field diameter of more than 60μm for the fundamental in-phase supermode) and its CW lasing properties in terms of threshold, slope efficiency, beam quality and wavelength tuneablility. The most novel results will be concentrated around the Q-switching laser action of these fibres using an acousto-optic modulator. Parameters like pulse duration, repetition rates and maximum pulse energy will be discussed.

6102-33, Session 10

Exploiting nonlinearity in femtosecond fiber amplifiers

F. W. Wise, L. Kuznetsova, A. Chong, S. Zhou, Cornell Univ.

Conventional wisdom holds that nonlinear effects must be minimized to obtain the best performance from chirped-pulse amplifiers. We show how nonlinearity can be used to advantage in short-pulse fiber amplifiers.

This approach offers practical benefits and promises substantial increases in the pulse energies available from femtosecond fiber amplifiers.

6102-34, Session 10

Ultrafast high energy amplifiers beyond the B-integral limit

L. Shah, Z. Liu, I. Hartl, G. Imeshev, G. Cho, M. E. Fermann, IMRA America, Inc.

High average power single-mode fiber lasers have attracted significant attention as alternatives to conventional solid-state lasers owing to their relative high brightness, compactness and robustness. Likewise the turn-key operation of industrially qualified ultrafast fiber oscillators is well established. In recent years the convergence of reliable ultrafast fiber oscillators, high brightness pump diodes and high power fiber amplifiers has enabled ultrafast fiber lasers to surpass ultrafast solid-state lasers in terms of average power. While fiber lasers have generally not been able to match the ultrashort pulse energies produced by solid-state lasers, careful management of nonlinearities can overcome the conventional B-integral limit of pi thereby permitting stable operation of practical ultrafast fiber lasers with pulse energies approaching the milli-Joule level. Here we review modes of nonlinear propagation in fibers which have enabled increases in ultrashort pulse energies from nano-Joule to milli-Joule levels, namely: solitons, similaritons and cubicons. As an example of a practical high energy ultrafast fiber laser, we demonstrate a cubicon Yb fiber chirped pulse amplification system producing 650 fs pulses with >100 micro-Joule energy and the utility of this laser in several applications.

6102-35, Session 10

20 W, 50 fs pulses from a fiber laser system using nonlinear fiber compression

F. Røser, T. Schreiber, A. Liem, J. Limpert, A. Tünnermann, Friedrich-Schiller-Univ. Jena (Germany)

High average power ultra-short laser pulses find a number of applications e.g. in medicine, spectroscopy and basic science. One very powerful technique for generating intense ultra-short laser pulses is the nonlinear femtosecond fiber compression. Intense short laser pulses are send through a waveguide wherein nonlinear effects, mainly self-phase modulation (SPM), lead to spectral broadening. By removing the imposed chirp a significant reduction of pulse duration compared to the initial pulse width can be obtained.

In this contribution we report on the generation of 50fs pulses with an average output power of more than 20W, achieved in a compact setup applying nonlinear compression using a large-mode-area photonic crystal fiber and a pair of chirped mirrors. Initial pulses are produced by a high average power ytterbium-doped fiber CPA system, delivering even up to 131 W in 220 fs pulse duration at a repetition rate of 73 MHz [1]. A portion of the power is launched with a coupling efficiency of 80% into a large-mode-area photonic crystal fiber with a mode-field area of ~1000 μm2 and a length of 1.5 cm. At 20 W transmitted average power the spectral bandwidth is increased to ~ 40 nm. Subsequent, the pulses are send through a pair of chirped mirrors. 12 bounces at mirrors with a GVD of -250 fs2 did result in a compression down to sub-50 fs pulse duration. Therefore, the compact system produces a peak power of 5.5 MW. Beyond the results, scaling possibilities and limitations will be discussed.

[1] F. Røser, J. Rothhard, B. Ortac, A. Liem, O. Schmidt, T. Schreiber, J. Limpert, A. Tünnermann, “131 W 220 fs fiber laser system“, accepted in Optics Letters.

6102-36, Session 10

Compact μJ-level all-polarization maintaining femtosecond fiber source

T. Schreiber, B. Ortac, C. K. Nielsen, J. Limpert, A. Tünnermann, Friedrich-Schiller-Univ. Jena (Germany)

Compact and environmentally stable high energy and high average power ultra-short pulse laser sources have many applications. Examples are eye surgery (ophthalmology), index modification in transparent materials (waveguide writing) and frequency conversion. Fiber based short-pulse lasers have been demonstrated to be an ideal candidate for compact femtosecond laser sources. However, so far mode-locked fiber laser systems suffer from lack of stability of non-polarization maintaining components and lack of self-starting.

In this contribution, we report on all-PM fiber femtosecond source delivering up to 1.2 μJ pulse energy at 17 MHz in 200 fs pulses. The compact system starts with a novel passively mode-locked fiber oscillator scheme comprising a polarization maintain ytterbium-doped fiber, polarization-maintaining couplers, a dispersion compensation stage using compact transmission gratings and a SESAM. All components are arranged in a linear cavity. The oscillator is self-staring and due to the PM fibers environmentally stable and delivers 2 mW of linearly chirped parabolic pulses (similaritons) of about 8 ps duration at 17 MHz repetition rate and 1030 nm center wavelength. The pulses can be recompressed to 200 fs duration. The output of the oscillator is spliced to a PM ytterbium-doped fiber preamplifier boosting the average power to 50 mW. The pulses are slightly stretched to about 12 ps. The main amplifier consists of a low nonlinearity single-polarization large-mode-area ytterbium-doped photonic crystal fiber. This fiber had a length of 1.2 m and a mode-field-area about 700 μm2. This amplifier is capable to produce an average power of 29 W with a slope efficiency of ~75 %. The polarization extinction ratio is better than 23 dB. Recompression to 200 fs duration is done with a pair of transmission gratings with a grating distance of just 2 cm resulting in 21 W average power corresponding to 1.2 μJ pulse energy. Beyond these results we will discuss the advantages of amplifying parabolic pulses instead of conventional pulse shapes such as sech2 or Gaussian.

6102-37, Session 10

High average power and energy-scalable fiber CPA at 1558-nm using chirped volume Bragg grating pulse stretchers and compressors

M. Cheng, Univ. of Michigan; V. I. Smirnov, E. Flecher, L. B. Glebov, College of Optics and Photonics/Univ. of Central Florida; A. Galvanauskas, Univ. of Michigan

Technological advantage of fiber-based chirped-pulse amplifiers is in their potential to provide high average power ultrashort pulses from compact and robust packaged systems. However, the currently used high-power-compatible compact compressors, such as chirped fiber Bragg gratings or hollow-core fiber compressors, are not energy scalable beyond ~1-μJ. Therefore, simultaneous high pulse energy and high average power generation from a compact fiber system is not achievable with these technologies.

Here we report development of high average power 1558-nm fiber CPA system using recently demonstrated novel compact pulse stretching/compressing technology based on linearly-chirped volume Bragg gratings in photo-thermal glass (PTR CVBG). The main advantage of this new compression technology is that it is compact, compatible with high average powers, and is energy scalable into >1-μJ to >1-mJ range.

We are developing an all-fiber high-power CPA system, which consists of a mode-locked fiber oscillator, a single-mode Er-doped fiber pre-amplifier, a polarization-maintaining double-clad Er/Yb-doped LMA-fiber power amplifier, and a PTR CVBG based 1-cm long pulse stretcher and compressor. In the initial demonstration we have achieved bandwidth-limited sub-picosecond recompressed pulses with >10-W of average power at 40-MHz repetition rate. CVBG stretcher/compressor has been used in a reciprocal configuration, where stretching of seed pulses from a fiber oscillator and recompression of amplified pulses has been performed in the same grating using pulse incidence from two opposite propagation directions along the grating. Effect of fiber amplifier dispersion has been compensated by using positive-dispersion fiber prior to the pre-amplifier stage. Further power scaling is in progress. It is important to note that such reciprocal configuration is free from the dispersion-mismatch limitations occurring in hybrid fiber or fiber-grating stretching and diffraction-grating compressing CPA systems.

6102-38, Session 11

Intense ultra-short fiber laser systems and their applications

J. Limpert, F. Røser, T. Schreiber, A. Tünnermann, Friedrich-Schiller-Univ. Jena (Germany)

We will review the performance of high average power and high energy femtosecond fiber laser systems. Remarkable evolutions in fiber technology made it possible to overcome restrictions due to nonlinear pulse distortions in the amplification fiber and revealed the full potential of rare-earth-doped fibers as a power-scalable solid-state laser concept in the short pulse regime. State-of-the-art femtosecond fiber lasers in our labs deliver average powers well above 100 W and pulse energies of several 100 μJ in the 1 μm wavelength region. This performance, in particular the significantly higher repetition rate compared to conventional femtosecond lasers, allows for unique approaches in several application fields.

Beyond the fiber designs, the setup, performance and limitations of these systems we will discuss applications e.g. high speed and high precision micromachining of metals and pumping of nonlinear optical processes such as parametric amplifiers.

6102-39, Session 11

High energy, short pulse fiber laser front end for kilo-Joule class CPA systems

J. W. Dawson, S. Mitchell, R. J. Beach, M. J. Messerly, C. W. Siders, C. P. J. Barty, Lawrence Livermore National Lab.

We are developing an all fiber laser system optimized for providing input pulses for short pulse (1-10ps), high energy (~1kJ) glass laser systems. Fiber lasers are ideal solutions for these systems as they are highly reliable and enable long term stable operation.

The design requirements for this application are very different than those commonly seen in fiber lasers. High-energy lasers often have low repetition rates (as low as one pulse every few hours), and thus high average power and efficiency are of little practical value. What is of high value is pulse energy, high signal to noise ratio (expressed as pre-pulse contrast), good beam quality, consistent output parameters and timing. Our system focuses on optimizing these parameters.

Our prototype system consists of a mode-locked fiber laser, a compressed pulse fiber amplifier, a “pulse cleaner”, a chirped fiber Bragg grating, pulse selectors, a transport fiber system and a large flattened mode fiber amplifier. In our talk we will review the system in detail and present theoretical and experimental studies of critical components. We will also present experimental results from the integrated system including high dynamic range background free auto-correlation data from recompressed pulses up to the 100 micro-Joule level.

6102-40, Session 12

Self-similar low-noise femtosecond ytterbium-doped double-clad fiber laser

B. Ortac, J. Limpert, Friedrich-Schiller-Univ. Jena (Germany); A. Hideur, C. Chedot, M. Brunel, G. Martel, Univ. de Rouen (France)

In recent years, femtosecond ytterbium-doped fiber lasers have attracted great interest because of their broad gain bandwidth and high optical efficiency. Ytterbium fiber oscillators with pulses width as short as 36 fs and energies as high as 5 nJ has been reported [1-3]. More recently, Ilday et al. have demonstrated the generation of self-similar pulses directly from an Yb fiber oscillator [4]. This new regime of operation tolerates pulses with higher non-linear phase shift than in soliton and stretched-pulse fiber lasers, opening the way to higher pulse energies. Theoretical calculations show that femtosecond pulses with hundreds of nanojoules could be generated in similariton fiber lasers [4]. All the experimental and theoretical demonstrations of self-similar pulse evolution have considered a minimal length of gain fiber (some tens of centimeters). Experimentally, this was possible using highly-doped Yb gain fiber, core pumped with single-mode laser diodes. Thus, self-similar femtosecond pulses with 14 nJ have been achieved [5]. The best way to reach higher energies is to use the double-cladding (DC) technology. Nevertheless, the weak absorption efficiency in the cladding-pumped DC fibers require the use of larger length of gain fiber.

In this communication, we report the generation of self-similar femtosecond pulses from a side-pumped ytterbium-doped double-clad fiber laser. Positively-chirped parabolic pulses with 6.4 ps duration and more than 3.2 nJ energy are obtained. These pulses are extra-cavity compressed to 140 fs. This regime of emission ensures very low-noise operation with less than 0.05 % amplitude fluctuations.

[1] F. Ö. Ilday, J. Buckley, L. Kuznetsova and F. W. Wise, Opt. Express 11, 3550 (2003).

[2] B. Ortac, A. Hideur, T. Chartier, M. Brunel, C. Õzkul, F. Sanchez, Opt. Lett. 28, 1305 (2003).

[3] F. Ö. Ilday, J. R. Buckley, H. Lim, F. W. Wise, W. G. Clark, , Opt. Lett. 28, 1365-1367 (2003).

[4] F. Ö. Ilday, J. R. Buckley, W. G. Clark and F. W. Wise, Phys. Rev. Lett. 92, 213902 (2004).

[5] J. R. Buckley, F. W. Wise, F. Ö. Ilday and Sonowski, ASSP’2005, paper WE5 (2005).

6102-41, Session 12

All-fiber, pigtailed, passively modelocked laser oscillator at 1.5μm with 2.2W average power and 160MHz repetition rate

P. G. Polynkin, A. Polynkin, D. Panasenko, M. Mansuripur, J. V. Moloney, N. N. Peyghambarian, The Univ. of Arizona

The heavily doped active fibers based on the soft phosphate glass offer an attractive gain medium for compact and high-power laser oscillators. We report for the first time to our knowledge, a passively modelocked, all-fiber laser at 1.5um based on such active fiber. The standing-wave laser cavity consists of a 20cm-long piece of the side-pumped, active phosphate fiber, which is heavily co-doped with Er and Yb ions, and a low-ratio fused coupler. The length of the fully spliced laser cavity is ~60cm. The cavity is terminated by a passive broadband mirror deposited directly on the cleaved fiber end from one side, and by a butt-coupled semiconductor saturable absorber mirror (SESAM) from the other. The modelocked operation of the laser is started and sustained by the SESAM, and neither any additional pulse narrowing mechanism such as nonlinear polarization evolution, nor dispersion compensation of any kind is used. In order not to over-saturate the SESAM, and therefore to achieve high peak pulse power at the output of the laser, the fiber end which is butt-coupled to the SESAM is tapered which expands the propagating fiber mode and decreases the power density incident on the absorber substantially. The stable modelocked operation of the laser occurs in the range between 1.53W and 2.23W of the average output power, which is limited by the maximum available pump power at 975nm. The optical-to-optical efficiency of the laser is ~10.5%. The peak pulse power is limited by the saturated SESAM at ~450W, and the pulse width grows linearly from 20psec to 45psec as the pump power is increased. At the pulse repetition rate of 160MHz, the pulse energy reaches 14nJ. The laser combines the convenience of the all-fiber construction with the performance previously achieved only with the modelocked solid-state laser oscillators.

6102-42, Session 12

Single pulse and bound state operation of a self-starting self-similar all-PM Yb-doped fiber laser

C. K. Nielsen, B. Ortac, T. Schreiber, J. Limpert, R. Hohmuth, W.

Richter, A. T¸nnermann, Friedrich-Schiller-Univ. Jena (Germany)

Fiber-based laser systems are well-suited for ultra-fast applications as they have a large amplification bandwidth supporting ultrashort pulses and exhibit improved stability and freedom from misalignment. In addition, they offer compact design with inexpensive components and are suitable for high average power applications because their geometry leads to efficient heat dissipation. However, the fundamental limit of the generation of high-energy ultrashort pulses directly from a fiber laser are nonlinear effects causing pulse distortions and pulse break-up. Usually, the pulse formation dynamics are controlled by interplay between the anomalous group-velocity dispersion and the Kerr nonlinearity to achieve soliton like pulses with pulse energies of some ten picojoule. To break the nonlinear limits, stretched pulse lasers with output energies up to some nanojoules have been demonstrated by incorporating an amount of normal dispersion inside the cavity. Recently, self similar propagation inside fibers with normal dispersion and gain have been exploited resulting in linearly chirped parabolic pulses with pulse energies higher than those in stretched pulse fiber lasers. However, so far self-similar pulses have only been generated from fiber lasers based on the non-linear polarization evolution in the ring geometry, which are sensitive to environmentally induced changes in birefringence of the non-PM fibers used. In contrast, we report, to the first time to our knowledge, on a linear cavity made of all PM Yb-doped single mode fibers, thus being intrinsically environmental stable. A saturable absorber mirror is used as a nonlinear loss to achieve mode-locking. Beside the stretched pulse regime we demonstrated self-starting self-similar pulse evolution inside this fiber oscillator. Clean single pulses with energies of 1 nJ at a repetition rate of 17 MHz were obtained. The pulses with a spectral bandwidth of 12 nm at center wavelength of 1035 nm could be externally compressed to 180 fs. Additionally, we observed stable self-starting bound state output at higher pump powers, where the temporally constant pulse separation of 10 ps is confirmed by autocorrelation and spectral measurements.

6102-43, Session 12

Wide and fast wavelength-tunable mode-locked fiber laser using dispersion tuning

M. Asano, S. Yamashita, The Univ. of Tokyo (Japan)

We demonstrate a wide and fast wavelength-tunable mode-locked fiber laser based on tuning the mode-locking frequency. The laser is a sigma-laser configuration composed of a wideband (3dB-bandwidth ~ 70nm) semiconductor optical amplifier (SOA) at 1.3μm as a gain medium, 20m-long dispersion compensation fiber (DCF), polarization beam splitter (PBS), a Faraday rotation mirror (FRM), and an output coupler. Because the devices are pigtailed with polarization maintaining fibers (PMF) except for the DCF, the DCF is placed between the PBS and the FRM to form the sigma-laser cavity. As the result, the intracavity polarization state is constant at any wavelengths. Mode-locking is achieved by direct modulation of the injection current to the SOA, and the DCF is used to provide the desired intracavity dispersion of -2.67ps/nm. By tuning the modulation frequency from 999.7MHz to 1000.5MHz, a wide tuning range over 80nm (1296nm to 1382nm) was achieved. Lasing wavelength was measured to be in linear proportion to the RF frequency applied to the SOA. The sweep rate over the entire wavelength range (80nm) could be raised to be as high as 20kHz. Instantaneous linewidth of the laser output was measured to be 0.38nm. The output was observed to be pulsed at the repetition rate equal to the modulation frequency, and the pulsewidth was ~130ps. Currently, the sweep rate is limited by the frequency modulation speed of the RF signal synthesizer. We expect faster sweep rate over 20kHz possible with the RF signal synthesizer having faster FM function.

6102-44, Session 12

Polarization-maintaining picosecond oscillator based on quantum dots SESAM

P. Crittenden, A. Starodumov, M. K. Reed, Coherent, Inc.

Passively mode-locked fiber lasers are very attractive for a wide range of applications including ultrafast spectroscopy, multi-photon excitation microscopy, micromachining, harmonic generation, and the pumping parametric amplifiers and oscillators. Those lasers do not require precise alignment and special measures to stabilize the cavity length against environmental changes and vibrations that make them a viable alternative to traditional solid-state ultrafast lasers [1,2]. However, use of non-polarization-maintaining components may result in temperature-dependent polarization drift in such lasers. A highly desirable polarized output can be achieved through coiling of non-PM fiber [3] or the institution of PM components with polarization selective properties.

We report a simple, environmentally stable, SESAM-based all-PM fiber oscillator, which can reliably output picosecond pulses operating at 1035nm or 1064nm. A polarization extinction ratio better than 20dB was achieved through the use of a PM coupler (or WDM) exhibiting an anisotropic splitting ratio and insertion loss for the fast and slow axis of the fiber. It is typical for those PM components to have different coupling ratio or insertion loss for each polarization state. In a laser cavity, a small difference in intracavity loss for two polarization states results in a strongly polarized output. Temperature variations from 20-40° C had no effect on output power and degree of polarization. The laser produced a stable pulse train ranging from 15 to 100 MHz repetition rates. Transform-limited 4-6ps pulses were produced at a threshold of 35-50mW of pump power. A slight decrease of pulse duration was observed with increase pump powers.

We have tested operation of the laser using different SESAM structure based on quantum wells (MQW) and quantum dots (QD) at 1035 nm. The cavity had a linear geometry and consisted of a fiber Bragg grating and SESAM as terminating mirrors. Although QD SESAM had much higher saturation fluence the pulse length of ~ 4 ps was the same for both SESAMs. Mode-locked operation with QD SESAM can tend to fall into Q-switch operation due to higher saturation fluence. In general, pulse properties and laser performance were comparable using a QD and MQW saturable absorbers.

REFERENCES

1. M. E. Fermann, “Ultrashort-Pulse Sources Based on Single-Mode Rare-Earth-Doped Fibers,” Appl. Phys. B, vol. 58, 197-209, 1994

2. L. A. Gomes, L. Orsila, T. Jouhti, O.G. Okhotnikov, “Picosecond SESAM-Based Ytterbium Mode-Locked Fiber Lasers,” IEEE Journal of Selected Topics in Quantum Electronics, vol. 10, 129-136, 2004

3. I. Hartl, G. Imeshev, L. Dong, G. C. Cho, M. E. Fermann, “Ultra-compact dispersion compensated femtosecond fiber oscillators and amplifiers,” CLEO 2005 Proceedings, CThG1, 2005

6102-45, Session 13

Fundamentals of incoherent and coherent beam combining (Tutorial)

J. R. Leger, Univ. of Minnesota

Abstract not available.

6102-46, Session 13

Coherent beam combining of fiber amplifier array output through spectral self-phase conjugation via SBS

V. I. Kovalev, R. G. Harrison, Heriot-Watt Univ. (United Kingdom)

Coherent combining of laser beams into a single giant coherent beam with diffraction limited beam quality is one of the most challenging problems in laser physics. The effort given to this problem since the early sixties has been and continues to be enormous since this is the only viable way forward to further power scaling of lasers. The general idea of this approach is to split a single diffraction limited coherent beam into many beams which are then amplified by a parallel array of similar power amplifiers and finally re-combined to a single diffraction limited beam. While there have been countless test-of-principle demonstrations at low power it is fair to say that none have had success in real high power systems. The main reason for this is the unavoidable and uncontrollable variation in phase shift (both linear and nonlinear) in the different amplification channels, rendering the combining process essentially incoherent even in a case when the original beam is perfectly coherent. The effect of spectral self-phase conjugation in SBS we recently discovered offers a solution to this. The main advantages of this effect in comparison to the well known spectral phase conjugation via non-degenerate four-wave mixing is high efficiency (~70% compared to ~0.1% for NDFWM) and it does not need in additional pump waves. It is also substantially faster compared to electro-optical phase compensators. We will discuss the basic principles of the effect, its main features and characteristics in regard to application for coherent beam combining of fiber amplifier array output.

6102-47, Session 13

Beam phasing multiple fiber amplifiers using a fiber phase conjugate mirror

B. W. Grime, W. B. Roh, T. G. Alley, Air Force Institute of Technology

Phasing of two-channel cw master oscillator/power amplifier beams using an SBS phase conjugate mirror has been demonstrated. The phasing was achieved for a two-channel master oscillator/power amplifier system, which used a single-frequency Nd:YAG master oscillator and two parallel fiber amplifiers, and a fiber phase conjugate mirror in a double-pass configuration. The successful phasing of two cw amplifier beams with a fiber phase conjugate mirror greatly enhances the prospects for phasing of multiple laser amplifiers without complex servo-loop control systems.

6102-48, Session 13

The effect of macro-bending on phasing in 6 and 7 core large mode area photonic crystal fibers

B. G. Ward, Air Force Research Lab.

In this paper, we present the results of a frequency domain analysis of the effect of coiling induced macro-bending on the phasing of the modes of 6 and 7 core large mode area photonic crystal fibers. These fibers may enable fiber laser CW power and pulse energy scaling due to their large effective mode area (~4000 square microns), however; phase differences between the cores degrade the output beam quality. We study the effects of bend axis, bend radius, and core geometry on the phasing of the fiber modes. Coiling causes the signals in the individual cores to suffer dephasing relative to each other in a predictable manner. This allows the possibility of recovering phased output, and thus near diffraction limited beam quality, from amplifiers employing these fibers. Preliminary experimental results are also presented.

6102-49, Session 14

Pulsed fiber laser with 20W output power at 532-nm

A. V. Babushkin, D. V. Gapontsev, N. S. Platonov, V. P. Gapontsev, IPG Photonics Corp.

We have generated 20W average power at 532nm by single-pass frequency doubling the output of the pulsed fiber 1064nm laser operating at 1.5MHz repetition rate with 1.5ns pulse duration and over 40W average power. Close to 50% conversion efficiency of the second harmonic generation in the bulk LBO crystal was achieved due to the high peak power pulses generated by the fiber laser to be presented. The developed laser have a truly solid-state design required for deployment into the industrial environment.

6102-50, Session 14

Multi-watt 589-nm fiber laser source

J. W. Dawson, A. D. Drobshoff, R. J. Beach, M. J. Messerly, S. A. Payne, D. M. Pennington, A. Brown, Lawrence Livermore National Lab.

We have demonstrated 2.7W of 589nm light from a continuous wave fiber laser using periodically poled KTP as the frequency conversion crystal. The system employs 938nm and 1583nm fiber lasers, which were sum-frequency mixed in periodically poled KTP to generate 589nm light.

The 938nm fiber laser consists of a single frequency diode laser master oscillator (200mW), which was amplified in two stages to \>15W using cladding pumped Nd3+ fiber amplifiers. The fiber amplifiers operate at 938nm and minimize amplified spontaneous emission at 1088nm by employing a specialty fiber design, which maximizes the core size relative to the cladding diameter. This design allows the 3-level laser system to operate at high inversion, thus making it competitive with the competing 1088nm 4-level laser transition. At 15W, the 938nm laser has an M2 of 1.1 and good polarization (correctable with a quarter and half wave plate to >15:1). The 1583nm fiber laser consists of a Koheras 1583nm fiber DFB laser that is pre-amplified to 100mW, phase modulated and then amplified to 10W in a commercial IPG fiber amplifier.

As a part of our research efforts we are also investigating pulsed laser formats and power scaling of the 589nm system. In our talk, we will discuss the fiber laser design and operation as well as our most recent results in power scaling at 589nm.

6102-51, Session 14

1 W average power at 589-nm from a frequency doubled pulsed Raman fiber MOPA system

P. Dupriez, C. Farrell, M. Ibsen, J. K. Sahu, J. Kim, C. A. Codemard, Y. Jeong, D. J. Richardson, J. Nilsson, Univ. of Southampton (United Kingdom)

We report a pulsed fiber laser operating at 589 nm from a frequency doubled pulsed Raman fiber MOPA system. The fiber laser generates sub-100 ps pulses at a repetition rate of 32 MHz with an average output power of 1 W. The Raman based fiber MOPA system is seeded by a CW narrow linewidth cascaded Raman fiber laser producing 156 mW and 534 mW at 1119 nm and 1178 nm respectively. This signal is then amplified by a Raman fiber amplifier pumped by 120 ps pulses at 1060 nm. The pump source is an ytterbium doped fiber (YDF) MOPA system in which the mater oscillator, a picosecond pulsed laser diode, is amplified by 2 cascaded ytterbium doped fiber amplifiers, reaching up to 250 mW of average output power. Both pulsed signal and CW pump beams are launched through a WDM coupler into a cladding-pumped YDF amplifier which provides high gain at 1060 nm and consequently Raman gain at 1178 nm. A 23 m long YDF with an active core of 8 μm in diameter was employed leading to the generation of 21 W of average output power into the second Raman Stokes order. This amplified signal is then launched into a 15 mm long LBO crystal for frequency doubling. The system produced 1 W of average output power at 589 nm in a clean spectrum with a 3.7 nm linewidth and a diffraction limited beam quality. With excellent spectral and spatial quality, and the potential for compactness and robustness, this fiber based configuration is an attractive alternative to bulk solid-state lasers for guidestar applications.

6102-52, Session 14

Nonlinear effects in optical fibers and their applications (Tutorial)

G. P. Agrawal, Univ. of Rochester

Fiber nonlinearities have long been regarded as being mostly harmful for fiber-optic communication systems. In recent years, their impact has also been felt in the context of high-power fiber lasers, whether operating con-

tinuously or designed to emit high-energy pulses. Over the last few years, the nonlinear effects in optical fibers are increasingly being used for practical applications, the Raman and parametric amplification being only the recent examples. In this tutorial I plan to review the various nonlinear effects from a fundamental standpoint while also pointing out their applications to fiber lasers and other devices.

The five major nonlinear effects occurring inside optical fibers are: Stimulated Raman scattering (SRS), stimulated Brillouin scattering (SBS), self-phase modulation (SPM), cross-phase modulation (XPM), and four-wave mixing (FWM). After considering the physics behind the stimulated Raman and Brillouin scattering processes, I would discuss their threshold power levels in the context of fiber lasers. The SRS process can also be exploited for making wideband Raman amplifiers. After describing the SPM and XPM processes, I discuss their role in realizing ultrafast nonlinear optical switches capable of responding at time scales of 1 ps or less. Many optical devices exploit these two nonlinear optical phenomena for application such as wavelength conversion, mode locking, time-domain demultiplexing, and ultrafast signal processing. FWM is the final nonlinear effect discussed in this tutorial. It is used for making parametric amplifiers that can be employed not only for wideband signal amplification but also for wavelength conversion and other signal processing applications. If time permits, I may cover the topic of supercontinuum generation in microstructure and tapered fibers.

6102-53, Session 15

Multiple-pump fiber parametric devices

S. Radic, Univ. of California/San Diego

Multiple-pump parametric processing in high confinement fiber provides practical means for phase-sensitive amplification, all-optical regeneration, conjugation, band conversion, ultrafast sampling and source construction. A single-pump parametric architecture can be described using degenerate four-photon mixing: two pump photons are annihilated in order to produce single signal (gain) and idler (conversion) photon. This conventional device is inherently limited by a narrow operating bandwidth, impaired idler generation and low Brillouin threshold. Multiple-pump parametric process possesses a number of fundamental advantages not associated with classical modulation-instability interaction. As a simplest example, two-pump parametric processor operates using at least three dissimilar four-photon processes (degenerate and non-degenerate), commonly referred to as modulational instability coupling.

Recent advances made in fabrication of high confinement fibers and multiple-pump physics have raised the expectation for a practical class of ultrafast, all-optical devices and sources. In contrast to a conventional, one-pump parametric scheme, multiple-pump interaction is used to generate equalized, high-gain operation across four operating bands. We will discuss the physics, design and limitations of multiple-pump parametric devices with highly nonlinear fibers. A recent set of record results related to signal regeneration, amplification, wavelength conversion, source construction and transport penalty erasure will be highlighted and contrasted with fundamental problems remaining in the field.

6102-54, Session 15

Dispersion varying fibers for optical signal processing

A. A. Sysoliatin, V. F. Khopin, General Physics Institute (Russia)

The single mode fibers with varying along length chromatic dispersion are attracting a considerable attention due to their value for optical soliton processing and applications in stable sources of ultrashort optical pulses. In particular, dispersion decreasing fibers (DDF) have been recognized to be useful for high-quality soliton pulse compression and stable against pump noise continuum generation. The fibers with varying along length dispersion can have a lot of applications in optical signal processing. The method to produce fibers varying along the length from standard preform had been developed. It is possible to draw fibers with a necessary length dependency on the dispersion with high accuracy. During the drawing process information about the current diameter is processed by digital control unit and compared with a calculated value. The dispersion deviation from the prearranged value is less than 0.1ps/nm/km. High-quality pulse compression has been obtained in DDF. The compression factor is determined by the ratio of input to output dispersion and typically limited to about 20. Using DDF with optimum dispersion profile it is possible to generate pedestal-free pulses of less than 50fs duration. In addition, a new DDF design has allowed to increase the SBS threshold by 7dB over conventional nonlinear fibers.

6102-55, Session 16

Q-switching of Yb-doped double-clad fiber laser using micro-optical waveguide on micro-actuating platform modulator for marking applications

Y. Jeong, Gwangju Institute of Science and Technology (South Korea); A. Liem, Friedrich-Schiller-Univ. Jena (Germany); K. Moerl, Institut für Physikalische Hochtechnologie e.V. (Germany); S. Höfer, Friedrich-Schiller-Univ. Jena (Germany); Y. Kim, Gwangju Institute of Science and Technology (South Korea); A. Tünnermann, Friedrich-Schiller-Univ. Jena (Germany); K. Oh, Gwangju Institute of Science and Technology (South Korea)

A novel all-fiber modulator using novel micro-optical waveguide(MOW) on micro-actuating platform(MAP) structure, which applied for Q-switched Yb-doped fiber laser, has been presented for the first time. Fused biconical taper(FBT) technology has been adopted for light modulator where mechanical stress was electronically applied over the waist of FBT couplers. With optimal cross-section morphology of the FBT waist, especially circular shape, an advanced photo-elastic mechanism is introduced by a new MOW on MAP structure, where micron scale FBT waist was placed on an electrically driven PZT mechanical actuating system.The MOW has initially 100% transmission through the output port at a certain wavelength. As the MAP induce compressive stress along the axial direction of MOW, the stress built in MOW on MAP will result in the coupling constant change by photoelastic effects and subsequently a portion of the input power is now coupled to the another output port.

To apply in Q-switching of Yb-emission we made a 2×2 coupler from specialty fiber having the cutoff wavelength at 920nm to secure single mode operation of the device in the wavelength range of 1060~1080nm. The Yb-doped double-clad fiber had a D-shaped silica cross section along with circular Yb-doped core to improve the pump-Yb absorption. The modulator has two output ports whose responses are reciprocal. One fed back to the cavity and another was used as the laser output. The system showed the peak power of 192mW at 4.1W pump power and 699mW at 5.2W. The repetition rate was 18.6kHz. It is noted that pulse duration did depend on pump power. Pulse repletion rate was determined only by the driving frequency of MOW on MAP modulator. Further optimization of connectorization between the gain fiber and the device could improve peak power and pulse duration.

6102-56, Session 16

Progress in all fiber components

D. J. DiGiovanni, OFS Fitel, LLC

Abstract not available.

6102-57, Session 16

Latest advances in LMA fiber based high power fiber laser and amplifier modules

M. O'Connor, Nufern

Large mode area (LMA) fiber technology has matured significantly in re-

cent years with a range of standard fiber geometries now becoming available from multiple vendors. This standardization has encouraged manufacturers to develop LMA compatible components such as couplers and Bragg gratings, thus enabling monolithic high power lasers and amplifiers to be developed. In this talk we review the recent progress on these devices in applications from high power (200W) CW fiber amplifiers and lasers through to high peak power pulsed amplifiers.

6102-58, Session 16

Tapered fused bundle coupler package for reliable high optical power dissipation

F. Seguin, A. Wetter, ITF Optical Technologies, Inc. (Canada)

Abstract not available.

6102-59, Session 16

Qualification of fiber lasers and fiber optic components for space applications

S. Hendow, S. Falvey, B. Nelson, Northrop Grumman Corp.

High power fiber lasers have many advantages over traditional lasers, such as power efficiency, ease of assembly and light weight. Such advantages make fiber lasers attractive candidates for space applications where weight and power consumption are serious limitations. The components used in these systems are typically commercial off-the-shelf fiber optic parts, most of which are developed for the traditional fiber communication and high power industrial markets. Although there is considerable overlap in these environments and certain space conditions, the differences suggest that there is further qualification needed for space. In this paper we examine the various components that conceivably may be used in fiber lasers, together with a suggested Taxonomy for testing these classes of parts. These classes include passives, actives and active modules. Test protocol is suggested for qualification based on current methodologies employed in the fiber optic communications industry, but adapted to space conditions. These modifications include the additional environmental conditions imposed by space, namely thermal, vibration and radiation. Additionally, this test protocol is verified by executing a series of vibration, thermal (including vacuum) and radiation tests to examine its validity. A selected set of recently-developed commercial off-the-shelf fiber optic components (at 106x nm) are chosen for these tests. These include doped fibers, combiners, sources, pumps, isolators and fiber Bragg gratings. Expected test results are discussed, together with a discussion of potential failure mechanisms when in space. The scope for this work is limited to the environmental conditions of lower Earth orbit satellites, 100 to 1000km orbital altitude and up to 60 degrees inclination.

This project was sponsored by the USAF Materiel Command, AFRL, Kirtland AFB with Jackson and Tull as the Prime Contractor, under contract number F29601-01-D-0078.

6102-60, Session 17

Power scaling of high power fiber lasers for micromachining and materials processing applications

S. Norman, A. Appleyard, P. Skull, D. Walker, I. Crowe, F. Ghiringhelli, L. Hickey, P. Turner, Southampton Photonics, Inc. (United Kingdom); T. Hoult, Southampton Photonics, Inc.

Fiber-integrated high power fiber lasers have demonstrated remarkable levels of parametric performance, efficiency, operational stability and reliability, and are consequently becoming the technology of choice for a diverse range of materials processing applications in the “micro-machining” domain. The design and functional flexibility of such HPFLs enables a broad operational window from continuous wave in the 100W+ power range, to modulated CW (to 50kHz prf and above), and to quasi-pulsed operation (kW/us/mJ regime) from a single design of laser system. A long-term qualification program has been successfully completed to demonstrate the robustness and longevity of this family of fiber lasers.

In this paper we report for the first time on the power-scaling extension of SPI’s proprietary side-coupled cladding-pumped GTWaveô technology platform to output power levels in the multi-hundred watt domain. Fiber and system design aspects are discussed for increasing both average power and peak power for CW and quasi-pulsed operation respectively whilst maintaining near-diffraction limited beam quality and mitigating non-linear effects such as Stimulated Raman Scattering. Performance data are presented for the new family of laser products with \>200W CW output power, M2 ~ 1.1 and modulation performance to 50kHz+; results are presented in relation to specific application examples in materials machining and welding.

6102-61, Session 17

300W single-frequency, single-mode, all-fiber format ytterbium amplifier operating at 1060-1070-nm wavelength range

O. Shkurikhin, N. S. Platonov, D. V. Gapontsev, R. Yagodkin, IPG Photonics Corp.; V. P. Gapontsev, IPG Laser GmbH (Germany)

300W single frequency ytterbium amplifier with M2<1.3 is demonstrated in all-fiber format for 1060-1070 nm wavelength band. Using an optimized splicing conditions and specially designed Yb-doped fiber at the booster stage, the amplifier provides single frequency amplification without any nonlinear effects including SBS. No output power saturation was observed and output optical power was only limited by pump power. We also did not observed any noticeable noises and roll off of output power due to high order modes excitation or other nonlinear phenomena. More resend results would be presented and discussed.

6102-62, Session 17

Novel SBS suppression scheme for high power fiber amplifiers

A. Liu, Aculight Corp.

We proposed a novel scheme for SBS suppression in high power fiber amplifiers by changing the core diameter along the fiber length. The fiber consisting of several sections with different core diameters has an extremely large core diameter at most locations to suppress SBS while at certain locations the core is relatively smaller and insensitive to bending. As a result, the fiber has lower SBS gain than the LMA fibers but still can be packaged in a compact, robust package. The change of core diameter along the fiber length can be made by either splicing several different fibers together or expanding the core diameter with a thermal diffusion process.

We have developed a numerical model based on rate equations for the fiber amplifiers with SBS involved to estimate SBS threshold. The model takes into account SBS gain dependence on temperature and strain distributions as well as inhomogeneous spectral broadening due to variation of fiber numerical aperture. The modeling results show that SBS threshold can be increased significantly when the seed power, fiber length, pump configuration, and fiber parameters are optimized. As a result, a single frequency fiber amplifier can generate up to kW output power without the onset of SBS. The new scheme also shows that the high power amplifier can be packaged much more compact than a conventional LMA fiber amplifier as the fiber can be bent very tight at certain locations.

6102-63, Session 17

Bent-waveguide modeling of large-mode-area, double-clad fibers for high-power lasers

G. R. Hadley, A. V. Smith, R. L. Farrow, Sandia National Labs.

The development of high-power fiber lasers requires a detailed under-

standing of limitations imposed by high optical irradiances present in the active core. In a well-designed high-power system, the onset of optical damage or nonlinear optical processes ultimately limits the attainable power. As a result, current designs employ large mode area active fibers, with the aim of achieving a dominant lowest-order spatial mode with the largest possible area. Since such fibers will generally support multiple modes, a common practice is to coil the fiber using a diameter small enough to induce mode-dependent bend losses[1]. The desired LP01 mode experiences lower bend losses than the higher-order modes, and, below a certain bend radius in the presence of gain, can completely dominate over the other modes. Optimizing the design of a fiber for use in bend-loss mode-filtered lasers or amplifiers requires consideration of the mode losses, mode-field spatial distributions and propagation constants of bent fibers and of beam propagation in fibers with varying bend radii or having orthogonal bend planes.

We have developed analytical and numerical models for simulating beam propagation in coiled fibers in the presence of gain and loss. The models range in complexity from a semi-analytical eigenmode solver for bent step-index waveguides to fully vectorial, triangular mesh, finite-difference eigenmode solvers and beam propagation models. The latter models can handle arbitrary refractive-index and rare-earth-ion doping distributions as well as arbitrarily varying bend radii. Both types of tools were found necessary for treating problems encountered in fiber amplifier simulation. One significant result concerns the degree of mode-field distortion occurring in bend-loss mode filtering. When a step-index fiber is coiled tightly enough to filter out high-order modes, the resulting LP01 mode is substantially distorted relative to LP01 of the unbent fiber and has a smaller effective mode area (Aeff). In addition, the intensity-weighted center of the bent-fiber mode is significantly shifted toward the outer core boundary in comparison with the unbent mode. Both of these effects could have an impact on amplifier performance and efficiency; the smaller Aeff could lead to a more rapid onset of damage or nonlinear process and the shift in mode position could reduce the overlap between the mode field and the rare-earth-doped region.

We will present these issues in more detail and will discuss the ramifications for fiber design. In addition, other modeling results concerning propagation of high-irradiance fields in bent and straight fibers, including the dependence of self-focusing effects on bend radius, will be presented.

Supported by Laboratory Research and Development, Sandia National Laboratories, U. S. Department of Energy, under contract DE-AC04-94AL85000.

[1] J. P. Koplow, D. A. V. Kliner, and L. Goldberg, Opt. Lett. 25, 442 (2000).

6102-64, Session 17

High order modes suppression in large mode area active fibers by controlling the radial distribution of the rare earth dopant

M. Hotoleanu, M. J. Söderlund, Liekki Oy (Finland); D. A. Kliner, J. P. Koplow, Sandia National Labs.; S. K. Tammela, V. Philipov, Liekki Oy (Finland)

Many high power fiber laser applications require doped fibers having large mode area but still working in single mode regime. The traditional technique to keep a large mode area fiber in single mode regime is either to reduce the core numerical aperture or to strip the high order modes by coiling the fiber (or the combination of the two methods). Both methods have limits and disadvantages.

In this paper we demonstrate by simulation the effectiveness of another method to suppress the higher order modes in large mode area active fibers by optimizing the rare earth dopant concentration across the core while keeping the step index structure of the core of the fiber. This method was not previously employed because the traditional doped fiber manufacturing technologies did not have the required capability to radially control the dopant concentration. However, DND (Direct Nanoparticle Deposition) can be used to manufacture large mode area fibers having any radial distribution of active element concentration and any refractive index profile. Thus, the DND fibers can be designed to benefit from this higher order modes suppression technique.

Using a modified version of Liekki Application Designer we have simulate LP01 (fundamental mode) and LP11 (second order mode) propagation at 1064nm along a 25um core / 250um cladding, step index core ytterbium doped fiber. The simulation demonstrates that in a uniform doped ytterbium fiber, LP11 mode experience more gain than LP01 mode. This is particularly detrimental in the effort to keep the fiber operating in single mode regime. The situation reverses for graded doping profile. For a parabolic doping profile, LP01 experience about 5dB more gain than LP11 while for a Gaussian profile the difference can be more than 7dB.

6102-67, Poster Session

Small signal intensity modulation of external cavity lasers

N. Dogru, S. M. Ozyazici, Gaziantep Univ. (Turkey)

A variety of applications ranging from optical communications to radar systems require picosecond optical pulses at high repitations rate. Active mode-locking with external cavity gratings is one technique used to generate such pulses from semiconductor lasers by applying an rf drive current at frequency matching the roundtrip of the laser cavity. Mode-locking of external cavity lasers is a well-established technique, with picosecond and subpicosecond pulses being achieved. The hybrid soliton pulse source (HSPS) is one such device, developed as a pulse source for soliton transmission system. This device has been demonstrated an extremely wide mode-locking frequency range due to a novel wavelength self-tuning mechanism.

In this paper, small signal intensity modulation (IM) of a HSPS utilizing Gaussian apodized fiber Bragg grating (FBG) is described using electric field approach. The HSPS is modeled by a time-domain solution of the coupled-mode equations.

It has been shown in previous papers that some laser diode parameters lead to increase resonance peak spectral splitting (RPSS) in the intensity modulation (IM) spectra. However, our simulation results show that type of external cavity is important effect on RPSS in IM response as well as effect of laser and FBG parameters. The RPSS can be suppressed by using linearly chirped Gaussian apodized FBG as an external cavity insted of Gaussian apodized FBG.

6102-68, Poster Session

Highly efficient double-clad Er/Yb co-doped single mode fiber lasers

A. V. Kazakevitch, J. Lit, Univ. of Ontario Institute of Technology (Canada)

Double-clad fiber (DCF) geometry and Yb co-doping of Er-doped fibers lead to higher power range of fiber lasers. The common value of a slope efficiency of these lasers described in literature is about 20-50%, whereas the quantum efficiency limit is 57-68% depending on the pump wavelength. This discrepancy encouraged us to investigate some possible loss mechanisms such as parasitical Yb emission. To achieve this aim a number of fiber lasers have been constructed. We have tested three single-mode Er/Yb co-doped DCFs. Made by different companies (Nufern, Haghwave, and Ofs) these fibers had different inner-cladding shape and dopant (Er, Yb, P_2O_5, Al, Ge) concentrations. The laser performance and behavior of Yb parasitical and residual pump radiation has been examined.

Our laser configuration is a modification of the conventional forward-signal configuration. It provided ~1.53 W of maximum launching pump power from a pump laser operating at 975 nm. The laser resonator was formed by a combination of a cleaved unpumped end of the DCF and a fiber Bragg grating (with reflectivity 79.4%)

Dependencies of lasers' slope efficiency, threshold, residual pump radiation, and parasitical ytterbium emission versus active fiber length were obtained and analyzed. Optimization of resonator parameters and minimization of splicing losses allowed us to achieve a maximum slope efficiency of 61.9% that is close to the quantum efficiency limit (63%) and 1.03 W of output power. At used launched pump power, the additive of

phosphorus in silica network did not affect the parasitical Yb emission behavior and it was about 0.3% of lasing power.

6102-70, Poster Session

A role of non-linearity in self-organization in fiber laser arrays

A. P. Napartovich, N. N. Elkin, V. N. Troshchieva, D. V. Vysotsky, Troitsk Institute for Innovation and Fusion Research (Russia)

Along with rapid progress in characteristics of single-fiber lasers much attention is paid these days to the problem of phase locking of multi-core fiber lasers. This approach promises to get a comparatively short device with high-power combined output beam of high quality. The small fiber length weakens stimulated scattering effects. Actually, the problem to make radiation in multi-core system coherent is a challenging task attacked earlier in other types of laser arrays. It was found that only strong-coupled system has a chance to be phase locked despite non-identity of channels. In case of the strong inter-channel coupling the traditional theoretical approach based on expansion over modes of individual cores fails. To treat correctly the limit of strong coupling one needs to employ methods of direct numerical simulations of wave field propagation in a compound structure. We have developed 3D diffraction numerical code [1], and results of its implementation to simulations of 7-core hexagonal fiber structure experimentally studied in [2] will be reported. Detailed analysis of light propagation in this system, where self-organization effect was observed, shows that there are not single but a few mechanisms of coherence formation in an array of co-propagating beams. The strongest is mode spatial filtering produced by the gain assembly. Non-linear refraction effect leads to some kind of synchronization of beams along propagation path. Influence of construction parameters on self-organization will be reported.

[1] N.N. Elkin et al, Opt. Comm. 177, 207, 2000

[2] P.K. Cheo et al, IEEE Photon. Technol. Lett., 13, 439, 2001

6102-72, Poster Session

Stimulated Raman scattering and broadband spectrum generation of nanosecond pulses from a directly modulated DFB laser

R. Rojas-Laguna, Univ. de Guanajuato (Mexico); J. Gutiérrez-Gutiérrez, E. A. Kuzin, B. Ibarra-Escamilla, S. Mendoza-Vázquez, Instituto Nacional de Astrofísica, Optica y Electrónica (Mexico); J. M. Estudillo-Ayala, Univ. de Guanajuato (Mexico); J. W. Haus, Univ. of Dayton

We report the investigation of SRS in a standard fiber using a directly modulated DFB laser with wavelength equal to 1549 nm, amplified by a two cascade erbium-doped fiber amplifier. The amplifier provides amplification of 2-mW peak power pulses to 100-W peak power pulses. This setup provides a simple source of high power pulses for nonlinear investigation. However, the directly modulation of DFB lasers causes the transient oscillations at the beginning of pulses. Our pulses consisted of a 2-ns transient part followed by a steady-state plateau. We found that the transient part generates a continuous spectrum broadband spectrum while the plateau causes conventional SRS with the spectrum maximum around 1660 nm. Additionally in the experiments with NOLM we have found chaotic polarization behavior of the transient part while the plateau had a stable polarization state. We attribute these specific features of the transient part behavior to the modulation instability causing pulse break, subsequent soliton pulse formation and the intrapulse Raman frequency shift. In our experiments we have found that the process of the broadband spectrum formations of the transient part begins before the regular SRS of the plateau. This fact opens the way of the nonlinear clearing of the pulses. For this aim the pulses passes first through fiber long enough to cause the broadband spectrum generation while the plateau power maintains below the SRS threshold, then the broadband part is filtered by the spectrum filter. The transient part of the pulses at the filter output was found essentially depleted.

6102-73, Poster Session

Generation of 560 fs soliton at 10 GHz from optically cross-gain-modulation mode-locked SOA fiber laser

I. Chiu, G. Lin, National Chiao Tung Univ. (Taiwan)

Optically harmonic mode-locking and femtosecond compression of a semiconductor optical amplifier fiber laser (SOAFL) induced by backward injecting a dark-optical-comb pulse-train at 10 GHz is demonstrated for the first time. The injected dark-optical-comb with 25-ps pulsewidth can be generated by seeding tunable laser into a Mach-Zehnder intensity modulator (MZM) at DC biased point of 0 V. The MZM is driven by a commercial electrical comb generator under an input microwave power of 28 dBm at repetition frequency of 10 GHz. Theoretical simulation indicates that the backward injection of dark-optical-comb results in a wide gain-depletion width (as well as a narrow gain window of <=25 ps) within one modulation period, providing a cross-gain-modulation mode-locking of the SOAFL with a shortest pulsewidth of 5.4 ps at 10 GHz. The difficulty in mode-locking the SOAFL by an optical short pulse (bright-optical comb) injection is also demonstrated and elucidated by the insufficient gain-depletion time (as well as modulation depth). After propagating through a 75m-long dispersion compensating fiber (DCF), the negatively chirped SOAFL pulsewidth that is mode-locked by the backward injected dark-optical-comb can be linearly dispersion-compensated and slightly shortened to 3.9 ps. By increasing the peak power of the dispersion-compensated SOAFL pulse to 51 W and propagating it through a 76.7m-long single mode fiber (SMF), an eighth-order nonlinearly soliton compression is achieved with the pulsewidth, linewidth, and time-bandwidth product of 560 fs, 4.5 nm and 0.31, respectively.

6102-74, Poster Session

Noise characteristics of an FM mode-locked erbium fiber ring laser stabilized with a semiconductor optical amplifier in anomalous dispersion or normal dispersion region

Y. J. Kim, D. Y. Kim, Gwangju Institute of Science and Technology (South Korea)

We have previously reported that FM mode-locked erbium fiber ring laser could be stabilized with high supermode noise suppression ratio when a semiconductor optical amplifier (SOA) is inserted in the cavity to act as a fast saturable gain medium even in a normal dispersion region. In this paper, we further investigate the noise characteristics including relaxation oscillation, timing and energy jitter in both positive and negative dispersion regions.

Nakazawa et al. suggested that random beating between up-chirped pulse and down-chirped pulse could be prohibited by employing proper amount dispersion and optical band-pass filtering in a laser cavity. With an anomalous dispersion fiber, up-chirped pulse is compressed and amount of chirp per pass is balanced between the phase modulator and the anomalous dispersion fiber. Conversely down-chirped pulse is broadened and dispersed out by experiencing loss through an optical filter. This mechanism is totally reversed when normal dispersion is dominant.

However supermode noise, which is considered the main noise source in an actively mode-locked erbium fiber laser, could not be eliminated by the suggested method. They introduced intensity dependent loss mechanism based on self-phase modulation (SPM) and optical band filtering to suppress supermode noise. Main drawback of this technique is that anomalous dispersion is required.

We achieved supermode noise suppression up to 70 dB in an anomalous dispersion region and also in a normal dispersion region by introducing a semiconductor optical amplifier biased just above threshold condition in the FM mode-locked erbium fiber laser operating at 2.5 GHz repetition rate. Relaxation oscillation peak measured by a spectrum analyzer was reduced by about 10 dB in the presence of an SOA in both dispersion regions. Supermode noise suppression improved from 50 dB to 70 dB. Energy jitter and timing jitter were measured by using a fast detector and

spectrum analyzer. 1.22 % energy jitter was reduced to 0.48 % and 690 fs timing jitter was reduced to 320 fs. We also observed the similar amount of improvement even in the normal dispersion region. We believed that this technique is a very effective method for pico-second tunable pulse generation with high repetition rate and good stability.

6102-75, Poster Session

Wavelength switching in an actively mode-locked FPLD coupled with a high dispersive external cavity

Y. J. Kim, D. Y. Kim, Gwangju Institute of Science and Technology (South Korea)

We propose a simple wavelength switching technique based on an actively mode-locked Fabry-Perot laser diode (FPLD) coupled with high dispersive external cavity. Wavelength switching was achieved by slightly detuning the modulation frequency applied to the FPLD. We have used a dispersion compensating fiber (DCF) with a dispersion coefficient of -100ps/km/nm at 1550 nm as a timing filter. When the external modulation frequency applied to the FPLD was slightly reduced we have observed that peak wavelength of the optical pulse is switched from a shorter longitudinal FP mode to a longer FP mode. Wavelength switching from the longer longitudinal FP mode to the shorter FP mode was achieved by replacing the DCF with a single mode fiber.When the dispersion of a ring cavity is highly dispersive, wavelength-dependent round trip time between discrete FPLD modes is slightly different. By slightly increasing the modulation frequency in a highly normal dispersion cavity, we observed the laser wavelength is switched to the longer wavelength region because the group velocity of longer wavelength pulse moves faster. In a cavity with a high anomalous average dispersion, the effect was just opposite. The external modulation frequency was around 2 GHz. When an 18 m DCF is inserted, the average dispersion of the cavity becomes -1.51 ps/nm. 14 kHz increment of the modulation frequency moved the lasing wavelength to the adjacent mode. Switching between five FPLD modes spanning 4.7 nm wavelength was observed. The wavelength switching rate per modulation frequency change was 0.078 nm/kHz, which was quite close to the expected value. Side mode suppression ratio (SMSR) was around 40 dB and supermode noise at each switching states was suppressed more than 50 dB. When 100 m length of an anomalous fiber was used for a timing filter, the average dispersion of the cavity was 2.08 ps/nm. We observed wavelength switching to the shorter wavelength region by increasing the modulation frequency. Switching rate was 0.16 nm/kHz and it also showed good agreement with the expected calculation value. SMSRs were around 40 dB and supermode noise at each switching states was suppressed more than 50 dB.

In conclusion, we established simple and cost effective method for wavelength switchable pulse system with good spectral and noise characteristics using actively mode-locked FPLD and a highly dispersive external cavity.

6102-76, Poster Session

All-fiber supercontinuum generation based on a low noise femtosecond fiber laser and highly nonlinear dispersion shifted fiber

H. Song, Y. J. Kim, D. Y. Kim, Gwangju Institute of Science and Technology (South Korea)

We report a wideband and almost flat spectrum Supercontinuum (SC) generation by using a femtosecond fiber pulse laser and a highly nonlinear dispersion shifted fiber (HN-DSF). Wide spectrum covering 1180 ~ 1700 nm wavelength range, is generated by putting the femtosecond fiber laser pulse at the wavelength of 1557 nm into the HN-DSF whose zero dispersion wavelength is 1537 nm.. We have constructed a passively mode-locked Er-doped fiber ring laser using nonlinear polarization rotation mechanism. Generated pulses are characterized with a conventional SHG-FROG setup. It generates ~ 800 fs pulses at a repetition rate of 13 MHz, with an average output power of 0.5 mW. These pulses are amplified in a short Er-doped fiber amplifier (EDFA). The output from the fiber amplifier is put into the HN-DSF whose nonlinear coefficient is about 10.5 /W/km at the input wavelength. The polarization state of the generate SC spectra is well defined such that it can be properly controlled by the polarization controller. The dependence of the SC spectral width on the HL-DSF length, the stability of the generated SC spectrum, and conditions for obtaining smooth spectra without a fine structure are investigated in detail. We believe that our proposed all-fiber laser based supercontinuum source has many important applications in recently developed frequency-domain measurement techniques such as OCT, OFDI, OFDR and their instrumentation applications.

6102-77, Poster Session

0.5 kW, 10μJ linearly polarized fiber laser operating at 977-nm

V. Khitrov, B. N. Samson, D. P. Machewirth, K. Tankala, Nufern

Pulsed fiber lasers emitting multiple-kW peak powers and pulse energies in the mJ range are looking to address many of today's more demanding applications. Such fiber-based devices have numerous advantages over other types of lasers, such as compactness, maintenance-free operation, robustness and high efficiency.

Although there is a great deal of interest in high-pulse power devices operating in the wavelength range of 970 - 980 nm, where Yb-doped fiber lasers could be a candidate, the usual operating wavelength range for fiber devices utilizing Yb+3 is limited typically to 1050-1100 nm. The 970-980 nm range, using Yb3+ doped fibers, presents challenges due to the need for high brightness pump sources, the highly inverted fiber condition required and the generated amplified spontaneous emission (ASE) that limits the gain.

Here we report our recent progress in the design of a linearly-polarized pulsed fiber laser operating at 977nm that addresses the aforementioned concerns. The laser consists of linearly polarized 977nm laser diode and a polarization maintaining (PM) fiber amplifier. The amplifier is based on PM Yb-doped fiber that is core-pumped at 915nm. The entire device has a compact, robust, all-fiber design. A peak power of 0.5kW and 10μJ pulse energy has been achieved from this laser. Further power scaling results will be presented at the conference.

6102-78, Poster Session

Product design issues relating to erbium doped fiber ring lasers and super fluorescence sources

J. M. Sousa, J. R. Salcedo, M. Melo, M. O. Berendt, Multiwave Photonics, S.A. (Portugal)

The high gain offered by Erbium doped fiber amplifiers has, since its first demonstration, been explored in lasers and super fluorescence sources. Although such devices have been the topics for numerous scientific publications only a few configurations have resulted in commercial products. We have identified the principal reasons for this as the difficulty in obtaining single polarization and single mode laser operation in the inherently long laser cavities and the tendency of super fluorescence sources to show spurious lasing in high power operation. In this presentation we show some results of our effort to deal with these obstacles. For long fiber ring lasers with mode spacing as small as 10 MHz a technique based on a saturable absorber population inversion grating filter is shown to assure stable single longitudinal mode lasing even when the cavity is subject to temperature variations. The advantage of the saturable absorber filter is that it has a narrow passband and dynamically tracks the lasing mode. Single polarization lasing may be obtain by using an in-cavity polarizing element. This approach however leads to mode hopping, induces by random polarization coupling in non polarization maintaining (PM) fiber cavities. An all PM fiber ring cavity in combination with saturable absorber filter provides a solution for stable single mode, single polarization laser operation.

Progress on amplified spontaneous emission super fluorescence sources is fueled by improvements in available pump power ratings. Even in single

mode pumping a regime is now reached where spurious lasing is limiting the spectral power density of the broad band emission. We present techniques based on tailored optical feedback using Fiber Bragg grating or Faraday rotator mirror which increases lasing threshold and thus the achievable output power. These advances have allowed manufacture of fiber optic sources which maintain their performance parameters over time and when subject to temperature and vibration perturbations found in real applications.

6102-79, Poster Session

High-peak-power, linearly-polarized, diffraction-limited pulses from a large-core Yb-doped photonic crystal fiber

F. Di Teodoro, C. Brooks, Aculight Corp.

Efficient and compact optical sources generating UV light at power levels suitable for remote sensing of biochemical agents and pollutants constitute an enabling technology for portable, in-the-field devices, which can be deployed in a variety of scientific, industrial, and national-security applications. Yb-doped fiber lasers and amplifiers operating at ~1μm-wavelength exhibit ideal characteristics for integration in such portable devices. Effective production of UV light through harmonic generation of these sources, however, has been hampered by difficulties in maintaining a stable polarization state at high peak power, due to nonlinear effects.

We report a fiber-based source featuring a large-core Yb-doped photonic-crystal fiber, which generates 1064nm, diffraction-limited, sub-ns pulses of peak power \>700kW and average power \>5W exhibiting a stable degree of polarization \>99% (polarization extinction ratio \> 20dB). To our knowledge, the obtained peak power is the highest in a linearly-polarized fiber amplifier output. The result bears great promise for high-power, effective UV light generation from a fiber source.

6102-80, Poster Session

High repetition rate high power femtosecond fiber laser

B. Ortac, Friedrich-Schiller-Univ. Jena (Germany); A. Hideur, M. Brunel, G. Martel, Univ. de Rouen (France)

The generation of high energetic ultra-short pulses from fiber lasers near the 1 mm wavelength region has been under high investigation for the last years. Since the first demonstration of femtosecond pulses in Yb-doped fiber laser in 1997 [1], a significant progress has been realized. Indeed, it was recently demonstrated that pulses with durations as short as 36 fs and energies as high as 5 nJ could be obtained from the stretched pulse ytterbium-doped fiber lasers systems[2,3]. An intense effort is now directed toward high repetition rate femtosecond laser development and thus harmonic-mode-locking.

We report passive harmonic mode locking of a high-power Yb-doped double-clad fiber laser operating in both the normal- and the anomalous-dispersion regime with a fundamental repetition rate of 20.4 MHz. First observations have been done in the anomalous dispersion regime. The total second-order cavity dispersion is fixed to -0.1 ps2. Harmonic mode locking can be achieved for pump power of 2.05 W. In this case, 20 pulses per round trip are created. These pulses can rearrange themselves to occupy uniformly the cavity leading to harmonic mode-locking. Because the free spectral range of the cavity is 20.4 MHz, the repetition of the laser in this case is 408 MHz. The supermodes suppression is more than 30 dB. The pulse duration is about 1 ps and its energy about 125 pJ. In the second step we reduced the total net dispersion to a value close to zero (about -0.004 ps2). For pumping power of 2 W, we generated simultaneously 91 pulses uniformly separated in the cavity. The resulted repetition rate is higher than 2 GHz. The supermodes suppression is lower in this case, it is about 25 dB. The pulse duration (energy) is about 700 fs (48 pJ).

It is well known that shorter and more energetic pulses could be obtained in the stretched-pulse regime. To test this configuration, we adjusted the total cavity dispersion to a positive value of +0.047 ps2. In this case, we generated five pulses of 5 ps duration uniformly separated in the cavity. The repetition rate is thus 102 MHz. The supermodes suppression is more than 60 dB. After extra-cavity compression, the pulse duration is reduced to about 120 fs. Pulse energy is about 1.7 nJ. Finally, we report a new regime of multiple pulsing emission observed with this fiber laser: the stable emission of two pairs of bound pulses exhibiting different time separations and uniformly separated in the same cavity round trip.

[1] V. Cautaerts, D. J. Richardson, R. Paschotta, D. C. Hanna, Opt. Lett. 22, 316 (1997).

[2] F. Ö. Ilday, J. Buckley, L. Kuznetsova, and F. W. Wise, Opt. Express 11, 3550-3554 (2003).

[3] B. Ortaç, A. Hideur, T. Chartier, M. Brunel, C. Özkul, F. Sanchez, Opt. Lett. 28, 1305 (2003).

Conference 6103: Nonlinear Frequency Generation and Conversion: Materials, Devices, and Applications V

Wednesday-Thursday 25-26 January 2006

Proceedings of SPIE Vol. 6103

6103-01, Session 1

New organic NLO material for blue-green laser generation

S. Dhanuskodi, J. J. Ramajothi, Bharathidasan Univ. (India)

Second order nonlinear optical (SONLO) materials capable of efficient frequency conversion of infrared or visible laser radiation to visible or ultraviolet (UV) wavelengths are of considerable interest in the field of telecommunications, high-density optical recording etc. During the last several years an extensive research was carried out on organic NLO materials due to their fast response over a broad frequency range, high optical damage threshold and inherent synthetic flexibility.

The nonlinear optical material L-histidinium tetrafluorophthalate (L-HFP) was synthesized at 55°C in a temperature controlled water bath. Good quality single crystals with regular shape and size of 12 x 6 x 3 mm3 were grown by slow evaporation solution growth technique (pH=3.2, 30°C). The grown crystal has been subjected to single crystal X-ray diffraction to determine the unit cell dimensions and morphology using a Enraf-Nanious CAD-4 X-ray diffractometer with MoK radiation of = 0.717 ≈. The crystal belongs to monoclinic system with volume 1297.006 ≈3. The FT-IR spectrum was recorded using a Jasco 460 Plus spectrometer by KBr pellet technique to analyze the functional groups present in L-HFP. From this spectral analysis it is confirmed that the imidazole and amino groups are protonated and counter balance the negative charges of the carboxylate functionality in the tetrafluorophthalic acid.

A good optical transmittance and lower cutoff value are important properties for NLO crystals. The UV-Vis spectrum was recorded for the grown crystal using a Varian Cary 5E UV-Vis spectrometer. This material has a lower cutoff wavelength at 230 nm with large transmission in the entire visible region enable it to be a potential candidate for optoelectronic applications and the second and third order harmonic generations of Nd:YAG laser. The powder SHG efficiency was measured for different particle size by Kurtz and Perry method and the phase matching condition was achieved. The thermal analyses (TG and DTA) show that the material melts at 138∫C. The microhardness was measured in the (100) plane and the work hardening coefficient was found to be 4.3. The laser damage threshold was found to be 56.58 MW/cm2 using a pulsed Nd:YAG laser (= 1064 nm, 10 Hz, 10 ns).

6103-02, Session 1

Periodically poled vapor transport equilibrated lithium niobate for visible light generation

R. V. Roussev, R. K. Route, J. Schaar, K. E. Urbanek, M. M. Fejer, Stanford Univ.; D. H. Jundt, C. Kajiyama, Crystal Technology, Inc.

The ability to achieve high quality periodic poling in lithium niobate (LN) has allowed quasi-phase-matching to be used for second-order nonlinear optics, leading to experimental demonstration of efficient optical frequency generation throughout its wide transparency range (0.36-4.5 um). Applications of congruent lithium niobate involving visible or ultraviolet wavelengths are limited to low power or high temperature operation due to the effects of photorefractive damage (PRD) and green-induced infrared absorption (GRIIRA). Methods of suppressing PRD include doping with 5 mol-% MgO or ZnO and varying crystal stoichiometry. We use a combination of vapor transport equilibration (VTE) and moderate MgO doping (<1%) to obtain near-stoichiometric PRD-resistant crystals with improved parameters for periodic poling compared to the commercially available 5% MgO-doped congruent crystals.

Efficient process for periodic poling at room temperature using baked photoresist as a patterned dielectric on one crystal surface and LiCl-solution electrodes was developed for periods as low as 8.3 microns for 0.5% and 7 microns for 0.3% MgO-doped VTE:LN. The quality of periodic poling improves with lowering MgO concentration. Stable second harmonic generation of 0.9-W continuous-wave 532-nm radiation was obtained at room temperature (31 degrees C) over 6 hours with no sign of degradation in a 1.5-cm long crystal of 0.3% MgO-doped VTE:LN periodically poled with a period of 7.05 microns.

6103-03, Session 1

Growth of new quaternary nonlinear optical crystals for 1-micron-pumped mid-IR generation

P. G. Schunemann, BAE Systems plc

Significant advances in mid-infrared nonlinear optical (NLO) crystals have been made in recent years due to the growing importance of laser applications in the 2-12 micron spectral range. However, there remains a need for improved NLO materials that can efficiently shift the output of 1.06-micron solid-state Nd-lasers to wavelengths beyond 4 microns (which is the practical limit of oxide-based crystals). The chalcopyrite AgGaS2 is one of the few crystals that meets this requirement, but it is plagued by a low laser damage threshold that severely limits its usefulness. The selenide analog AgGaSe2 has a higher damage threshold but has insufficient birefringence for phase matching a 1.06-micron pump source.

Two new quaternary compounds have recently been reported which overcome these limitations: AgGaGeS4 and AgGaGe5Se12. AgGaGeS4 has orthorhombic (mm2) symmetry, is phase-matchable for Nd-laser pumping, and offers a larger bandgap and higher damage threshold than the parent compound AgGaS2. Similarly, AgGaGe5Se12 (also mm2) exhibits a larger band gap and a much larger birefringence (~0.18) that extends the phase-matching range of AgGaSe2 to allow pumping at wavelengths of 1-micron and below.

In order to more accurately assess the usefulness of these materials for mid-IR laser frequency conversion, the quaternary compounds were synthesized by vapor transport in sealed ampoules from high purity elemental starting materials, and crystals were grown by the horizontal gradient freeze technique in transparent furnaces. AgGaGe5Se12 exhibited incongruent melting behavior, and small optical samples extracted from an as-grown polycrystalline boule had high scattering losses. AgGaGeS4 growth was far more favorable, resulting in a crack-free single crystal measuring 19mm in diameter and >60mm in length with as-grown 2.05-micron absorption losses < 0.05 cm-1. The measured laser damage threshold of an uncoated AgGaGeS4 crystal at 2.05um was 1 J/cm2 (100 MW/cm2), and room-temperature measurements of thermal diffusivity, heat capacity, and thermal conductivity yielded values of 0.224 mm2/s, 0.448 J/g/K, and 0.399 W/mK respectively for the sulfide.

6103-04, Session 1

Thermal poling and high efficiency second harmonic generation in sulfide glasses

F. Smektala, M. Guignard, V. Nazabal, J. Troles, Univ. of Rennes I (France); H. Zeghlache, Y. Quiquempois, A. Kudlinski, G. Martinelli, Univ. des Sciences et Technologies de Lille (France)

Chalcogenide glasses are known for their high non linear optical properties from the third order, 100 to 1000 times the non linearity of the reference silica glass. By inducing an internal static electrical field (Eint) in these glasses, one can expect, from the coupling between Eint and their third order non linear characteristics, the generation of a high second order non linearity. We describe here the thermal poling of sulfide glasses.

The poling parameters like temperature (100-310°C), applied voltage (2.5-4 kV) and duration (5-60min) are explored. An adapted treatment has permit to reach a high efficiency second harmonic generation in the Ge25Sb10S65 sulfide glass. Indeed, a large non linear second-order susceptibility of about 10 ± 0.5 pm/V is measured for this glass, with the help of a Maker fringes experiment, with a pump beam at the wavelength of $\lambda\omega$ = 1.904 µm. The nonlinear susceptibility profile as a function of the depth under the anode for the Ge25Sb10S65 poled glass is determined using the analyze of the remaining second harmonic signal after several NaOH etching treatments. In parallel, a study of the concentration variation of elements being able to be involved in the formation of a charge space is achieved by using the secondary ion mass spectroscopy.

6103-05, Session 1

Laser-induced defect reactions governing damage performance in KDP and DKDP crystals

P. P. DeMange, R. A. Negres, H. B. Radousky, S. G. Demos, Lawrence Livermore National Lab.

The formation of laser-induced bulk damage sites in optical materials, particularly in potassium dihydrogen phosphate (KDP) and its deuterated analog (DKDP) nonlinear crystals is a major factor impeding goals for greater operational intensities in large-aperture laser systems. Laser annealing is demonstrated to provide nominal improvement to the damage performance of KDP and DKDP. The presence of impurity nano-particles and/or native defect clusters has been hypothesized to be responsible for damage initiation but the laser-defect physics associated with material damage performance are still not well understood. In this work, damage initiation mechanisms are investigated by measuring the damage resulting without and with laser annealing under various damage testing conditions. The results are compared against current models for damage initiation that favor either a linear absorption (particle heating) mechanism or a multi-step or nonlinear mechanism.

The damage testing approach we have used provides rapid measurements of the damage site density as a function of laser parameters, including fluence, wavelength, and pulse-length. Laser annealing effectiveness and behavior is cataloged using variable laser pre-exposure fluences at different wavelengths. Damage initiation under simultaneous exposure to variable fluence at different wavelengths is also explored. Our results indicate that there are at least two populations of defects leading to damage initiation over different wavelength ranges of the testing pulses. Moreover, multiple paths leading to laser annealing of a defect population exist.

6103-06, Session 1

Large spatial self-phase modulation in castor oil enhanced by gold nanoparticles

M. A. R. C. Alencar, C. M. Nascimento, M. G. A. da Silva, M. R. Meneghetti, J. M. Hickmann, Univ. Federal de Estado de Alagoas (Brazil)

Spatial self-phase modulation (SSPM) was observed when a CW laser beam propagated along a cuvette containing castor oil. This effect depends on the laser intensity and it presents a threshold behavior with the incident light power. The threshold power decreases when the sample length is increased, as well as when the laser wavelength approaches to the absorption band of the medium. This phenomenon can be explained by solving the nonlinear Schrödinger equation, which predicts the generation of conical emission when an intense laser beam interacts with a nonlinear medium. Using this model, the effective nonlinear refractive index of castor oil was estimated. This SSPM was also observed when a laser beam interacts with a colloidal solution of gold nanoparticles in castor oil. The gold nanoparticles were synthesized by reduction of Au(III) from an aqueous solution of HAuCl4 and immobilized in castor oil. The particle sizes were estimated using transmission electronic microscopy, yielding average size of ~ 10 nm. For this system the SSPM threshold power decreased dramatically, which indicates that the nonlinear refractive index for this system is enhanced due to the gold nanoparticles. Indeed, the estimated value for the nonlinear refractive index of the colloidal system is one order of magnitude larger than the observed value for castor oil. Moreover, for laser wavelength near to the plasmon resonance of the gold nanoparticles, this enhancement factor is even higher. Although the large value of this nonlinearity, its temporal response is slow. This fact suggests that this phenomenon is due to a combination of thermal and electronic effects. The contribution of each effect is currently under investigation.

6103-07, Session 2

Blue light generation using a broad-area diode-laser in two passively coupled ring-resonators

D. Skoczowsky, V. Raab, R. Menzel, Univ. Potsdam (Germany)

In recent years we have demonstrated an external resonator design for improving the spectral and spatial beam quality of broad area diode lasers. These concepts are now adapted to the needs of efficient second harmonic generation (SHG). This led to a new resonator design which consists of two optically coupled ring resonators. These passively coupled ring resonators are oscillating at a common wavelength by design to dispense with active length control. In a first ring resonator an AR coated diode laser is used as a gain medium. This resonator has a relatively low finesse to prevent the facette of the diode from catastrophic optical damage. Furthermore this resonator drives the second ring resonator which has a relatively high finesse to enhance the low output power of the diode laser. Inside this second ring resonator a critically phasematched potassium niobate crystal is placed for efficient SHG.

The optimal reflectivities of the mirrors were calculated and varied to estimate the behavior of the high finesse cavity i.e. for the occurrence of losses or variations in input power. Furthermore considerations on the spectral behavior of the two ring resonators, particularly the spectral matching of the two ringresonators, were undertaken. Based on these investigations an experimental setup was realized using an additionally grating to control the center wavelength of the emission. This experiment revealed a 10 mW cw emission of 465 nm light which is close to the theoretical predictions.

Danilo Skoczowsky, Volker Raab, Ralf Menzel

Institute of Physics, University of Potsdam, Am Neuen Palais 10, D-14469 Potsdam, Germany

6103-08, Session 2

Frequency conversion concepts for the efficient generation of high power 935-nm - 942-nm laser radiation

H. Rhee, T. Riesbeck, F. Kallmeyer, S. Strohmaier, H. J. Eichler, Technische Univ. Berlin (Germany); A. A. Kaminskii, Institute of Crystallography (Russia); K. Petermann, Univ. Hamburg (Germany)

For weather forecast, especially for civil protection from high-impact weather events, measuring the three-dimensional distribution of water vapour by DIAL techniques is a fundamental concern. Especially for development and evaluation of atmospheric models, knowledge of water vapour distribution is important.

With suitable wavelengths around 935 - 942nm measurement of water vapour concentration in the atmosphere is possible.

No efficient high power laser sources emitting at 935 - 942nm are available so far. The comparison between frequency converters based on Stimulated Raman Scattering (SRS), Ti:Sapphire and Mixed Garnet shows the favourable properties of each concept and helps to evaluate the most suitable concept.

The use of SRS in solids to shift the wavelength of existing lasers is becoming more widespread due to the investigation of a large number of Raman-active materials with promising nonlinear properties. Development

of Raman frequency converters for high pulse energies concentrates on linear resonator designs and seeding using the Raman material as a direct amplifier based on Raman four-wave-mixing.

A seeded and frequency stabilized high pulse energy Ti:Sapphire (TISA) laser system with high average power and 35mJ at 930nm with an unseeded linear resonator has been developed. Injection-seeded pulses of 20mJ at the water vapour absorption line at 935.684nm with a spectral purity of 99.6% were demonstrated.

Direct generation of the wavelengths 935nm and 942nm required for water vapour detection is possible with diode-pumped, Nd-doped YGG- and GSAG-crystals. First experiments resulted in high efficiencies of up to 20% and pulse energies of 12mJ at 942nm wavelength.

6103-09, Session 2

High efficient generation of tunable visible light by means of DFG in self-controlled conversion processes

J. Wueppen, B. Jungbluth, M. Vierkoetter, D. Hoffmann, R. Poprawe, Fraunhofer-Institut für Lasertechnik (Germany)

Generating the difference frequency of a frequency-doubled, widely tunable Ti:Sapphire laser and a Nd:YAG laser provides tunable laser radiation in the visible spectrum range. The generated wavelength region closes the spectral gap between the fundamental and the second harmonic of the Ti:Sapphire laser. A prototype has being developed with a fully automated wavelength tuning, i.e. the wavelength tuning of the Ti:Sapphire laser and the angel tuning of the nonlinear crystals and the tuning of the temporal delay between the Ti:Sapphire and the Nd:YAG laser operate self-controlled. Design, theoretical modeling and experimental characterization of the system are closely discussed. At a repetition rate of one kilohertz, the frequency-doubled Ti:Sapphire laser provides pulses of approximately 20 ns, a spectral line width of 20 GHz, a nearly diffraction limited beam quality and pulse energies of up to 850 μJ. The tuning range reaches from 340 nm to 510 nm. For the three wave interaction process in a 8 mm long BBO crystal the Ti:Sapphire pulses (pump wave) are mixed with 3.5 mJ pulses of a Nd:YAG laser (signal wave). The generated idler wave has pulse energies of up to 280 μJ and pulse durations of approximately 10 ns in the spectral range between 510 nm and 680 nm. This yields to a conversion efficiency of about 33% and a quantum conversion efficiency of more than 50%. To our knowledge, this clearly exceeds the values that has been obtained with comparable setups so far. Further increase of the efficiency is currently under investigation.

6103-10, Session 3

Random frequency accessible broad tunable THz-wave source using phase-matched DAST crystal DFG

K. Suizu, A. Nawahara, Tohoku Univ. (Japan); T. Yamashita, Tohoku Univ. (Japan) and Advantest Lab. (Japan); H. Ito, Tohoku Univ. (Japan) and The Institute of Physical and Chemical Research (Japan)

Ultra broad band (from 1.5 to 37 THz) THz-wave generation using difference frequency generation (DFG) in an organic 4-dimethylamino-N-methyl-4-stilbazolium tosylate (DAST) crystal was demonstrated. A DAST crystal is one of the promising materials for efficient and high power THz-wave generation because of its very high nonlinearity and low refractive index dispersion between the near infrared region and the THz-wave region. We can use DAST's highest nonlinear component, d11 (about 230pm/V), to generate THz-wave by means of DFG because the co-linear phase matching condition of the Type0 configuration is satisfied. We constructed a dual-wavelength optical parametric oscillator (OPO) with two KTP crystals pumped by frequency doubled Nd:YAG laser. Each KTP crystal was set on a Galvano scanner and the angle of each crystal was controlled independently. The OPO has a tunable range from 1300 - 1900 nm, resulting in an ultra broad tunable range of the THz-wave. We successfully generated ultra broad tunable THz-wave using only one DAST crystal without any change of the experimental setup, except the computer controlled Galvano scanner angle change. The highest THz-wave energy of 10 nJ was obtained at around 26 THz region under 2 mJ of pumping energy. Finally, the THz-wave source can access an arbitral THz frequency for every pulse (50 Hz at present). The Galvano scanner has a 1 kHz response and we can obtain 1 msec of frequency access speed.

6103-11, Session 3

Backward parametric interactions

Y. J. Ding, Lehigh Univ.

During this presentation, we will highlight the investigations of the parametric processes in the backward configuration such as second-harmonic generation, sum-frequency generation, difference-frequency generation, and parametric oscillation, from infrared to acoustic waves in the electromagnetic spectrum. These processes have been studied in a variety of the nonlinear materials and structures such as periodically-poled LiNbO3, periodically-poled KTiOPO4, KTP/RTP waveguides, and a few bulk crystals. We will also discuss the fundamental importance and potential applications of these parametric processes.

6103-12, Session 3

High-efficiency high-energy wavelength-doubling optical parametric oscillator

D. J. Armstrong, A. V. Smith, Sandia National Labs.

We have numerically modeled an efficient method of converting 1064 nm light to 2128 nm light using a wavelength-doubling optical parametric oscillator (OPO). The wavelength doubling OPO cavity is based on the four-mirror nonplanar RISTRA geometry, denoting rotated image singly-resonant twisted rectangle, and contains a single type-II KTP crystal. By using the polarization-rotating properties of this cavity, and modifying its geometry to incorporate polarization-selective mirrors with angles of incidence near Brewster's angle, this design obtains stable oscillation at degeneracy. When the pump is injection-seeded, and the cavity contains an intra-cavity etalon for single-longitudinal-mode oscillation, the wavelength-doubled light remains phase-locked to the pump, independent of cavity length, with little or no active stabilization. Numerical analysis indicates that a pulse-injection-seeded wavelength doubling OPO can obtain 1046 nm to 2128 nm conversion efficiency exceeding 65%. A more complete analysis of a system containing a low-energy seeder-doubler OPO followed by high-energy pulse-seeded doubler suggests total 1064 nm to 2128 nm efficiency greater than 55%. An Nd:YAG pumped 2128 nm source based on high-efficiency wavelength doubling may offer a cost-effective alternative to conventional two micron laser sources such as Tm:Ho:YAG.

6103-13, Session 3

High quality efficient intracavity UV, IR generation in image rotated KTP OPO

S. Wu, California Institute of Technology

We present our results in a image rotated KTP OPO cavity where we added harmonic generator and mixing module inside to enhance UV generation. The cavity is desgined to provide efficient UV generation at 226nm (for NO detection), 282nm (for OH detection) and 390nm (for CH detection).

Our initial results at 390nm, which is direct intracavity SHG of 780nm, show record high efficiency from 1064nm. We get 69mJ/pulse at 390nm from 900mJ of 1064nm input.

Efficiencies at 282nm and 226nm are also quite high.

The beam quality at these UV wavelengths are also very high — they are round beams with divergence less than 0.5mrad in both directions. This setup provides a good UV light source for combustion PLIF research.

6103-14, Session 3

Optical performance monotoring using a A poled lithium-niobate (PP-LNO3)

M. B. Tayahi, Univ. of Nevada/Reno

Optical second harmonic generation in dense wavelength division multiplexing were used to monitor the performance of each channel in all optical networks. A poled Lithium-Niobate (PP-LNO3) device is used to convert C and L- Band optical WDM channels into half wavelength channels where silicon arrayed detectors and CMOS electronics were used to perform advanced digital signal processing to predict optical channel presence, channel power, signal to noise ratio and the quality (Q) factor parameter. With further processing, the bit error rate per channel can be estimated from the Q factor. The technique is realized on a system-on-a-chip CMOS technology which can potentially improve all optical networking architectures.

6103-15, Session 3

Polarization properties of nonlinear optical loop mirror with twisted fiber and birefringence bias in the loop

B. Ibarra-Escamilla, E. A. Kuzin, P. Zaca-Moran, R. Grajales-Coutiño, F. Mendez-Martinez, Instituto Nacional de Astrofísica, Óptica y Electrónica (Mexico); O. Pottiez, Faculté Polytechnique de Mons (Belgium); J. W. Haus, Univ. of Dayton; R. Rojas-Laguna, Univ. de Guanajuato (Mexico)

The nonlinear optical loop mirror (NOLM) is used in application like optical switching and demultiplexing, all-optical active mode locking, passive mode locking, pedestal suppression, pulse shaping, etc. This device offers a versatile way to obtain a nonlinear transmission behavior through the nonlinear differential phase shift between the two interfering beams due to the self-phase modulation. Recently we discussed a NOLM device using a symmetrical coupler, highly twisted fiber, and a quarter-wave (QW) retarder introducing the polarization asymmetry in the loop. We have shown high contrast operation, flexibility of characteristics, and stability in time. In this report we analyze theoretically and study experimentally the transmission behavior for different input polarization considering as well different output polarizations. We propose a simple description of the NOLM transmission for right- and left-hand circular output polarization at different output polarization states. The nonlinear characteristics depend on the QW retarder plate angle, but also on the polarization state at the NOLM input. Experiments were carry out with the NOLM consisted of a 500-m length SMF-28 fiber with twist rate of 7 turns/meter. Experiments show a good agreement with our theoretical approach. Appropriate choice of the input and output polarizations allows very high contrast, at least higher than 5000. Our measurements were restricted by sensitivity of our detection system to measure low power pulses at conditions when theoretically transmission must be equal zero. Experiments show flexibility and stability of characteristics. Adjustment of the QW retarder and input polarization allows tuning the critical power over a wide range.

6103-16, Session 4

Picosecond mid-IR generation by means of MHz-rate optical parametric amplification of white-light continuum

V. V. Yakovlev, Univ. of Wisconsin/Milwaukee

We used a specially prepared optical fiber to generate a red-shifted white-light continuum from a MHz-rate picosecond all-solid-state laser. This continuum is parametrically amplified in GaSe crystal to generate broadly tunable picosecond pulses in the Mid-IR spectral region. Other highly efficient nonlinear optical interactions in nanoscopic materials will be discussed.

6103-17, Session 4

Ultrafast parametric amplifier pumped by a fiber laser system

C. Aguergaray, F. Röser, T. Schreiber, J. Limpert, Friedrich-Schiller-Univ. Jena (Germany); E. Cormier, Univ. Bordeaux 1 (France); A. Tünnermann, Friedrich-Schiller-Univ. Jena (Germany)

Several applications rely on high repetition rate (and therefore high average power) and ultra-intense ultra-short pulse laser systems. If one considers the properties of ytterbium-doped short pulse fiber lasers [1] and ultrafast optical parametric amplification systems [2] one easily realizes the well matched compatibility of those techniques to achieve both challenging parameters. It is well known that fiber laser systems are scalable to high average power due to the fiber design itself. Parametric amplifiers are, one the other hand, inherently immune against thermo-optical problems due the absence of energy absorption by the crystal during the nonlinear amplification process. The generation of ultra-short energetic pulses in rare-earth-doped fibers is restricted by the limited amplification bandwidth (~5 THz in the case of Ytterbium doped fibers) and pulse distortion due to nonlinearity in the fiber core. However, parametric amplification offers an enormous amplification bandwidth (~ 200 THz in noncollinear configuration). Furthermore, an overall gain of 106 or even 108 can be achieved in just few millimeter long crystals, therefore, the B-integral (accumulated nonlinear phase) is typical negligible. So far parametric amplification suffers from the lack of a high energy high repetition rate pump laser source, whose parameters potentially can be transferred into pulse durations in the sub-10 fs range using the parametric process. High performance short-pulse fiber laser have the potential to fill this gap.

In this contribution we report on an ytterbium-doped fiber CPA system pumping a parametric amplifier working at degeneracy. The fiber CPA system delivers 100 μJ pulses at a repetition rate of 200 kHz and 1 ps pulse duration at 1040 nm center wavelength. In a 5 mm long BBO pumped by the second harmonic (SHG) of the fiber CPA system broadband pulses at 1040 nm are amplified to the μJ-level. The pulses are compressible to sub-50 fs using a prism pair compressor.

[1] A. Tünnermann, T. Schreiber, F. Röser, A. Liem, S. Höfer, H. Zellmer, S. Nolte, and J. Limpert, “The renaissance and bright future of fibre lasers,” J. Phys. B: At. Mol. Opt. Phys. 38, 681-693 (2005).

[2] G. Cerullo and S. De Silvestri, “Ultrafast optical parametric amplifiers,” Review of Scientific Instruments 74, 1, 1 (2003).

6103-18, Session 4

Applying sum frequency generation vibrational spectroscopy to deduce detailed structural information from complicated chemical and biological surfaces

Z. Chen, Univ. of Michigan

Sum frequency generation (SFG) vibrational spectroscopy has been applied to study surface structures of various polymer and protein molecules. Carefully analyzing SFG spectra collected using different polarizations of input and output laser beams can elucidate surface structures of complicated surfaces and interfaces, such as polymer surfaces and interfacial proteins. For example, we characterized the detailed surface structure of poly(methyl methacrylate) (PMMA) in air using SFG. Our research indicates that the PMMA surface is dominated by ester methyl groups in air. These ester methyl groups stand up on the surface. Surface restructuring behaviors of poly(n-butyl methacrylate) in water have been quantified using the polarization combinations and absolute intensity measurements of SFG. Similarly, we studied surface changes of other polymer materials when exposing to water. Our results indicate that different polymers have varied surface changes in water.

Using intermediate polarization combinations, we demonstrated that we can fit the SFG spectra more reliably, and weak chiral SFG spectra can

be deduced from interference with the non-chiral SFG signal. Molecular structures of buried polymer interfaces have been examined using SFG. Such structures have been related to adhesion properties of these polymer materials, providing a molecular level understanding of adhesion mechanism. Interfacial structures of various biological molecules, including proteins, peptides, and lipids, have been elucidated using SFG at the solid/liquid interface in situ in real time. For example, we observed time-dependent structures of fibrinogen after adsorption to polymer surfaces. At different polymer surfaces, such time-dependent structural changes are different. We also examined interactions between lipid bilayers and antimicrobial peptides to understand antimicrobial behavior of such peptides.

We showed that combinations of linear vibrational spectroscopy such as attenuated total reflection Fourier transform infrared spectroscopy with nonlinear vibrational spectroscopic techniques such as SFG and four-wave mixing provide more detailed structure of surfaces/interfaces than that from a single technique.

6103-19, Session 4

Propagation of ultrashort solitons in the presence of nonlinear gain

M. F. Ferreira, S. C. V. Latas, Univ. de Aveiro (Portugal)

The evolution of picosecond soliton pulses in optical transmission lines and mode-locked fiber lasers can be described, to a good approximation, by the complex Ginzburg-Landau equation. Single-pulse transmission and generation have been investigated in detail within this framework. However, in the case of subpicosecond or femtosecond optical pulses, the higher-order effects such as third-order dispersion, self-steepening, and self-frequency shift become important and must be taken into account. On the other hand, to reduce the soliton timing jitter, optical bandpass filters are generally used. The excess gain that must be provided to compensate for the filter induced loss amplifies also the linear waves coexistent with the soliton trains, leading to instability of the background. An approach to avoid this instability consists in the use of an amplifier having a nonlinear property of gain, or gain and saturable absorption in combination.

In this paper we consider the propagation of pulses in fiber-optic systems in the presence of self-frequency shift, narrow-band filtering, linear and nonlinear gains. We show that, using these control techniques, stable optical pulse propagation over long distances can be achieved. We analyse the system using a perturbative approach and obtain steady-state solutions and their existence conditions. These steady-state solutions are studied by linear stability analysis. The results are verified by directly solving the main governing equation numerically. Our results are also suitable for investigation of the stable soliton in fiber lasers.

6103-20, Session 5

Thermal dephasing and control of second harmonic generation in periodically poled LiNbO3 and LiTaO3 crystals

O. A. Louchev, National Institute for Materials Science (Japan); N. E. Yu, Gwangju Institute of Science and Technology (South Korea); S. Kurimura, K. Kitamura, National Institute for Materials Science (Japan)

Second harmonic generation (SHG) using quasi-phase-matching (QPM) in periodically poled (PP) crystals has shown significant progress over last decade and continues to remain in the focus of research efforts aimed towards greater efficiency SHG devices working at higher input powers. PP LiNbO3 (PPLN) and PP LiTaO3 (PPLT) remain among the best SHG materials due to their high second order susceptibility. Nevertheless, experimental efforts to use these and also similar crystals for high power SHG devices encounter the problem of efficiency loss, difficult temperature tuning during operation and thermally induced long term degradation. In this report we report the results of our simulations of the optical problem of SHG in PPLN and PPLT crystals coupled with a time dependent three-dimensional (3D) thermal model. The optical computations are based on plane wave slowly varying amplitude approximation for fundamental ans second harmonics coupled with 3D heat transfer model inside the temperature controlled crystal. The model takes into account thermal effects of linear and non-linear absorption.

Our simulations are performed for 20 nanosecond pulsed 300 micron diameter laser beam of a 1.06 mm fundamental wavelength. This moded shows the onset of increasing thermal dephasing and very significant SHG efficiency loss for input powers \>10 W. Our study also shows that PPLT crystals which have a lower value of the effective non-linearity,10 pm/V (compared with 16 pm/V for PPLN), provide a significant advantage over PPLN due to the higher heat conductance, 8.5 W/m K, and the lower absorption, which become the critical parameters controlling SHG efficiency at high input powers. Performed computational study reveals very strong coupling of FH and SH laser energy fields with the onset of significant temperature non-uniformities along and across the laser beam arising in PPLN and PPLT crystals which leads to a significant thermal dephasing and SHG efficiency loss. Conformal temperature tuning along the crystal during operation with temperature gradient is shown to inhibit effectively temperature non-uniformity along the laser beam propagation and thermal lensing effects, and to increase SHG efficiency at high input powers. For instance, selected PPLN conformal cooling parameters lead to the formation a high SHG efficiency (ª60 %) temperature uniform QPM channel for laser beam at 20 W input power.

6103-21, Session 5

Measurement of the nonlinear coefficient profile of quasi-phase-matched gratings using iterative error-reduction algorithms

A. Ozcan, M. J. F. Digonnet, G. S. Kino, Stanford Univ.

It is theoretically well known that the measurement of the second-harmonic power generated by a quasi-phase-matched (QPM) grating as a function of the frequency detuning parameter yields the Fourier transform (FT) magnitude of the complex nonlinear coefficient profile along the QPM device. This measurement can be achieved by tuning either the wavelength of the fundamental laser beam or the temperature of the QPM grating. However, without the FT phase, the magnitude of the FT cannot be unambiguously inverted to uniquely recover the nonlinear coefficient profile of the QPM grating, and this technique yields only approximate profiles. In this work, we demonstrate that this ambiguity can be completely lifted by placing a stronger and thinner nonlinear sample against the input (or output) of the QPM device of interest and measuring the detuning curve of this composite assembly. The crux of this method is that by construction, the nonlinear profile of this assembly has a sharp peak due to the thinner sample, followed by the weaker, broader profile of the QPM grating, which essentially constitutes a minimum-phase function. As such, its FT phase can be simply and exactly calculated from its measured FT magnitude, for example by applying to the FT amplitude the Hilbert transform or an error-reduction algorithm. The nonlinear coefficient profile of the QPM device can thus be fully recovered by processing the measured tuning curve with a fast and simple iterative error-reduction algorithm. In this paper, we demonstrate with numerical simulations that this powerful new technique can accurately recover the period, envelope, and chirp parameters of any QPM grating.

6103-22, Session 5

Engineered ferroelectrics and hybrid semiconductor-silica fibers for tunable optical devices

V. Gopalan, L. Tian, The Pennsylvania State Univ.; D. A. Scrymgeour, Sandia National Labs.; D. J. Won, The Pennsylvania State Univ.; K. L. Schepler, Air Force Research Lab.

Considerable source development work has been done that exploits frequency up- and down-conversion through quasi-phase-matched interactions in microstructured ferroelectric domains in planar crystal geometry. Optical modulation, guiding and steering have received less attention in comparison, although the same basic concept of microstructuring ferroelectric domains can result in numerous other functionalities such as electro-optic beam steering, dynamic focusing, beam shaping and modulation. In addition, the micro-and-nanostructuring of dielectrics and semiconductors into 2- and 3-dimensions for creating photonic bandgap structures offers new and interesting ways of guiding and modulating light in tailored dispersion media.

In this talk, we describe 2 classes of nonlinear optical media and devices: (1) Domain microengineered planar devices to demonstrated electro-optic phased array beam steering, dynamic focusing, and electro-optic switching. (2) Semiconductor filled microstructured optical fibers for infrared guiding and optical switching of light within the fiber.

6103-23, Session 5

Second harmonic generation in quasi-phase matched AlGaAs waveguides with low loss pumped at 1.55um

X. Yu, L. Scaccabarozzi, P. S. Kuo, J. Fu, M. M. Fejer, J. S. Harris, Jr., Stanford Univ.

GaAs is desirable for nonlinear optical wavelength conversion because of its high nonlinear coefficient. It is also desirable to fabricate GaAs/AlGaAs waveguides in order to take the advantage of the high optical mode confinement. Unfortunately, highly efficient nonlinear waveguide devices based on GaAs/AlGaAs system has not been realized. The high propagation loss at either fundamental wavelength or second harmonic wavelength kills the optical power in long waveguide devices and short waveguide (1~3mm) devices have produced the highest (although moderate) conversion efficiency. We have developed all-epitaxially fabricated, orientation-patterned AlGaAs waveguides with reduced waveguide corrugation height. The waveguide structure is optimized to reduce the waveguide corrugation height to below 45nm. The regrowth condition is investigated to improve the domain boundary quality. This reduced waveguide corrugation height and improved domain boundary quality dramatically reduce the waveguide loss. The power attenuation coefficient at 1.55um for the waveguide with QPM grating periods at 4.8um is measured to be 1.6/cm using Fabry-Perot method. This loss is close to the unpatterned waveguide in the same wafer. The loss at 780nm is estimated to be 3~5/cm. The second harmonic generation was measured by tuning the fundamental wavelength around 1.55um. Taking into account of the waveguide coupling efficiency, the reflection from input and output facets, and the detector efficiency, we estimate a record internal SHG conversion efficiency of 25%/W under continuous wave operation with a 5mm long waveguide.

6103-24, Session 5

Efficient broadband difference frequency generation in a direct-bonded periodically poled lithium niobate ridge waveguide and the bundle observation of carbon monoxide isotopomer absorption from 2300-nm to 2450-nm

T. Yanagawa, O. Tadanaga, Y. Nishida, NTT Photonics Labs. (Japan); H. Miyazawa, NTT Electronics Corp. (Japan); K. Magari, M. Asobe, H. Suzuki, NTT Photonics Labs. (Japan)

It is reported that efficient difference frequency generation (DFG) in the 2000-nm region is obtained by using a direct-bonded periodically-poled LiNbO3 (PPLN) ridge waveguide. The direct-bonding technique can utilize the bulk LN characteristics, which provide certain advantages including non additional absorption, precise device design and reproducible device fabrication.

We achieved a conversion efficiency of 100%/W in the fabricated waveguide with a 940-nm pump laser diode (LD) and a 1550-nm band tunable signal LD source. We also confirmed a wide tunable range of over 100 nm in a 50-mm-long waveguide with a single-pitch PPLN at a constant temperature. This is because the DFG bandwidth is decided by the phase mismatch dk and dk=0 is only obtained at a certain wavelength, however, Sellmeier equation shows dk~0 is easy to realize in the 2000-nm region when the pump is set at 900-960 nm. Subtle dk changes around 0 realized group velocity matching and a broadband output could be obtained.

Compact and broadband tunable light sources are expected to be used for trace gas sensing in the near to medium infrared regions. This report also describes bundle observation of carbon monoxide isotopomer absorption lines. The DFG output bandwidth is sufficient to observe 12CO and 13CO simultaneously. The absorption lines of the P and R branches for each gas are clearly observed between 2300 and 2450 nm.

DFG in the 2000-nm region using direct-bonded PPLN ridge waveguides is a promising approach for opening up new broadband applications.

6103-25, Session 5

Material improvement of LiTaO3 single crystals for QPM applications

Y. Furukawa, O. Nakamura, M. Matsukura, OXIDE Corp. (Japan); Y. Liu, S. Takekawa, K. Kitamura, National Institute for Materials Science (Japan)

Lithium Niobate (LiNbO3:LN) and Lithium Tantalate (LiTaO3:LT) single crystals are the most excellent and useful ferroelectric materials for piezoelectric, linear electro-optic and nonlinear optical device applications. In recent years there has been increasing interest in the use of quasi-phase-matched (QPM) nonlinear crystals for a variety of frequency conversion applications. Using the QPM technique, periodically poled lithium tantalate (PPLT) have been demonstrated to give efficient second-harmonic generation and optical parametric oscillation in both the cw and the Q-switched regimes. However, there are still some fundamental problems in the conventional materials for fabricating precise domain structures. High electric field (above 20 kV/mm) required for domain switching at room temperature and large internal field in both cases of conventional LN and LT pose limitations on the sample thickness and the ability to control domain periodicity. High power operation by QPM devices has been limited by material issues such as photorefractive beam distortion and green-induced infrared absorption (GRIIRA). Recently, it has been revealed that all these undesirable problems are closely related with intrinsic non-stoichiometric defects of LN and LT.

Recently Stoichiometric LiTaO3 single crystals have been commercialized by a spin-out company from NIMS called “Oxide Corpora-tion.” Stoichiometric crystals are superior to their conventional congruently grown counterparts in almost every respect, and will find widespread use in telecommunications, optical storage and frequency doubling and parametric conversion. Unlike congruently grown crystals which are typically lithium deficient, stoichiometric materials maintain the almost ideal 50/50 lithium to niobium ratio, thereby reducing the defect density by two orders of magnitude. This in turn leads to larger nonlinear and eltro-optic coefficients, improved transparency in the UV, increased resistance to optical damage, and most importantly for nonlinear and parametric processes, factors of between 5 and 10 reduction in the poling field required. Commercial availability of these materials has been long awaited, and the expectation is that improved device performance can be expected imminently.

In this paper we are going to present recent development of crystal quality of stoichiometric LiTaO3 for QPM applications. The relationship between material quality and QPM devices will be discussed.

6103-26, Session 6

Microresonator-enhanced four-wave mixing

K. Zheng, S. Blair, Univ. of Utah

Four-wave mixing (FWM) is an important tool for frequency conversion and fast

optical switching in all-optical communication networks. Semiconductor optical amplifiers are popular media for wavelength conversion via FWM for wavelength division multiplexing optical communication owing to their compact size and large conversion efficiency. In this paper, we demonstrate that microring resonator based filters can also generate significant conversion efficiency with sub-millimeter physical lengths. Microresonator based filters have not only high finesse, which can enhance nonlinear efficiency, but also periodic passbands, which satisfy the phase matching

condition of FWM automatically (when implemented in weakly dispersive media). Non-degenerate FWM in direct-coupled ring resonator (DCRR) filters and ring-based Mach-Zehnder interferometers (RMZI) is studied in this paper. Both structures give us greater than 10% conversion efficiency (defined by the converted intensity divided by the initial signal intensity) with low values of n2 Ip, where n2 is nonlinear refractive index and Ip is the initial pump intensity, whereas DCRR allows greater frequency conversion bandwidth within the filter passbands. We also compare the efficiency of the ring-based filters and a straight waveguide with same the effective length. The result shows that the efficiency ratio of the ring-based filter over the straight waveguide is approximately the finesse of the filter. We thus demonstrate that ring-based filters are effective devices for on-chip wavelength conversion for WDM network.

6103-27, Session 6

Coherent Raman solitons in hollow-core photonic crystal fibers

F. Biancalana, Tyndall National Institute (Ireland)

The propagation of laser light in a Hollow-Core Photonic Crystal Fibre (HC-PCF) using photonic bandgap (PBG) guidance has been demonstrated relatively recently [R.F.Cregan et al., Science 285, 1537 (1999)]. The PBG fibre consists of a 2D periodic lattice of refractive index variations in the transverse direction (cladding), with a break in the periodicity ('defect') in the form of a hollow core. Light coupled into the core at frequencies lying in its bandgap is therefore confined in it, by a multiple Bragg reflection mechanism, along the transverse direction.

Rather paradoxically, despite the smallness of direct nonlinearities due to the Kerr effect in the core, HC-PCF represents undoubtedly one of the most interesting nonlinear microstructured optical devices created in the last decade. In fact, strong nonlinear interactions can be obtained by filling the core with nonlinear gases or liquids, providing a practically unlimited interaction length between matter in the core and the mode field. This interaction is particularly suitable for the study of resonant nonlinear optics. For instance, in a recent experiment on stimulated Raman scattering due to vibrational states of molecular hydrogen [F.Benabid et al., Science 285, 1537 (1999)], threshold energies of Stokes generation in HC-PCF have been reported that are two or three orders of magnitude less than in any other published experiment.

In this work [D.V.Skryabin, F.Biancalana, D.M.Bird and F.Benabid, Phys. Rev. Lett. 93, 143907 (2004)] we give an exhaustive numerical and analytical description of two new classes of solitary waves propagating in a strongly dispersive HC-PCF and supported by the Raman resonant interaction between the light and the ensemble of matter molecules present in the fibre core. These two classes of soliton, which we have called 'off-resonance' and 'on-resonance' solitons respectively, both consist of two optical components with different frequencies (two-colour solitons), their frequency difference being in the proximity of the Raman resonance. These two kinds of soliton possess completely different properties. The first kind (off-resonance) lives in the far (negative) detuning region of the lorentzian Raman resonance, and it is analysed in the framework of the Maxwell-Abraham-Lorentz equations. The second kind (on-resonance) lives at resonance, and for this reason must be analysed using the full version of the Maxwell-Bloch equations.

Precise conditions for the experimental excitation of Raman solitons in HC-PCFs will be given. In the case of off-resonance solitons, both bright-bright solitons and 'inverted' dark-bright solitons (with the dark component living in the anomalous dispersion and the bright component living in the normal dispersion) have been found. These are likely to be observed experimentally in the immediate future.

6103-28, Session 6

Gain optimization of Raman-mediated fiber optical parametric amplifier

K. K. Wong, N. Wong, The Univ. of Hong Kong (Hong Kong China)

Fiber optical parametric amplifiers (OPAs) and Raman amplifiers (RAs) are both based on the third-order nonlinear susceptibility of glass fibers. Recently, there are some efforts in combining these two nonlinear phenomenons in order to extend the amplification and wavelength conversion windows to S-band or lowering the required parametric-pump power in order to achieve the same signal gain. We propose a new technique of utilizing these two amplifying principles in a single piece of highly-nonlinear dispersion-shifted fiber (HNL-DSF). We call this Raman-mediated fiber OPA (RM-OPA), which is different from the previous Raman-assisted OPA (RA-OPA) work. The previously investigated RA-OPA required an extra Raman pump in the power level of around 1 W, on top of the erbium-doped fiber amplifier (EDFA) required to amplify the OPA pump. Therefore, Raman amplification is simply employed as a power booster for the OPA pump, i.e. RA "assists" OPA. On the other hand, the new approach we propose here does not require an extra EDFA as pre-amplifier and the single piece of HNL-DSF provides both RA and OPA effects. In other words, there is essentially no parametric amplification without the presence of the Raman pump.

While combined RA and OPA have been investigated both analytically and experimentally before, it involves only introducing some extra Raman terms in the nonlinear Schrödinger equations (NLSE) additively, which is sufficient for the case when a single pump is used to amplify the signal (and idler) through both RA and OPA. However, the situation is significantly different here, where the parametric pump is amplified by the RA, while the OPA gain will be varied along the gain medium as the parametric pump itself is a function of the distance along the HNL-DSF. In this paper, we will present an analytical model for this RM-OPA, in both co-propagating and counter-propagating configurations. We also propose an advanced convex programming technique to optimize the Raman-mediated fiber OPA, given the coupling amongst the parametric pump, Raman pump, signal and idler, which is the first attempt to optimize such kind of fiber amplifiers.

6103-29, Session 6

Generation of phase-conjugate wavefront from dye-doped thin films using He-Ne laser

P. Palanisamy, T. Geethakrishnan, Anna Univ. (India)

Optical phase-conjugation (OPC) is of interest for many applications such as high-speed turbulence correction, optical resonator and image processing. With the rapid growth of photonics technology, considerable effort is being directed towards the development of new materials. Better materials are still needed for implementation of ideas. Present report is on low-power optical phase-conjugation (OPC) based on the degenerate four wave mixing (DFWM) arrangement in gelatin films doped with methyl green and acid blue 7 dyes. The 633nm beam from a He-Ne laser was split to form two counter-propagating pump beams and one probe beam. The experiment was carried out varying writing beam intensities, angle of the probe beam with respect to the pump beam and concentrations of dyes in the gelatin matrices. Phase-conjugate signal contribution from the individual holographic gratings were measured. High reflectivity optical phase conjugation is hereby reported for low power laser.

6103-30, Session 6

Enhancement optical phase conjugation reflectivity in doped III-V semi-conducting in a magnetic field

M. N. Singh, P. Aghamkar, Guru Jambheshwar Univ. (India)

Optical phase conjugation (OPC) is a fascinating nonlinear optical phenomena and offers manifold applications in wide class of optoelectronic devices. The origin OPC lies in the third-order nonlinearity of the medium. In this paper, keeping in mind importance of piezoelectric semiconductors in modern optics, an analytical investigation of optical phase conjugation via Brillouin-enhanced four wave mixing has been made in doped III-V weakly piezoelectric semi-conducting crystals in presence of a strong magnetic field (B). The third order nonlinear susceptibility (c(3) of the III-V semiconductors and resultant phase conjugate reflectivity are derived analytically using coupled mode approach. The role of piezoelectricity and doping on phase conjugacy factor is also analysed. The external magnetic field substantially enhances magnitude and alters sign of c(3) Numerical estimates have been made for moderately n-type doped InSb crystal at 77K duly irradiated by pulsed 10.6 μm CO2 laser. The magnitude of complex c(3) at B = 0 are found to be in good agreement with literature [1,2]. However, values of c(3 at B = 10 T and 14.2 T are nearly hundred times larger than the values obtained at B=0 and therefore reflectivity of phase conjugate signal enhances by a few orders of magnitude. In conclusion, it is expected that n-type moderately doped III-V piezoelectric semi-conducting crystal such as InSb, GaAs in presence of a strong magnetic field are smart materials for the fabrication of efficient phase conjugate mirrors.

References:

1. Y.R. Shen, Principles of Nonlinear Optics (John Wiely, NY, 1984), p. 101.

2. B.S. Wherrett, A.C. Walker and F.A.P. Tolley, in Optical Nonlinearities and Instabilities in Semiconductors, eds. by H. Haug (Academic, Sandiego, 1988), p.239.

6103-31, Session 7

Supercontinuum in silica nanowires

R. R. Gattass, G. T. Svacha, E. Mazur, Harvard Univ.

Fibers are gaining widespread acceptance for generating ultra-broad spectra. The most common approach involves a photonic crystal fiber with carefully designed core size and dispersion characteristics. Although this system provides confinement of light to micrometer (and sometimes submicrometer) dimensions, this confinement is achieved at the expense of a complex core structure. An alternative to microstructured fibers is the use of silica fibers with sub-wavelength diameters whose waveguiding properties were initially demonstrated by our group. Silica nanowires are a model system because they are a step-index, all-core cylindrical waveguide, and therefore easily modeled. The nanowires have applications in integrated photonics and sensing.

We present recent results for supercontinuum generation using femtosecond laser pulses in nanowires of various diameters and lengths. We observe supercontinuum generation in over interaction lengths as short as 10 mm. The evolution of the spectra is examined with respect to self-phase modulation and solition self-splitting. We will discuss the nonlinear effects and the resulting spectra as a function of the dispersion characteristics for the fibers and of the input laser power.

6103-32, Session 7

Tunable fiber optical parametric wavelength converter with 900 mW of CW output power at 1665-nm

M. E. Marhic, Opal Labs.; G. M. Williams, L. Goldberg, J. P. Delavaux, Keopsys Inc.

The 1620-1700 nm region of the optical spectrum is important as it contains numerous molecular resonance lines of chemical species. We have investigated, theoretically and experimentally, the possibility of designing an efficient frequency converter based on a fiber OPA, to generate high-power in that range, by mixing radiation generated by C- and L-band fiber amplifiers.

We have theoreetically investigated the possibility of obtaining strong pump depletion in a one-pump fiber OPA, and of maintaining high conversion efficiency as the signal is tuned over a wide range. We have shown analytically that strong punp depletion can be obtained over a broad tuning range, when the signal input power is about one third of the pump input power. This conclusion was also verified by numerical simulations including: Raman gain; spurious four-wave mixing; amplified spontaneous emission due to the high-power signal and pump amplifiers; longitudinal variations of the zero-dispersion wavelength.

In experiments with a 40-m long highly-nonlinear fiber (HNLF) we have generated 900 mW of CW output power at 1665 nm, when pumping with 3W at 1612nm and 0.82W at 1562nm. The optical conversion efficiency was 23%. The linewidth was less than 0.1 nm. To our knowledge this is the highest CW output power reported to date for a fiber OPA WC. We have also obtained similar output characteristics at 1684 nm, demonstrating the tunability of the device, which can in principle be tuned over the 1662-1697 nm region by tuning the signal wavelength over the C-band (1535 to 1565 nm). We anticipate that the ouput power can be scaled to higher powers.

6103-33, Session 7

Supercontinuum generation with femtosecond dual pumping

T. V. Andersen, T. Schreiber, D. Schimpf, J. Limpert, A. Tünnermann, Friedrich-Schiller-Univ. Jena (Germany)

Supercontinuum generation (SCG) in optical fibers has been extensively investigated in the last decade due to the improvements in production of micro-structured fibers (MFS). Supercontinua spanning more than 1000 nm can now be generated with low-energy pulses directly from oscillators resulting in new coherent sources of white light. Such light sources are already used in optical metrology and tomography and are believed to become important in telecommunication systems and bio-medical applications.

Usually SCG in MSF have been obtained by pumping the fiber in the anomalous dispersion regime where fission of solitons provide a wide spectrum through various nonlinear effects such as self-phase modulation, Raman-scattering and four-wave mixing. Recently, it was reported that wide and flat spectra could be obtained in the visible by simultaneously pumping a MSF in the normal and anomalous regime with picosecond pulses [1].

In this contribution, we report, for the first time to our knowledge, on SCG with a femtosecond dual-pumping scheme. A 9 MHz oscillator delivering 300 femtosecond pulses at 1028 nm is frequency doubled and both the fundamental and second harmonic are coupled into a MSF. When the two pulses are temporally overlapped in the fiber a broad supercontinuum appear. By tuning the temporal delay between the two pulses, different regions of the spectrum can be enhanced which allows either improved flatness of the spectrum or selective amplification of regions of interest.

Results from different fibers will be presented and differences between femtosecond and picosecond pumping will be considered. Furthermore, numerical simulations will be presented discussing the physical mechanisms behind dual-wavelength pumping supercontinuum generation.

[1] Champert et al, White-light generation in normally dispersive optical fiber using original multi-wavelength pumping system, Optics Express, Vol. 12, p. 4367 (2004)

6103-34, Session 7

Wide-band supercontinuum generation for sub-micron-resolution OCT by using a laser-diode-seeded amplified pulse source

S. Moon, D. Kim, Gwangju Institute of Science and Technology (South Korea)

We propose a new compact supercontinuum source based on mature fiber-optic telecom technologies. A laser diode with gain switching technique was used to produce the initial seeding pulses. And cascaded EDFAs were employed to boost the peak power of these pulses effectively. In order to maximize the pulse power for a given saturation output of the EDFAs, the pulse repetition rate was reduced to few MHz or even less than 1 MHz. We have obtained 1-kW peak pulse power by using a 1550-nm DFB laser diode and three cascaded EDFAs in maintaining the pulse-width less than 40 ps. By launching these high-power pulses into dispersion-shifted fibers (DSFs), ultra-wide bandwidth supercontinua were generated. The wavelength range only for the blue-shifted spectrum of our supercontinuum covers an octave from 800 nm to the pumping wavelength of 1550 nm. To understand the mechanism, we have investigated the influences of the length and the dispersion property of the DSF used for the supercontinuum as well as time-domain spectral evolution. Four-wave mixing, modulation instability and Raman scattering were found to play major roles in our supercontinuum generation. It was also observed that the excessive Raman interaction caused by using too long DSF degrades the flatness of the output spectrum. With the fiber length optimization, flat wide-band supercontinuum centered at 1200 nm was obtained after a short-wavelength pass filter. This compact supercontinuum source can enable sub-micron longitudinal resolution when used in optical-coherence tomography (OCT).

6103-35, Poster Session

Nonlinear optical properties of triphenylmethane (malachite green and methyl green) dyes as studied by Z-scan using low power He-Ne laser

P. Palanisamy, R. Madhana Sundari, Anna Univ. (India)

The optical nonlinearities of organic dyes namely malachite green and methyl green from triphenylmethane family are measured using the Z-scan technique. The third-order optical nonlinearity of the dyes is explored in aqueous solution form. For different concentrations of aqueous solutions of the dyes, the third order nonlinear refractive index and nonlinear absorption coefficient measured are presented. The dyes (in aqueous form) under study are found to exhibit negative nature of non-linearity, which is mainly due to the thermally induced refractive index change. He-Ne laser (633 nm) is used for Z-scan technique. The third-order susceptibility of these dyes in aqueous form is found to be of the order of 10-7 esu.

6103-36, Poster Session

Optical data atorage in acid red dye-doped thin films

P. Palanisamy, D. Sankar, Anna Univ. (India)

High Density Optical Data Storage is a current field gaining importance where research work is done in abundance to bring about Holographic CDs to light. Dye doped gelatin films are promising candidates as recording materials for holographic data storage because of the ease of preparation and low cost. In this report we suggest some Acid red dyes as useful recording materials for optical data storage. Acid red dyes namely Acid Red 73, Acid Red 91 and Acid Red 114 that are completely water soluble are used to sensitize gelatin thin films for data storage. These dyes have their absorption peak around 514nm. Two coherent beams of Argon ion laser (514.5nm) are used to form grating in the dye sensitized gelatin films. The grating formed is found to be permanent. The diffraction efficiency of each material as a function of different parameters such as dye concentration, writing beam intensities and their ratio and spatial frequency has been studied and presented.

6103-37, Poster Session

Studies on third order nonlinearity of oxazine dye using Z-scan technique

P. Palanisamy, M. A. H. Qusay, Anna Univ. (India)

The single beam Z-scan technique is used to determine the nonlinear optical properties of the solution of oxazine dyes, nile blue chloride and nile blue A in the solvent ethanol. The experiment is performed with He-Ne laser at wavelength 632.8 nm. The measurements are carried out at different concentrations of the dyes for several incident beam intensities. The nonlinear refractive index n2 shows negative sign (self-defocusing) nonlinearity for all concentrations of the samples. The defocusing effect is attributed to the thermal nonlinearity resulting from absorption of radiation in dyed solution at 632.8 nm. The intensity-dependence of nonlinear refractive index was investigated. The third-order nonlinear refractive index is found to be linearly dependent on the dye concentration within the concentration range studied. The results showed that the solution of nile blue chloride and nile blue A in solvent ethanol exhibited large nonlinear refractive coefficient. These results show that theses dyes have potential applications in nonlinear optics.

6103-39, Poster Session

Intervalence band solitons in semiconductor quantum wells

F. Biancalana, Tyndall National Institute (Ireland)

Many coherent optical phenomena related to Optical Bloch Equations (OBE) for dilute atoms are known to have analogues occurring in bulk semiconductors and semiconductor quantum wells, where the effects of Coulomb interactions and many-body exchange terms cannot be neglected, and the Semiconductor Bloch Equations (SCBE) must be used instead. The most important of these effects are: optical Stark effects, semiconductor photon echo, generalized Rabi oscillations, and partial self-induced transparency (SIT) due to exciton resonances [D.S.Chemla et al., Nature 411, 549 (2001)]. The importance of these comparative studies relies on the fact that they allow us to understand the role of the various quantum many-body interactions in dense materials.

While the two-level analogies between atomic and semiconductor physics have been successfully exploited, the question of what it is possible to learn from a comparison of coherent three-level molecular systems and three-band semiconductor structures is currently under intense investigation [M.E.Donovan et al., Phys. Rev. Lett. 87, 237402 (2001); R.Binder et al., phys. Stat. Sol. (b) 221, 169 (2000); R.Binder et al., Phys. Rev. B 61, 2830 (2000)].

In the present work we study the propagation of a novel kind of short temporal optical soliton in type-I GaAs/AlGaAs semiconductor quantum wells. These solitons have a lorentzian profile, they live in a 1-dimensional parameter space, and are based on the propagation of two components at different frequencies, and rely on the existence of a two-photon Raman-like transition between the light-hole (LH) valence band and the heavy-hole (HH) valence band, coupled indirectly through the conduction band (CB). The frequency difference between the two optical components is tuned in resonance with the frequency difference between the LH band and the HH band, therefore introducing an indirect coherence between these bands. This coherence generates a polarization in the semiconductor medium, which is able to lock the two optical components, which will therefore travel at the same group velocity, determined by the material parameters. These solitons have a direct analogue in the gas of three-level Raman molecules [A.Kaplan, Phys. Rev. Lett. 73, 1243 (1994)].

By solving the full SCBE for the two-photon case and other related simplified models based on a local-field model, we provide an extensive numerical and analytical feasibility study of the conditions of excitation of two-photon Raman solitons in quantum wells. We show the existence of

threshold values in energy and pulse durations for the soliton generation. The influence of the Rabi frequency renormalization and excitation-induced dephasing effects, which mark the difference with a set of uncoupled three-level systems, is therefore clarified.

6103-40, Poster Session

Semiorganic nonlinear optical material for frequency doubling: Sodium p-Nitrophenolate

S. Dhanuskodi, R. Pricilla Jeyakumari, Bharathidasan Univ. (India)

Materials with large second order optical nonlinearities, lower cutoff wavelength and stable physicochemical performance are needed in order to realize many of photonics and optoelectronic applications. During the last several years, according to the idea of combining the inorganic distorted polyhedron with asymmetric π conjugate organic molecules, semiorganic materials have been attracting a great deal of attention in the NLO field, because such materials have the potential for combining the high optical nonlinearity and chemical flexibility of organics with temporal and thermal stabilities and excellent transmittance of inorganics.

Sodium p-nitrophenolate (SPNP) a semiorganic nonlinear optical material possessing large values of hyperpolaraizability because of an organic entity p-nitrophenol. The organic ligand (nitrophenoxy ion) is ionically bonded to the metal ion (sodium) along with the intermolecular hydrogen bonding imparts higher structural stability to the crystal. SPNP useful for frequency doubling (in the IR region) has been synthesized and the solubility studies have been carried out in the temperature range 30-50*C. Single crystals (10 x 7 x 3 mm3) of SPNP (methanol as solvent) have been grown by slow evaporation of the saturated aqueous solution at 30*C using a constant temperature bath. The lattice parameters of the grown crystals have been determined by single crystal X-ray diffraction technique. The UV-Vis-NIR transmittance spectrum has been recorded in the range 200-1500nm and the cutoff wavelength is 530 nm. The molecular structure was confirmed by FT_IR and FT-NMR. SPNP was thermally stable up to 103*C determined by TG/DTA curves. The powder SHG efficiency was found to be 5 times that of KDP using a Q-switched Nd:YAG laser (=1064 nm, 10 ns, 10Hz) and its phase matching property was established. Laser damage threshold of the SPNP was determined as 52 MW/cm2 .

6103-41, Poster Session

Sellmeier and thermo-optic dispersion formula for AgGa(S1-xSex)2 with application in mid-IR generation

S. Banerjee, Chitose Institute of Science and Technology (Japan); N. Umemura, Japan Defense Agency (Japan); K. Kato, Chitose Institute of Science and Technology (Japan)

The ternary chalcopyrite semiconductors (example AgGaS2 & AgGaSe2) are at present one of the most widely used non-linear optical materials for frequency conversion in the mid-IR, owing to their high nonlinear coefficient (d36(1.054mm)=23.6pm/V for AgGaS2 & d36(10.591mm)=39.5pm/V for AgGaSe2) and high transparency in the mid-IR. These chalcopyrite semiconductors have also been demonstrated as narrow band pass filters by Horinaka et al and Badikov et al, utilizing the accidental isotropy and optical activity of these compounds. While until now only one paper has been published for the mixture crystal of AgGaS2 and AgGaSe2, we have studied the linear and nonlinear optical properties of this material using the index data of Mikkelsen and Kildal. In this paper we present Sellmeier equations for various concentration (x=0.3, 0.55, 0.75), which correctly reproduce the isotropic wavelength (ne=no) of the mixture crystal reported by Yamamoto et al and the thermo-optic dispersion formula for x=0.55, which is highly useful for predicting the Nd:YAG pumped OPO wavelength near 5.75mm for medical applications.

6103-42, Poster Session

Light field transformation by intracavity four-wave mixing

O. G. Romanov, O. A. Ormachea, A. L. Tolstik, Belarusian State Univ. (Belarus); J. L. Arce Diego, D. Pereda Cubián, F. Fanjul Vélez, Univ. de Cantabria (Spain)

Advances in the development of nonlinear interference and holographic systems based on four-wave mixing point to great potentialities of these systems for real-time processing and correction of the light fields, formation of the desired space-time structures of laser radiation, image transfer, realization of logic and mathematical operations, creation of bistable devices and adaptive optics elements. This work presents the results of theoretical and experimental studies into the processes of light field transformations upon frequency-degenerate and -nondegenerate four-wave mixing in nonlinear Fabry-Perot interferometer. The principal aim is to develop a theory of intracavity four-wave mixing in complex molecular media in conditions of exhibited internal (scattering from dynamic gratings) and external (resonator) feedback, to determine a mechanism of light field transformations at the dynamic holograms and by nonlinear interferometers, to work out and introduce into practice novel nonlinear-optical methods for the control over the spatial-temporal characteristics of light beams. For theoretical description of typical experimental situations we used the round-trip model of interferometer adapted for the geometry of four-wave mixing, which can be realized in the scheme of symmetrical oblique incidence of reference and signal beams to the front and back mirrors of cavity. The conditions of magnification of dynamic gratings efficiency due to contribution from multiple interference of recording and reading light beams have been studied experimentally and by means of theoretical modelling. The methods aimed at the realization of various types of optical bistability, spatial hysteresis, regular and chaotic intensity oscillations, formation of coupled resonator solitons are proposed and investigated.

6103-43, Poster Session

Wide-band wavelength conversion using a dispersion-flattened nonlinear PCF

Y. Yu, S. Ruan, C. Du, J. Zhao, J. Zeng, Shenzhen Univ. (China)

Microstructure fibers (MFs) have received a lot of attention owning to their high nonlinearity per unit length. In fact, all of the nonlinear effects that are present in standard optical fibers are expected to be observed in MFs with reduced length and pump power requirements. A number of MF-based telecommunication applications have already been demonstrated, including Raman amplification, 2R regeneration, wavelength conversion, and optical switching, optical parametric amplifiers.

In particular, Four-wave mixing (FWM) is a promising technique for wavelength conversion in optical networks owing to its ultrafast response and high transparency to bit rate and modulation format. However, it is difficult to maintain phase matching in a long fiber FWM-based wavelength converter, because the group velocity dispersion is wavelength dependent. Also, the necessity of fixing the pump in the dispersion-zero wavelength region may limit the flexibility of the optical networks. In order to obtain broad-band efficient wavelength conversion, the fiber should have high nonlinearity, low dispersion, low dispersion slope, and short length.

In this letter, a 100-m dispersion-flattened nonlinear PCF prepared by Crystal Fiber A/S was applied to obtain wide-band wavelength conversion using FWM. Since the PCF has a very small dispersion slope in the 1550-nm range, a wavelength converter with widely tunable operation range over 80 nm(1510-1580 nm) and with a conversion efficiency of about -10 dB has been obtained pumped by CW 1480 nm fiber laser. It is indicated that such converters with dispersion-flattened nonlinear PCFs are promising for wide-band wavelength conversion applications in all-optical networks.

6103-44, Poster Session

Performance comparison of advanced optical modulation formats in wavelength division multiplexing (WDM) systems employing G.655 fibers

I. Neokosmidis, T. Kamalakis, T. Sphicopoulos, D. Syvridis, Univ. of Athens (Greece)

The need for wavelength division multiplexing (WDM) systems with high bit rates and increased spectral efficiency has led to the examination of various alternatives to the standard return-to-zero (RZ) and non return-to-zero (NRZ) modulation formats. NRZ alternatives include duobinary NRZ and NRZ Differential Phase Shift Keying (NRZ-DPSK). The RZ amplitude modulation alternatives consist mainly of alternate mark inversion (AMI), carrier suppressed (CS) and alternate phase (AP). RZ-DPSK and CS-DPSK are also gaining popularity. This paper addresses the issue of the choice of optical modulation format in a multi span WDM system using G.655 fiber. Various modulation formats are assessed by numerical simulation in the presence of fiber non linearities with Four Wave Mixing (FWM) being the dominant effect. The simulations include the influence of the Amplified Spontaneous Emission (ASE) noise which can cause nonlinear phase noise through fiber nonlinearity. It is shown that the various amplitude modulation alternatives result in more or less the same performance. Phase modulation schemes such as DPSK drastically increase the system performance leading to an increase of the Q-factor by at least 3dB. It is also shown that RZ modulation formats can provide increased nonlinear tolerance in the presence of channel misalignments. If the channels are all aligned however, RZ modulation does not lead to performance enhancement.

6103-45, Poster Session

Experimental observations of diffraction of ultrashort

H. Zhang, Univ. of Nebraska/Lincoln

Inspired by previous theoretical work, experiments on diffraction of 10 femtosecond ultrashort pulses passing through a single slit have been performed. Fringes are dramatically reduced or even eliminated in the diffraction of ultrashort mode locked (ML) laser in the near field compared with that of the continuous wave (CW) laser. This can be explained in the frequency domain as a result of the broadband spectrum of ultrashort pulses. Simulations are performed for Fresnel diffraction for both ML and CW mode lasers and they correspond well with experimental observations. The result of this work has important implication in biomedical imaging and remote imaging applications to name only a few.

Conference 6104: High-Power Diode Laser Technology and Applications IV

Monday-Tuesday 23-24 January 2006

Proceedings of SPIE Vol. 6104

6104-01, Session 1

Non corrosive micro coolers with matched CTE

T. Ebert, ProLas Produktionslaser GmbH (Germany)

After the first beginnings with micro coolers made with selective laser melting, the results with stainless steel coolers shows the need of new materials. The choosen new material is a nickel alloy which is used in the nuklear industry as an anti-corrosion-coating. The results regarding thermal conductivity were as good as common micro coolers made of copper. This presentation describes the next steps from the pure cooling system to an integrated part with a matched CTE.

Using different materials only in the mounting area leads to a matched CTE without having bad influence of thermal resistance. In addition to that, the hard and stabile material of the cooler corpus opens the possibility to integrate more functions then only the cooling, for example integrated holder for micro lenses and electrical contacts.

6104-02, Session 1

Reliable high power diode lasers: thermomechanical fatigue aspects

G. Klumel, Y. Gridish, I. Szafranek, Y. Karni, SCD-Semi Conductor Devices (Israel)

High power water cooled diode lasers are finding increasing demand in biomedical, cosmetic and industrial applications where repetitive CW (continuous wave) and slow pulse (switched CW) operation modes are required. When operating in such modes the lasers experience numerous complete thermal cycles between "cold" heat sink temperature and "hot" temperature typical for thermally equilibrium CW operation. It is clearly demonstrated that the main failure mechanism directly linked to repetitive CW operation is thermo-mechanical fatigue of solder joints adjacent laser bars, especially when "soft" solders are used. Analyses of the bonding interfaces were carried out using acoustic imaging and scanning electron microscopy. It was observed that intermetallic compounds, formed already during bonding process, lead to the solders fatigue both on p- and n-side of the laser bar. Fatigue failure of solder joints reduces useful life time of the stacks to hundreds hours in comparison with more than 10,000 hours life time typically demonstrated in commonly adopted non-stop CW reliability testing programs. It is shown, that proper selection of package materials and solders, careful design of fatigue sensitive parts and burn-in screening in the hard pulse operation mode allow considerably increased life time and reliability, not compromising the devices efficiency, optical power density and compactness.

Microchannel cooling, requiring the deionised water, permanent control and fine filtration, remains a serious maintenance and reliability problem. The coolers leakage and clogging are frequently occurring because of the deionised water aggressive corrosion. A novel high power laser diode stack that eliminates the above problems and immune to cyclic fatigue failures is demonstrated. The solution is especially effective for pulsed applications in duty cycle range of 20-50%.

6104-03, Session 1

Expansion-matched passively-cooled heatsinks with low thermal resistance for high-power diode laser bars

M. Leers, C. Scholz, K. Boucke, R. Poprawe, Fraunhofer Institut für Lasertechnik (Germany)

The lifetime of high-power diode lasers which are cooled by standard copper heatsinks is limited. The reasons are the aging of the indium solder normally employed, the mechanical stress caused by the mismatch between the copper heatsink (16 - 17ppm/K) and the GaAs diode laser bars (6 - 7,5 ppm/K). For micro - channel heatsinks corrosion and erosion of the micro channels additionally limit the life time.

The different thermal behaviour and the resulting stress cannot be totally compensated by the solder. Expansion matched heatsink materials like tungsten-copper or aluminium nitride reduce this stress. A further possible solution is a combination of copper and molybdenum layers. But all these materials have a high thermal resistance in common. For high-power electronic or low cost medical applications novel materials like copper/carbon compound, compound diamond or high-conductivity ceramics are developed during the recent years.

Based on these novel materials, passively cooled heatsinks are designed and their properties are are checked by thermal and mechanical simulations. The expansion of the heatsink and the induced mechanical stress between laser bar and heatsink are the main tasks for the simulations. A comparison of the simulation with experimental results for different material combinations illustrates the advantages and disadvantages of the different approaches. Together with the boundary conditions the ideal applications for packaging with these materials are defined.

The goal for the development of passively-cooled expansion-matched heatsinks has to be a long-term reliability of several 10.000h and a thermal resistance below 1 K/W.

First long-term results of different heatsinks will be shown.

6104-05, Session 1

Comparative performance studies of indium and gold-tin packaged diode laser bars

D. Lorenzen, Jenoptik Laserdiode GmbH (Germany); M. Schröder, Jenoptik LaserDiode GmbH (Germany); J. Meusel, P. Hennig, Jenoptik Laserdiode GmbH (Germany); H. König, M. Philippens, OSRAM Opto Semiconductors GmbH (Germany)

The increased efficiency and quality of high-power laser diode material is about to lead to a paradigm change in the packaging technology: Laser diode temperature during operation seems to be no longer the main issue for reliability but the solder itself: The widely employed indium solder exhibits reliability lacks at high current densities. High-power operation is thus limited by the solder more than by the laser itself. This issue is even more obvious when the laser is operated in a long-puls mode that leads to harmful mechanical fatique in the soft solder layer.

We present the results of a broad study that compares both, continuous wave and long-puls mode operation of lasers diode bars that were soldered with indium and gold-tin.

6104-06, Session 2

An overview of DARPA's SHEDS and ADHELS programs

C. M. Stickley, Defense Advanced Research Projects Agency

An overview will be given of progress in DARPA's program in Super High Efficiency Diode Sources (SHEDS) by the performers as they strive to achieve 80% efficient edge-emitting diodes operating at 50C junction temperature and producing 480 Watts from a stack, or 480 Watts/cm2 from array of VCSELs, and with a linewidth of 2-4 nm. The presentation will also include the status of DARPA's program in the Architecture of Diode High Energy Lasers (ADHELS).

6104-07, Session 2

Ongoing development of high-efficiency and high-reliability 9xx-nm bars and fiber-coupled devices at Coherent

H. Zhou, K. Kennedy, E. Weiss, J. Du, P. Reichert, J. Li, Coherent, Inc.

Established and emerging markets for laser diodes demand continuous improvements in power, conversion efficiency, brightness, and reliability, while also requiring reduced operational costs through simplified system designs. Offering convergent solutions to these often incompatible goals, Coherent presents recent product releases and development results on the next generation passively-cooled, high efficiency, high reliability bars and fiber-coupled products at 915 nm, 940 nm, and 980 nm.

Ongoing optimization of epitaxial designs and rigorous device engineering has led to a family of high power-conversion-efficiency (PCE) fiber-array-package (FAP) products. Powered by our latest generation of high-efficiency 9xx nm diodes, those FAP devices have consistently exceeded 55% PCE at 40W and 50W power levels, with 62% PCE demonstrated out of the fiber. High-temperature optimization has produced 60% PCE on the bar level with passive cooling at a TEC temperature of 50°C, and 65% PCE is typical for these 9xx nm bars when operating at 50W to 60W CW level with TEC = 25°C. 280W QCW has been demonstrated from a 20% fill-factor bar, with no indication of catastrophic optical mirror damage (COMD). Leveraging these improvements has enabled high brightness FAPs demonstrating 100W CW from a 600μm-core fiber bundle with 0.12 N.A .

At Coherent, reliability has always been at the very core of any product release or developmental effort. We have observed over 220,000 total real-time device hours at a variety of accelerated and non-accelerated operating conditions with a random failure rate <0.9% per kilo-hours and gradual degradation rate <0.4% per kilo-hours. For a 30% fill- factor 50W CW 9xx nm bar, this equates to a >30,000 hour median lifetime with 90% confidence level. Similar type of 30% fill-factor 9xx nm bars with longer cavity length are under development for 80W CW application with extrapolated median lifetimes greater than 20,000 hours.

6104-08, Session 2

Highly reliable high-power broad area laser diodes

V. V. Rossin, M. G. Peters, E. P. Zucker, B. Acklin, JDS Uniphase Corp.

High-power broad area 9xx nm lasers are used to pump fiber lasers and amplifiers in a wide range of telecom and industrial applications. Increase of reliable power from a single laser results in smaller number of lasers per system and significant cost savings. A multi-cell life test performed on our new generation of very efficient high power laser diodes showed a steep power acceleration with the exponent of nearly 6. Improvement in facet passivation process resulted in significantly less power acceleration of failures. Subsequent multi-cell life test on upgraded lasers showed median lifetime of 500,000 hours at operating conditions of 8W and 25C. Optical powers as high as 16.5W for thermally limited CW operation and 30W for 20∝s pulsed operation were recorded. Results of the life test performed at power cycling conditions (1Hz repetition rate, 50% duty cycle) show significant improvement.

6104-09, Session 2

High-power, reliable 808-nm laser bars for QCW and CW applications

M. Mondry, M. Fouksman, H. Zou, J. Li, J. Haapamaa, Coherent, Inc.

Manufacturers of Nd:YAG lasers continue to demand 808 nm pump sources that deliver ever lower operating costs (measured in $/kW-hour). Responding to this demand, Coherent has developed a new generation of high power, 808 nm laser bars. These lasers are most ideal for high power, QCW applications, but also perform very well in CW pumping applications. The key to the improved power for QCW bars is increase in catastrophic optical mirror damage (COMD) threshold. Through a combination of advances in epitaxial structure design and coating technology after aging COD limit for new generation of bars has been increased by 50%. This allowed us to achieve reliable QCW operation at 270W of peak power. Lifetest results shows that lifetime of these bars at these conditions exceed 2e109 shots. We also developed similar structure optimized for CW operations. When mounted on microchannel water cooled packages CW bars operate at an output power of 150 W. Power conversion efficiency (PCE) for CW bars was more than >50%.

6104-10, Session 2

Diode laser efficiency increases enable >400-W peak power from 1-cm bar and shows clear path to peak powers in excess of 1kW

P. A. Crump, J. Wang, S. Patterson, D. Wise, A. Basauri, M. DeFranza, S. Elim, W. Dong, S. Zhang, M. Bougher, J. Patterson, S. Das, M. Grimshaw, J. Farmer, M. A. DeVito, R. Martinsen, nLight Photonics

Peak optical power from single 1-cm diode laser bars is advancing rapidly across all commercial wavelengths. We demonstrate > 400W output from single 800-nm bars and 360W output from 975-nm 1-cm bars, complementing the high powers we have achieved from single 1-cm laser bars at other wavelengths (100W at 1470nm and 70W at 660-nm). Advances in diode laser efficiency and low thermal resistance packaging technology continues to drive these powers higher. The most critical improvements have been the reduction in the diode laser operating voltage through optimization of hetero-barriers (leading to 73% efficient 100W bars on copper micro-channel) and a reduction in packaging thermal resistance by optimizing micro-channel performance (leading to < 0.2C/W thermal resistance). Progress in material performance is reviewed and we show that current trends imply there is no fundamental barrier to achieving peak powers of 1kW per 1-cm diode laser bar, with 700W per bar being a realistic near term goal.

6104-11, Session 2

High-performance, high-reliability 880-nm diode laser bars and fiber-array packages

M. Fouksman, S. Lehconen, J. Haapamaa, K. W. Kennedy, J. Li, Coherent, Inc.

The 880 nm diode laser is emerging as the source of choice for pumping Nd:YV04 laser crystals because it offers higher pumping efficiency than 808 nm diode lasers. This paper reports on recent progress in the development of high power, high reliability, 880 nm laser bars. Specifically, high performance has been achieved based on Coherent's aluminum-free active (AAA) epitaxial structures while maintaining lifetimes greater than 10,000 hours. This includes 30% fill factor, 1 cm bars on conductively cooled packages (CCP) operating at 55 W with proven manufacturability. We observed power conversion efficiency (PCE) of up to 56%. These lasers have a far field fast axis divergence of 32° (FWHM), and slow axis divergence of <7° (FWHM). Typical value of the FWHM of output spectrum is 2.5 nm. These bars were used to build fiber array packages (FAPs) operating at 45 W. We have achieved FAP PCE of 50% and numerical aperture of <0.12. Reliability of both bars and FAP was shown to exceed 10000h MTBF.

6104-12, Session 2

Effect of compressive and tensile strain on the performance of 808-nm QW high power laser diodes

M. Levy, B. Yuri, Y. Karni, SemiConductor Devices (Israel)

The effect of compressive and tensile strain of Quantum Wells (QWs) on the gain and transparency current density of high power laser diodes was studied. Material composition of InGaAlAs/AlGaAs and GaAsP/InGaP were utilized for the study of compressive and tensile strain QWs, respectively. Variation in the strain degree was achieved by changing the In and P mole fraction accordingly. We found that the transparency current densities of compressively strained QWs do not vary significantly as a function of strain and are about 105 A/cm2. In contrast, the transparency current in tensile strained QWs decrease from 150 to 130 A/cm2 as the strain is increased. These differences are correlated with the low temperature photoluminescence excitation spectra, which show that the valence subbands energy separation are much larger for compressively strained QWs (40-70 meV) than for tensile strained QWs (20-30) meV. The material gain of compressively strained QWs is insensitive to the variation of strain degree (~1000 cm-1), while the material gain increases from 1000 cm-1 to 1300 cm-1 when the tensile strain is increased. In spite of the higher transparency densities the gain achieved at maximum strain is larger for tensile strained QW laser. This result is explained by the strain influence on the electron-hole recombination strengths.

Consequently the effect of strain on the performance of High Power QCW/CW laser bars was also investigated. The threshold current and slope efficiency of bars with compressively strained QWs are almost constant (1.05 W/A). On the contrary, as the tensile strain is increased the threshold current reduces and the slope efficiency increases (1-1.2 W/A). As a result, tensile strain QWs bars are more efficient at high power operation.

6104-13, Session 3

8 W high-efficiency high-brightness tapered diode lasers at 976-nm

M. T. Kelemen, Fraunhofer-Institut für Angewandte Festkörperphysik (Germany); J. Weber, G. Kaufel, R. Moritz, M. Mikulla, G. Weimann, Fraunhofer Institut für Angewandte Festkörperphysik (Germany)

Tapered diode lasers are mainly used today in external resonator configuration for non-linear spectroscopy or frequency doubling for blue-green outputs. Now increased brightness and lifetime make tapered lasers even attractive for material processing and for pumping of fibre amplifiers or lasers.

We have realized high-power ridge-waveguide tapered diode lasers emitting at 976 nm. The high material quality of the MBE-grown laser structures yields a high internal efficiency of more than 97% and low internal losses of 0.5/cm. Tapered single emitters consist of a ridge section with a length of 500 μm and a taper section with a length of 3000 μm. The taper angle was 6°.

A threshold current of 1.07 A corresponding to a threshold current density of 222 A/cm2 has been obtained. The maximum slope efficiency of 1.09 W/A together with the low series resistance of 35 mW results in a high wall-plug efficiency of 58% at 5.5 W output power. This high wall-plug efficiency remains nearly constant up to operation currents of 9 A corresponding to output powers of more than 8 W. At an operation current of 15 A an output power of 12.5 W has been achieved, which is to our knowledge the highest output power in continuous wave mode for tapered diode lasers reported so far. At 8 W a nearly diffraction limited behavior with values for M2 of less than 1.5 have been observed resulting in a brightness of more than 660 MW/cm2.

6104-14, Session 3

High brightness laser diode bars

N. Lichtenstein, Y. Manz, J. Müller, S. Pawlik, A. Thies, J. Troger, S. Weiss, C. Harder, Bookham AG (Switzerland)

Future high power laser systems are using fiber laser (FL) or direct laser diode (DLD) architectures as pump sources. While today's high power laser diode bars are able to deliver in excess of 300 W under CW operation from high fill-factor designs, most important for FL and DLD applications is excellent reliability at enhanced brightness levels at competitive cost.

Bookham's advanced (Al)Ga(In)As laser technology has been continuously improved over the last two decades with respect to power, reliability and cost maintaining the classical ridge-waveguide design and the effective elimination of catastrophical optical mirror damage (COMD) using E2 facet passivation. For superior longterm stability of the packaged devices AuSn-based mounting technologies are used similar as for our telecom products.

Based on the most recent generation of Bookham's laser diode bars in the 9xx nm wavelength range which are able to deliver in excess of 250 W of output power from 50% filling factor 2.4 mm cavity length design, we have developed low 20% fill-factor bar devices for improved brightness delivery. The bar design contains standard 19 emitters at 500 um pitch while the width of the individual emitters is as small as 100 um to enable high brightness fiber coupling schemes. Close to 200 W of output power has been achieved in CW mode from actively cooled micro-channel cooler devices without signs of damage. Mounted on conductively cooled copper blocks, still more than 130 W (CW) have been obtained, indicating the high conversion efficiency of >60% reducing the thermal load on the mounting assembly. The high power density at the front facet of more than 100mW / um depicts the robust device design and enables high operating power levels. Based on extensive reliability testing in excess of 5000 h at power densities ranging up to 30mW / um and beyond, highly reliable operation of these 20% fill-factor bars is expected.

To facilitate fiber coupling into wide-core multi-mode fibers a further reduction of the emitter aperture has been realized. From a single 3.6 mm cavity length by 800 um wide emitter design about 50 W output power has been obtained in CW mode from devices mounted on standard conductively cooled 1x1 inch copper blocks. While CW operation has been thermally limited, extremely high peak power operation can be expected in qCW operation. Due to the narrow aperture of this MaxiChip efficient and easy to achieve coupling into wide aperture multimode fibers can be achieved. From extensive multi wafer stress tests of multimode single emitters reliable operation in excess of 10 kh is anticipated. While first samples have been realized at 940 nm emission wavelength, scaling at wavelengths ranging from 0.8 to 1 um is expected in the future.

6104-15, Session 3

Very high power operation of 980-nm single-mode InGaAs/AlGaAs pump lasers

M. A. Bettiati, C. Starck, F. Laruelle, V. Cargemel, P. Pagnod-Rossiaux, P. Garabedian, D. Keller, G. Ughetto, J. Bertreux, L. Raymond, G. Gelly, R. Capella, Avanex France s.a. (France)

We report on the development of a new generation of very high power 980 nm single lateral mode ridge-waveguide quantum-well lasers. An asymmetric-waveguides vertical structure has been optimized for very low internal losses while keeping the vertical mode-size large, thus allowing a low vertical far-field beam angle of less than 19°. Careful optimization of the doping profiles, and epitaxial interfaces optimization for reduced scattering, allowed to obtain internal losses as low as 0.6-0.7 cm-1. Such low losses are necessary to keep the external efficiency high in very long cavities, together with a high internal quantum efficiency. We thus reached our goal of keeping the external efficiency above 70% even for cavity lengths of 4.5 mm. The flared ridge waveguide has been designed to strongly filter higher order lateral modes, and kink-free operation has been obtained up to over 1.5 W output power, with very stable

vertical and horizontal beam patterns. High saturation powers above 2 W have also been demonstrated at 25°C, and over 1.5 W at 75°C. Wavelength stabilized chips, by means of a fiber Bragg grating, reached linear fiber powers above 1.0 W with strong suppression of gain-peak lasing at all currents and good power stability.

6104-16, Session 3

Comparison between 50 W tapered laser arrays and tapered single emitters

C. Scholz, K. Boucke, R. Poprawe, Fraunhofer-Institut für Lasertechnik (Germany); M. T. Keleman, J. Weber, M. Mikulla, G. Weimann, Fraunhofer Institut für Angewandte Festkörperphysik (Germany)

During the last few years high power diode laser arrays have become well established for direct material processing due to their high efficiency of more than 50%. But standard broad-area waveguide designs are susceptible to modal instabilities and filamentations resulting in low beam qualities. The beam quality increases by more than a factor of four by using tapered laser arrays, but so far they suffer from lower efficiencies. Therefore tapered lasers are mainly used today as single emitters in external resonator configurations. With increased output power and lifetime, they will be much more attractive for material processing and for pumping of fiber amplifiers.

High efficiency tapered mini bars emitting at a wavelength of 980 nm are developed, and in order to qualify the bars, the characteristics of single emitters and mini bars from the same wafer have been compared. The mini bars have a width of 6mm with 12 emitters. The ridge waveguide tapered lasers consist of a 500 μm long ridge and a 2000 μm long tapered section.

The results show very similar behavior of the electro-optical characteristics and the beam quality for single emitters and bars. Due to different junction temperatures, different slope efficiencies were measured: 0.8 W/A for passively cooled mini bars and 1.0 W/A for actively cooled mini-bars and single emitters. The threshold current of 0.7 A per emitter is the same for single emitters and emitter arrays. Output powers of more than 50 W in continuous wave mode for a mini bar with standard packaging demonstrates the increased power of tapered laser bars.

Defect measurements by LBIC (Laser beam induced spectroscopy) and photoluminescence microscopy provide an insight into the defect development in single emitters and emitter arrays.

6104-17, Session 4

Advances in high brightness semiconductor laser bars and arrays

R. M. Lammert, S. W. Oh, M. L. Osowski, C. Panja, P. Rudy, T. S. Stakelon, J. E. Ungar, Quintessence Photonics Corp.

We present recent advances in high power semiconductor lasers including increased spectral brightness, increased spatial brightness, and reduced cost architectures at wavelengths from the near infrared to the eye-safe regime. Data are presented which demonstrate both edge emitter devices and high power surface emitting 2-dimensional arrays with internal gratings to narrow and stabilize the spectrum. Diodes with multi-mode high spatial brightness and high power single mode performance in the 808 and 976nm regime are described, and advances in high power bars at eye-safe wavelengths are presented. These devices have the potential to dramatically improve diode pumped systems and enable new direct diode applications.

6104-18, Session 4

9xx high power pump modules

S. Pawlik, B. Sverdlov, R. Bättig, B. Schmidt, N. Lichtenstein, H. Pfeiffer, J. Müller, B. Valk, C. Harder, Bookham AG (Switzerland)

High power pump modules are used for industrial as well as telecom applications such as for high power fiber lasers and cladding pumped erbium doped fiber amplifiers (EDFASs). Key element of a pump module is a single emitter laser diode, which normally has an aperture of around 90 μm, in order to provide best coupling into an optical multi-mode fiber with a 105 μm core diameter.

Our design approach for multi-mode chips is based on Bookham's "single-mode" laser diode technology, which is used for telecom grade high power single-mode pump modules with less than 500 FIT at maximum operating powers of up to 600 mW. Main features of Bookham's mature chip technology are the InGaAs/AlGaAs structures grown by MBE, the ridge-waveguide manufacturing process and the E2 facet passivation. The combination of these technologies enables us to realize high performance broad area single emitters, on which we recently reported a maximum light output power of more than 22.5 W in Q-CW operation and a differential quantum efficiency of 90%.

In this communication we report on the fiber coupled performance characteristics of Bookham's latest generation of high power pump laser diodes. Coupling efficiency into a multi-mode fiber with a 0.22 NA exceeds 95% due to the low divergence of the laser beam. The modules were tested at various temperatures in CW operation. Ex-fiber light output powers of 12 W are shown. Additional performance and lifetest results of the modules will be presented in the final communication.

6104-19, Session 4

9xx-nm single emitter pumps for multi-kW systems

A. Ovtchinnikov, V. Gapontsev, I. Berishev, G. Ellis, A. Komissarov, N. Moshegov, O. Raisky, P. Trubenko, V. Solodovnikov, IPG Photonics Corp.

Single emitter multimode pumps outperform traditional monolithic laser diode arrays in power efficiency, reliability and brightness. Distributed pumping architecture realized with discrete single emitter diodes makes multi-kilowatt class systems robust against individual pump failures and ensures a lower cost of ownership.

Here we report on developments in fiber-coupling and packaging technologies as well as on chip-on-submount performance and reliability improvements. Combining these advances allowed us to increase the brightness of pumping noticeably: 20 W CW power from a standard 100 um dia. fiber is launched into less than 0.13 numerical aperture. Improvements of operating parameters did not require an increase in the footprint of the packaged device; it has been maintained at below 1.2 sq. inch.

New generation single emitter diodes with optimized layered structure, device geometry and increased cavity length demonstrated better performance at high driving currents. Also stability of lasing parameters against the heatsink temperature variation is much better than that of the previous generation pumps. Multicell stress test performed on these devices indicates reliability similar to the previously reported data but at 50% higher driving currents.

We also describe manufacturing approaches and practices that result in cost-effective high-volume manufacturing of single emitter diodes. Efficient semiconductor manufacturing along with higher reliability make single emitter distributed pumping an economically appealing solution compared with diode bar pumping schemes. This applies to low power and to kilowatt-class devices (fiber lasers and direct laser diode systems).

6104-20, Session 4

Monolithic integration of collimating fresnel lens for beam quality enhancement in tapered high power laser diode

F. K. Lau, C. W. Tee, X. Zhao, A. Wonfer, K. Williams, R. Penty, I. White, Univ. of Cambridge (United Kingdom); M. Calligaro, M. Lecomte, O. Parillaud, N. Michel, M. Krakowski, Alcatel-Thales

III-V Lab. (France)

We demonstrate, for the first time, a monolithic integrated lens for wide aperture gain-guided tapered laser beam quality enhancement by compensating the quadratic phase curvature. The 3mm long tapered laser with an output aperture of 170µm adopted in this design consists of a gain-guided tapered section and an index-guided ridge section and operated at 980nm. The lens design is implemented by focus ion beam etching (FIBE) technique, whereby the laser diode is mounted p-side up in order to facilitate the etching process. The lens is located 600µm away from the junction of the tapered and ridge sections, and is 40µm wide and 300µm long with a focal length of 800µm. The laser diode is characterised by light-current characteristics together with near- and far-field measurements before and after etching. The device is biased by current pulses of 1µs width and 0.1% duty cycle. Light-current measurement shows a drop of 10.5% in threshold current from 380mA to 340mA after the inclusion of lens. This is an evidence that the lens effectively equalised the curved phase in order to reduce the laser cavity loss by improving the coupling efficiency of backward travelling wave at the output facet. Throughout the whole current range tested, the width of near-field at waist is broadened by an average of 36% after the inclusion of lens. By successfully compensating the quadratic phase curvature of the mode, the beam divergence in the far-field is significantly narrowed by an average of 28.5%. M≤ factor is improved by an average of 12%.

6104-21, Session 5

Dense spatial multiplexing enables high brightness multi-kW diode laser systems

H. Schlueter, U. Bonna, G. Charache, J. Hostetler, T. Li, C. Miester, R. Roff, T. Vethake, TRUMPF Photonics Inc.

Primary characteristics of multi-kW cw laser systems are absolute power level, brightness, cost per watt, wavelength and spectral emission width.

Diode laser systems can match CO2 and solid state laser system performance on all those characteristics but brightness. This has limited their field of use and therefore their commercial success.

Dense spatial multiplexing (DSM) enables multi-kW diode lasers systems that approach the brightness of lamp-pumped solid state lasers while providing better efficiency and lower cost per watt.

Based on available, highly reliable diode lasers with 5 watts of output power per 100 um wide emitter, this technology will open new markets for high power diode laser systems.

6104-22, Session 5

Development of high power high brightness fiber coupled diode laser systems

N. Ostrom, M. Gall, B. O. Faircloth, Nuvonyx Inc.

The improved wall-plug efficiency and minimal maintenance of diode laser systems over Nd:YAG and CO2 lasers has been admired by many manufacturers. Until recently, most diode laser systems could not compete at high-power levels or with the same beam quality. Nuvonyx reports the development of a diode laser system that delivers 2000 W from a 600 µm core fiber with a 0.22 NA. This system is suitable as a standalone industrial direct diode laser system or as a multi-kilowatt fiber laser pump source. The development of a high brightness bar technology by Nuvonyx and its collaborators along with the use of polarization beam combining is the core of this laser system. Each emitter operates with a single lateral mode resulting in a high brightness bar that outputs up to 50 W. The wavelength of the laser is centered at 975 nm with a width of less than ± 3 nm. The demonstration of this laser system defines a clear path to scale this technology to 4000 W.

6104-23, Session 5

Dense wavelength multiplexing for a high power diode laser

C. Wessling, M. Traub, H. D. Hoffmann, R. Poprawe, Fraunhofer Institute fu Lasertechnik (Germany)

At present methods of polarization and wavelength multiplexing with dielectric coatings are used to increase the brigthness of diode lasers. The number of suitable diode laser wavelengths is limited by the temperature- and current-dependent spectral width of the diode laser and the slope of dielectric edge-filters. By use of external volume holographic gratings it is possible to constrict the emission spectra of diode lasers and to reduce the wavelength shift related to temperature or current injection. Due to the stabilization of the wavelengths multiplexing of diode laser beams at small distance of the centre wavelengths can be realised.

The performance of wavelength stabilization by use of volume holographic gratings adapted to AR-coated diode laser arrays in an external cavity as well as to standard high power diode laser arrays is discussed. Furthermore modules of two diode laser beams are combined by wavelength dependent diffraction of an adapted volume holographic grating. The spectra of the diode lasers of the same wafer are stabilized with a centre wavelength spacing of about 3 nm and more than 95% of the optical output power of each beam within a spectral width less then 0.7 nm. An efficiency of more than 80% for multiplexing of two diode laser bars with good beam quality in fast axis of M≤ < 2 is achieved. A set up for scaling up the power to a 1 kW fibre coupled diode laser by utilization of additional coarse wavelength and polarization multiplexing of diode laser bars of the wavelengths in the range of 940 nm and 980 nm is presented.

6104-24, Session 5

A compact high brilliance diode laser

F. Bammer, B. Holzinger, Technische Univ. Wien (Austria)

We present a high power diode laser based on time-multiplexing of four multi-mode 4W cw-laser diodes with 100µ aperture width. Each diode is operated in pulsed mode with a pulse width of 300ns, a peak power three times cw-power (~12 W) and a repetition rate of 1.1Mhz and emits an optical power of 3.6W (90% cw-power). To investigate reliability one diode has been operated in this mode of operation with an average power equal to cw-power for more than 80 hours without degradation of power or diode failure. The laser pulses are emitted at different times and guided onto a common optical path by a digital electro-optical multiplexer. The resulting quasi continuous laser beam has the beam quality of a single laser diode. Addressing different optical paths is done by a setup of polarization filters and polarization switches. The latter are made of z-cut LiNbO3-crystals driven by a harmonic voltage course. Due to the typical nonlinear transfer characteristic of a Pockel's cell between parallel polarizers this enables high switching efficiency while avoiding unintended ringing. Up to now our setup generated 10.5W, 13W are expected for an optimized one. With new 8W laser diodes the device will deliver 25W. While the principle was already shown with a rather large laboratory setup we can now demonstrate a compact design suitable for direct use or for conventional multiplexing of several such devices.

6104-25, Session 5

Homogenization of high power diode lasers for pumping and direct applications

M. Traub, D. Plum, D. Hoffmann, P. Loosen, R. Poprawe, Fraunhofer Institut für Lasertechnik (Germany)

High power diode lasers have become an established source for numerous direct applications like metal hardening and polymer welding due to their high efficiency as well high reliability. Diode lasers are also used for efficient pumping of solid state lasers as Nd:YAG lasers. To increase the output power of diode lasers, the emitters are scaled laterally by forming a diode laser bar and vertically by forming a diode laser stack. These devices offer an output power of several kilowatts in combination with a small footprint. For most applications, though, the undefined far field distribution of most commercially available high power diode laser stacks states a major drawback of these devices. This is especially valid for illumination applications, but also direct material processing like hardening suffer from very high peak intensities causing local melting of the metal and smooth edges of the distribution. These edge areas cannot be used for the process, and thereby its efficiency is reduced significantly. For pumping applications, high peak intensities introduce unwanted thermal lenses. Furthermore, the distribution changes offer time as single emitters and/or bars degrades and finally fails. This change in output power can be compensated by adjusting the injection current, but the influence on the distribution cannot be equalized. By this effect, the process stability is decreased significantly for direct applications, and for pumping applications, they decrease the beam quality of the solid state laser.

To overcome this problem of high power diode lasers, its distribution can be homogenized by two different approaches. For the first one, a waveguide is used, while for the second one, microoptic elements are used to homogenize the diode laser beam. The waveguide divides the far field distribution by several total reflections and overlay these segments at its exit surface. This exit surface is imaged on the workpiece. Thereby, power fluctuations are equalized, and a flat top hat distribution is achieved. To adapt this technology to two dimensional homogenization of very high peak powers in pulsed mode operation, the homogenizer can be split by using an anamorphotic device.

By microoptic elements, the aperture is subdivided in a number of small apertures, and these apertures are overlaid spatially by a field lens. By this approach, a flat top hat distribution can also be achieved.

Within this paper, several diode laser optics using a waveguide both for one and two dimensional homogenization developed at ILT are presented. These optics are suited for an output power up to 6 kW. We will also present the results for a microoptic homogenizer used for pumping a solid state slab laser. The two approaches will be compared by presenting the results of raytracing analysis as well as experimental results.

6104-26, Session 5

Laser beam transformation technique for high-power laser diode linear arrays

P. Grenier, Y. Taillon, M. Wang, P. A. Topart, D. Asselin, A. Parent, Institut National d'Optique (Canada)

High power laser diode linear array generally emit a laser beam in the form of an elongated thin line of 10 mm x 0.001 mm and a divergence of 10° x 80°. Due to its large asymmetry such beam can not be efficiently focused or coupled to an optical fiber. Several techniques have been devised to reshape such laser beam. Nevertheless, limitation and challenge coming among other things from the increasing CW bar fill factor keep the development interest. A new design addressing these limitations and challenges is proposed. The microoptic design is described. Simulation results are showing good performance with up to 75% fill factor bar. The fabrication microoptic's fabrication technique is presented. It permitted to achieve the required complex surface profile of the microoptic master form (free-form, large profile height). Still low cost production can be achieved owing to the use of a replication technique of the master form. The fabricated microoptic has been used for the transformation of the laser beam of a 10 mm laser diode bar. The resulting laser beam has been coupled to an 0.4 mm NA .22 optical fiber with an efficiency of 74%. Furthermore, the design features and measurement results indicate good potential of the microoptic for laser diode bar with higher fill factor. This will permit to couple larger optical power in the fiber and achieve higher brightness.

6104-27, Session 5

Stable coherent coupling of laser diodes by a volume Bragg grating in PTR glass

G. B. Venus, A. Sevian, L. B. Glebov, College of Optics and Photonics/Univ. of Central Florida; V. I. Smirnov, OptiGrate

Coherent coupling of lasers for increasing of brightness of laser systems is intensively studied for more than 25 years and published in numerous papers. There are two basic approaches for coherent coupling. The first one is to inject coherent radiation to the separated lasers and force them to emit coherently. The second one is to design a multichannel resonator which provides coherent emission of all its components. However, no stable coherent emission with high efficiency was reported for such scheme. The main problem preventing stable efficient coupling is a tendency of multichannel system to switch between different modes of a complex resonator. This paper reports the use of thick Bragg grating recorded in a photo-thermo-refractive glass with an extremely narrow spectral width and angle selectivity that provided coherent coupling of two semiconductor laser diodes. In the described construction no oscillations of output power was observed and an interference patter with visibility close to unity was observed for a long time.

6104-28, Session 6

6.8 W cw-output power from a 976-nm external cavity diode laser with narrow linewidth and 40-nm tuning range

A. Jechow, V. Raab, R. Menzel, Univ. Potsdam (Germany)

We present an external cavity design for a single broad area laser diode as gain medium. To suppress internal longitudinal modes the front facet of the diode is highly anti-reflection coated. The diode is frequency stabilized and bandwith narrowed by a diffraction grating in Littrow-arrangement, with grating lines positioned parallel to the plane of epitaxy. The first diffraction order is coupled back into the active region of the laser chip. Additionally, the external cavity consists of a fast axis collimator and a cylindrical lens to collimate the light of both axis onto the grating. Frequency narrowing is maintained because the FAC together with the grating and the aperture of the chip serves as a spectral filter with a linewidth of 0.15 nm.

The beam is coupled out via the zero diffraction order, while the diffraction efficiency into the Littrow-order of less than 10 % corresponds to the feedback reflectivity. Even though the grating is placed the way the diffraction efficiency is low, because of the high gain of the GaAs semiconductor no polarizing components are needed.

With that setup a full tuning range of more than 40 nm could be reached with center wavelength around 970 nm. For the emission a typical side-mode suppression ratio of more than 30 dB was obtained. The bandwith (FWHM) was in the order of 100 pm. Stable operation could be managed up to injection currents of 9 A at a maximum cw-output power of 6.8 W, where thermal rollover set in.

6104-29, Session 6

Effect of the threshold reduction on a catastrophic optical mirror damage in broad area semiconductor lasers with optical feedback

Y. Takiguchi, T. Asatsuma, S. Hirata, Sony Corp. (Japan)

Avoiding degradations is the most important issue in high power semiconductor laser applications. We experimentally and theoretically studied degradation phenomena and their mechanism in broad area semiconductor lasers (BALs) with optical feedback (OFB). We made two types of BALs (one is consisted of AlGaAs emitting at 808nm in TE mode, and another one is consisted of AlGaInP emitting at 642nm in TM mode), and investigated conditions of the degradations caused by the OFB. The both types of BALs showed degradations depending on feedback rate and output power. For example, both BALs were damaged with about 20% of intensity feedback rate at half of an output power of a catastrophic optical mirror damage (COMD) levels. To describe a theoretical model for the degradation, the optical power at a front facet of the BALs was calculated and compared with the COMD level of the solitary BALs. In the

theoretical model, we included a threshold reduction caused by the OFB. We found that the degradation was explained by a constructive interference between internal and the feedback optical fields. The BALs are damaged when a coherent sum of those fields exceeds the solitary COMD level. We found that the threshold reduction decreases a critical value of the feedback rate corresponding to the damage at low output power regime, and also found that there is an optimum reflectivity of the front facet. The theoretical results show a good agreement with experimental results. According to this model, we can avoid the damages induced by the OFB in the various applications.

6104-30, Session 6

m2k-laser GmbH (Germany)

J. Weber, M. T. Kelemen, S. Moritz, M. Mikulla, Fraunhofer-Institut für Angewandte Festkörperphysik (Germany)

Tapered lasers have been well established for different fields of applications in the last few years. For some applications such as nonlinear frequency-conversion for green and blue outputs or Raman-spectroscopy a small spectral linewidth, and in addition a nearly diffraction limited high optical output power is needed. One possibility to fulfill these requirements is to use tapered lasers in an external cavity configuration. However at the moment only 1 W of nearly diffraction limited output power is commercially available. The wall-plug efficiency in external cavity configurations is significantly lower as for standard lasers. Therefore to achieve a remarkable increase in output power an excellent heat-management is substantial.

We have developed a new heat-sink concept which allows to access both facets and simultaneously enables a sufficient heat removal. In combination with this packaging we have realized tapered diode lasers for high output powers in external cavity setups. The design of the laser consists of a gain guided taper-section and an index guided ridge section. The overall resonator length is 2.5 mm. Both facets were highly anti-reflection coated to guarantee an optimal operation in Littrow-configuration. We have obtained output powers of more than 3 W together with a longitudinal single mode operation and nearly diffraction limited behaviour. The beam-quality parameter remains well below M≤ < 1.8. At a tuned wavelength of 976 nm a sidemode-supression of 40 dB was measured. A tuning range of 40 nm between 940 nm and 980 nm has been demonstrated.

6104-31, Session 6

V-shaped external cavity for tunable 1W diffraction limited cw-power at 976-nm

V. Raab, A. Jechow, R. Menzel, Univ. Potsdam (Germany)

Based upon previous results with diode lasers in external cavities the unstable V-shaped resonator design is applied to very broad stripe array diodes of 400 μm width. Here we show that it can generate almost fundamental Gaussian light even at high powers. The setup consists of the laser chip, a fast axis collimator, a grating in Littrow arrangement, and a l/2-plate for adapting the high efficiency of the grating to the polarization of the laser chip. This results in a preferred off-axis emission under an angle of 49 mrad with respect to the surface normal. One of the two arms acts as feedback and the other as outcoupler.

The GaAs semiconductor has a very broad gain bandwidth which manifests itself in a luminescence of 60 nm spectral width for the chips that are 1500 mm long and 400 mm wide and have a highly reflecting back facet and an AR-coating on their front facet. The system is tunable over a range of 40 nm from 945 to 995 nm with maximum output power at 970 nm.

For the emission a typical side-mode suppression ratio of over 40 dB was obtained. For a measurement of the beam quality an additional aperture was introduced into the outcoupling beam to suppress stray light and ASE (amplified spontaneous emission). The caustic of the second moments of the beam width behind that aperture yields an M2 = 1.35 in the slow axis and an M≤ = 1.1 in the fast axis for the beam of 1W output power at 2.7 A pump current.

6104-32, Session 6

Compact tunable diode laser with diffraction limited 1000 mW in Littman/Metcalf configuration for cavity ring down spectroscopy

S. Stry, J. R. Sacher, Sacher Lasertechnik GmbH (Germany); S. Thelen, P. Hering, M. Mürtz, Heinrich-Heine-Univ. Düsseldorf (Germany)

High resolution spectroscopy of environmental and medical gases requires reliable, fast tunable laser light sources in the mid infrared (MIR) wavelength regime between 3 and 5 microns. Since this wavelength cannot be reached via direct emitting room temperature semiconductor lasers, additional techniques like difference frequency generation (DFG) are essential. Tunable difference frequency generation relies on high power, small linewidth, fast tunable, robust laser diode sources.

We report a new, very compact, alignment insensitive, robust, external cavity diode laser system in Littman/Metcalf configuration with an output power of 1000mW and an almost Gaussian shaped beam quality (M2<1.2). The coupling efficiency for optical waveguides as well as single mode fibers exceeds 60%. The center wavelength is widely tunable within the tuning range of 20 nm via remote control. This laser system operates longitudinally single mode with a mode-hop free tuning range of up to 30GHz without current compensation and a side-mode-suppression better than 50dB. This concept can be realized within the wavelength regime between 750nm and 1060nm.

We approved this light source for high resolution spectroscopy in the field of Cavity-Ring-Down-Spectroscopy (CRDS). Our high powered Littman/Metcalf laser system was part of a MIR-light source which utilizes difference-frequency-generation in Periodically Poled Lithium Niobate (PPLN) crystals. At the wavelength of 3.3μm we were able to perform a high resolution absorption measurement of 5ppb Ethane. This application clearly demonstrate the suitability of this laser for high-precision measurements.

6104-33, Session 6

Wavelength tunable injection locking of high power super luminescent diode with 1.4 watt diffraction-limited output

Y. Su, C. Lin, C. Tsai, National Taiwan Univ. (Taiwan)

High power and good beam quality are desired for semiconductor light sources in many applications. We propose a new type of semiconductor light sources that can provide 1.4watt high output power; 35nm wavelength tunable range and diffraction limited beam quality. The key active element of this light source is a 1.4watt super luminescent diode with diffraction limited beam quality. This new device is a modification from angled broad area waveguide laser. With this modification, the cavity of this angled broad area waveguide laser is destroyed, and this device becomes a super luminescent diode with broad emission bandwidth. The output power is 1.4 watt per facet at 12Amp. The emission spectrum has 20nm FWHM. In addition, the far field has a single lob distribution, which is only 2degree in width. The output is emitted at 33degree away from the direction of facet normal and the far field divergence is at the diffraction limit of the corresponding near field distribution.

The external feedback setup requires only two components, a C330TM-C collimator from Thorlab and a grating. With external grating feedback, the emission wavelength is locked by the feedback. The emitted power is 1.4 watts at 8Amp. The emission spectrum concentrates at the wavelength of the grating feedback. The peak wavelength can be tuned from 1275nm to 1310nm. The main character of beam profile is not affected by the external feedback. The far field divergence remains at 2degree, while the near field broadens slightly from 43umto 48um.

6104-34, Poster Session

Successive phase change and stability of near-field patterns for broad-area laser diodes

T. Asatsuma, Y. Takiguchi, S. Frederico, A. Furukawa, S. Hirata, Sony Corp. (Japan)

For the application of broad-area laser diodes (BA-LDs) to display or printing, uniform distribution and stability of their near-field pattern (NFP) are the most important demand. In order to control the NFP, we have fabricated BA-LDs with index-guided structure and got better top-hat and stabler NFP than that for gain-guided BA-LDs. However, this mechanism is not understood yet. Therefore, we study the features of BA-LDs' NFP systematically, and set up a new model to understand their behaviors. The NFPs of BA-LDs evolve via three phases with increasing operation current: the first phase is "mode-progressing phase" in which the number of the spatial modes increases orderly, and the second phase is "transition phase" in which the spatial modes become unstable and fluctuate. The third phase has different properties according to the waveguiding structure of BA-LDs: "disordered phase" appears for gain-guided structure in which several specific modes dominate in the whole distribution (filamentation behavior), on the other hand "ordered phase" appears in the case of index-guided structure in which a top-hat distribution is observed. This top-hat NFP is almost unchanged with increasing output power. With these experimental results, we propose the new model, in which the emitting area of a BA-LD is divided into several parts and they are discussed separately.

6104-35, Poster Session

In-line implant and RTP process monitoring using the carrier illumination technique for 65-nm and beyond

H. L. Chuang, P. Y. Y. Chen, C. I. Li, United Microelectronics Corp.

This paper describes the application of the Carrier Illumination technique to non-destructively measure the dopants behavior before and after annealing for 65nm technology. The pattern wafers were implanted with different SDE energy and dosage. The detected signals form laser diode show good correlation with electrical performance (drive current, overlap capacitance). Another crucial application is to in-line monitor thermal process. By splitting spike anneal temperature, we found detected signals were proportional to the junction depth of SIMS. The non-destructive, non-contact, and small spot size nature of the CI measurement method is capable to trace low energy implant and spike anneal.

6104-36, Poster Session

Properties and reliability of improved large acceptance optical fibers

B. J. Skutnik, C. Smith, K. B. Moran, K. Bakhshpour, CeramOptec Industries, Inc.

The high power diode laser systems with their laser diode bars and arrays not only require special fibers to couple directly to the diode emitters, but also require special fibers couple from the laser to application sites. These power delivery fibers are much larger than the internal fibers, but must be flexible, and have not only good strength but also good fatigue behavior. This is particularly important for industrial systems using robotic arms or robots to apply the high power laser energy to a treatment site. The optical properties of hard plastic clad silica (HPCS) fibers are well suited for the needs of delivery of high power from diode laser bars and arrays to an application site. New formulations for HPCS fibers have been developed which earlier demonstrated fibers with good mechanical strength in preliminary tests. A systematic study has been undertaken to determine the strength and fatigue behavior of these 'new' HPCS fibers and to compare them with results for earlier HPCS fibers. Early benefits of stronger median dynamic strengths and tighter flaw distributions for the fibers with the new formulations appear to continue. In addition to discussing the benefits, including mechanical reliability, of these 'new' HPCS fibers in power transmission for high power diode laser bars and arrays, more complete results for strength and fatigue behavior of these fibers will be presented.

6104-37, Poster Session

Can superluminescent LEDs be more efficient than Fabry Perot lasers?

O. A. Konoplev, S. Park, P. J. Heim, J. Wei, D. Bowler, Covega Corp.

High-power, high-efficiency superluminescent light emitting diodes (SLEDs) represent an interesting alternative to other high-power semiconductor diode sources such as Fabry-Perot laser diodes (FPLs). By principle of operation, by performance and by geometric design SLED can be compared to three well-established devices: LED (a SLED is LED with large optical gain), SOA (a SLED is a SOA seeded with its own noise) and FPL (a SLED is a FPL with frustrated resonator feedback).

Up till now, the average optical power level and wall-plug efficiencies reached from single-spatial mode semiconductor FPLs were never matched by any other semiconductor device for optical power levels above 100 mW. We recently demonstrated a SLED with optical power in excess of half-Watt and with the peak wall plug efficiency of 28%. (Proc. SPIE vol 5739, p.66-80, March 2005). Scalability of SLED to Watt-level power was presented, while creation of SLED with efficiency competing to that of the best FPLs is yet to be done. The electro-optical efficiency of SLEDs achieved so far was approximately half of that reported in the literature for the best FPL devices.

We discuss the possibility of creating of very high efficiency and high average power SLEDs that may be more efficient than FPLs. It is admitted that SLEDs are inferior to FPLs due to reduced internal quantum efficiency caused by much higher excited carrier densities. However, two other factors such as lower mirror loss and lower R-I-square Joule loss factor favors SLEDs with respect to FPLs in electro-optical efficiency. In SLEDs, the gain is not clampled at lasing. This allows to better suppression of higher order lateral modes at wider lateral waveguide sizes. The possibility of a wider ridge while maintaining high qualifty of fundamental mode allows scalability to higher output power with lower RI^2 loss. Taking all factors into account we believe that it is possible not only match but also probably exceed both output power and electro-optical efficiency of the best FPLs.

6104-38, Poster Session

Laser ignition of propellants

M. S. Singh, M. K. Gupta, Rajkumar, L. Kumar, S. Bansal, V. S. Sethi, Government of India (India)

We studied the laser ignition characteristics of eight different types of standard gun propellants used in small arms to high caliber guns. The experimentation were conducted to study threshold laser ignition energy density and ignition delay of different propellants. Dependence of threshold ignition energy on optical fiber dia and ignition behavior of different propellants to different pulse widths of laser is discussed. We also studied the over driven combustion phenomenon with micro sec laser pulses from Nd: YAG laser.

6104-39, Poster Session

Characteristics and reliability of high power multi-mode InGaAs strained quantum well single emitters with CW output powers of over 5W

Y. Sin, J. Scarpulla, N. Presser, G. Stupian, S. C. Moss, The Aerospace Corp.

High power multi-mode broad area InGaAs strained quantum well single emitters in the wavelength range of 920-980nm have been mainly used for industrial applications. In recent years, these broad area lasers with CW output powers of over 5W have also found applications in communications as pump lasers for Er-Yb co-doped fiber amplifiers. This application requires very demanding characteristics from these devices including higher reliability compared to industrial applications. In contrast to 980nm single mode InGaAs strained quantum well lasers that are widely employed in both terrestrial and submarine applications, the fact that multimode lasers have never been used in optical communications necessitates a careful study of these lasers. We thus report on the performance characteristics, reliability, and failure modes of high power multi-mode single emitters.

The lasers studied were broad area strained InGaAs-GaAs single quantum well lasers either grown by MOCVD or MBE. Typical apertures were around 100μm wide and cavity lengths were 3.5mm. AR-HR coated laser diode chips were mounted on carriers with junction down configuration to reduce thermal impedance. The laser threshold was 450mA at room temperature. At an injection current of 5A typical CW output powers were 5W at 20C with a wall plug efficiency of ~50%. Various characteristics were measured from these devices including thermal impedance, optical beam profiles, and gain spectra that are critical in understanding performance and reliability of these devices. ACC burn-in tests with different stress conditions were performed on these devices and log (I)-V characteristics were measured at RT to find a correspondence between degradation in optical output power and an increase in trap density estimated from the 2κ T term in bulk recombination current. Also reported will be initial analysis of lifetest results and failure modes from these lasers.

Conference 6105: Free-Space Laser Communication Technologies XVIII

Tuesday-Wednesday 24-25 January 2006

Proceedings of SPIE Vol. 6105

6105-01, Session 1

Optical phased arrays for laser communications

T. A. Dorschner, W. J. Miniscalco, I. W. Smith, K. L. Fisher, Raytheon Co.

Abstract not available.

6105-34, Session 1

The Mars laser communication demonstration: what it would have been

D. M. Boroson, MIT Lincoln Lab.; A. Biswas, Jet Propulsion Lab.; B. L. Edwards, NASA Goddard Space Flight Ctr.

Abstract not available.

6105-36, Session 1

OICETS on-orbit laser communication experiments

T. Jono, Y. Takayama, K. Ohinata, N. Kura, Japan Aerospace Exploration Agency (Japan); Y. Koyama, Japan Aerospace Exploration Agency

Abstract not available.

6105-02, Session 2

Optimal GEO lasercomm terminal field of view for LEO link support

B. Engberg, C. W. Hindman, K. Walchko, Air Force Research Lab.

As alternatives to the traditional gimbaled terminal design, future satellite based laser communications terminals are envisioned that utilize a wide field of view or field of regard (WFOV/WFOR). This approach can be advantageous in situations requiring rapid switching between user terminals, support for multiple terminals simultaneously (via TDMA, SDMA or WDMA) or other non-standard mission requirements. However, a traditional gimbaled terminal has the capability to continuously track a single user over very large angles, such as the 18-20° spanned by a LEO satellite as seen from GEO. WFOV/WFOR designs face increasing cost and/or complexity issues with each incremental increase in angular coverage. The methodology and results from a trade study are presented here that attempts to maximize the available connectivity to a LEO satellite while minimizing cost and complexity metrics by choosing an optimal FOV/FOR size for a GEO terminal.

6105-03, Session 2

Simplified optical communication system architecture

C. Chen, H. Hemmati, A. Biswas, G. G. Ortiz, W. H. Farr, Jet Propulsion Lab.; N. Pedreiro, Lockheed Martin Advanced Technology Ctr.

Abstract not available.

6105-04, Session 2

Multilevel coding for FTTH and metro networks

L. Hofmann, Technische Univ. Chemnitz (Germany); M. B. Tayahi, Univ. of Nevada/Reno; J. Carstens, Technische Univ. Chemnitz (Germany); S. Lanka, Univ. of Nevada/Reno

PAM 4-ary at 2.5 Gbaud/s was experimentally and numerically investigated. A graded index multimode fiber link was investigated using short-wavelength VCSELs operating at 850 nm, a error free transmission for 1 km was obtained. Multilevel signalling in Metro networks using SSMF links were investigated for three scenarios: directly modulated DFB lasers operating at 1.3 um, 1.55 um, and external modulation were also investigated. Power budget and system requirements were met for 100 km SSMF with no need for dispersion compensation.

6105-05, Session 2

Development of optical antennas utilizing free form surface optics for the high speed laser communication systems

K. Takahashi, Olympus Corp. (Japan); Y. Arimoto, National Institute of Information and Communications Technology (Japan)

Next generation optical communication systems will require small optical antennas and fine tracking system.

Such optical communication systems might be applied not only to space communications such as optical feeder links, intersatellite links and/or stratospheric platforms but also optical links for long distance communication on the ground.

We have developed a high speed laser communication system including the small optical antenna which utilizes off-axis free form surface optics system, and a fine tracking system which feeds back an incident angle signal detected by QD(quadrant detector) to a small fine positioning mirror. In particular, the available mirror actuator response frequency for tracking is approximately 2kHz.

6105-06, Session 2

Real-time combining of optical array signals

V. A. Vilnrotter, C. Lau, K. Andrews, P. Vo, M. Srinivasan, D. Lee, Jet Propulsion Lab.

Abstract not available.

6105-07, Session 2

4-ary PAM signaling for increasing the capacity of metro light-wave systems

S. Lanka, M. B. Tayahi, Univ. of Nevada/Reno; L. Hofmann, J. Cartsens, Technische Univ. Chemnitz (Germany)

We investigated both experimentally and by simulation, non-return-to-zero (NRZ) and return-to-zero (RZ) 4-ary PAM operating at 20 Gb/s. A simple scheme to realize the quadratic signal leveling by suitably driving a MZ modulator is proposed, which provides >5 dB improvement in receiver sensitivity as compared to equal level spacing. We experimentally demonstrated NRZ and RZ 10 Gbaud/s 4-ARY PAM transmissions over

an 80 km standard single mode fiber (SSMF) link as a proof of concept and more detailed experimental results over longer reach will follow. Numerical simulations for the 4-ary PAM performance over longer distances (\>200 km) are also presented.

6105-35, Session 2

140 km free-space laser link verification based on homodyne BPSK

B. Smutny, R. Lange, Tesat-Spacecom GmbH & Co. KG (Germany); R. H. Czichy, Synopta GmbH (Switzerland); B. Wandernoth, D. Giggenbach, DLR (Germany)

Abstract not available.

6105-08, Session 3

Analysis of capacity and probability of outage for free-space optical channels with fading due to pointing and tracking error

R. J. Barron, D. M. Boroson, MIT Lincoln Lab.

The transmitter of a free-space laser communications system operating in the far field points to the receiver using a tracking control loop that has a non-zero tracking error. The tracking error moves the transmitted Gaussian beam relative to the receiver, inducing a dynamic fading process at the receiver. This report analyzes the effects of fading due to tracking error on communications performance of lasercom systems employing pulse-position-modulation (PPM) with interleaving and a photon-counting receiver; one such system is the Mars Lasercom Demonstration System (MLCD) . We provide general expressions for the probability of outage as a function of interleaver depth, which serve as useful proxies for codeword error performance for systems using capacity-approaching iterative codes.

The downlink transmitter for MLCD tracks on both the earth itself and a beacon sent from earth using a two-pole tracking loop. The two-dimensional dynamic tracking error is well-modeled as a circularly symmetric wide-sense stationary Gaussian process. Using this model we derive the following analytic quantities that are essential for lasercom link-budgeting: an expression for unrecoverable tracking loss (unrecoverable by interleaving or any other means); an expression for probability of outage in the absence of interleaving; and an expression for the probability of outage with interleaving. As a result of our analysis, we have determined that the MLCD interleaver memory of 500 thousand PPM symbols is sufficient to keep the receiver impairment caused by dynamic fading due to tracking error below 0.3dB for even the highest supported data rates.

6105-09, Session 3

Performance of a laser communication system with acousto-optic tracking: an experimental study

V. V. Nikulin, R. Khandekar, J. Sofka, Binghamton Univ.

Laser communication systems hold great promise for broadband applications. This technology uses much higher-than-RF region of the spectrum and allows concentration of the signal within a very small spatial angle, thus offering unsurpassed throughput, information security, reduced weight and size of the components and power savings. Unfortunately, these intrinsic advantages do not come without a price: small beam divergence requires precise positioning, which becomes very critical at high bit rates. Complex motion patterns of the communicating platforms, resident vibrations, and atmospheric effects are known to cause significant signal losses through the mechanisms of the pointing errors, beam wander and other higher-order effects. Mitigation of those effects is achieved through the multiple means of fast tracking and wavefront control. In this paper we focus on the application of a beam steering technology and its effect on the communication performance of the system. We present the results of an experimental study of a laser communication link subjected to pointing distortions. These distortions are generated by a special disturbance element in the optical setup, which recreates specific operation environments with particular spectral characteristics. The acousto-optic technology is used to build an agile tracking system to assure the maximum signal reception in spite of the harsh operational conditions. The received communication signal is recorded and statistically analyzed to calculate the bit-error-rates. This paper presents the synthesis of a tracking system and the experimental results characterizing the communication performance under uncompensated pointing disturbance and with tracking.

6105-10, Session 3

Star-tracker-based tracking and pointing for deep-space communications

G. G. Ortiz, S. Lee, Jet Propulsion Lab.

Abstract not available.

6105-12, Session 3

Centroiding accuracy estimate of the long wavelength infrared earth images

S. Lee, Y. Chen, G. G. Ortiz, Jet Propulsion Lab.

Abstract not available.

6105-14, Session 4

High performance single photon detector to enable next generation free space laser communication systems

K. Linga, E. Godik, J. Krutov, Amplification Technologies, Inc.

Optical communications have the potential to provide performance advantages over conventional RF communications by as much as 60-80 dB. One of the important elements of a free-space optical communication system is a photodetector. Currently, the lack of a fast sensitive photodetector is a key constraint on the development of free space laser communication systems.

We will review the main performance requirements to a detector for use in laser communications. Next, the technology required for realizing such a detector will be described, followed by the description of the technologies that are being currently used. With these basics, a novel design of a high performance detector that could enable the next generation laser communications systems will be presented. Finally, the applications areas for this new detector technology will be described.

We have designed and developed a new family of photodetectors with Internal Discrete Amplification (IDA) mechanism for the realization of free space optical communications in the visible and near infrared spectral region. The first prototypes of these photodetectors can operate in linear detection mode with gain-bandwidth product of over 5 x 10^15 and in photon counting mode with count rates over 10^9 counts/sec. These key performance characteristics exceed those of Photomultiplier tube (PMT) and Avalanche Photodiode (APD) devices. The measured parameters of these detectors have a gain > 10^5, excess noise factor as low as 1.02, rise/fall time < 300 ps with significant room for improvement, and a wide internal linear dynamic range. Additional applications include remote sensing and laser spectroscopy. Potential benefits of this technology over conventional avalanche photodetectors include ultra low excess noise factor, very high gain, lower reset time (~ 0.1 μs).

6105-15, Session 4

Daytime use of astronomical telescopes for deep-space optical links

G. G. Ortiz, W. T. Roberts, T. A. Boyd, Jet Propulsion Lab.

Tests at the 200-inch Hale Telescope on Palomar Mountain have demonstrated this telescope's ability to withstand considerable thermal stress, and subsequently produce remarkably unaffected results. During the day of June 29, 2005, the Hale telescope dome was left open, and the telescope was exposed to outside air and direct sunlight for 8 hours. During this time, portions of the telescope structure in the telescope's optical path experienced temperature elevations of 30 C, while the primary mirror experienced unprecedented heating of over 3 C. The telescope's measured blind pointing accuracy before and after this exposure were not noticeably affected. The telescope also produced good 1.6 arc sec images of stars during the daylight hours immediately following the exposure, and seeing was remarkably good (sub-arc sec) during the subsequent night hours. The adaptive optics system was able to lock the tip-tilt loop during daylight hours, and acquired full lock-up of the deformable mirror during the evening and night hours. This data is the first step in co-opting astronomical telescopes for daytime use as astronomical receivers, and supports the contention that this can be done with little impact to astronomy.

6105-17, Session 4

Progress toward experimental demonstration of quantum-optimum receiver

J. Geremia, California Institute of Technology; S. J. Dolinar, C. Lau, V. A. Vilnrotter, Jet Propulsion Lab.

Abstract not available.

6105-18, Session 4

A novel monolithic beam steering high power transmitter for low cost free space optical wireless links

X. Zhao, F. K. Lau, C. W. Tee, A. Wonfer, R. Penty, I. White, Univ. of Cambridge (United Kingdom); M. Calligaro, M. Lecomte, O. Parillaud, N. Michel, M. Krakowski, Alcatel-Thales III-V Lab. (France)

A novel transmitter for directed-beam infra-red wireless that utilizes a combination of both gain-guiding and index-guiding mechanism to ameliorate the shortcoming of the state-of-the-art technology is proposed and demonstrated. The experimental results are supported by comprehensive time-domain laser modelling. The 3mm long tapered laser consists of an index-guided ridge straight section and a gain-guided tapered section with a full angle of 6°. By implementing multiple contact with a sufficiently high inter-contact resistance, discrete switching between different angles can be obtained by selectively pumping current to different contact (gain-guiding effect), while fine-tuning of a given angle can be achieved by adjusting the injection current of nearby contacts (index-guiding effect). The tapered laser's metal cover is removed using focus ion beam etching technique to form three separate sections: base section as filter, left section and right section for beam steering. The device is biased by current pulses of 1μs width and 0.1% duty cycle. With a 1.6A injection current, an output power of 2W is achieved, which would be suitable to overcome large free space optical loss and facilitate the use of transmitting methods. The beam profile steered by 3.2° and -5.4° from the central lobe when injection current is limited to the left and right section respectively is measured. It is also observed that as injection current increases, the beam profile is steered towards the central position. This is because as the injection current increases, the local refractive index is decreased, thereby shifting the beam profile towards the opposite direction.

6105-19, Session 4

Non-polarization and non-absorbing beamsplitters for laser communications

K. Zhang, A. Smajkiewicz, Barr Associates, Inc.

We report the most recent advances of optical beamsplitters for laser communications developed at Barr Associates. The challenges for meeting the two key requirements, polarization control and wavefront control, of the lasercom beamsplitters are discussed. The paper will first show the design result for various type beamsplitters, followed by an analysis of the requirement of controlling thickness, refractive index and stress of thin films to meet some typical specifications. Finally, the latest result of various lasercom beamsplitters is presented. For a typical 50% reflection and 50% transmission beamsplitter at 22.5 degree angle of incidence, we have achieved s and p polarization split less than 0.3% from 1530nm to 1590nm and less than 1/40 waves (at 632.8nm) of substrate distortion caused by the coating stress.

6105-33, Session 4

Expansion of receiver area by spherical mirror for optical free space communication

T. Yazaki, M. Shibuya, M. Usami, KDDI R&D Labs. (Japan)

Free-space optical communication system is promising for high-speed and short-reach space data communication because of its ultra-high speed (\>1Gbps), compactness, and low driving power in comparison to radiowave system. However, alignment between transmitter and receiver is rather difficult in optical than in radiowave. In this paper, we proposed the use of a spherical mirror as a focusing medium to expand the receiver area, where the power density exceeds a threshold for 1Gbit/s receiver sensitivity. We successfully confirmed that the receiver area was expanded due to a rather planar beam profile owing to an aberration of the spherical mirror.

In the experiment, we carried out 100 mm transmission experiment using 1310 nm FP-LD with FFP angle of 7 degree and InGaAs PIN-PD of 0.3 mm in diameter as transmitter and receiver, respectively. An output power of FP-LD was 5mW and the PD was located at the optimum defocus position where a maximum receiver area was obtained. The threshold optical sensitivity of the receiver was -16dBm to accommodate 1 Gbit/s data rate. The spherical mirror was tilted by 10 degree from the main axis to prevent shading effect by the PD.

We measured the receiver area with the spherical mirror and with a plane-convex lens of which the diameters and the focal lengths (F) were 10mm and 15mm, respectively. The flattened beam profile was obtained at the optimum defocus position in the spherical mirror system due to the aberration. Consequently, the receiver area was expanded from 16.0 mm to 18.2 mm by the use of the spherical mirror. Moreover, the receiver area was further expanded to 19.5 mm when F is decreased to 10 mm.

In summary, the use of spherical mirror with short focal length was confirmed to be effective to expand the receiver area of free-space optical communication system.

6105-20, Session 5

Ultra-light weight telescope coupled with portable AO system for laser communications applications

S. R. Restaino, J. Andrews, C. Wilcox, T. Martinez, Naval Research Lab.; D. Payne, Narrascape

The use of Micro-Electro-Machined (MEM) devices as deformable mirrors (DM) for active and adaptive optics has enabled the demonstration of portable adaptive optics systems, with compact form factor and very low power consumption. At this we can add a new generation of ultra-light telescopes that can be easily coupled with the aforementioned AO systems to deliver a powerful laser communication station. In this paper we present the status of both our AO system and the status of our ultra-light telescope program. We will present laboratory and field results for both systems and analysis of the performances.

6105-21, Session 5

FSO antenna with high speed tracking for improved atmospheric turbulence effects mitigation

K. R. Kazaura, K. Omae, T. Suzuki, M. Matsumoto, T. Sato, Waseda Univ. (Japan); K. Asatani, Kogakuin Univ. (Japan); M. Hatori, Chuo Univ. (Japan); T. Murakami, Koito Industries Ltd. (Japan); K. Takahashi, Olympus Corp. (Japan); H. Matsumoto, Showa Electric Wire & Cable Co., Ltd. (Japan); K. Wakamori, Hamamatsu Photonics K.K. (Japan); Y. Arimoto, National Institute of Information and Communications Technology (Japan)

When a free space optical beam propagates through the atmosphere it experiences deterioration and deformation of its wave-front. These degradation modes are caused from small scale, randomly localized changes in the atmospheric index of refraction, resulting in beam wander and scintillation effects which can reduce the link availability and may introduce burst errors.

Unlike previous Free Space Optical System (FSOS) research, we are experimenting on a free space optical communication system which connects an optical signal directly to a single mode fiber (SMF) without any OE conversion.

In order to efficiently couple the 1550 nm transmitted optical beam to the SMF it is necessary to be able to control the beam arrival angle fluctuations. To achieve this we have developed a high-speed tracking optical antenna.

From our experiments we have demonstrated the relation between the arrival angle fluctuations and the frequency characteristics of the scintillation effects for a free space optical beam propagating through a turbulent atmosphere. We use this information to determine the optimum antenna tracking speed for improved performance and error free transmission under various atmospheric conditions. The long-term performance of this free-space optical communication system is under investigation.

6105-22, Session 5

Wavefront correction of low-cost large apertures for optical communication receivers

H. Hemmati, Y. Chen, Jet Propulsion Lab.

Abstract not available.

6105-23, Session 5

Airborne laser communications and performance enhancement by equalization

S. Lee, B. Hamzeh, M. Kavehrad, The Pennsylvania State Univ.

Free Space Optics (FSO) has recently attracted considerable attention for a variety of applications. FSO is a promising candidate for emerging broadband applications, considering that RF spectrum is already congested, rendering accommodation of additional RF broadband channels difficult and costly. Communications via RF signals are reliable but cannot support emerging high data rate services unless they use a large portion of the costly radio spectrum. FSO communications offer enormous data rates but operate much more at the mercy of the atmospheric environment, such as scintillation and multi-scattering through fog and clouds. Since RF paths are relatively immune to these phenomena, combining the attributes of a higher data rate but bursty link (FSO) with the attributes of a lower data rate but reliable link (RF) could yield attributes better than either one alone, enabling a high availability link at high data rates. This transmission configuration is typically called a hybrid RF/FSO wireless system. The focus of this paper will be on applying well-known equalization techniques to FSO, to further enhance availability of RF/FSO wireless system.

In FSO, atmospheric turbulence can degrade the performance severely, particularly over ranges in the order of 1 km or longer. Also, multi-scattering due to aerosol particles in atmosphere induces temporal and spatial dispersion, which at high bit rates cause intersymbol interference (ISI), severely degrading the performance. A recent study found that under the assumption of ground-to-air link through the air, the link suffers more from multi-scattering than from atmospheric scintillation, causing ISI. In this paper, the authors will study the performance of an FSO link through highly dispersive multi-scattering medium as clouds, and its enhancement through well-known equalization techniques.

6105-24, Session 5

Mitigation of dynamic wavefront distortions using a nematic liquid crystal spatial light modulator and simplex optimization

R. M. Khandekar, V. V. Nikulin, Binghamton Univ.

Laser beam propagating through the atmosphere is subjected to severe wavefront distortions due to the optical turbulence. This leads to the reduction in the received power, ultimately resulting in the BER degradation, even for short ranges. Optical properties of the atmospheric channel change over time; hence, maintaining a reliable link requires dynamic wavefront control to mitigate the effects of the atmospheric turbulence. An electrically addressed programmable nematic liquid crystal spatial light modulator (SLM) is proposed to perform this task. Wavefront correction is achieved by computing a phase shift for each pixel of the SLM, which could be a rigorous and time-consuming procedure. Hence, the aim is to obtain a stable and relatively simple approach to dynamically control the modulator elements. The phase profile of the distorted beam can be approximated using Zernike formalism or another type of wavefront polynomial, which provides efficient mapping between a large number of SLM pixels and a much smaller number of approximation coefficients. Furthermore, wavefront correction needs to be performed in real-time; hence the Simplex method by Nelder and Mead, known for fast improvement of an optimization metric, is used to adjust the approximation coefficients. The phase profile obtained from the optimization procedure is imposed on the received beam by the SLM. This facilitates the reduction of the optical path difference (OPD) present in the distorted wavefront by applying an inverse OPD, and mitigating the effects of the optical turbulence. This paper presents a basic algorithm as well as the experimental results.

6105-25, Session 6

Multichannel coherent optical receiver for PPM signals in the presence of atmospheric turbulence

M. Muñoz Fernández, California Institute of Technology; V. A. Vilnrotter, Jet Propulsion Lab.

We present the performance analysis and experimental verification of a multichannel coherent free-space optical communications system in the presence of simulated atmospheric turbulence. Bit Error Rate (BER) performance is analyzed for the case of extremely weak signals received from Deep Space. The key components include two lasers operating at 1064 nm wavelength for use with coherent detection, a 16 element (4X4) focal plane detector array, and data acquisition and signal processing assembly needed to sample and collect the data and analyze the results. The detected signals are combined using the least-mean-square (LMS) algorithm.

6105-26, Session 6

Atmospheric turbulence effects on a wavelength diversified ground-to-UAV FSO link

A. Harris, J. J. Sluss, Jr., H. H. Refai, Univ. of Oklahoma; P. G. LoPresti, Univ. of Tulsa

The use of free-space optical (FSO) communications links are envisioned as a viable option for providing a temporary high-bandwidth communication link between a ground station and an unmanned aerial vehicle (UAV). The presence of atmospheric turbulence causes three different phenomena to occur, namely beam wander, scintillation and beam spread, each of which is a wavelength dependent phenomenon. In this paper, simulation tools are used to investigate the effects of atmospheric turbulence on a wavelength diversified ground-to-UAV FSO communications link. This paper compares the effects of atmospheric turbulence on four different wavelengths, 1.55 μm, 1.06 μm, 0.85 μm and 10 μm. Each of these wavelengths has different advantages in depending on prevalent weather conditions and atmospheric turbulence conditions. Based on the effects of atmospheric turbulence on each wavelength, a wavelength diversity scheme is proposed in order to optimize the performance of the FSO link. The largest problem associated with establishing a ground-to-UAV FSO link is alignment and tracking of the FSO link. For this reason, the wavelength diversity scheme is further analyzed as a method to optimize link acquisition and tracking of the ground-to-UAV link by exploiting various characteristics of each wavelength. Based on this analysis, the benefits of employing a wavelength diversity scheme as a method to optimize link acquisition for ground-to-UAV FSO communications links are described.

6105-27, Session 6

Adaptive techniques for reducing fade probability in LaserCom systems

P. N. Crabtree, M. Goda, Air Force Institute of Technology

Adaptive techniques are investigated for the purpose of reducing fade probability in free-space laser communication (LaserCom) systems. The overarching goal of our approach is to identify failure mechanisms and explore techniques to improve the fade rate performance and robustness of LaserCom systems. Here we are concerned with the mitigation of two types of fades. First, challenging operating scenarios can lead to spot breakup in the focal plane image. During moments of spot breakup a traditional centroid tracker can force an intensity valley to the on-axis position and cause unnecessary drops in received power. We previously investigated correlation tracking techniques to prevent this type of fade. Here we explore adaptive techniques to prevent the correlation tracker from jumping from spot to spot during periods of image breakup. Our initial approach is to identify a threshold below which the current peak must fall before allowing the tracker to jump across a valley to a new peak. Second, scintillation is identified as a primary failure mechanism for any LaserCom system operating in severe conditions. Scintillation can cause the captured power to fall below threshold. In this case and with the assumption of a fixed threshold, one must increase source power and/or incorporate adaptive optics in the transmitter. Alternatively, one could use an adaptive threshold to determine whether the signal at a given point in time represents a 1 or a 0. This technique is explored here, initially with a simple boxcar average.

6105-28, Session 6

The experimental determination of on-off keying laser communications probability models and a comparison with theory

W. C. Brown, Colorado State Univ./Pueblo

It is well known that atmospheric turbulence diminishes the performance of laser communications systems. Among the multiple degradations caused by turbulence is fading and surging of the received signal, usually referred to as scintillation. If a minimum probability of error receiver is employed for on-off keying (OOK), it is necessary to understand the two conditional probability densities (pdfs) corresponding to the transmission of ones and zeros. These probability densities are the distributions of signals received when the laser is on when sending ones and when the laser is off sending zeros. Many theoretical studies have determined the form of the expected pdfs. An ongoing experimental study operating a low-power, low data rate link over a range of 9.5 Km has been started at Colorado State University-Pueblo to carefully examine the effects of atmospheric turbulence on laser communications. Experimental models of actual, true and typical pdfs have been done. The results do not always match theoretical predictions. The non-stationary nature of these pdfs is also a problem that must be and is addressed. This paper summarizes the experimental testing and shares a number of its conclusions.

6105-29, Session 6

Control of the intensity fluctuations of random electromagnetic beams on propagation

O. Korotkova, Univ. of Rochester and College of Optics and Photonics/Univ. of Central Florida

We discuss fourth-order correlation properties of a wide-sense statistically stationary, quasi-monochromatic, electromagnetic beam. In particular, we derive expressions for the covariance function and for the contrast (scintillation index) of the fluctuating intensity of an electromagnetic Gaussian Schell-model beam, propagating in free space. For such beams we also derive expressions relating to fluctuations in the power and discuss the effects of transmitter and receiver aperture averaging. We show that the fluctuations of the intensity and of the power of the beam can be controlled by suitable choice of the states of coherence and of polarization of the source. The results presented in this paper may find applications in the theory of optical detection and for optimization of free space communication links which involve random electromagnetic beams.

6105-30, Poster Session

Research on 1.06μm laser atmospheric propagation in low elevation

Y. Liu, Shandong Institute of Business and Technology (China)

The property of 1.06μm laser atmospheric propagation in low elevation was researched. Some valuable data and results were obtained.

First, the atmospheric propagation property of laser on sea surface was analyzed. The laser atmospheric transmittance was chiefly discussed. And the atmospheric transmittance of 1.06μm laser atmospheric propagation in low elevation was calculated. Some valuable conclusions about the atmospheric propagation in low elevation on sea surface were obtained. The atmospheric transmittance of 1.06μm laser atmospheric propagation was calculated by the simple formula. And then the atmospheric propagation property of high power laser was analyzed. Finally, the compensation technology of laser atmospheric propagation was given.

Conference 6106A: Laser Applications in Microelectronic and Optoelectronic Manufacturing XI

Monday-Wednesday 23-25 January 2006

Proceedings of SPIE Vol. 6106A

6106A-02, Session 1

Review: 40 years of laser-marking industrial applications

B. Gu, GSI Lumonics Inc.

One of the early applications of lasers was marking electronics components. Today laser marking has found its way into a wide range of applications, from wafer marking at the chip scale package level to beer bottles and food package identifications, and to marking of the buttons of clothes. In many cases, laser marking has become a standard manufacturing process. We will review the laser marking technology over the last four decades. This would include the review on evolution of the different laser technologies and beam delivery systems used in various laser marking systems for the past 40 years. Finally, the latest laser marking technologies will be presented and future directions will be discussed.

6106A-03, Session 1

Laser patterning of ITO in flat panel display manufacture

S. Venkat, Coherent, Inc.

A necessary step in the fabrication of many different flat panel display types is the selective removal of a thin layer of indium tin oxide (ITO) or other conductor from the substrate to create circuit patterns. The conventional method of performing this patterning utilizes photolithography. Specifically, an image of the desired pattern is projected on to a photoresist coated substrate, and this substrate is then developed and etched with wet chemicals. However, it is possible to use a laser to directly ablate ITO without damaging the substrate, and thus eliminate all the expense, time and environmental concerns associated with a wet chemical process. First generation laser based systems for ITO patterning were too slow to be competitive with traditional means, however, laser manufacturers are focused on developing sources that enable the required process speed, and also possess desirable characteristics in terms of lifetime, maintenance downtime, and overall cost-of-ownership. This paper examines current developments in both excimer and solid-state laser technology that are intended to meet the needs of ITO patterning for the flat panel display industry. It reviews the relative merits of these two different laser technologies for this application, and also presents the latest process results from the Coherent Applications Lab.

6106A-04, Session 2

Laser processing of advanced materials with high brightness solid-state lasers at 532nm

T. Riesbeck, Technische Univ. Berlin (Germany); A. Binder, Laser- und Medizin-Technologie GmbH, Berlin (Germany); H. J. Eichler, Technische Univ. Berlin (Germany)

High beam quality is one of the most important properties for micro material processing with lasers. It facilitates slight focus diameters and due to high Raleigh length even at strong focusing drilling of holes with high aspect ratio. Together with high average output powers it allows fast processes with high quality. Another important point is the wavelength of the laser radiation. Many materials e.g. diamond or silicon show no sufficient absorption at fundamental wavelength of Nd based solid-state laser sources. Frequency conversation to the second and forth harmonic allows the efficient processing of these materials. At least flexible pulse peak power and repetition rate is necessary to optimize the process. Two laser sys-tems which fulfill these requirements are investigated. A pulsed pumped Nd:YAP System which delivers an average output power of 315 W with M≤ = 2.6 at the fundamental wavelength and 124 W at the second harmonic. Another pulsed pumped System based on Nd:YAG with an average output power up to 125 W with M≤ = 2.2 at the fundamental wavelength, 49.5 W at the second harmonic and 4.75 W at 266 nm. Due to its active Q-switch the pulse peak power of this system is variable in a wide range. With an emphasis on silicon and ceramic materials several examples comparing IR with “green” processing will be given in this presentation, as well as some applications in the UV-range.

6106A-05, Session 2

High quality laser milling of ceramics, dielectrics and metals using nanosecond and picosecond lasers

D. Karnakis, G. Rutterford, M. R. Knowles, Oxford Lasers Ltd. (United Kingdom); T. Dobrev, P. Petkov, S. S. Dimov, Cardiff Univ. (United Kingdom)

Laser milling of industrial materials like ceramics, dielectrics and metals is of significant commercial interest for microfabrication of micro-moulds and other micro-system devices. 2.5D laser machined structures were generated in alumina, tungsten and steel substrates using a nanosecond copper vapour laser (511nm) at 10 kHz. Preliminary results in fused silica, alumina and steel are also presented from a high repetition rate amplified mode-locked picosecond Nd:vanadate laser. It is shown that high quality surface finish can be achieved with both laser types; for example, average surface roughness, Ra ~ 300nm has been demonstrated in steel. Fused silica could only be processed with picosecond laser pulses. Volume removal rates are analysed, which are especially high for difficult materials like tungsten (~0.1mm3/min) and are greater compared to other milling technology like micro-EDM. Surface roughness measurements in these materials using white light interferometry are reported along with SEM analysis.

6106A-07, Session 2

Production excimer drilling process for producing micron exit holes in polyimide

T. E. Lizotte, O. P. Ohar, Hitachi Via Mechanics USA, Inc.

Producing micron level exit holes or vias interconnects for applications involving critical drug delivery and microelectronic packaging is no easy task. The design of excimer beam delivery optics, the physical system configuration, construction materials used and laser material interaction play significant roles in the ultimate process results. As a result of higher density microelectronic package designs and the critical nature of drug delivery, these processes need to be robust and repeatable to a six sigma level. Many companies who look to source new laser systems to meet these new demands come face to face with the reality of this dilemma. Matching laser process to material selection sets the stage for a successful integration, of most concern is the materials ability to resolve the features desired and the ease of cleaning the debris once the features are formed. This paper will present application specific laser beam delivery methods, focus/image stability techniques, beam shaping and inline inspection technology to stabilize such processes and present statistical and quality data on a process that was developed to form (1) one micron exit holes through 25 micron thick polyimide for a critical drug delivery application. The data will cover a 30 day period of processing.

6106A-08, Session 2

High power excimer laser micromachining

L. Herbst, R. Paetzel, Lambda Physik GmbH (Germany)

Excimer lasers are well-established tools for a wide array of micro-machining tasks. Their unique combination of high pulse energy, high average power and deep ultraviolet (UV) wavelength make them capable of ablating a wide range of materials, including polyamide, PMMA, copper, and diamond. Furthermore, UV output enables the production of small feature sizes, making the excimer laser an ideal technology for the fabrication of microvias in semiconductor packages, ink jet nozzle arrays and small holes in medical devices. Extending the reach of excimer laser micro-machining requires both higher output power to increase process throughput, along with good output stability and reliability. This paper examines the newest generation of high power industrial excimer lasers specifically designed to enable high duty-cycle, high-throughput micromachining. It will review the technology behind these lasers, as well as beam delivery systems and important applications.

6106A-09, Session 3

A Neuro-Fuzzy Approach to Failure Detection and Diagnosis of Excimer Laser Ablation in Microvia Formation

R. Setia, G. S. May, Georgia Institute of Technology

Excimer laser ablation is used for microvia formation in the microelectronics packaging industry. With continuing advancement of laser systems, there is an increasing need to offset capital equipment investment and lower equipment downtime. This paper presents a neuro-fuzzy methodology for in-line failure detection and diagnosis of the excimer laser ablation process. Response data originating directly from laser tool sensors and the characterization of microvias were used as failure symptoms of the deviations of four laser system parameters from their corresponding baseline values. The response characteristics consist of via diameter, via wall angle, and via resistance. The resistance measurement on copper deposited in the ablated vias was conducted to characterize the degree to which debris remaining inside the vias affected quality. The laser system parameters include laser fluence, shot frequency, number of pulses, and helium pressure flow. The adaptive neuro-fuzzy inference system (ANFIS) was trained and subsequently validated for its capability in evidential reasoning using the data collected. Results indicated only a single false alarm occurred in 19 possible failure detection scenarios. In failure diagnosis, a single false alarm and a single missed alarm occurred.

6106A-10, Session 3

Developments in laser singulation to support higher integrated circuit density

S. Venkat, Coherent, Inc.

Continuing progress in the development of integrated circuits for logic and memory with smaller geometries, higher performance and lower cost requires a move from traditional silicon substrates to thinner wafers and wafers that utilize low-κ dielectrics. However, the mechanical characteristics of these new substrates make them difficult to singulate (separate into individual units) using traditional mechanical sawing. This paper reviews the needs of the semiconductor industry for material singulation, particularly as it moves towards the 45 nm node, and examines laser process solutions and laser technologies that are being developed to meet these current and future requirements.

6106A-11, Session 3

New advances in dry and steam laser cleaning of opaque and transparent critical substrates: with IR-lasers to new laser cleaning mechanisms

S. D. Allen, S. Shukla, K. Lyon, S. I. Kudryashov, Arkansas State Univ.

Dry and steam laser cleaning, DLC and SLC, of nano-and micro-contaminant particles from opaque and transparent critical substrates has been studied using nanosecond IR- and UV-lasers and different energy transfer media (ETM) fluids. In the case of SLC, microscopic details of lyophobic and lyophilic particle-ETM-substrate interactions in pre-deposited micron-thick ETM layers have been revealed preliminarily by means of time-resolved optical microscopy. Fundamental DLC and SLC mechanisms of UV/vis opaque and transparent critical substrates have been studied in front-side and back-side laser illumination geometries with the help of time-resolved optical and photoacoustic techniques. Optimal conditions for nearly complete laser cleaning have been chosen for different combinations of contaminating nano- and micro-particles and substrates.

6106A-12, Session 3

Laser Annealing of LTPS

R. Paetzel, L. Herbst, F. Simon, Lambda Physik GmbH (Germany)

Laser annealing has become the primary production method for the Low-Temperature-Poly-Silicon (LTPS) panels used in the Flat Panel Display (FPD) industry. LTPS backplanes for Active Matrix Liquid Crystal Display (AMLCD) displays offer substantial advantages over those based on amorphous silicon. The trend to higher pixel density, the integration of more driver and logic ICs on the glass, and the advent of Active Matrix Organic Light Emitting Displays (AMOLED) have all lead to significant interest in the laser annealing process. Currently, there are several different approaches to the annealing process based on excimer lasers, CW-green DPSS lasers, modelocked-green DPSS lasers and Q-switched Nd:YAG lasers. This paper reviews the various laser technologies and annealing techniques, such as line beam or SLS. These approaches will be compared in terms of crystal quality, electron mobility, throughput, yield and operating cost.

6106A-13, Session 3

A hybrid SLS approach for obtaining orientation-controlled single-crystal Si regions on glass substrates

P. C. van der Wilt, B. A. Turk, A. B. Limanov, A. M. Chitu, J. S. Im, Columbia Univ.

Sequential lateral solidification (SLS) is a pulsed-laser-based crystallization technique that can be used to produce a variety of low defect-density polycrystalline Si films for high-performance TFTs on glass substrates. We have previously shown that location-controlled single-crystal Si regions can be obtained by implementing a specific version of the SLS process, referred to as dot-SLS. In this paper, we will report on advances we have made on obtaining location-controlled single-crystal regions with a controlled surface crystallographic orientation. We accomplish this by performing dot-SLS on textured poly-Si precursor films that were obtained using laser-crystallization processes. We will in particular report on two specific well-known laser techniques for obtaining either (100) or (111) textured poly-Si films.

6106A-14, Session 4

High-spatial coherence excimer laser for production of fiber Bragg gratings

R. F. Delmdahl, Lambda Physik AG (Germany)

Excimer lasers are unique ultraviolet laser sources ideally suited for a wide range of applications driving innovations in almost every branch of industry including microsystem manufacturing, flat panel display production and dense wavelength division and multiplexing to name a few.

The success of fiber Bragg gratings in the last years is based on their unique properties which make them extremely valuable for numerous applications in optical telecommunication networks. Expectations for the continued growth of demand for internet services and more bandwidth show a promising future also for passive optical components. Components which serve not only one but several purposes have a good possibility to participate in this success proportionally.

Excimer laser written fiber Bragg gratings (FBGs) stabilize the frequency of laser diodes, flatten the non-linear gain of fiber amplifiers, compensate for the fiber's dispersion and filter communication channels. Developments and optimization of 248 nm excimer laser systems for production environments are ongoing.

6106A-15, Session 4

Laser-induced formation of an array of periodic submicron resistors in silicon covered by SiO2

Y. Liao, J. Degorce, M. Meunier, École Polytechnique de Montréal (Canada)

Arrays of periodic submicron conductive links were fabricated in silicon, covered by SiO2, when a polarized frequency doubled Nd:YAG pulsed laser irradiation is focused on the gap between two highly doped regions. The principle of the process is based on the fact that the laser forms a periodic melting in silicon, thus inducing a preferential dopant diffusion and creating an array of fine conductive links between the highly doped regions. The formation mechanism of the periodic resistors was studied using transmission electron microscopy (TEM), scanning electron microscopy (SEM) and numerical simulation. By performing careful plan-view TEM samples and cross-sectional SEM samples prepared by focused ion beam (FIB), we observed that two-dimensional (2-D) periodic coexisting of liquid and solid exists (0.9 < I < 1.08 W) and is responsible for the formation of periodic resistors. The periodicity of these structures is 360 nm, related to the wavelength of frequency doubled Nd:YAG laser (532 nm) and the index of refraction of SiO2. We propose a model based on the fact that oxygen atoms are diffusing locally from SiO2 into the melted Si, thus forming SiOb with a lower melting point than that of pure Si; successive laser pulses melt preferentially these regions giving rise to a positive feedback. Scanning capacitance microscopy (SCM) was employed to detect these submicron structures and to measure their electrical properties. It was found that between 2 to 7 submicron conductive links are observed in the focused spot size of 3 μm and their number depends only on laser intensity ranging from 3.10 W to 3.75 W, while their average width (151 - 300 nm) and depth (108 - 147 nm) strongly depends on both laser intensity and number of laser pulses. The resistances of these links are between 363 - 493 W and the effective average doping levels are from 1.5x1018 to 2.4x1019 cm-3. Dynamic nanoscale modeling, based on variations of melting points of Si and dielectric and reflection coefficient, confirms the experimental results.

6106A-16, Session 4

Inkjet printed flexible electronics components fabrication by low temperature subtractive laser processing of functional nano-ink

S. H. Ko, Univ. of California/Berkeley

The low temperature fabrication of passive electrical components (resistor, capacitor) on the flexible substrate is presented in this paper. A drop-on-demand(DOD) ink-jetting system was used to print passive electrical components from gold nano-particles suspended in Alpha-Terpineol solution on flexible polymer substrate. PVP(poly-4-vinylphenol) in PGMEA(propylene glycol monomethyl ether acetate) solvent was inkjet printed as dielectric layer for capacitor. Pulsed laser was irradiated to make finer electrical components to overcome limitation of inkjet process. Continuous Ar laser was irradiated locally to evaporate carrier solvent as well as to cure gold nano-particles. Simple conductor lines and capacitors were fabricated on polymer substrate and the performance was analyzed.

6106A-17, Session 4

Laser-induced oxidation of zinc film for direct-write grayscale photomask material

G. H. Chapman, J. Wang, M. Chang, R. Y. Tu, C. Choo, D. K. Poon, J. Peng, Simon Fraser Univ. (Canada)

Previous research showed that bimetallic films (Bi/In and Sn/In) exhibit good grayscale levels after laser exposure due to controlled film oxidation. While giving a large alteration in optical density (OD) from 3.0OD to 0.22OD at 365 nm, Bi/In and Sn/In films show a very nonlinear OD change with laser power, making fine control of grayscale photomask writing difficult at some gray levels. This paper studies zinc and zinc alloy films as possible candidates for improved direct-write grayscale photomask applications. Zn laser oxidation has been reported previously, but without optical measurements. In this paper Zn films, 50nm ~ 150nm thick, were RF-sputtered onto glass slides. Under focused (f=50 mm) argon laser (514 nm) exposure the Zn film OD changes from 1.7OD to 0.10OD (at 365 nm). The zinc OD change versus laser power curve is nearly linear, unlike that of Sn/In films which starts with a steep slope at low power and changes slowly at higher power levels. For a 100nm zinc film the average OD change rate versus laser power is only -0.0065 OD/mW, ranging from -0.002 to -0.013 OD/mW. This is much less than that of Bi/In and Sn/In films (average OD rate -0.02 OD/mW, ranging from -0.001 to -0.113 OD/mW for a 10at.%, 80nm Sn/In film), thus suggesting finer gray-level control. Profilometry test demonstrates that the exposed area thickness increases by 10% - 100% (depending on the power). Surface roughness of a 100 nm thick zinc is <15nm, which is much smoother than Sn/In or Bi/In.

6106A-18, Session 4

Real-time optical characterization of laser oxidation process in bimetallic direct write gray scale photomasks

G. H. Chapman, D. K. Poon, M. Chang, J. Wang, C. Choo, R. Tu, Simon Fraser Univ. (Canada)

Previous research demonstrated that DC-sputtered Sn/In and Bi/In bimetallic thin films turn transparent under laser exposure with an optical density (OD) that changes smoothly with increasing laser power from ~3.0OD (unexposed) to <0.22OD (fully exposed). This laser-induced oxidation of bimetallic films produces direct-write binary and analogue grayscale photomasks. In this paper we explored how Sn/In and Bi/In films' OD changes with time during laser exposure from minimum conversion to maximum transparency using a silicon photodiode to measure film transmission in real time. In one example with an Argon laser (488/514 nm) of 0.17W focused to 10 um spot, a 10at.%, Sn/In, 80 nm film changed from 3.2OD to 3.5OD in 57 micro-second due to heating of the material. The Sn/In thin film then began to oxidize and its OD dropped abruptly from 3.5OD to 0.65OD in 142 micro-second. The Sn/In slowly reached its final value of 0.23OD in another 311 micro-second. This agrees with the measured film OD versus laser power curves which show after reaching a threshold an initial rapid decrease in OD with laser power, but large laser power required to reach the maximum transmission. The real-time measurement of film transmission using a photodiode combined with X-ray material analysis gives a better understanding of the laser-induced oxidation process. These experiments suggest the film OD can be precisely controlled real-time during the laser writing process if we are able to monitor and adjust both the laser power and optical shutter open time.

6106A-19, Session 5

Femtosecond laser micromachining

E. Mazur, Harvard Univ.

When femtosecond laser pulses are focused tightly into a transparent material, the intensity in the focal volume can become high enough to cause nonlinear absorption of laser energy. The absorption, in turn, can lead to permanent structural or chemical changes. Such changes can be

used for micromachining bulk transparent materials. Applications include data storage and the writing of waveguides and waveguide splitters in bulk glass, fabrication of micromechanical devices in polymers, and subcellular photodisruption inside single cells.

6106A-20, Session 5

Tailored excitation sequences for optimized laser induced modifications in bulk transparent materials exposed to sub-ps irradiation

A. Mermillod-Blondin, Univ. Jean Monnet Saint-Etienne (France) and Max-Born-Institut für Nichtlineare Optik und Kurzzeitspektroskopie (Germany); R. Stoian, Univ. Jean Monnet Saint-Etienne (France); A. Rosenfeld, Max-Born-Institut für Nichtlineare Optik und Kurzzeitspektroskopie (Germany); E. Audouard, Univ. Jean Monnet Saint-Etienne (France); I. V. Hertel, Max-Born-Institut für Nichtlineare Optik und Kurzzeitspektroskopie (Germany)

Tightly focusing of ultrashort laser pulses in the bulk of various transparent materials induces significant modifications of the optical properties by locally changing the material refractive index. Such laser-induced phase objects are of major technological interest, notably for direct writing of embedded optical functions.

While extensive studies have been reported on ultrashort pulsed laser-induced modifications in several materials, especially with regard to focusing conditions, incubation effects, or the influence of the energy content of the pulse , we emphasize here the role of the temporal design of the excitation sequence.

We present phase-contrast microscopy investigations of the resultant morphology and discuss the refractive index topological map induced by different temporal pulse intensity envelopes in various transparent materials.The consequences of complex temporal profiles generated by a pulse shaping apparatus on the morphology of the interaction zone are illustrated, emphasizing the benefits of the synchronization between the excitation temporal profile and the material response. Additionally, adaptive optimization procedures based on dynamic temporal pulse shaping are implemented to create user-designed phase objects. These results suggest that temporal pulse tailoring is a viable concept in the perspective of realizing efficient guiding elements in optical materials.

6106A-21, Session 6

Laser nanoprocessing using near-field probes

C. P. Grigoropoulos, Univ. of California/Berkeley

Recent research results on the nanoscale laser-induced surface modification will be presented. Ultra-fast and nanosecond pulsed lasers have been coupled to near-field-scanning optical microscopes (NSOMs) in apertureless configurations as well as through apertured bent cantilever fiber probes. Calculations of the electromagnetic field show effective enhancement of the near-field intensity distribution on the target surface. The feature size depends on the pulse length, and the near-field absorption distribution. Experiments have been conducted on the surface modification of metals, polymers and semiconductor materials in both ambient air and controlled gas environments. By combining nanoscale ablative material removal with subsequent chemical etching steps, ablation nanolithography and patterning of fused silica and crystalline silicon wafers has been demonstrated. Confinement of laser-induced crystallization to nanometric scales has also been shown. Laser Chemical Vapor Deposition (LCVD) has been utilized to deposit nanoscale metal and semiconductor patterns. Experiments have been conducted on the pulsed laser-induced functionalization of monolayer coatings.

6106A-22, Session 6

Dynamics of femtosecond laser-induced cluster emission from silicon

A. V. Bulgakov, Institute of Thermophysics (Russia); I. Ozerov, W. I. Marine, Univ. de la Méditerranée (France)

Ultrashort laser pulses have opened unique opportunities for studying mechanisms of laser-matter interactions by analyzing particles emitted from the irradiated surfaces. A number of recent experiments indicate that efficient emission of clusters can occur under certain conditions of fs-laser ablation/desorption of semiconductors. Analysis of cluster emission could provide a considerable insight into the complex interplay of thermal and ultrafast, non-thermal processes in the laser-irradiated targets.

Here we report time-resolved pump-probe measurements of the yield of singly-charged positive cluster ions (n = 2-11) from a silicon surface and theoretical modeling of the laser-induced excitation of the Si target for the experimental regimes. A 80-fs Ti:sapphire laser pulse was split into two subthreshold pulses with a variable time delay and cluster emission was monitored after each pair of pulses. When temporal separation between the pulses is around few hundred femtoseconds, the emission is found to be stronger than that with a single laser pulse of the same total energy. We demonstrate also that there is significant incubation in silicon in respect of cluster yield which is maximized after 30-40 pulses applied to the same spot. Temporal and spatial behavior of electron and ion temperatures in the Si target as well as surface charge density were simulated as a function of pump-probe delay. Both modeling results and observations imply a new mechanism of cluster emission involved. We suggest that the first pulse induces the lattice destabilization and surface structural changes while the second pulse, applied to the unstable surface, acts as a trigger resulting in efficient emission of clusters. The role of surface defects and premelting in cluster formation process will be discussed.

6106A-23, Session 6

Suited simulations for optimal ultrafast laser processing of metals

E. Audouard, J. Colombier, A. Mermillod Blondin, N. Huot, R. Stoian, Univ. Jean Monnet Saint-Etienne (France); H. Soder, Impulsion SAS (France)

Due to a large material removal rate and a minimal collateral damage, subpicosecond laser pulse offers many advantages for material processing. Post-experimental examination of ultrashort laser material ablation shows that the heated surface of the bulk does not exhibit thermal damage.

A lot of complicated physical processes follow intense laser irradiation and have often been modeled in over-simplified way to explain experimental results. Because a more complete understanding of the damage mechanisms would be very interesting and would open new applications in the scientific research community and industry. A detailed model of the ultrashort response to reproduce ablation process is presented, describing dynamical electronic properties such as temperature, pressure and energy. To simulate the interaction between the laser and the metallic target, these theoretical models are inserted inside a 1D Lagrangian hydrodynamic code.

It is still a very challenging task to disentangle the cumulative/competitive effects of all physical processes if included at once in numerical simulations. Adding the different processes into numerical simulations on a one by one basis allow to assess their contributions to the quantity of ejected matter on a large range of laser intensity.

Experimental results related to the influence of multi-pulses or tailored pulses for ablation efficiency with ultrafast pulses (pulse duration up to 5 ps) has been obtained. A significant improvement of the micro structuring quality in metals is demonstrated, and the theoretical approach presented allow to manage the optimal temporal shape of pulses. An effi-

cient process control can be reached and the industrial applications will be evidenced.

6106A-24, Session 7

Generation of new nanomaterials by interfering femtosecond laser processing and its applications

Y. Nakata, Kyushu Univ. (Japan)

New nanomaterials such as nanobump, nanomesh, nanobelt were generated by thin film processing by interfering femtosecond laser beams. To split and correlate femtosecond laser, a demagnification optical system with a transmission beam splitter was used. Different interference patterns can be generated depending upon the number of beam, magnification factor and period of the transmission grating. Using the system, a material surface can be processed according to the interference pattern. Metallic single- or multi-layered film was used as a target.

With four interfering beams and at relatively low fluence, a conical nanobump array was generated within a single shot. The size became larger and a bead was formed on a top of a bump at higher fluence. Moreover, with three or two beams, ellipsoidal or linear nanobump array was generated. As an application, field emission device was fabricated. With further higher fluence of four beams, a nanohole array was generated. By exfoliating the structure, a nanomesh was generated. On the other hand, a grating was generated with two beams, and nanobelts were generated by exfoliation. Bimetallic nanobelts were generated from multilayered thin film.

These top-down techniques for the generation of nanomaterials have advantages as follows; the structures are unique and controllable, and automatically aligned. Moreover, adaptability to many kinds of materials is very good, which can be amorphous, crystalline, single- or multi-layer, composite, or even living material. No special ambient condition such as high vacuum, temperature control, special gas or liquid is required. This technique is expected to improve the existing applications and open new opportunities for nanomaterials.

6106A-25, Session 7

Fabrication of periodic arrays of gathering titania-organic hybrid pillars derived from multi-beam laser interference technique

H. Segawa, Tokyo Institute of Technology (Japan); H. Misawa, Hokkaido Univ. (Japan); T. Yano, Tokyo Insititute of Technology (Japan); S. Shibata, Tokyo Institute of Technology (Japan)

Periodic arrays, which are composed of two materials with large different refractive indices, are applicable for photonic crystals. A multi-beam laser interference (MLI) technique is known to one of the fabrication techniques of photonic crystals. In the technique, laser is interfered on a scale of the wavelength of light and is irradiated to photosensitive films. The periodic arrays can be formed by the removal of the unirradiated portions, because the laser irradiation caused a change in the solubility of the film.

We have paid attention to photosensitive TiO_2-organic hybrid film, which has high refractive index. In this work, TiO_2-oranic hybrid periodic pillar arrays are fabricated by the MLI technique.

The TiO_2 hybrid film was prepared from Ti-alkoxide and beta-diketone by the sol-gel method. The interference pattern of femtosecond pulses at 800nm wavelength was irradiated on the film. By the laser irradiation, the beta-diketonato ligands between Ti alkoxide and beta-diketone decomposed and TiO_2 network was formed. The structural change caused a decrease of the solubility of the irradiated parts in 2-ethoxyethanol.

Two-dimensional periodic arrays, which correspond to the MLI pattern, have been obtained on the film after the chemical development. Depending upon the laser energy or film thickness, the several pillars have gathered on the top by the self-organization and they have arranged with new larger period. From the observation of the drying process during the development, it is found that the self-organized periodic pillar arrays are fabricated by the unbalance between the cohesive and restoring powers for the pillars.

6106A-26, Session 7

Femtosecond laser writing of Bragg gratings using a single-pulse processing

I. Sohn, M. Lee, T. Kim, Information and Communications Univ. (South Korea); S. Lee, J. Chung, Phoco Co., Ltd. (South Korea)

We report microfabrication of periodic photonic band gap structures in transparent materials using a single pulse femtosecond laser processing. This technique has the potential to generate line and dot patterns with ultrahigh processing speed of 1 kbit/s. We create the line patterns with a slit, which is applicable to fabricate a Bragg grating. The pulse width was 100 fs, the wavelength was 800 nm, and the repetition rate was 1 kHz. The laser beam was guided into a microscope and focused by a 50x objective (NA, 0.42) into the core. The sample was placed on a computer-controlled stage. The average power of the laser beam was controlled by neutral density filters inserted between the laser and the microscope objective. The laser pulse-induced refractive index change is 0.006-0.01. The refractive-index changes were estimated by coupling light from an He:Ne laser into the waveguides and measurement of the numerical aperture (NA) of the waveguides.

6106A-27, Session 8

Picosecond time-scale heat transport in metallic layers

D. G. Cahill, B. C. Gundrum, R. S. Averback, Univ. of Illinois at Urbana-Champaign

While a great deal of attention has been given to the rate at which a material can be heated by an ultrafast laser pulse, practical applications of laser processing of materials will also have to be concerned with the rate at which the processed material can dissipate heat on picosecond time scales. We have studied several aspects of this problem using measurements of time-domain thermoreflectance and computer simulation. The experimental system we are studying is a thin layer of Al deposited on a much thicker layer of Cu. The Al/Cu interface introduces electron scattering which helps confine heating to the thin Al layer but this interface also introduces a thermal resistance that limits the cooling rate of the Al layer. Measurements of the thermal conductance of this metal-metal interface using a small temperature excursions produced by a mode-locked Ti:sapphire laser give a value of 4 GW/m2-K at room temperature, in good agreement with a “diffuse mismatch model” for interface electron transport. An amplified laser is used to produce large temperature excursions that are beyond the near-equilibrium assumptions of the theory. Computer simulations are used to explore the maximum cooling rate that can be achieved when the latent heat of crystallization is dissipated only by lattice vibrations.

6106A-28, Session 8

Fundamentals of laser-induced plume dynamics in ambient gas environment

N. M. Bulgakova, Institute of Thermophysics (Russia)

Gasdynamic behavior of plasma plumes induced by pulsed laser ablation of solids determines substantially different processes taking place in the vaporized matter (chemical reactions, plasma-associated processes, condensation, etc) with major consequences for various laser applications such as thin film deposition and nanoparticle production. Extended knowledge about formation and evolution of the plume under different irradiation conditions (type of irradiated material, laser pulse duration and wavelength, ambient gas pressure and sort, etc.) will lead to development of

concepts for optimizing a variety of applications.

In this presentation the dynamics of the laser ablation plumes expanding in ambient gases are considered for a wide range of the irradiation conditions. Plume analysis is carried out with a new modeling approach based on the Navier-Stokes equations taking into account the diffusion processes. The approach allows to follow the ablation products propagation and their mixing with the ambient gas. It is demonstrated that, depending on ablation conditions, the plume can either propagate near-spherically or form intricate vortex structures in the plume periphery and its front. Moreover, in some cases, side spreading of the plume is found to take place with subsequent generation of a tiny jet of the ablation products along the plume axis. Generally, the different plume structures do not exist alone but accompany each other or replace one another in the temporal scale. All these aspects are discussed with demonstration of particular examples of the complicated vortical structures arising in the plumes. Other approaches to the analysis of plume dynamics such as the spherical model, Monte-Carlo method, and double-layer theory are also involved.

6106A-29, Session 8

Ablation of silica glass using laser plasma soft x-rays at around 10nm and ablation mechanism

T. Makimura, H. Miyamoto, S. Uchida, K. Murakami, Univ. of Tsukuba (Japan); N. Hiroyuki, National Institute of Advanced Industrial Science and Technology (Japan)

Micromachining inorganic transparent materials at high precision is required for nanometric chemical analyzers, chemical reactors and optical devices. We have investigated direct micromachining of inorganic transparent materials using laser plasma soft X-rays. The soft X-rays were generated by irradiation of Ta targets with 532 nm Nd:YAG laser light with a pulse duration of 7 ns, at an energy density of 10E4 J/cm2. The soft X-rays were focused on samples, using an ellipsoidal mirror that we desined so as to focus soft X-rays at around 10~nm efficiently. We found that synthetic quartz glass, fused silica, Pyrex, LiF, CaF2, Al2O3, LiNbO3 and Si can be machined smoothly. Typically, quartz glass is ablated at 40 nm/shot, and has a surface roughness less than 10 nm after 10 shots. In order to investigate ablation mechanism, silica glass was irradiated with laser plasma soft X-rays in innert gas, which can be used as X-ray band pass filter. It is suggested that silica glass is ablated by soft X-rays at around 100 eV (=10 nm), above which Si 2p core electrons are excited. Further, nonomachining using the 10-nm X-rays is demonstrated using a WSi contact mask fabricated on a synthetic quartz glass plate and patterned by electron beam lithography technique. We found that a line-and-space pattern is fabricated on the glass plate with a resolution less than 100~nm. In summary, we have established a technique for micromachining a vriety of inorganic materials using laser plasma soft X-rays.

6106A-30, Session 8

Modeling focused pulsed laser-induced charge injection in silicon

M. Meunier, E. Boulais, J. Degorce, G. Wild, V. Binet, Y. Savaria, École Polytechnique de Montréal (Canada)

It is well known that by focusing a pulsed visible laser on silicon, photoexcited charges are injected into the material. This phenomena could have important transient and even permanent effects on surrounding circuits when laser processes are directly used on microelectronics chips. This could be the case for instance in the recently developed laser fine tuning technology (1) which consist of creating an accurate resistor by applying laser pulses on a gateless MOSFET transistor to melt the silicon and diffuse dopants from the source and the drain into the gap. In order to monitor lased-induced charge injection effects on surrounding microelectronics devices, we have designed and fabricated a specially very sensitive frequency-monitoring circuit in the 0.18μm CMOS technology. Frequency changes of the ring oscillator have been measured as a function of laser power, pulse width and distance from the laser spot and the circuit. Using conventional circuit analysis software, we have shown that this behaviour is mostly due to a charge injection from the substrate into the well of the surrounding transistors thus strongly affecting their characteristics and the ring oscillator frequency. In order to understand this charge injection and assuming a cylindrical symmetry, complete two-dimensional (2-D) simulations were performed. Modeling this process involves to solve two coupled sets of equations: (i) the first one deals with the thermodynamics and heat transfer equations to obtain the 2-D temperature profile including phase transformation (2); (ii) the second set involves the semiconductor equations based on the Poisson and continuity equations to obtain the 2-D electron and hole concentrations and voltage distribution. Modeling results showing temporal and spatial current distribution are in good agreement with experiments.

[1] M.Meunier, Y. Gagnon, Y. Savaria, A. Lacourse and M. Cadotte “A novel laser trimming technique for microelectronics,” Applied Surface Science, 186, 52-56 (2002).

[2] J-Y. Degorce, J-N. Gillet, F. Magny and M. Meunier “Three-dimensional transient temperature field model for laser annealing” J. Applied Physics, 97, 033520 (2005)

6106A-31, Session 8

Laser-induced transient stress-field studied by time-resolved photoelasticity technique

Y. Ito, Nagaoka Univ. of Technology (Japan)

Interaction between an intense laser pulse and a material surface is a key issue to understand and control photo-induced surface processes. It is rather difficult to study the interaction in detail because it occurs in a very narrow area and a very short period. In addition, it is often accompanied by plasma formation, which causes difficulties for the most of observation and measurement techniques.

We have developed a time-resolved imaging technique which uses a pulse laser as a probe light and an ICCD, and successfully observed the dynamical change of the spatial distribution of laser induced transient stress fields by both shadowgraph and photoelasticity images using transparent materials. The methods allowed us to estimate the effects of surface roughness and incident angle to the laser-matter interaction. These results, however, have remained quantitative levels because these images were not so clear to allow us quantitative estimations.

Recently, we have found that photoelasticity imaging of epoxy resin observed under water provide clear images which allowed us the semi-quantitative estimation of the magnitude of laser induced stress. We can make the semi-quantitative estimation of the laser-induced stress by comparing images to those obtained for designated pulse energies. Effects of surface roughness has been re-examined in detail. We deposited a metal film on the surface of the block to examine the interaction of laser to the metal surface. Details of our time-resolved photoelasticity imaging technique and the results obtained by the technique will be discussed.

6106A-32, Session 9

The cross-beam pulsed laser deposition

A. Gorbunoff, Hochschule für Technik und Wirtschaft Dresden (Germany)

The talk surveys the principles of operation and peculiarities of the cross-beam pulsed laser deposition (CBPLD). The film deposition in this particular high vacuum PLD variant takes place from intersecting plumes from two simultaneously laser ablated targets. The reliable elimination of the debris in this technique allows on one hand the implementation of a wide number of surface averaging characterization methods of structure and properties of the PLD films. On the other hand, the specific shallow implantation (“subplantation”) film growth mode, extended asymmetric transition layers between the neighboring materials, the formation of abnormal crystal structures makes CBPLD itself an advantageous highly non-equilibrium hyperthermal particle beam deposition technique.

6106A-33, Session 9

Laser welding of silica microspheres to silicone rubber

M. Okoshi, J. Cho, N. Inoue, National Defense Academy (Japan); J. Li, P. R. Herman, Univ. of Toronto (Canada)

Photochemical welding of silica glass to silicone rubber has been successfully demonstrated by photochemical modification of silicone to silica with 157-nm F2-laser radiation. Fused silica microspheres of ~2.5-micron diameter were physically contacted with a 2-mm-thick silicone rubber substrate, and the interface irradiated by the F2-laser beam through the slightly transparent fused silica microspheres. Photochemical modification of the silicone rubber surface into silica yielded a strong chemical weld between the silicone and the fused silica microspheres. An F2-laser fluence of ~10 mJ/cm2 was applied to the silica microspheres surface at 10 Hz pulse repetition rate for 5 min. exposure. The laser photochemical welding was carried out at room temperature and showed no evidence of thermal degradation of either the silicone or silica surfaces. An alignment of the fused silica microspheres into a linear array and other geometries provide means for fabricating optical resonators and optical waveguides on a flexible substrate.

6106A-34, Session 9

Laser surface modifications for improved bio-compatibility and cell adhesion

L. C. Ionescu, J. Chen, W. O. Sobojeyo, C. B. Arnold, Princeton Univ.

Laser surface modifications of bio-compatible materials have been shown to be an effective method to improve compatibility and promote cellular growth and adhesion. In this presentation, we examine the influence of laser parameters on the resulting surface characteristics. Nanosecond laser micromachining (355 nm DPSS Nd:YVO4) is used to produce periodic grooves on the surface of Titanium-6 Aluminum- 4Vanadium alloy. The groove width and pitch are varied as well as depth and roughness through control of the translation distance between sequential laser pulses. Surfaces are characterized for chemical composition, corrosion resistance, and roughness on multiple length scales prior to testing cell interactions. Osteosarcoma cells are seeded on these surfaces and examined with respect to their growth and adhesion after different incubation times and compared to results on control surfaces. These results will be discussed in the context of laser induced surface modifications and control of machining parameters.

6106A-35, Session 9

Laser treatment of micro-components' surface for improved tribological applications

K. Ye, Y. Goh, National Univ. of Singapore (Singapore); C. Cheng, C. Yeo, Sony Singapore Research Lab. (Singapore); M. H. Hong, National Univ. of Singapore (Singapore)

The demand for small and compact mechanisms is increasing due to the requirements of mobile products. Many technologies have been explored to fabricate micro-scale components. However, the fabricated micro-components often result in rough surface, which will produce high abrasion, heat and noise when used for tribological applications such as sliding and rotating. These characteristics will shorten the lifetime of the micro-components. Conventional machining techniques for improving these surfaces are often unacceptable due to the small size and non-planar shapes that is often difficult to reach.

We are proposing a method and system to mount and treat the surface of a fabricated micro-component by irradiating an infrared laser on it. Upon irradiation, the heat from the laser will penetrate the micro-component's surface, causing it to melt and flow to reduce the amount of irregularity. This method can create a desired surface finishing with good repeatability on selected regions of the micro-components. It can also work on surfaces of various material types as well as internal surfaces of thin planar or circular structure. The process can be conducted under ambient conditions. By changing the laser power, the repetition rate and the scanning speed, the process can deal with surfaces with different roughness. The final surface roughness can be reduced from micro-meter level to sub-100nm level. The laser treated micro-components have improved tribological performance as the friction is reduced; the abrasion, heat and noise are also reduced. The improvement can enhance the lifetime of the micro-component when used in micro rotating or sliding mechanism.

6106A-36, Session 9

CW-laser induced modification in glasses by laser backside irradiation (LBI)

M. Yoshioka, H. Hidai, H. Tokura, Tokyo Institute of Technology (Japan)

We describe modification of various glasses by a CW Laser Backside Irradiation (LBI) method. In this method, an absorbent which was attached on one side of a glass sheet, was irradiated from the other side through the glass with CW laser beam. Ar ion laser was used and copper foil was chosen as an absorbent. Silica, Pyrex and soda-lime glasses were tested as sample glasses.

When the absorbent was irradiated, heated spot appeared in the glass adjacent to the absorbent and it ran to the other side of the glass in the path of laser beam. Then cylindrical modified zone that was transparent and crack-free was produced. Diameter of the modified column was 30~200 μm and the cylinder could grow up to 30 mm. The growth rate was approximately 200 mm/s. The dimension of modified zone depended on irradiation conditions, such as laser fluence or beam profiles. The threshold fluence for Pyrex glass was 4.4x105 W/cm2.

Then the characteristics of modified zone were examined by etching in 8 wt. % HF solution. As a result, it turned out that modified zone consisted of two layers and etching rate of the inner part was lower than that of the outer part. The Raman spectroscopy revealed that the density of the inner part increased by the modification.

6106A-37, Session 9

Micro/nanoscale surface modification and structuring using lasers

Y. Lu, Univ. of Nebraska/Lincoln

Laser material processing demonstrated its significance in many areas such as microelectronics, data storage, photonics and nanotechnology, since versatile laser sources provide flexible and unique energy source for precise control of material processing. The extreme conditions created by laser irradiation have provided strong impact on material research. To achieve nanoscale laser material machining and processing, we need to overcome the diffraction limit of the laser wavelengths. Recently, different approaches have been explored to overcome the diffraction limit and to achieve feature sizes down to 10 nm order, way beyond the diffraction limits. The author will provide an overview in the areas of laser-based micro/nanoscale surface modification and structuring, including his own research experience on laser-assisted scanning probe microscope, superfocusing by optical resonance in spherical particles, laser nanoimprinting, laser synthesis of quantum dots, laser annealing of ultrashow pn junctions, nanometer-order film thickness detection using rotational Raman spectroscopy, near-field-induced nanoscale deposition, multi-laser-beam material processing, and laser cleaning of nanoparticles.

6106A-38, Session 10

Optical-maskless patterning for nanostructuring

R. Menon, M. E. Walsh, LumArray Inc. and Massachusetts Institute of Technology; D. Chao, A. Patel, Massachusetts

Institute of Technology; H. I. Smith, LumArray Inc. and Massachusetts Institute of Technology

Optical projection lithography (OPL) has been one of the primary driving forces behind the technological progress in the semiconductor industry. In OPL, a fixed pattern on a photomask is imaged onto a photoresist-coated substrate by means of a complicated optical system. Resolution-enhancement techniques used to print at the diffraction-limit often constrain the geometries of these patterns [1]. Furthermore, OPL is inherently inflexible since the patterns once defined in the photomask cannot be changed. Obtaining a new set of photomasks is an expensive and time-consuming proposition. This is significantly important in emerging applications, where frequent experimentation of pattern geometries is often essential to achieving the optimum design. Maskless-patterning techniques ameliorate these issues by not requiring a photomask [2, 3], which provide significant advantages for low-volume manufacturing, prototyping, and research and development. In this presentation, we describe an optical-maskless-patterning technique, which we refer to as Zone-Plate-Array Lithography (ZPAL) [4].

Although scanning-electron beam lithography (SEBL) is capable of higher resolution than optical lithographies, SEBL suffers from very low writing speeds (being a serial process), often has poor pattern-placement accuracy (since electrons are deflected by all electromagnetic and electrostatic fields), requires vacuum, and often imparts energy into the substrate, which might cause damage. In ZPAL, an array of high-numerical aperture diffractive lenses (for example, zone plates) creates an array of highly focused laser beamlets onto the surface of a photoresist-coated substrate. The beamlets are modulated by pixels on an upstream spatial-light modulator, while the substrate is scanned. Patterns of complex geometries are thus created in a “dot-matrix” fashion. Since patterns are created by an incoherent addition of focused spots, there are no undue restrictions on the geometries, even while patterning at the diffraction limit. This is illustrated by scanning-electron micrographs of an arbitrary pattern of minimum linewidth 140nm as well as gratings of period less than 300nm, both of which were patterned using an exposure wavelength of 400nm and NA = 0.85. Recently, we also demonstrated the use of an immersion fluid between the zone-plate array and the substrate to increase the resolution to 115nm [5]. The use of shorter wavelength sources will enable the patterning of features below 100nm.

In this presentation, we will describe the latest results from our commercial prototype ZPAL system. We will also describe various applications of this technology in the fabrication of devices in micro-magnetics, and micro-optics. Extendibility of this technology to smaller features as well as faster writing speeds will be discussed.

References:

[1] M. E. Mason, Proc. SPIE, v. 5379, p. 10-19 (2004).

[2] R. Menon et al., Materials Today, p.26-33 (2005).

[3] R. F. Pease et al, Microelectron. Eng., v. 53 (1-4), p. 55-60 (2000).

[4] H. I. Smith, J. Vac. Sci. Technol. B 14(6), p. 4318-4322 (1996).

[5] D. Chao et al., To be published in J. Vac. Sci. Technol. B, Nov/Dec (2005).

6106A-39, Session 10

Application of UV transparent polymer ablated by F2 laser to a lab-on-a-chip

K. Obata, The Institute of Physical and Chemical Research (Japan); Y. Hanada, Tokyo Univ. of Science (Japan) and The Institute of Physical and Chemical Research (Japan); K. Sugioka, The Institute of Physical and Chemical Research (Japan) and Tokyo Univ. of Science (Japan); K. Midorikawa, The Institute of Physical and Chemical Research (Japan)

The UV transparent polymer is a promising material in fields of not only optoelectronics but also biophotonics, since such devices sometimes request transmission of UV light. The commercially available CYTOP (Asahi glass Co. Ltd.) is the fluoropolymer, which has excellent properties of high-transmission in the wavelength range from 200nm to 2nm, high-electrical insulation, and high-chemical stability. Therefore, the CYTOP would be a good candidate for a substrates of integrated optoelectronic and biophotonic devices. For fabrication of such devices, development of precise and simple microfabrication process is essential. However, conventional plasma etching process requires specially designed resist for micropatterning of the CYTOP due to its high-chemical stability. Laser ablation is an alternative way since it presents maskless patterning, high-flexibility, high-spatial resolution, and high-processing speed. However, ArF excimer laser of 193 nm wavelength can not perform high-quality ablation due to little absorption. In addition, we confirmed that femtosecond laser of 180 fs pulse width also can not perform high-quality ablation. In this study, F2 laser of 157nm wavelength is used for high-quality ablation of CYTOP. Then, the developed technique is applied to fabrication of bio-chips, in which UV light can be used for analysis.

In this experiment, CYTOP sheet was used as the sample and ablated by F2 laser of 157nm wavelength and 20ns pulse width in the chamber filled with dry nitrogen gas. In this case, F2 laser beam were shaped to a rectangular using a stencil mask and then projected to the sample surface. High-quality ablation with little debris deposition surrounding the ablation area and without deterioration of transmission characteristics was performed. The ablation rate linearly increases with the logarithm of the F2 laser fluence up to 1 J/cm2. It reveals that the ablation of CYTOP using F2 laser takes place by single-photon absorption. Additionally, the F2 laser ablation at 165 mJ/cm2 achieves to form the open channel with linewidth of 70 nm on the CYTOP surface. Thus, it reveals that the ablation of CYTOP using F2 laser can be expected as a high-quality etching technique for fabrication of the microchips.

6106A-40, Session 10

Femtosecond laser lithography and applications

B. N. Chichkov, Laser Zentrum Hannover e.V. (Germany)

I will report on the recent progress in the development of femtosecond laser lithography. Special attention will be given to two-photon polymerization technique. Applications in photonics and bio-medicine will be addressed.

6106A-41, Session 10

Optical driven nano robots for micro biology

K. Ikuta, Nagoya Univ. (Japan)

We have been proposing and developing unique nano manipulator fabricated by our original high speed two-photon nano stereolithography with high speed scanning. No micro motor is needed to drive it, because laser trapping technique is utilized for real-time remote control by human or computer. Unlike conventional nano manipulators in research phase, our manipulator can work in the liquid. This feature is indispensable for most of biotechnology and cell biology. Several type of nano manipulators with multi degrees of freedom motion have been developed and basic performances were verified experimentally.

1. Optical driven nanomanipulator with three degrees of freedom

Fig.1 shows a newly developed nanomanipulator with three degrees of freedom. This mechanism has an arm, a wrist and a gripper connected by rotating hinges and moving slider. To actuate three nano parts, Yag and Ar laser beam traps three trapping points shown as bright points in Fig.1. The length of the nanomamipulator is about 10 micron m. Fig.2 is a nano cell-mover to handle a living cell in buffer solution. The cell-mover successfully grasp a yeast cell and pushing it to the wall to measure mechanical property of the cells.

2.Master-slave (remote) control system for optical driven nano manipulator

Fig.3 shows master control device for three degrees of freedom motion of the nanomanipulator. One hand operation is possible and 100mm linear motion of the master controller corresponds 10micron m. Maximum response speed reaches 12Hz.

3. Merits of optical driven micro/nano robotic sysytems

The main advantages of the optically driven manipulators are as follows: remote drive in an aqueous solution, force control on the order of femto-Newton to pico-Newton, and elimination of the need to use ultrahigh precision 3D stages to move the probe tips. In addition, the flexible, rapid fabrication using the two-photon microstereolithography technique enables tailor-made nanotools for versatile applications.

6106A-42, Poster Session

In situ crystal growth during explosive crystallization

M. S. Rogers, Univ. of California/Berkeley

Explosive crystallization is a macroscopic kinetic phenomenon involving the self-sustaining transformation of an amorphous phase to a crystalline phase driven by the difference in enthalpy and melting temperature between the two phases. In situ images of the explosive crystallization grain growth have been captured for the first time. These dark field images reveal the crystallization front shape and speed of propagation. The experiments were carried out on a 1.2 micron germanium sample sputtered on a quartz substrate. Images were captured using a 12 bit CCD camera and a double cavity ND:YAG 532nm laser for illumination. Crystallization initiation was accomplished from a line focused 355nm ND:YAG. The calculated speed of propagation agrees well with established work in the literature.

6106A-43, Poster Session

Nitrogen-doped TiO2 thin films grown on various substrates

T. Sakano, T. Okato, M. Obara, Keio Univ. (Japan)

TiO_2 is the mostly commercially used photocatalytic material which has indirect bandgap of 3.0~3.2 eV depending on crystal phases. Rutile and anatase are the most well-known crystal phases of TiO_2 and their bandgap are 3.0 and 3.2, respectively. Rutile has lower bandgap, however, anatase shows higher photocatalytic efficiency. Therefore, considerable efforts have been paid to enhance the optical absorption of anatase which has rather large bandgap. Repeatedly taken techniques are introduction of defect levels between the bandgap. For instance, cationic- (Fe^{2+}, Zn^{2+} or Nd^{3+}) or anionic- (N^{2-}, Sb^{2-}) impurity or oxygen vacancy (VO) levels are created, and their enhanced efficiency are reported. Mixing of rutile and anatase phase is also an interesting approach. Among them, N-doping lately attracts attentions, since it was found that the N causes bandgap narrowing of anatase through O2p and N2p orbital mixing. More recently, however, the bandgap narrowing is considered rather difficult due to the difficulty of unstable monatomic N doping into O site, which results in controversial reports, where bandgap narrowing is doubted. N-doping into rutile is even more complicated, because the bandgap broadening are observed instead, nonetheless, rutile and anatase mixtured phase clearly shows bandgap narrowing.

The aim of this research is to demonstrate the effect of N-doping in various phases, where N-doped states, bandgap shift, and photocatalytic efficiency are determined. The N-doped thin films were grown by pulsed-laser deposition technique from home-made TiON targets. The crystal structures were analyzed using x-ray diffraction and Raman spectroscopy. The crystalline phases of TiO_2 were artificially controlled by choosing appropriate substrates, respectively. The anatase and rutile were epitaxially grown on (100) $LaAlO_3$ and (0001) sapphire substrates. Rutile-anatase mixtured phase were grown on soda lime glass substrates. Here, we should note that N-concentration quite strongly depends on the growth temperature, so that we have kept the growth temperature at 300 ∫C to discuss fairly. Chemical bonding states of N within the matrix were investigated by x-ray photoelectron spectroscopy. The optical absorption and bandgap were measured using UV-VIS spectrometer. Then, the photocatalytic activity of the films was evaluted by measuring the decompositon rate of methylene blue solution with the UV and visible light illumination.

6106A-45, Poster Session

Growth of ZnO thin films with ZnO low-temperature buffer layer for blue LED

T. Osada, T. Okato, M. Obara, Keio Univ. (Japan)

Zinc oxide (ZnO) is a wide bandgap (3.37 eV) transparent semiconductor and intensively studied for many applications. Recently, many studies have been directed toward the demonstration of ZnO blue light-emitting device because of its interesting excitonic properties. However, the technical difficulty of preparation of p-type layer with low resistivity prevents ZnO from its potential applications, since it is naturally an n-type semiconductor due to the native donor defects of O vacancy or interstitial Zn. Therefore, reduction of such defects is crucial as in the case of GaN-LED. Nowadays, many methods, such as the use of lattice matched ZnO or $ScAlMgO_4$ substrates or introduction of buffer layers, are proposed and many researchers are successfully obtained high quality thin film of ZnO by either or both techniques. However, the growth of a high quality ZnO thin film on sapphire substrate, having ~18% lattice mismatch, is of significant interest for commercial applications. Here we explore the growth of ZnO on c-plane sapphire substrates with low-temperature buffer layer, stimulated by the success of GaN epitaxial growth.

There are several reports of ZnO-LTBL, however, the effect of LTBL is still unclear. Also most of the LTBLs are crystallized through thermal treatment inside the chamber at low-pressure. In this study, we crystallized the LTBL in air ambient. ZnO thin layers are first prepared on the substrate by KrF excimer laser ablation of a ZnO sintered target. They are then crystallized through thermal treatment in an electrical furnace (ex-situ annealing). The growth conditions of the ZnO LTBL were experimentally optimized through changing the parameters of growth temperature, thickness, and annealing temperature. Characteristics of ZnO thin films were determined by x-ray diffraction (XRD), field emission scanning electron microscope (FE-SEM), and atomic force microscopy (AFM). The electrical properties of the ZnO thin films were measured by the van der Pauw method. The effects of LTBLs were discussed by comparing ZnO/ZnO-LTBL/sapphire and ZnO/sapphire using transmission electron microscope (TEM). In addition, the comparison between ex-situ and in-situ annealing (crystallization of LTBLs inside the vacuum chamber) are also discussed.

6106A-46, Poster Session

Synthesis and treatment of nano-structured ZnO by laser ablation

T. Okada, K. Kawashima, M. Ueda, Kyushu Univ. (Japan)

Nano-structured ZnO crystals were synthesized by nano-particle assisted pulsed laser deposition. In order to use these crystals as an element of the nano-optics, it is necessary to take individual nano-structured crystal out of the substrate. We have investigate the possibility for it using back side laser ablation of crystals. We also investigated the nano-structuring of the crystals by laser irradiation using near field effect.

6106A-47, Poster Session

Fabrication of ZnO nanoparticles with visible photoluminescence using pulsed lLaser ablation in aqueous media

C. He, T. Sasaki, Y. Shimizu, N. Koshizaki, National Institute of Advanced Industrial Science and Technology (Japan)

The pulsed laser ablation of a zinc target in aqueous solutions has been used to produce ZnO nanoparticles with controlled surface chemistry. The phase structure and particles size were characterized by XRD, SEM and TEM. Surface chemistry effects on photoluminescence of ZnO nanoparticles were also investigated. The ZnO particles produced in KCl or NaCl solution aggregated strongly and these faster agglomerations are consistent with the measured decrease of surface charge of the particles leading to a reduction of the electrostatic repulsion between the

nanoparticles. However, the stable suspensions consisting of well-dispersed ZnO nanocrystals with small sizes were obtained by ablation Zn target under the acidic or basic condition. The coalescence of the particles can be effectively limited in the acidic or basic media due to the electrostatic repulsion, and led to a significant reduction of their size. An effective size control was achieved in the acidic or basic media (18 nm for HCl, pH 5.36; 20 nm for NaOH, pH 11.98) with a considerable improvement compared to particles prepared in deionized water (23 nm), under identical ablation conditions. As the pH value decreased or increased than the crucial point (pH 9.5), the intensity of the visible emission of the nanoparticles increased while that of the exciton emission decreased. The increase of the green light emission intensity as the particle size decreases suggests that there is a greater fraction of oxygen vacancies in the ZnO due to higher surface area to volume ratio for smaller nanoparticles.

This study was partially supported by Industrial Technology Research Grant Program '04 from New Energy and Industrial Technology Development Organization (NEDO) of Japan.

6106A-48, Poster Session

Nucleation and growth of single-wall carbon nanotubes in the laser ablation products

A. Gorbunoff, Hochschule für Technik und Wirtschaft Dresden (Germany); O. Jost, Technische Univ. Dresden (Germany)

The talk presents a survey of the physical and chemical processes which lead to the formation of bundles of single wall carbon nanotubes (SWNTs) through the laser ablation of metal-containing graphite pellets in the atmospheric pressure gases. This is the only known technique today which enables to precisely controlling the two basic stages of the process - the nucleation and the growth of SWNTs, and consequently the quality (the length and the diameter scattering) of the final product. It is demonstrated that SWNTs form in a multistep non-equilibrium physico-chemical phase transformation process which is discussed in the frames of the proposed solid-liquid-solid mechanism. Both the nucleation and the growth of SWNTs are mediated by carbide forming metal nanoparticles after the relaxation of the ablation products to ambient pressure and temperature. The peculiarity of the process consists in the excess free energy of the nanoparticles, which forces them to melt and to catalyze the liquid state graphitization of amorphous carbon flakes at surprisingly low temperatures. The unusual tubular form of the transformed carbon subunits in bundles of SWNTs appears to be a result of the interaction of forming graphitic network with the supersaturated surface layer of the catalyst nanoparticle. The importance of trivalent catalyst impurities for the promotion of the SWNT growth is underlined.

6106A-49, Poster Session

Active control of the ablation plume for laser ablation atomic fluorescence spectroscopy

D. Nakamura, T. Takao, Y. Oki, M. Maeda, Kyushu Univ. (Japan)

We have developed an extreme sensitive trace element detection technique that has been called Laser ablation atomic fluorescence (LAAF) spectroscopy. This technique consists of laser-induced fluorescence (LIF) spectroscopy combined with a pulsed-laser ablation. The LAAF spectroscopy was applied to a nanometer-scale solid surface analysis. The absolute weight of the detection limit of 870 ag (10^-18g) and high depth resolution of 3.6 nm had been demonstrated in trace sodium detection of polymethylmethacrylate. In the LAAF analysis, the behavior of the ablation plume is a very important factor for high sensitivity. When the ablated atoms are kept a certain position for a long time, an effective large LIF signal can be attained due to a long LIF duration time. In this time, we tried to control the plume by an ambient gas and an assist mask for more sensitive analysis. To investigate the behavior of the plume, two dimensional LIF imaging spectroscopy was applied. Time-resolved images of the ablation plume could be observed by a gated ICCD camera. The diffusion speed of the ablated particles was modified in collision with the gas molecules. Furthermore, it was found that the form of the plume was changed by the mask. Thus, improvement of the detection sensitivity of the LAAF was expected using this approach.

6106A-50, Poster Session

A study of angular dependence in the ablation rate of polymers by nanosecond pulses

J. E. Pedder, A. S. Holmes, Imperial College London (United Kingdom)

Measurements of ablation rate have traditionally been carried out only at normal incidence. However, in real-world applications ablation is often carried out at oblique angles, and it is useful to have prior knowledge of the ablation rate in this case. Detailed information about the angular dependence is also important for the development of ablation simulation tools, and can provide additional insight into the ablation mechanism. Previously we have reported on the angular dependence of direct-write ablation at 266 nm wavelength in solgel and polymer materials [1]. In this paper we present a systematic study of angular dependence for excimer laser ablation of several polymer materials of interest for microfabrication, including polycarbonate, SU-8 photoresist and polyimide. The results are correlated with the predictions of known ablation models, modified for non-normal incidence with the aid of independent refractive index measurements.

REFERENCE

[1] George D.S., Onischenko A., Holmes A.S., "On the angular dependence of focussed laser ablation by nanosecond pulses in solgel and polymer materials", Applied Physics Letters, vol. 84, no. 10, 2004, pp. 1680-1682.

6106A-51, Poster Session

Lateral melt expulsion and debris formation during small-scale femtosecond laser ablation

S. I. Kudryashov, Arkansas State Univ.

Strongly-oriented lateral expulsion of molten material and re-deposition of ablative debris around resulting craters have been observed during small-scale femtosecond laser ablation of both crystalline silicon and dielectric films. The orientations of melt expulsion and debris deposition correlated with minor axis of the fs-laser spot onto the target surfaces and with orientation of transient plasma/vapour plumes above the surfaces. Characteristic parameters of expulsion/debris re-deposition processes and the underlying fundamental hydrodynamic mechanisms are discussed in terms of potential shortcomings of small-scale fs-laser ablative micro-structuring.

6106A-52, Poster Session

Mechanisms study of laser-induced plasma-assisted ablation (LIPAA)

Y. Hanada, K. Sugioka, K. Obata, K. Midorikawa, The Institute of Physical and Chemical Research (Japan)

Laser-induced plasma-assisted ablation (LIPAA) developed by our group is known for microfabrication of glass materials. In this process, the glass substrate must be transparent to the wavelength of the laser beam, so that the laser beam irradiates the metal target placed behind the substrate. For a laser fluence above the ablation threshold for the target and below the damage threshold for the substrate, the plasma generated from the target surface propagates forwards to the rear side of the substrate at high speed. Then, the absorption site of the laser beam is generated at the rear surface of the substrate by the plasma attack, resulting in high-quality ablation by the incident laser beam. This process can be proceeded by a single pulse irradiation of an adequate ns pulse width laser with an adequate distance between the target and the substrate. However, mechanisms of this process are still unknown. In this paper, double-

pulse irradiation of femtosecond laser is performed to investigate the time-dependent influence of the laser-induced plasma. Then, the transient absorption of the laser beam by the rear surface of the glass substrate where the plasma attacks is measured. To determine the origin of the transient absorption, electron excitation and recombination process induced by the plasma attack is examined by measuring the transient polarization change when the external high electric field is applied to the substrate. A possible mechanism is discussed based on the results obtained. Additionally, some of the new applications of LIPAA are also demonstrated.

6106A-53, Poster Session

Surface micro-fabrication of silica glass by DPSS-UV laser irradiation

H. Niino, Y. Kawaguchi, T. Sato, A. Narazaki, T. Gumpenberger, R. Kurosaki, National Institute of Advanced Industrial Science and Technology (Japan)

Silica glass is an important material in optics and optoelectronic devises because of its outstanding properties, such as transparence in a wide wavelength range, strong damage resistance for laser irradiation, and high chemical stability. In order to develop simpler processes of micro-fabricating silica glass using a pulsed laser, we have investigated a one-step method to microfabricate a silica glass plate using laser-induced backside wet etching (LIBWE) upon irradiation with ns-pulsed UV lasers. A laser irradiation system based on Galvanometer-based point scanning and single-mode laser beam from a diode-pumped solid state (DPSS) laser at 266 nm was employed for the fabrication. We have succeeded in a fine micro-fabrication of silica glass surface. The point scanning on a high repetition rate is suitable for flexible rapid prototyping.

6106A-54, Poster Session

Increase of stability geometrical parameters of microholes

M. V. Volkov, St. Petersburg Institute of Fine Mechanics and Optics (Russia); V. A. Serebryakov, A. A. Timofeev, S.I. Vavilov State Optical Institute (Russia); X. Zhang, Beijing Aeronautical Manufacturing Technology Research Institute (China)

The report focused on experiments directed on reduction of diameter entrance funnel, and increases cylinder-like of microholes. In experiments was used YAG:Nd laser working in a pulse train mode.

Very important parameter in laser drilling microholes with diameter 100-150 microns and aspect ratio more than 30 is the geometrical form of microholes - minimal entrance funnel on a surface and high cylinder-like. The entrance funnel is formed as a result of interaction of “wings” laser irradiation, and also ablation products with a surface. To minimize influence of “wings” is possible by means of transfer the image on a sample.

In experiments was determined influence on geometry microholes of such parameters at drilling as:

Blow gas from nozzle;

Direct focusing laser beam with distribution TEM00;

Transfer of image TEM00 on a sample;

Change of intensity pulse train.

Comparison was carried out with direct focusing laser irradiation with TEM10, and with transfer of image TEM10 on a sample. In all cases a focal plane or a plane of the image moved in depth of sample on various distances.

Optimum variants of an insertion of apertures have been determined.

6106A-55, Poster Session

Finishing of non-metallic materials including real-time laser ellipsometry monitoring

Y. D. Filatov, V. I. Sidorko, National Academy of Sciences of Ukraine (Ukraine); A. Y. Filatov, National Taras Shevchenko Univ. of Kyiv (Ukraine)

The quality of the surfaces of nonmetallic materials is estimated by roughness and reflection by different optical methods: profilometry, reflactometry, interferometry, optical and atomic force microscopy. The ellipsometry method of research was used because another methods can not give us a possibility of measurement directly in surfaces processing. The aim of the work was theoretical and experimental research on transformation of the surface layer of nonmetallic materials when mechanical processing and real time monitoring of influence of processed surface quality on ellipsometric and optical constants of the processed material. For conducting researches the samples from transparent dielectric (optical glass, silica, etc.) with diameter of 60 mm were used. Before polishing the samples were thin and super-thin ground by tools based on diamond powders with grit size of 40/28, 20/14, 10/7, 7/5. The polishing tools based on CeO2 powders were used. The processing was conducted on optical grinding-polishing machine.

Ellipsometrical parameters of polarized light reflected by the polished surfaces were determined with help of ellipsometer at constant value of angle of incidence of laser beam (on the wave length 632,8 nm), that was 70 degrees.

Detailed study of process of roughness formation on surfaces of samples from optical glass was made with help of grinding -polishing device installed on ellipsometer. Such modernization of the ellipsometer allowed in-situ ellipsometric researches on surface layer of nonmetallic materials in case of their finishing. The glass sample was rigidly fixed relatively ellipsometer table. The sample surface that reflects polarized beam was preliminary polished with help of AQUAPOL polishing tool by conventional technology. The back surface of the sample was processed by lapping procedure with help of polishing tool based on CeO2. Continuous observation of optical characteristics of the surface makes it possible to real time monitoring of quality of sample.

6106A-57, Poster Session

Inspection of defects and metallic contamination in SiGe:B CMOS using an in-line photoluminescence monitor

C. Liao, United Microelectronics Corp. (Taiwan); A. Buczkowski, Accent Optical Technologies; C. C. Chien, K. T. Huang, United Microelectronics Corp. (Taiwan); Z. Li, T. Walker, S. G. Hummel, Accent Optical Technologies

Selective area epitaxial (SAE) growth of strained SiGe:B (Boron) in the recessed source/drain (S/D) region of an MOS device is known to improve Si-PMOS performance due to enhancement of hole mobility and reduction of S/D resistance. However, the process may be adversely affected by pattern loading effects, SiGe relaxation, dislocation formation, dopant precipitation and contamination. These effects, if not controlled, will deteriorate device performance and yield. A nondestructive, in-line SAE process monitoring approach on patterned wafers is especially desired. A specialized, contact-less, carrier lifetime-based Room Temperature - Photoluminescence (RT-PL) method meets this demand. The RT-PL tool, which uses a novel excitation path design to achieve carrier confinement, device-suitable probing depth, submicron scanning resolution and a micron probe size, offers a quick, non-destructive assessment of strain, defects and contamination for SAE.

In this paper, a systematic evaluation of SiGe:B layers is illustrated using layers with a Ge content of 15-25% and B doping level of undoped-2E20 cm-3, which is not only on monitor (blanket) wafers but also on CMOS SAE pattern wafers. For the as-grown conditions, we observed that SiGe remains in an unrelaxed state without extended dislocations being formed. These results suggest that SiGe composition could be further modified to optimize the associated mobility enhancement. Uniformity variations associated with SiGe composition and B-doping were identified. Excessive boron precipitation, metallic particle-originated defects and large contamination regions induced by processing tools were also exposed.

The multiple and unique insights enabled through the RT-PL technique provide significant benefits towards decreasing process development and integration time, maintaining SiGe process in control and reducing device fabrication costs.

6106A-58, Poster Session

High Repetition Rate Excimer Laser

H. Esser, Lambda Physik (Germany); H. Schillinger, TuiLaser AG (Germany)

For many years, excimer lasers have been well established in industry as reliable UV light sources. For each application, the beam characteristics have to fulfil different requirements and demands, in terms of technology and cost efficiency. One of the biggest advantages of the excimer laser is that it generates light at DUV-wavelengths at high repetition rates. Many applications benefit from these characteristics.

The trend toward smaller feature sizes in microlithography requires both a shift to shorter writing wavelengths, as well as the use of special techniques for photomask manufacture. These so-called Resolution Enhancement Techniques (RET) utilize more sophisticated mask making methods, thus increasing mask manufacturing costs. Furthermore, more advanced metrology methodologies must also be employed in order to inspect RET based masks, and this inspection much often be performed at the wavelength of use (193 nm) in order to accurately identify potential errors. Excimer lasers with high repetition rates and excellent beam characteristics are used for the detection and classification of mask defects in order to maximize yields during wafer fabrication.

Excimer lasers are also used with spatial light modulators (SLM) to generate photomask patterns directly. This approach presents a way to manage the decreasing feature sizes at low operating cost compared to conventional e-beam photomask writing technology. This technique also requires an excimer laser that delivers the high repetition rates necessary to sustain adequate process throughput and extremely well stabilized energy output for writing accuracy.

This paper reviews the performance and technology of high repetition rate excimer lasers specifically for use in photomask inspection and optical mask writing.

Conference 6106B: Synthesis and Photonics of Nanoscale Materials IV

Monday-Thursday 16-26 January 2006

Proceedings of SPIE Vol. 6106B

6106B-59, Session 12

Design, fabrication, and characterization of nanometer-scale ridged aperture optical antenna

X. Xu, E. X. Jin, S. M. Uppuluri, L. Wang, Purdue Univ.

We investigate light concentration and enhancement in nanometer-scale ridged aperture antennas. Resent numerical simulations have shown that nanoscale ridged apertures can concentrate light into nanometer domain. Most importantly, these ridge apertures also provide an optical transmission enhancement of several orders of magnitude compared to regularly shaped nanoscale apertures. We employ the finitedifference time-domain (FDTD) method to optimize the design of these apertures and fabricate them in thin metal films. A home-built near field scanning optical microscope (NSOM) is used to map the near field intensity distribution of the light transmitted through these apertures. It is shown that the ridged apertures can produce a concentrated light spot far beyond the diffraction limit, with transmission enhancement orders ofmagnitude higher than regularly shaped apertures. Potential applications of these nanoscale ridged aperture antennas will be discussed.

6106B-60, Session 12

Extremely high efficiency carrier multiplication in semiconductor nanocrystals

R. D. Schaller, J. M. Pietryga, M. A. Petruska, V. I. Klimov, Los Alamos National Lab.

We have observed that absorption of a single photon by a semiconductor nanocrystal can produce multiple excitons with extremely high efficiencies (up to 100%) depending upon the energy of the photon [Phys. Rev. Lett. 2004, 92, 186601]. Generation of multiexcitons from a single photon also begins to occur once the process is energetically possible in semiconductor nanocrystals. This is in contrast with bulk materials, which undergo this process (generically termed "carrier multiplication" or "impact ionization") with low efficiency and only for significantly higher photon energies relative to the semiconductor band gap. Using transient absorption, we directly monitor multiexciton generation as a function of absorbed photon energy and observe that multiexcitons are produced on an ultrafast timescale following the photon absorption event. This effect of efficient exciton multiplication can affect many semiconductor nanocrystal-based technologies (optical amplification, quantum computing, optical nonlinearity) and is particularly attractive as a means of increasing solar cell power conversion efficiency via an increase in photocurrent for photon absorption at the blue end of the solar spectrum and has been cited as a possible operation mechanism for low-cost, high-efficiency Generation III solar cells.

6106B-61, Session 12

Selective area immobilization of Avidin on (001) GaAs surface

X. Ding, K. Moumanis, J. J. Dubowski, Univ. de Sherbrooke (Canada)

To immobilize bio-moieties is the critical issue in the development of biodetector devices based on the optical/electronic properties of III-V semiconductors. Herein we demonstrate the successful immobilization of avidin, a robust and well-studied protein, on (001) GaAs surface. The immobilization was carried out via specific binding to biotin, which was connected to the GaAs surface through amino terminated alkanethiols.

6106B-62, Session 12

Preparation of indium tin oxide nanoparticles using laser-induced fragmentation of the particles dispersed in water and their optical properties

T. Sasaki, H. Usui, Y. Shimizu, N. Koshizaki, National Institute of Advanced Industrial Science and Technology (Japan)

Indium tin oxide (ITO) is well known as a transparent conductor. The ITO particles can also be applied for the coating material of ultraviolet and infrared light shielding. The smaller particles size can depress the scattering and increase the transmittance in visible light. In this study, ITO particles were irradiated by pulsed laser beam in water to fabricate much smaller ITO particles, and the particle size and the transmittance spectrum of the irradiated particles were investigated.

ITO particles (Sn:In=1:9, average size: 30 nm) dispersed in a deionized water of 40 dm3 were irradiated by the nanosecond pulse Nd:YAG laser (355 nm). The laser beam was focused in the solution by optical quartz lens (focal distance df = 50 mm). The laser energy was changed from 20 to 150 mJ/pulse. The structures of the obtained nanoparticles were examined by TEM, SEM and XRD. The optical transmittances of the suspensions after laser irradiation and of the nanoparticles deposited on glass substrates were recorded.

The average size of the fragmented particles was decreased with increasing the laser energy. The fragmented particles showed the high transmittance in the visible light region and the lower transmittance in the ultraviolet and infrared light region. The optical band gap of the fragmented particles was increased with decreasing the average particle size. This result is possibly caused by Burstein-Moss effect due to the increasing concentration of the carrier which was generated by the surface defects of the oxygen vacancies.

This study was partially supported by Industrial Technology Research Grant Program '04 from New Energy and Industrial Technology Development Organization (NEDO) of Japan.

6106B-63, Session 12

Second harmonic generation from centrosymmetric arrays of metal nanoparticles

M. D. McMahon, R. Lopez, L. C. Feldman, R. F. Haglund, Jr., Vanderbilt Univ.

It is generally taken for granted that symmetry considerations forbid the generation of even-order harmonics in centrosymmetric nanoparticle systems. Even if noncentrosymmetric particles are arranged so that the overall array has inversion symmetry with respect to the illuminating beam, SHG is completely suppressed along the beam direction. Autocorrelation measurements in metal-island films and lithographically prepared arrays have demonstrated symmetry-induced quenching of the "real-surface" contribution to SHG, in contrast to volume or "bulk" effects originating within the optical skin depth of the nanoparticle. Even the volume component, however, vanishes in the transmission direction for light normally incident on a nanostructured sample that is spatially centrosymmetric on average. However, a Bragg diffraction grating can spatially isolate nanoparticle-generated second-harmonic light from both the fundamental beam and second-harmonic contributions from the interface, facilitating among other things the measurement of small signals.

In this paper, we describe recent experiments that take advantage of this grating effect to demonstrate that SHG is a viable tool for studying elec-

tron dynamics and nanoparticle interactions even in centrosymmetric nanoparticles. We have detected particle-plasmon-enhanced, Bragg-diffracted (and thus coherent) SHG from lithographically-prepared Au nanorods aligned in a symmetric grating geometry, even when optically excited at normal incidence with light polarized perpendicular to a symmetry axis of the grating and nanorods. Due to symmetry considerations, the trend in the diffracted amplitudes is just reversed from that of a typical diffraction pattern: that is, there is virtually no zero-order peak, and the SHG intensity increases with diffracted order for a single array and with increasing angle of observation from the normal. The SHG depends strongly on resonant enhancement, accessed here by tuning the particle plasmon mode to the frequency of the excitation laser. We will describe a variety of experiments testing the effects of resonant vs non-resonant excitation, nanoparticle shape and array structure.

6106B-64, Session 13

Tailored femtosecond pulses for nanoscale laser processing

L. Englert, L. Haag, C. Sarpe-Tudoran, M. Wollenhaupt, T. Baumert, Univ. Kassel (Germany)

We present a systematic study regarding ablation in dielectrics with tailored femtosecond pulses. To that end we focus single pulses selected from a Titanium:Sapphire amplifier through a microscope objective (NA 0.5; working distance 7 mm). The sample (fused silica) is mounted on a 3D piezo translation stage that also serves for characterization of the pulses in the focal region. We measure pulses of 40 fs duration in a beam diameter of 1.4 μm. The mikro- and nanomachining platform is additionally equipped with a spectrometer coupled to an intensified and gated camera for plasma luminescence detection. Tailoring of the pulses is accomplished via phase shaping using a spatial light modulator in a 4-f set-up. So far we investigated unmodulated pulses, quadratic phase masks, cubic phase masks, sine masks (leading to pulse trains) and double pulses with different intensities of the two pulses. For each pulse z-scans at various pulse energies are measured. The obtained structures are analyzed with the help of a scanning electron microscope. In certain parameter ranges we obtain reproducible lateral substructures that are an order of magnitude below the diffraction limit. By timing the double pulse sequence these substructures can be switched on and off.

6106B-65, Session 13

Synthesis of novel colloidal nanomaterials by femtosecond laser ablation in liquids

A. V. Kabashin, M. Meunier, S. Besner, P. Boyer, École Polytechnique de Montréal (Canada)

We report progress in the development of femtosecond laser ablation-based method for nanofabrication in liquid environment. The method uses femtosecond radiation to ablate a solid target in aqueous or organics solutions, yielding to a production of colloidal nanoparticles. In this case, the properties of nanoparticles produced (size distribution, surface chemistry, stability to agglomeration) can be controlled by both varying physical conditions of ablation (laser fluence, geometry of radiation focusing) and using chemically active agents. This approach was originally used to produce colloidal gold nanoparticles with variable mean size (down to 2-3 nm) and extremely low dispersion. We report our results on the synthesis of a variety of novel nanomaterials, including semiconductor-based quantum dots and magnetic nanostructures. We also show that in many the method enables to avoid toxicity problems, which promises biosensing and bioimaging applications of nanostructures produced.

6106B-66, Session 13

Production of dichroitic 3D structures by fs laser irradiation in composite glass containing Ag nanoparticles

G. Seifert, A. V. Podlipensky, A. Abdolvand, H. Graener, Martin-Luther Univ. Halle-Wittenberg (Germany)

By using successively fs laser irradiation at different wavelengths, three-dimensional, permanent anisotropic modifications in glass containing spherical Ag nanoparticles were produced. This novel method is able to create dichroism in the visible and near IR part of the spectrum by deformation of nanoparticles to oblong shapes oriented parallel to the laser polarization. Using samples with a vertical gradient of the fill factor of Ag nanoparticles in the glass substrate and an accordingly inhomogeneous broadening of the surface plasmon band, modifications in various depths can be made using different excitation wavelengths. The induced modifications are reversible: heating to 600°C restores the spherical shape of Ag nanoparticles. This technique could be useful for manufacturing of different, 3D, polarization and wavelength selective micro-devices such as polarizers, filters, gratings, display and rewriting optical 3D data storage devices.

6106B-68, Session 13

Ferrocene-based monolayers: self-assembly via rigid bidentate anchor groups

T. Weidner, C. Bruhn, Univ. Kassel (Germany); D. Fenske, Univ. Karlsruhe (Germany); A. Krämer, B. Krohn, Univ. Kassel (Germany); A. Priebe, Univ. Heidelberg (Germany); A. Rothenberger, Univ. Karlsruhe (Germany); D. Rother, U. Siemeling, F. Träger, Univ. Kassel (Germany)

Self-assembled monolayers have found strongly increasing interest in science as well as in technology. Such films can be used, for example, for catalysis, sensors, and molecular switches. Molecules self-assembled on surfaces usually consist of head-groups that bind to the substrate, spacer units that may have different length, and finally functional groups. Due to our interest in redox-active interfaces we have focused on ferrocene as a functional unit.

In earlier work ferrocene has been attached to surfaces via monodentate thiol head groups in combination with aromatic or aliphatic spacer units. In our study the ferrocene moieties are provided with two anchor groups and no spacer units so that ferrocene is pinned down on the surface in a well-defined orientation and distance.

The interface processes were observed by optical second-harmonic generation, infrared spectroscopy, ellipsometry, scanning tunneling microscopy, and X-ray diffraction. The most important results are the following:

Diisocyanoferrocene (1) self-assembles into monolayers by binding to Au surfaces via its two isocyano units in an upright orientation [1]. This view is corroborated by a crystal structure analysis of the Au complex (1)(AuCl)2.

Bis(diphenylphosphanyl)ferrocene (2) plays an important role in catalysis and coordination chemistry, but its binding to Au surfaces has remained unexplored thus far. Our data show that 2 aggregates into stable monomolecular films via its two diphenylphosphanyl groups.

[1] U. Siemeling, D. Rother, C. Bruhn, H. Fink, T. Weidner, F. Träger, A. Rothenberger, D. Fenske, A. Priebe, J. Maurer, R. Winter J. Am. Chem. Soc. 2005, 127, 1102.

6106B-74, Session 13

Sub-wavelength ripple formation on dielectric and metallic materials

J. Gottmann, R. Wagner, RWTH Aachen (Germany)

Subwavelength ripples (spacing</4) are obtained by scanning a tightly focused beam (~1μm) of femtosecond laser radiation (tp=100fs, =800nm & 400nm) over the surface of various materials, e.g. LiF, SiO2, Si, Cu. The ripple pattern extends coherently over many overlapping laser pulses parallel and perpendicular to the polarisation of the laser radiation. Investigated are the dependence of the ripple spacing on the the material and the applied wavelength. New results concerning the evolution of the ripples are presented. Some possible models for the origin of the ripple growth

are discussed and conditions under which these phenomena occur are contained. Potential applications are presented.

Ripples or, in general, laser-induced periodic surface structures (LIPSS) have been observed substantially near the ablation threshold by many authors since the beginning of investigation of laser ablation four decades ago [1]. The great variety of experimental LIPSS was subsumed into theoretical approaches [2, 3, 4]. In the most common type of surface topography, a periodicity of about the wavelength of the laser radiation is observed. This has been attributed to interference between the incident laser radiation and scattered or excited surface waves [5]. In most cases the ripples orientation is found to be perpendicular to the incident polarisation. Smaller and bigger spacing between the ripples occur if the laser radiation has an inclination to the surface normal which is attributed to the downwards and upwards running surface wave on the inclined surface. The dependence =/(1±sin) has been found[2], which just could explain ripple spacings down to =/2. A supplement to the classical theorie or a new one has to be derived.

In opposition to the classical ripple theory[2,3,4], the observed ripple spacing is dependent on the material, giving indication to understand the processes during the subwavelength ripple formation by femtosecond laser radiation.

[1] M. Birnbaum, J. Appl. Phys. 36, 3688 (1965)

[2] Z. Guosheng, P. M. Fauchet, A. E. Siegman, Phys. Rev. B 26 (10) 5366 (1982)

[3] J. E. Sipe, J. F. Young, J. S. Preston, H. M. van Driel, Phys. Rev. B, 27 (2) 1141 (1983)

[4] A. Barborica, I. N. Milhailescu; V. S. Teodorescu, Phys. Rev. B, 49(12), 8385 (1994)

[5] D. C. Emmony, R. P. Howson, L. J. Willis, Appl. Phys Lett. 23(11), 598 (1973)

Fig. 1: Ripples in Al2O3 with changing scanning direction (SEM), =800nm, tp=90fs, f=1kHz, dpulse=20nm.

6106B-70, Session 14

Synthesis of single wall carbon nanotubes and carbon nanohorns by high power laser vaporization

A. A. Puretzky, The Univ. of Tennesse; D. J. Styers-Barnett, C. M. Rouleau, Oak Ridge National Lab.; B. Zhao, Oak Rdige National Lab.; H. Hu, H. Cui, Z. Liu, Oak Ridge National Lab.; I. Ivanov, The Univ. of Tennesse and Oak Ridge National Lab.; P. F. Britt, D. B. Geohegan, Oak Ridge National Lab.

The practical applications of single-wall carbon nanotubes (SWNTs) for multifunctional composites require large quantities of nanomaterials with well-controlled diameters, lengths, and purity. Unlike chemical vapor deposition techniques, laser vaporization (LV) of composite metal-carbon targets produces SWNTs with a narrow range of diameters (typically 1.2-1.4 nm) that are attractive for electronics applications. However typical yields for as-produced LV-SWNTs are only ~ 0.2 g/hr using scientific lasers, and when one considers that roughly 50-70 wt. % of this raw product is SWNTs and that ~ 90% of this material is lost during chemical purification, it is clear that scaling up the laser vaporization production process utilizing high-power, industrial lasers is very appealing. Several different types of lasers are being used worldwide for this purpose.

Our in situ spectroscopic diagnostics studies allowed us to develop a highly efficient method of single wall carbon nanotubes (SWNT) synthesis based on “long” pulse (~ 0.2 ms) laser vaporization with an average power of ~ 16 W. The choice of long laser pulses was found to be essential to limit the graphitic impurities that tend to prevent chemical purification of material to high levels. Since the ablation yield was roughly equal to that employed for ns-pulses per unit energy, the ablation mechanism was thought to involve preheating of the target surface utilizing several overlapping laser pulses.

In this study we present the results of high volume, high yield synthesis of SWNTs based on a high power industrial Nd:YAG laser (600 W average power, 1-500 Hz repetition rate, 0.5-50 ms pulse width) laser vaporization of a composite C/Co/Ni target at elevated temperatures. The high power laser provides a wide range of laser parameters that must be optimized in order to synthesize large amounts (up to 6 g/h) of SWNTs with a relatively high yield (up to 60%). The chemical purifiability of the raw material is an overriding concern in these studies, so nanotube yield must be compromised with chemical purifiability.

The high power laser also allows us to synthesize single wall carbon nanohorns (SWNHs). SWNHs are formed by high-power laser vaporization of pure carbon targets into room temperature and pressure argon, helium, or other rare gases. SWNHs are similar to (SWNTs), except they are shorter, closed structures containing numerous defect sites and different interstitial pore sizes within their flower-shaped aggregates which provide a rich variety of possible preferred adsorption sites for hydrogen storage and proven success in stabilizing small metal nanoparticles against aggregation for use in catalysis, fuel cells, and drug delivery. SWNHs are single-walled carbon structures, can be formed in high yield (up to 95% vs. amorphous carbon) without catalyst.

In this study, single-walled carbon nanohorns (SWNHs) and SWNTs are synthesized using a high-powered (600 W) industrial Nd:YAG laser. Efficiencies for their production into room temperature and elevated temperature background gases are compared, and similarities between the conditions for SWNH synthesis are compared with those of SWNTs. Ex situ transmission electron microscopy, scanning electron microscopy, optical absorption spectroscopy, Raman spectroscopy, thermogravimetric analysis, are compared with in situ diagnostic techniques to correlate the synthesis conditions with the resulting products and gain insight into their formation processes.

Research on Functional Nanomaterials at the Center for Nanophase Materials Sciences is supported by the U. S. Department of Energy, Division of Materials Science, Basic Energy Sciences. The SWNH part of this research is supported by DOE Center of Excellence on Carbon-based Hydrogen Storage Materials.

6106B-71, Session 14

Position-controlled, rapid growth of single-walled carbon nanotubes

D. J. Styers-Barnett, Z. Liu, Oak Ridge National Lab.; A. Puretzky, The Univ. of Tennessee; C. Rouleau, H. Cui, D. B. Geohegan, Oak Ridge National Lab.

‘Fast-heating’ chemical vapor deposition (CVD) is a proven efficient approach for the growth of long individual single walled carbon nanotubes (SWCNTs). However, obtaining insights into the growth mechanism of how fast a carbon nanotube can grow is still of both scientific and technical importance for designing future experiments to achieve better control of the nanotube growth. Further, “fast-heating” CVD in a furnace requires uniform heating of the entire sample. In this paper, we describe a new laser-irradiated CVD technique to synthesize SWCNTs using laser irradiation as a source of heat. A high power industrial Nd:YAG laser (600 W average power, 1-500 Hz repetition rate, 0.5-50ms pulse width) was employed. By adjusting the laser power, repetition rate, pulse width and duration of exposure, the heating time can be precisely controlled. Additionally, using a laser provides localization of the thermal energy, allowing for position controlled growth determined by both laser spot size and substrate catalyst composition. The temperature was measured and controlled using fast, in situ optical pyrometry. By varying the intensity and beam diameter of the laser, it is possible to control the rate of heating as well as the final temperature. During the growth process the heated area temperature remains stable. Temperature profiles of the substrate show controlled heating to CVD temperatures occurring in a few seconds. Scanning electron microscopy (SEM), microRaman scattering spectroscopy, transmission electron microscopy (TEM) and atomic force microscopy (AFM) were used to characterize the nanomaterials produced at different regions within the laser-irradiated zone. Growth rates, yield, and diameter distributions of SWCNTs are estimated for various thermal treatments for different hydrocarbon feedstock gases. These rates vary dramatically depending on catalysts and parameters of the heating profile, indicating laser-CVD technique may provide local control over growth conditions and may pave a way for investigating the growth mechanism of 'fast-heating' carbon nanotubes. Research on Functional Nanomaterials at the Center for Nanophase Materials Sciences is supported by the U. S. Department of Energy, Division of Materials Science, Basic Energy Sciences.

6106B-72, Session 14

Nanoscale vibrational analysis of carbon nanotubes using near-field Raman spectroscopy

T. Yano, Osaka Univ. (Japan); Y. Inouye, S. Kawata, Osaka Univ. (Japan) and The Institute of Physical and Chemical Research (Japan)

When light is incident on a metallic probe tip, an enhanced electric field is generated at the tip apex due to localized surface plasmon polariton excitation. The strong light field can enhance Raman scattering from molecules existing only in the vicinity of the tip. This technique has been applied to nanoscale vibratioanl analysis of single-wall carbon nanotubes (SWCNTs). Individual SWCNT bundles (height: 2~9 nm) were dispersed on glass coverslip and illuminated by frequency-doubled Nd:YVO4 laser (λ: 532 nm). We performed super-resolved near-field Raman imaging of an isolated bundle with spatial resolution of ~40nm by raster-scanning the bundle under a silver-coated AFM cantilever tip. Observation wavenumbers were set to specific vibrational bands, radial breathing mode (RBM) bands at 195 cm^{-1}, 244 cm^{-1} and 278 cm^{-1}. Since diameter (*d* nm) of a SWCNT is inversely proportional to its frequency (ω cm^{-1}) of RBM (i.e. $d= 248/\omega$), the Raman images at 195 cm^{-1}, 244 cm^{-1} and 278 cm^{-1} show spatial distribution of the SWCNTs having diameters of 1.27 nm, 1.02 nm and 0.89 nm, respectively. Considering a resonant Raman condition of the SWCNTs, the chiralities (n, m) the SWCNTs with d = 1.27 nm, 1.02 nm and 0.89 nm were also assigned to (13, 5), (9, 6) and (8, 5), respectively.

6106B-73, Session 14

The effect of tip-enhancement in near-field Raman scattering of C-60

P. Verma, K. Yamada, Y. Inouye, Osaka Univ. (Japan); S. Kawata, Osaka Univ. (Japan) and The Institute of Physical and Chemical Research (Japan)

Optical microscopy has long been a well-established no-destructive technique to characterize and understand the basic properties of materials, including carbon 60 (C-60), which went through enormous research efforts after the discovery of this interesting material. However, the resolution of such analysis is diffraction-limited. The basic idea to overcome this diffraction-limited resolution in Raman scattering leaded to the discovery of tip-enhanced near-field Raman scattering (TERS). The concept of utilizing TERS to investigate C-60 is expected to reveal many new interesting features, and makes it possible to observe molecular dynamics at sub-nano scale. Due to the presence of strong evanescent field in TERS, not only the vibrational modes are enhanced, but also the symmetry and the selection rules are modified leading to a shift in some modes and the observation of some new modes. Here, we present some TERS results from C-60. The sample was prepared by spin-casting C-60 molecules on a cover-slip, which was then investigated by Raman scattering under both, far-field and near-field configurations. A tip with 40 nm apex was prepared by evaporating silver on a commercial silicon AFM cantilever. Under the near-field configuration, the Ag mode around 492 cm-1 and the Hg mode around 1470 cm-1 were strongly enhanced and shifted in the higher frequency direction. In all, 2 Ag and 7 Hg modes were found to be enhanced with different enhancement factors, ranging up to a factor of several tens. Furthermore, the effect of unidirectional pressure was also observed when C-60 molecules were pressurized by the tip.

6106B-78, Session 14

Laser engineering of nanohybrid materials for bioapplications

W. I. Marine, L. Sajti, A. Said, S. Giorgio, V. Khodorkovsky, Univ. de la Méditerranée (France)

The important development in nanobiophotonics is a synthesis of new nanohybrides materials for biological and medical applications with properties fabricated "at the request". Nanohybrid materials formed by assembling of inorganic core (oxide or metallic nanoparticles), with typical dimension 2-30 nm, and organic functional molecule with specific properties. The core nanoparticle can be used as template to collect and to transport functional molecules or it can be used as an efficient absorber of electro-magnetic excitation with following excitation transfer between inorganic nanoclusters and organic molecule.

In spite the fact that physical aspects of laser ablation in liquids are still not well understood, it is clear, now, that this method can be used for nanoparticles synthesis. In this communication we review the basic principles on nanoclusters formation by f-PLA of oxides materials and we present new experimental studies of nanoparticles and nanohybrids formation in different pure or functional molecules containing liquids. We show that femtosecond laser ablation (f-PLA) is an excellent method of synthesis of complex nanohybrid materials in situ. We demonstrate the possibility to manipulate the nanoparticle size, the size distribution, and nanohybrids morphology by varying the conditions of f-PLA. Optimised nanohybrids show very efficient energy transfer between inorganic and organic parts of nanohybrids.

Finally we propose the way of engineering the optical and electronic properties of nanohybrids

6106B-75, Session 15

Angle resolved XPS study of self-assembled monolayers of thiols on GaAs

D. M. Wieliczka, Univ. of Missouri/Kansas City; X. Ding, J. J. Dubowski, Univ. de Sherbrooke (Canada)

Self-assembled monolayers (SAM) of several alkanethiol molecules, with varying chain length and terminal groups, were investigated using angle resolved x-ray photoelectron spectrometer (Kratos AXIS-HS). Carbon, oxygen, gallium, arsenic and sulfur core level spectra were obtained on all surfaces as a function of angle. The impact of atmospheric exposure was examined by storing one set of samples under atmospheric conditions with a second set stored in a nitrogen atmosphere prior to analysis. The intensity of the gallium and arsenic core levels indicated a considerable difference in the Ga/As ratio dependent on the terminal group of the alkanethiol. Additionally, the carbon and oxygen spectra indicate varying chemical bonding on the surface with the alkanethiol's having a carboxylic acid terminal group showing a more complex carbon and oxygen bonding.

6106B-77, Session 15

Using UV light to achieve micrometer sized sterically oriented immobilisation of proteins

S. B. Petersen, Aalborg Univ. (Denmark)

Fundamental knowledge on protein structures and the effect of ultraviolet light on these structures has paved the way for the development of a unique light-based immobilization technology that allows oriented protein immobilization onto micrometer sized spots. The methodology is considered to be a strong alternative to the conventional procedures which often include the use of harsh conditions such as strong chemicals and elevated temperatures. The technology behind this immobilization technique -here termed "light assisted immobilization" - is based on the fact that disulphide bridges that are naturally present within the protein structure can be broken as a result of UV illumination. The free thiol groups (-

SH) created upon disruption of a disulphide bridge are very reactive and can be used as linkers for covalent attachment to a surface. The surface can for example be gold or thiol-derivatized silicon,making this technology extremely useful for a large range of application areas, including biosensors.

We have successfully immobilised a range of enzymes, immunoglobulin and MHC-I onto thiol derivatized flat surfaces, such as quartz, glass and silicium. Enzymes have also been immobilized enzymes directly onto nanometer sized gold particles, both in solution and deposited on surfaces. They retained their biological activity after the immobilisation - even after being stored in dry form for extended periods.

A number of experiments have been done in order to illucidate in more detail the underpinning molecular mechanism. Using our femtosecond laser system equipped with a streak camera, we have obtained pico second resolved detailed fluorescence decay information. A Flash photolysis study has revealed a number of discrete events including the transient formation of solvated electrons as a result of UV illumination.

6106B-76, Poster Session

Research on laser damage of IR detector

Y. Liu, Shandong Institute of Business and Technology (China)

Pointing at the key problems of laser weapon, laser damage of IR dot seeker was researched. Some valuable data and conclusions were gained

First, laser damage of anti-ship missile was analyzed. IR seeker is most destructible than other parts of anti-ship missile. And IR dot seeker was chiefly discussed, including its function and its optics system. IR detector has strong sensitivity to light. IR detector is prone to be attacked by laser. Then the model that ship-borne laser weapon damages infrared detector of anti-ship missile was founded. Emulation calculation of laser damage was completed. Laser power needed was obtained in order to damage IR detector in a distance. Finally,feasibility was analyzed from two aspects. One is whether laser power settles for need, the other is whether IR detector is damaged.

Conference 6107: Laser-Based Micropackaging

Wednesday-Thursday 25-26 January 2006

Proceedings of SPIE Vol. 6107

6107-01, Session 1

A new laser bonding method of anisotropic conductive films in flat panel display and semiconductor packaging applications

G. Nam, K. Ryu, M. Seo, Institute for Adv Engineering (South Korea); N. Kwak, Jet Tech, Ltd. (South Korea)

Anisotropic conductive films(ACFs) consist of conducting particles and adhesive resins and have been widely used for packaging technologies in FPDs(Flat panel displays) such as LCDs(Liquid crystal displays) for last decades. So far various packaging technologies such as TCP(Tape carrier package) on LCD panel, COF(Chip on flex) on LCD panel and COG(Chip on glass) using ACFs have been carried out by using a hot plate as a heat source for cure. But this method is difficult to meet the requirement of fine pitch capability and make the flat panel displays smaller, lighter and thinner because of inhomogeneous thermal distribution of hot plate and thermal expansion of a film.

New ACFs bonding processes by making use of high power diode laser have been proposed and investigated. Laser ACF bonding is worthy of attention, not only because this method is non-contact bonding method to solve the problem of decreasing the reliability of contact due to the difficulty of flatness of hot plate surface when temperature is rising, but also because we can save total process time due to rapid reach by cure temperature.

6107-02, Session 1

Laser joining of glass to silicon using adhesive for MEMS packaging applications

F. Bardin, S. Kloss, A. J. Moore, Heriot-Watt Univ. (United Kingdom); I. De Wolf, IMEC (Belgium); C. Wang, D. P. Hand, Heriot-Watt Univ. (United Kingdom)

Laser-based joining (primarily welding and soldering) techniques have become standard manufacturing tools in many manufacturing processes, mainly due to the ability of the laser to provide a highly-localised, remote heat source. However, there has to date only been limited application of laser-based joining for micro-manufacture. To overcome the drawbacks of the standard wafer-level bonding techniques, i.e. high temperature and/or high electric fields applied to a complete MEMS package, localised heating can be applied using a laser source.

We have demonstrated a technique for joining glass to silicon by using a laser cured intermediate adhesive layer. It is based on localised heating of polymer via absorption of high power laser diode light at the surface of the silicon, with negligible absorption in the glass cover. The polymer we used is easy to process, suitable for non-uniform surfaces and displays minimal outgassing and low moisture. We show that a semi-hermetic cavity can be produced in few seconds at typical laser intensity of 1 W/mm2 resulting in a local temperature of ~ 300C. Tests show that physical properties of the polymer are not significantly affected by the laser heating. Leak and bond strength tests are being carried out and will be presented.

6107-03, Session 1

Laser micro welding of copper and aluminum

I. Mys, M. H. Schmidt, Bayerisches Laserzentrum gGmbH (Germany)

Aluminum combines comparably good thermal and electrical properties with a low price and a low material weight. These properties make aluminium a promising alternative to copper for a large number of electronic applications, especially when manufacturing high volume components. However, a main obstacle for a wide use of this material is the lack of a reliable joining process for the interconnection of copper and aluminum. The reasons for this are a large misalignment in the physical properties and even more a poor metallurgical affinity of both materials that cause high crack sensitivity and the formation of brittle intermetallic phases during fusion welding.

This paper presents investigations on laser micro welding of copper and aluminum with the objective to eliminate brittle intermetallic phases in the welding structure. For this purpose a combination of spot welding, a proper beam offset and a special filler material is applied. The effect of silver, nickel and tin filler materials in the form of thin foils and coatings in a thickness range 3-100 μm has been investigated. The use of silver and tin filler materials yields to a considerable improvement of the static and dynamic mechanical stability of welded joints. The analysis of the weld microstructure shows that already an application of small amounts of suitable filler materials helps to avoid critical, very brittle intermetallic phases on the interface between copper and solidified melt in the welded joints.

6107-04, Session 1

Diode laser welding for packaging of transparent micro-structured polymer chips

T. Klotzbücher, T. Braune, M. Letschert, K. S. Drese, Institut für Mikrotechnik Mainz GmbH (Germany)

Laser transmission welding in recent years has been established as a versatile method for interconnection of thermoplastics, at least for macroscopic parts. The technology also offers interesting possibilities for packaging of transparent, micro-structured polymer chips, as used for life science or biotechnology applications. A method for transmission welding, based on a diode laser bar in combination with a thin layer of IR-absorbing dye, is introduced, that allows for fast, mask-less welding of two thermoplastic substrates, at least one of which contains micro structures. The process strongly depends on the ratio of the IR-absorbing dye layer thickness to the depth of the microstructures and should be <<1. Detailed results of the absorption of the dye layers as a function of the spin coating parameters used for preparation of the films are presented, including depth profile analysis. It is demonstrated that the formation of good quality weld seams mainly depends on the energy per unit length coupled to the substrate, which is adjustable by the feed rate and the laser power applied. As an example the process window for welding CGE chips made of PMMA, containing 50 μm wide and deep channels, separated by 100 μm wide webs is shown. The applicability of the technology to other polymer chip geometries together with concepts for further improvement is demonstrated.

6107-05, Session 1

Laser patterning and multilayer welding of transparent polymers for microfluidic device fabrication

W. Pfleging, O. Baldus, C. Ziebert, Forschungszentrum Karlsruhe (Germany); I. Tahhan, Albert-Ludwigs-Univ. Freiburg (Germany)

CO2-laser-assisted micro-patterning of polymethylmethacrylate (PMMA) or cyclo-olefin copolymer (COC) has a great potential for the rapid manufacturing of polymeric devices including modification, cutting and structuring. Channel widths of about 50μm as well as a large area patterning of reservoir structures or the drilling of vias are established. For this purpose a high quality laser beam is necessary as well as an appropriate beam forming system. In combination with laser transmission welding a fast fabrication of two- and three-dimensional micro-fluidic devices was possible. Welding as well as multilayer welding of transparent polymers was investigated for different polymers such as PMMA, polyvinylidene fluo-

ride (PVDF), COC, and polycarbonate (PC). The laser transmission welding process is performed with a high-power diode laser (wavelength 940nm). An absorption layer of several nanometers in thickness is deposited onto the polymer surfaces. The welding process has been established for the welding of polymeric parts containing micro-channels, if the width of the channels is equal or larger than 100µm. For smaller feature sizes the absorption layer is structured by UV-laser radiation (wavelength 248nm or 355nm) in order to get a highly localized welding seam, e.g., for the limitation of thermal penetration and thermal damaging of functional features such as channels, thin walls or temperature-sensitive substances often contained in micro-fluidic devices. This process strategy was investigated for the welding of capillary blood separation chips, including channel widths smaller than 30µm. Analysis of the thickness of the absorption layer and the topography after laser patterning is carried out with atomic force microscopy in contact mode.

6107-06, Session 1

Laser micro welding of polymer components for dental prothesis

M. Hustedt, A. von Busse, M. Fargas, O. Meier, Laser Zentrum Hannover e.V. (Germany); H. Biflinger, dentacon GmbH (Germany)

In dental prosthesis, miniaturized unit assembly systems are increasingly used in order to enable the optimized adaptation of the prosthesis to the individual anatomic situation. To manufacture and package these miniaturized systems, there is the need to cover the complete device, in the reported case made of polycarbonate, comprising among others springs that apply pressure to fix the prosthesis. The laser is a suitable joining tool for applications in micro technology. Laser transmission welding was therefore investigated for joining the miniaturized components. The carrier was made of PC with carbon black. The cover consisted of transparent PC with thickness of 400 µm along the joining contour. The wall thickness of the joining partners amounted to 400 µm. The investigations presented in this paper cover detailed examinations of the welding process with and without laser mask. It was examined how far the mask geometry determines the formation of the weld seam. For both process variants, the joining geometry and the clamping was optimized. The influence of the main process parameters laser output power, welding speed and focal position was studied. The welding process was qualified especially with regard to joining strength, swelling, process time, reproducibility, accuracy and functionality of the complete assembly system. It turned out that the clamping of the components is crucial for a reliable process. Optimized process conditions enable the micro welding of plastic components for dental products considering the high requirements regarding functionality, biocompatibility, lifetime, and esthetics. Laser transmission micro welding proved to be a suitable method to package the final assembly without any refinishing operation.

6107-07, Session 2

Optimization of laser microsoldering by mathematical modelling of joints kinetic formation

V. P. Veiko, A. A. Allas, Saint-Petersburg State Univ. (Russia)

Optimal soldering modes prognosis by the help of “Solution withing the gap with account of boundary kinetics” model is done. This model describes the condition of mass balance in solid and liquid phases, interphase boundary movement in dependence of mutual solibility at different stages of the process. As a result of kinetics of computer simulation of soldered joints forming, practical investigations of soldering modes influence at the joints strength and analysis of micro section metallographic specimens fulfilled with the aid of electronic microscope, the possibility of three-five fold enhancement of soldered joints strength in comparison with manual soldering. Technological process and automated equipment based on Nd:YAG pulse laser are developed for laser soldering of microelectronic components with planar leads at the printed circuit boards.

The task of formation of adhesive compound having enhanced strength properties can be solved by using of laser soldering and comes to the reduction of time of solid and liquid phases contact at the temperature not exceeding essentially T of solder melting to minimum value, in order to limit the stage of solution saturation. By this it is necessary to provide good moistening of surfaces being soldered and fast solder crystallization. It is required to pay attention to the selection of flux activity, thus providing the concordance of moistening time with soldering time. High fluxing activity together with long soldering time with help the formation of intermetallic compounds, thus increasing the time of contact of solid and liquid phases. Lowered activity of flux hinders from soldering time reduction and increasing of strength properties of soldered joints.

6107-08, Session 2

Numerical prediction of drilling rates for ultra-high intensity nanosecond laser pulses

V. V. Semak, The Electro-Optics Ctr.

The results of numerical simulation of laser drilling of aluminum, copper and steel samples using nanosecond pulses are presented. The drilling rates were predicted for a wide range of laser beam irradiance. The theoretical model utilized for the simulation was upgraded to include phase transition at the critical temperature. In the new theoretical approach the latent heat of evaporation was assumed to be temperature dependent, such that in the range below the critical temperature its value is practically constant, decreases rapidly as the temperature approaches the critical temperature and is zero at the temperatures exceeding the critical temperature. The computed drilling rates for 4 ns laser pulses are in agreement with the experimental data. The upgraded model provides explanation to the observed saturation of drilling rate dependence on laser pulse energy. A new method of determining critical temperatures of metals and metallic alloys is proposed.

6107-09, Session 2

Ultra-deep drilling of solids by high-power nanosecond lasers: theory and experiments

S. Paul, K. Lyon, S. I. Kudryashov, S. D. Allen, Arkansas State Univ.

A new mechanism of threshold-like ultra-deep (up to tens of microns per pulse, sub-mm total hole depths) ablative drilling of optically opaque and transparent materials by high-power nanosecond lasers has been studied experimentally and theoretically. Average crater depth per laser shot and real change in crater depth from shot to shot (including energy deposition depths into bulk) have been measured as a function of laser power density (intensity) in these drilling experiments using, respectively, optical transmission and contact photoacoustic techniques. These techniques were also used to study material removal involving, as shown in this and previous studies, predominantly delayed expulsion of multi-micron materials droplets. According to experimental and theoretical results of this work, the underlying ultra-deep drilling mechanism can be divided in several stages including ultra-deep “non-thermal” energy delivery by a short-wavelength radiation of the surface high-temperature ablative plasma, bulk heating and melting of these materials, accompanied by the following subsurface boiling in the melt pool and resulting melt expulsion off of the target.

6107-10, Session 2

Investigation of CO2 gas breakdown using optical emission spectroscopy

H. Ling, Y. X. Han, Y. Lu, Univ. of Nebraska/Lincoln

CO2 gas dissociation through optical and plasma collision breakdown was investigated by optical emission spectroscopy (OES), using an Andor iStar ICCD. The evolution of the luminous plasma was examined by time-

resolved optical spectra. The emission lines of carbon and oxygen species, such as C(I) and O(I), were observed to understand the process of CO2 dissociation. Excimer Laser and Nd:YAG laser were used to provide energy for the gas breakdown processes. Effects of different gas pressures in the experiments on the plasma evolution were studied. Some emission lines could be obviously distinguished under various gas pressures indicating that the emitting species had different behaviors in the evolution. They were frequently ionized and excited after the laser irradiation.

6107-11, Session 3

Developments in laser processing for silica-based planar lightwave circuits

Y. Nasu, M. Abe, M. Kohtoku, NTT Photonics Labs. (Japan)

Laser processing offers an attractive way of manufacturing both optical devices and biomedical devices including microfluidic channels and biochips. Laser processing is also promising for the trimming and fabrication of silica-based planar lightwave circuits (PLCs). PLCs are key functional components for use in optical telecommunication systems since they offer compactness and high functionality in addition to excellent stability. A laser light that strongly interacts with glass, such as ultraviolet (UV) light or femtosecond pulses, can increase the refractive index of glass. This phenomenon can be used to improve the performance of PLCs as well as to enhance their functionality.

UV laser trimming is useful in that it can be used to change the refractive index of fabricated waveguides and thus compensate for fabrication errors. Manufacturing tolerances are not always sufficient as regards fabrication errors, and such errors have various detrimental effects on PLC performance including deviation from the designed wavelength, polarization dependence and crosstalk degradation in an arrayed waveguide grating. UV laser trimming can greatly improve PLC performance by compensating for these errors.

In addition, laser processing can provide PLCs with new functionalities. For example, a UV laser can be used to produce Bragg gratings, which are employed as band-reflection mirrors used in external cavity lasers in PLCs. Direct waveguide writing is also an attractive way to enhance circuit layout flexibility. Recently, a femtosecond laser was found to be effective for writing 3-dimensional waveguides, and it can also be used to interconnect waveguides flexibly. This enables us to expand PLC geometry from two to three dimensions.

This talk will review both trends in laser processing for PLC fabrication and recent R&D topics.

6107-12, Session 3

Micro-fabrication of advanced photonic devices by means of direct point-by-point femto-second inscription in silica

V. Mezentsev, M. Dubov, A. Martinez, T. P. Allsop, I. Y. Khrushchev, I. Bennion, Y. Lai, D. J. Webb, F. Floreani, Aston Univ. (United Kingdom)

We present recent results on experimental micro-fabrication and numerical modeling of advanced photonic devices by means of direct writing by femtosecond laser. Transverse inscription geometry was routinely used to inscribe and modify photonic devices based on waveguiding structures. Typically, standard commercially available fibers were used as a template with a pre-fabricated waveguide.

Using a direct, point-by-point inscription by infrared femtosecond laser, a range of photonic devices was fabricated including Fiber Bragg Gratings (FBG), Long Period Gratings (LPG). Waveguides with a core of a couple o microns, periodic structures with a period as short as 0.5 micron, and couplers have been also fabricated in planar geometry using the same method. Fine tuning of extremely stable laser setup is required to achieve pinpoint accuracy of the focused femto-second pulses which allows for robust reproducible sub-micron fabrication of virtually arbitrary geometric structures with a distributed variation of refractive index. We describe the characterization of the inscription procedure which requires shorter femtosecond pulses about 100 fs for wider window between the thresholds of inscription and material damage. The described method requires neither phase-masks nor photosensitised fibres and hence offers remarkable technological flexibility. For example, unlike known point-by-point methods of making FBGs and LPGs, very short inscription time of less than 60 s per grating is required. High quality FBGs and LPGs were produced using this method in commercial, non-photosensitised, unhydrogenated fibres. We have also fabricated radially asymmetric and more complicated 3D structures such as spiral, or chiral, gratings. Such structures demonstrate unprecedented sensitivity to directional bending and polarization properties. The prototypes of FBG- and LPG-based vector bending and polarisation sensors have been developed. The femtosecond inscription also allows for more complex hybrid devices such as superimposed non-overlapping fibre Bragg gratings laterally separated by inscription in separate segments of the fibre core.

Thermal properties of the above described structures fabricated with point-by-point femtosecond inscription were examined. For example, response FBGs to thermal annealing at temperatures in the range 500 C to 1050 C was studied. Gratings were thermally stable at temperatures up to 900 C, representing a significant improvement in comparison with the comnventional, UV-inscribed, gratings.

6107-13, Session 3

Use of non-digitized diffractive optical elements for high-throughput and damage-free laser materials processing

J. Amako, E. Fujii, Y. Yamazaki, T. Shimoda, Seiko Epson Corp. (Japan)

An important issue in laser materials processing is how to attain high-throughput and damage-free processes. Using a diffractive beam splitter in the processing increases the throughput substantially. However, using digitized diffractive optical elements can cause higher-order diffraction beams, which fall outside process areas, to irradiate the workpiece and damage it.

To realize damage-free processes it may be highly effective to use non-digitized elements that can afford to fully suppress those higher-order diffractions by containing as much photon energy as possible inside a fan-out of beams meant for the process. We have designed and fabricated non-digitized diffractive beam splitters to appraise their performances. The surface-relief structures of the splitters are optimized using an iterative algorithm and are formed on high-quality fused silica substrates using direct laser-writing and reactive ion-etching. For a 13-beam splitter, a non-digitized element gives a light-use efficiency of 97% with SN=38, whereas a binary counterpart can be as efficient as 78% with SN=5; SN is defined as the ratio between the minimum of the fan-out beams and the maximum of higher-order diffraction beams. Note that non-digitized elements have rather small tolerances for fabrication errors, which have turned out to be on the order of ~10nm.

We have used the two types of elements, continuous and binary, in various laser-processing experiments and verified that the continuous type is far superior to the binary type regarding process yield and process window.

6107-14, Session 3

Fabrication, characterization, and simulation of inverse opal 3D photonic crystals using laser-assisted imprinting

H. Wang, Y. Lu, Z. Y. Yang, Univ. of Nebraska/Lincoln

3-D photonic crystals were fabricated by laser-assisted imprinting of self-assembled silica particles into silicon substrates. The multilayer self-assembly of silica particles were formed on silicon substrate using isothermal heating evaporation approach. A short pulse (pulse duration 23 ns) of

a KrF excimer laser instantaneously melts the silicon substrate surface, which infiltrates and solidifies over the assembled silica particles. By removing silica particles embedded in the silicon using hydrofluoric acid, inverse-opal photonic crystals were produced. This technique is capable of fabricating the complete PBG, which is predicted by theoretical calculations with plan wave method. This might enable us to engineer the position of PBG by flexibly varying the silica particle size. Ellipsometry and spectrophotometer were used to identify specific bandgaps at various crystal directions for both opal and inversed structures. The transmission matrix method is used to simulate the transmission spectra of the structure, which agrees with the experimental results.

6107-15, Session 4

Laser-nanostructure interactions and applications for parallel nanomanufacturing

S. Chen, The Univ. of Texas at Austin

Lasers are becoming important tools for scientific research and industrial applications. In this invited paper, I will discuss laser interactions with nanostructures and associated issues of nanoscale optical enhancement, thermal/fluid transport, and nano-manufacturing.

In laser interactions with a monolayer of silica nanospheres, I will report a Marangoni effect in nanosphere-enhanced laser direct nanopatterning of silicon surface. The monolayer of nanosphere array was formed on the silicon substrate by self-assembly. A 248 nm excimer laser was used to irradiate the sample surface. Due to optical field enhancement between the nanosphere and the substrate, the silicon surface was locally melted. The molten material was redistributed due to surface tension forces, resulting in the formation of a nanodent array. The morphology of the nanodents changed from bowl-type to “Sombrero” with increase of laser intensity as a result of a Marangoni effect that arises due to the competition between a thermocapillary force and a chemicapillary force acting on the molten material.

In laser interaction with metallic nanostructures, we will demonstrate that photolithography can be extended to a sub-wavelength resolution for patterning of virtually any substrate by exciting surface plasmons (SPs) on both a metallic mask and a substrate. A polarized laser beam of 355 nm wavelength was used as light source to photoinitiate an 80nm-thick photoresist on a silicon substrate coated with titanium of 80 nm thick. Array of line apertures of 100 nm in width were made on a gold film or titanium film deposited on a quartz substrate, serving as the mask. Simulation results by Finite-Difference Time-Domain (FDTD) method have shown that surface plasmons excited on both the metallic mask and the Ti shield help to spatially confine the light behind the apertures. Experimental results show a strong dependence of pattern transfer on the polarization of light as well as the energy dosage of the light.

6107-16, Session 4

Excimer laser material processing: state of the art and new approaches in microsystem technology

W. Pfleging, Forschungszentrum Karlsruhe (Germany); M. Przybylski, ATL Lasertechnik GmbH (Germany); H. J. Brückner, Univ. of Applied Sciences (Germany)

In this contribution the current state of the art and new trends in excimer laser material processing are presented. Below the ablation threshold material modification is possible. For this purpose we present the fabrication of optical single-mode waveguides in polymers for the visible optical range and for 1550nm. The obtained structures reveal absorption losses in the order of 1.7dB/cm up to 5dB/cm. Laser exposure using contact masks or direct scanning of planar structures are appropriate methods for the integration of optical waveguides in PMMA sensor devices (Y-branch, interference couplers). Above the ablation threshold excimer laser micromachining is a powerful tool for a rapid manufacturing of complex three-dimensional micro-structures in polymer surfaces with depths between 0.1μm and 1000μm and aspect ratios up to 10. An intelligent mask-technology enables a flexible formation of complex periodical and non-periodical structures. Typical application fields are presented in micro-optics, micro-fluidics and rapid tooling. Micro-Laser-LIGA is established in order to fabricate nebulizer membranes, micro-fluidic devices and integrated single mode waveguides. Furthermore, the fabrication of 3d-shapes in metallic mold inserts is successfully demonstrated. Debris formation is completely suppressed. A low power short pulse excimer laser with high repetition rates up to 500 Hz is compared to a “conventional” high power excimer laser with a repetition rate of about 10-100Hz. These “high-repetition-rate-excimer lasers” with relatively small pulse energies but with much shorter laser pulse duration (< 8 ns) provide a significant improvement of pattern quality. Furthermore, the high repetition rate enables a fast material processing which is discussed in detail for several application fields.

6107-17, Session 4

Thermal damage of silicon wafer in thermal cleaving process with pulsed laser and CW laser

K. Yamada, Hiroshima Univ. (Japan); T. Ueda, A. Hosokawa, Kanazawa Univ. (Japan); Y. Yamane, K. Sekiya, Hiroshima Univ. (Japan)

The laser cleaving method is a cutting process of brittle materials such as glass panel for LCD, semiconducting material substrate. In this dry process, the laser irradiation causes the thermal stress which essentially controls the crack propagation, therefore the work materials are not contaminated but the thermal damage is caused on the irradiated surface and fracture surface of material.

The objective of this paper is the prevention of thermal damages in the laser cleaving process of silicon wafer. The cleaving experiments are conducted with pulsed Nd:YAG laser and cw Nd:YAG laser. In the cleaving with pulsed laser, the temperature required for crack propagation is investigated by measuring with a two-color pyrometer developed. The critical temperature at which the stress intensity factor slightly exceeds the fracture toughness depends on the pulse frequency, the pulse width, the scanning velocity of laser spot and the material properties. The temperature is also confirmed by the thermal stress analysis.

And then, for the cleaving with cw laser, a refrigerating-chuck system is developed to reduce the thermal damage of workpiece. The system refrigerates the working table below the freezing point of water, and the material is fixed on the table by the frozen water between the material and the table. While the silicon oxide is caused on the surface of wafer in the room temperature, the refrigerating-chuck can prevent the thermal damage at all and improve the reliability of the cleaving process. By use of the chuck, the smooth fractured surface is achieved and the linearity of the cleaving trajectory is also improved.

6107-18, Session 4

Laser slotting of inkjet printer chips

B. Richerzhagen, D. Perrottet, A. Spiegel, Synova SA (Switzerland)

Inkjet printers use a series of nozzles to eject drops of ink directly onto the paper. A silicon chip is used as a barrier between the orifice plate, which contains hundreds of nozzles, and the ink reservoir. The barrier is made directly from a silicon wafer, whose thickness varies between 600 and 700 microns. In order to let the ink pass through, the silicon barrier of the print head has to be drilled. Silicon wafer slots can be created by sandblasting. So far, this method has not provided satisfactory results, especially for narrow slots below 150 microns. Sandblasting limits the width of the slots and their density, as the edges tend to be conical; it is also incompatible with clean room conditions. Alternative processes, such as etching and dry laser cutting, are too slow. Etching is also expensive and requires masks. Dry laser slotting creates slag and micro cracks. The water jet guided laser, a hybrid technology which uses a water jet to guide a laser beam, has recently been used to create blind or through slots in

silicon chips with very accurate control of the depth. With this process, variations at the bottom of the slots are kept to a minimum. The water jet guided laser creates long and clean slots, free of any length or depth limitations. Straight walls are also produced with high quality and repeatability. Finally, speed is high due to a very efficient material removal and high laser power of up to 100 Watts.

6107-19, Session 4

Applications of laser patterning to fabricate innovative thin film silicon solar cells

W. Shinohara, M. Shima, S. Taira, M. Matsumoto, K. Uchihashi, A. Terakawa, SANYO Electric Co., Ltd. (Japan)

A Laser patterning is a key technique to realize integrate-type solar cells. In order to fabricate integrated-type solar sells, metal electrodes, semiconductor layers and Transparent Conductive Oxide (TCO) should be separated by laser irradiation. In case of separation of semiconductor layers mainly consists of hydrogenated amorphous silicon (a-Si: H), crystallization of a-Si: H often takes place around removed portions by laser irradiation. And a crystallized portions of a-Si: H behaves as a leak pass of photo-current. Because crystallized portions have low electrical resistance compared with original a-Si: H. On the other hand, in case of removal of TCO formed on a-Si: H layers, penetrated laser energy through TCO causes crystallization of underling a-Si: H easily.

In this work, a layer removal technique of stacked-type thin film silicon solar cells using Nd: YAG laser and KrF Excimer laser is investigated. In order to remove a-Si: H layers, Second-Harmonic Generation (SHG) of Nd: YAG laser is used. It is found that the removal of a-Si: H is occurred by a pressure of Hydrogen emitted from a-Si: H by the laser irradiation. Therefore, the removal is achieved mechanically without any thermal damages. Using this method, an amorphous silicon/amorphous germanium-silicon alloy stacked-type solar cell, which has large area of 8,252cm2 and a high conversion efficiency of 11.2%, has been obtained.

On the other hand, to remove TCO on the underlying a-Si: H layer, Excimer laser patterning is investigated experimentally. Raman spectra of an a-Si: H which is formed under TCO, suggest that Excimer laser can remove the TCO without crystallization of underlying layers. And this technique makes it possible to integrate amorphous silicon/thin film crystalline silicon stacked solar cells in series on a non-transparent substrate.

6107-20, Session 4

Rapid manufacturing of lattice structures using selective laser melting

O. Rehme, C. Emmelmann, Technische Univ. Hamburg-Harburg (Germany)

Since the development of layered freeform fabrication processes some technologies have emerged such as the Selective Laser Melting process (SLM) which uses layers of metal powder to manufacture 3D-Objects from CAD-data by melting targeted geometries. The main goal using this process is to obtain functional products from engineering materials that feature desired properties such as given strength, hardness, surface roughness and residual stress behaviour. Rapid production with short throughput times due to only few process steps, a high individuality (comp. lot size 1) and a high degree of geometric freedom are considered to be it's major advantages.

However one disadvantage to all laser-based freeform fabrication is the immense consumption of time since only considerably small quantities of material can be processed per time unit. Therefore it is desirable to review old-fashioned engineering design rules and develop part geometries that allow for hollow shaped parts with interior lattice structures that provide the part with virtually the same stiffness and strength. Thus the process cost could be massively cut down due to reduced production time and less need for costly powder material. The SLM-process is meeting the requirements to fulfil this intention. Based on using fiber laser technology that delivers high beam quality the process is capable of producing thin walled structures of high tensile strength.

Here the process of the development, production and testing of such lightweight yet sustainable SLM-parts will be presented along with their possible applications.

6107-21, Session 5

Silica nanowires: manipulating light at the nanoscale

E. Mazur, Harvard Univ.

Can light be guided by a fiber whose diameter is much smaller than the wavelength of the light? Can we mold the flow of light on the micrometer scale so it wraps, say, around a hair? Until recently the answer to these questions was “no”. We developed a technique for drawing long, free-standing silica wires with diameters down to 50 nm that have a surface smoothness at the atomic level and a high uniformity of diameter. Light can be launched into these silica nanowires by optical evanescent coupling and the wires allow low-loss single-mode operation. They can be bent sharply, making it possible to control the propagation of light around micrometer-sized corners. The nanowires have applications in microphotonic devices for optical processing and environmental sensing.

6107-22, Session 5

Synthesis of carbon nanotubes by laser-assisted chemical vapor deposition

J. Shi, Y. Lu, X. Wang, Univ. of Nebraska/Lincoln

With the recent advances of the aligned growth of carbon nanotubes (CNTs), there are great interests in CNT based field-emission and MOS transistor applications. In conventional thermal chemical vapor deposition method, substrates as well as chambers need to be globally heated to a sufficiently-high reaction temperature. Thus fabrication period lasts long and growth points cannot be well controlled. In this paper, we will report a method for direct synthesis of CNTs on pre-defined electrodes on silicon wafers using laser-assisted chemical vapor deposition. Catalytic Ni/Fe layers (1 nm) were deposited on top of the pre-defined electrodes first. A CO2 laser (CW 10.6 μm, beam diameter 1 mm) was irradiated on the defined structures as the thermal source for the CNT growth. The temperature of the substrate was measured by a pyrometer, ranging from 850~1000°C. SEM and TEM microscopy were carried out for the morphology and structural characterization of CNTs.

6107-23, Session 5

Resonant infrared pulsed laser deposition of polyimide

N. Dygert, R. F. Haglund, Jr., K. E. Schriver, Vanderbilt Univ.; M. R. Papantonakis, Naval Research Lab.; M. Anthamatten, Univ. of Rochester; A. P. Gies, D. M. Hercules, Vanderbilt Univ.

Resonant infrared pulsed laser deposition (RIR-PLD) is a conformal, low-temperature, dry transfer deposition technique based on resonant excitation of vibrational modes rather than ablation by electronic excitation. Because RIR-PLD substantially reduces the photochemical damage that occurs during laser ablation, it is uniquely effective in depositing a wide variety of thermoplastic polymers [e.g., polyethylene glycol, polystyrene, polytetrafluoroethylene], light-emitting polymers [e.g., MEH-PPV] and functionalized sensor polymers [e.g., fluoropolyol, fluorinated polysiloxanes] as thin films on semiconducting and insulating substrates. RIR-PLD thus can facilitate the development of alternative strategies for incorporating polymers and organic molecules into and onto MEMS and MOEMS devices.

Polyimide is a member of a quite different class of polymers, known as thermosetting plastics, that form in a rigid three-dimensional network and are stronger than thermoplastics. They have a number of desirable prop-

erties for technological applications. They are thermally stable at temperatures above 500 C; chemically inert; self-extinguishing; and have excellent dielectric properties (as with the well-known insulating film KaptonÆ). In general, they are synthesized in a two-step process that involves two precursors; they mix when heated to form the thermosetting polymer.

In this paper, we report the first demonstration that polyimide can be deposited by RIR-PLD. A precursor solution of 16% polyamic (PAA) acid was dissolved in N-methyl pyrrolidinone (NMP) and frozen in liquid nitrogen. A picosecond free-electron laser was tuned to 3.45 μm, corresponding to a strong vibrational absorption line in the NMP, and a mixture of string- and droplet-like moieties was deposited by laser ablation in vacuum at fluences above 0.5 J/cm2. Similar ablation results were achieved by ablation of PAA-NMP solutions in air at fluences between 0.5 and 3.0 J/cm2. At higher fluences, it is possible to suppress string-like moieties in favor of transferring primarily large droplets of the mixed material. Heating of the mixture following deposition on the substrate results in the formation of the polyimide thermosetting plastic. Time-resolved bright-field imaging of the laser ablation plume showed clear differences between the polymer solution (NMP and PAA) and the neat NMP solvent, showing that the PAA clearly affects the ablation mechanism. Interestingly, all attempts at RIR-PLD of polyimide directly from KaptonÆ proved to be impossible; visible damage and droplet ejection were observed at 1.5 J/cm2, but with very evident signs of thermal damage.

We shall present experiments on the dependence of the ablation process and the properties of the deposited polyimide on processing parameters, including wavelength, concentration, post-processing temperature and laser fluence. The transferred material is characterized by matrix-assisted laser desorption-ionization mass spectrometry and Fourier-transform infrared spectroscopy. We also note that because the PAA-NMP mixture is transferred without reaching the temperature required for curing the thermoset plastic, it is possible to pattern the deposited material by laser annealing, thus creating thermosetting polymer micro- and even nanostructures.

6107-24, Session 5

2D surface characterization of laser-deposited carbon films using Raman scattering

K. Yi, Y. Lu, H. Ling, Univ. of Nebraska/Lincoln

We will report an apparatus designed to characterize 2-D surfaces of carbon films based on the principle of inelastic light scattering (Raman scattering). The design and construction details will be presented. The system has a backscattering configuration, constructed using a high-power argon ion laser with a 514.5nm wavelength, an XYZ motion control stage with a movement resolution of 10 nm, a microscope lens, a confocal spatial filter, a holographic notch filter, to achieve extremely low crosstalk and maximum resolution spectroscopy. The beam size focused on the film surface is around 3 μm. The radial resolution for film surface is much enhanced by confocal spatial filter due to its stray light suppression capability. A large depth of sampling field is achieved using an object lens with a middle NA of 0.55, a long working distance of 8 mm, thus auto-focusing requirement can be avoided. Unlike general scanning Raman microscope, film surface characteristic is obtained directly through Raman shift instead of Raman image. A specific algorithm is designed to decide the film boundaries as well as the outline of surface structures. LabviewTM software will be developed for controlling movement of sample stage, data acquisition and visualization. Amorphous and diamond-like carbon films prepared by laser deposition will be studied to demonstrate the capability of this system. The results from this approach will be compared with those using general scanning Raman microscope. This low-cost system will be used to characterize carbon nanotubes and laser-induced diamond formation.

6107-25, Session 5

Laser-assisted synthesis of diamond-like carbon from cyclohexane liquid

Y. Han, H. Ling, Y. Lu, Univ. of Nebraska/Lincoln

Diamond and other high-pressure phases of carbon were synthesized by KrF excimer laser irradiation on single-crystal silicon substrates immersed in a cyclohexane liquid. The deposition process was performed with a peak laser intensity of about 10^8 W/cm2 at room temperature. Scanning electron microscopy, Raman spectroscopy and XPS studies showed diamond-like characters of the deposited films. Optical emission spectroscopy of laser-induced cyclohexane plasma indicated the decomposition of cyclohexane. A mechanism based on the dissociation of the cyclohexane molecules and condensation of energetic carbon atoms into diamond-like films is proposed to explain the process.

6107-26, Poster Session

Hybrid laser technologies for processing of dielectric materials

V. K. Syssoev, Lavochkin Association (Russia); Y. N. Bulkin, RFNC-VNIIEF (Russia); A. V. Zaharchenko, P. A. Vyatlev, Lavochkin Association (Russia)

The results of the study of application of the hybrid laser technology for processing of dielectric material are using in work.

Such hybrid technologies are based on sharing the laser sources the different on spectral ranges, including and incoherent polychromatic lamps.

As technological operation of processing material are considered:

* welding of polymeric and glassy materials by light-laser equipment (polychromatic source with CO2-laser)
* controlled thermocracking of oxide materials on biradiate laser mounting (CO2 and Nd-lasers)
* reception nano-powder on base light-laser equipment (polychromatic source, CO2 and Nd-lasers).

Using of such technologies has allowed successfully realizing the reception:

* strong welded joins of polymeric and glass products
* high-quality samples of the panels for display screens
* to get high-clean powders of SiO2
* carbon nanotubes.

6107-27, Poster Session

Adaptive modeling of the femto-second inscription in silica

V. Mezentsev, Aston Univ. (United Kingdom); J. Dreher, Ruhr-Univ. Bochum (Germany); J. Petrovic, Aston Univ. (United Kingdom); R. Grauer, Ruhr-Univ. Bochum (Germany)

We present a comprehensive investigation of plasma filament dynamics during the process of direct laser inscription dynamically resolved in time and space by means of adaptive mesh refinement. Direct inscription of the complex microstructures in refractive materials by means of intense femtosecond radiation is one of the novel enabling technologies in modern photonics. This technology implies that pre-focused femtosecond light pulses produce phase transitions and create domains with modified refractive index. Self-focusing of the intense laser pulse is a key physical phenomenon leading to a multi-photon ionization at its final stage. In fact the very formation of plasma filaments limits the catastrophic damage due to defocusing and multi-photon absorption. Eventually, the thermalization and recombination of the plasma filament leads to the modification of medium and a distributed variation of refractive index is produced. The dynamics of the light-induced plasma filaments is extremely complex and defined by many factors. It is an extremely fast process evolving

at the very fine spatial scales. We have studied the detailed evolution of plasma filaments and the role of pulse and media parameters on the shape of resulting filaments.

We report on the development of a computational framework for the parallel, mesh-adaptive solution of system of a 3D parabolic wave equation for envelope amplitude of electromagnetic field coupled with the rate equation for plasma density. Local mesh refinement is realized by the recursive bisection of grid blocks along each spatial dimension, implemented numerical schemes include standard finite-differences. Parallel execution is achieved through a configurable hybrid of POSIX-multi-threading and MPI-distribution with dynamic load balancing. The above mentioned model is widely used to describe the process of the femtosecond optical pulse propagation in dielectrics. High intensity of the optical pulse leads to the beam self-focusing due to the Kerr nonlinearity.

Eventually the collapsing cavern saturates due to mutiphoton absorption and ionisation and plasma defocusing. The results are compared with experimentally obtained shapes of domains with modified refractive index.

6107-28, Poster Session

Selective laser removal of nano- and micro-particles

S. Shukla, K. Lyon, S. I. Kudryashov, S. D. Allen, Arkansas State Univ.

Selective laser removal of micro-particles of one chemical type from its mixture with micro-particles of another chemical type pre-deposited on hydrophobic and hydrophilic surfaces have been demonstrated by means of Steam Laser Cleaning method realized with nanosecond IR and UV lasers and various liquid energy transfer media (ETM). Different particles mixtures and supporting substrates have been studied using this principle, and the corresponding optimal combinations for selective targeting and removal of specific particles in their mixture have been revealed. Microscopic imaging of final particle removal has been performed with the help of time-resolved optical microscopy.

6107-29, Poster Session

Microstructures on Si and graphite surfaces fabricated by single intense femtosecond laser pulses

S. I. Kudryashov, Arkansas State Univ.

“Frozen” concentric micro-structures on Si and graphite surfaces were fabricated by single intense femtosecond laser pulses. The number of concentric surface shells was found to depend on incident laser fluence, while the threshold for the structure formation in the case of Si surfaces was close to the femtosecond laser-induced Coulomb explosion threshold in this material, reported in previous studies. Possible formation mechanisms and applications of these structures are discussed.

Conference 6108: Commercial and Biomedical Applications of Ultrafast Lasers VI

Sunday-Wednesday 22-25 January 2006

Proceedings of SPIE Vol. 6108

6108-01, Session 1

Femtosecond laser dissection of neural networks

A. D. Samuel, Harvard Univ.

The nematode C. elegans has emerged as an ideal model organism for studies of brain and behavior. The worm has an attractive simplicity with a neural network of only 302 neurons, and recent advances in molecular biology have given us a powerful toolbox to manipulate the genetic makeup of its neural networks. However, equally essential physiological methods to manipulate or monitor neural activity in the living worm are only starting to emerge. The transparent millimeter-sized worm is an ideal substrate for the development of physiological methods based on optics and microscopy. We will discuss the use of tightly-focused femtosecond laser pulses which enable us to dissect individual nerve fibers with submicrometer precision in the living worm. For the first time, we are able to snip individual wires in the otherwise intact neural circuit of the worm in the study of behavioral encoding.

6108-02, Session 1

Blood flow changes following optically-induced microstrokes in rat brain

N. Nishimura, B. Friedman, N. Kort, P. D. Lyden, D. D. Kleinfeld, C. B. Schaffer, Univ. of California/San Diego

Blood supply to the brain is maintained by a tortuous, often redundant vascular network, in which the topology varies as arteries and arterioles progress to capillaries and then to venules and veins. Small strokes are thought to be caused by the occlusion of the microvessels (arterioles, capillaries, and venules) of this network, and are linked to many types of dementia in aging humans. Here we present studies of the physiological consequences of localized microvessel occlusions in the cortex of live, anesthetized rat. We use two-photon laser-scanning microscopy of intravenously injected fluorescein-dextran to visualize the vascular architecture and quantify the blood flow velocity in individual vessels. We induce clot formation by locally damaging a microvessel, triggering the natural blood clotting cascade. For vessels that lie on the surface of the brain this injury is caused by reactive oxygen species produced through optical excitation of an intravenously injected photosensitizer. For sub-surface vessels, the injury is induced using photodisruption, where an intense femtosecond laser pulse is nonlinearly absorbed in the vessel. Our studies of the blood flow following single-vessel occlusions reveal that the redundancy of the vascular network architecture determines the extent to which compensatory flow maintains tissue perfusion. In particular, we find that flow is maintained downstream from occlusions in arterioles on the surface of the brain through reversals in blood flow direction in some downstream vessels, while occlusions to sub-surface capillaries lead to severe drops in downstream flow.

6108-03, Session 1

Sub-cellular nanosurgery in live cells using ultrashort laser pulses

I. Z. Maxwell, E. Mazur, Harvard Univ.

We use femtosecond laser pulses to selectively disrupt the cytoskeleton of a living cell and probe its mechanical properties. The nanosurgery setup is based on a home-built two-photon microscope. To image, we use a 80-MHz, 100-pJ/pulse laser beam, which is scanned across the sample; to cut, we introduce a second, 250-kHz, 1 to 5-nJ/pulse, laser beam and locally ablate sub-cellular structures. Simultaneous cutting and imaging allows us to study immediate cellular response with several hundred-nanometer spatial and less than 500-ms time resolution.

We severed single actin bundles inside live cells to probe the local dynamics of the cytoskeleton and correlate it to global changes in cell shape. The targeted actin bundle retracts rapidly after laser cutting as it releases its tensile energy. We show that actin bundles in living cells behave like viscoelastic elements. This nanosurgery technique will further the understanding and modeling of stress and compression in the cytoskeleton network of live cells.

6108-04, Session 1

Nanosurgery of sub-cellular organelles in living cells using a femtosecond laser oscillator

W. Watanabe, T. Shimada, S. Matsunaga, T. Higashi, H. Ishii, K. Fukui, K. Itoh, Osaka Univ. (Japan)

Femtosecond laser pulses in the near-infrared region have potential applications in nanosurgery in cell biology. This paper reports on the disruption of sub-cellular organelles in living cells by focusing femtosecond laser pulses from Ti:sapphire laser oscillator.

6108-49, Session 1

Non-destructive micro-patterning of living cells and protein crystals by focused femtosecond laser

Y. Hosokawa, Osaka Univ. (Japan)

Micro-patterning of living cells and proteins has been attracted much attention as a potential technique to realize bio-microdevice. In this work, focused femtosecond laser was applied to micro-pattern living cells and protein crystals without biological damages. The micro-printing was performed to transfer living cells which were adhered on a source substrate to a target substrate which was underlaid on the source substrate. An 800-nm femtosecond laser was focused in a water buffer between the source and target substrates by an inverted microscope equipped with a 100x objective lens. When the laser was scanned at the position of a few um distance from the source substrate, the cells were detached by a stress due to the femtosecond laser induced shockwave and cavitation bubbles and transferred to the target substrate as a line pattern. The line width of the patterned cell was 100 um when the scanning speed was 100 um/sec. Here, 80 % cells detached from the source substrate were adhered and grew again on the target substrate. It means that these cells have no damage by the patterning process. This method can be also applied to multiple patterning of living cell and protein crystals with size of a few um. The pattering resolution may be better than that by inkjet printing. Furthermore, in the presentation, as the relative techniques with this patterning, nondestructive manipulations of the animal and plant cells by the focused femtosecond laser beam were introduced.

6108-05, Session 2

Manipulation of morphogenetic movements in live Drosophila embryos using femtosecond pulses

W. Supatto, Institut Curie (France); D. Débarre, J. Martin, M. Schanne-Klein, École Polytechnique (France); E. Farge, Institut Curie (France); E. Beaurepaire, École Polytechnique (France)

Femtosecond near-infrared lasers are progressively becoming familiar to life scientists owing to the success of multiphoton microscopy, currently the most appropriate technique for high resolution fluorescence imaging inside scattering tissues. Besides two-photon-excited fluorescence (2PEF) microscopy, other nonlinear optical processes are being explored as contrast mechanisms, such as third-harmonic generation (THG).

We show that femtosecond pulses appear as a promising tool for both perturbing and analyzing cell movements in vivo in developing embryos. Focused nanoJoule pulse trains were used to perform controlled intravital microdissections that altered the embryo structural integrity without significantly perturbing cytoskeleton dynamics and gene expression in adjacent cells. In turn, such targeted ablations were used to remotely perturb cell movements [1, 2].

In addition, lower energy pulses from the same laser source were used to visualize morphogenetic movements in developing Drosophila embryos, either in GFP-tagged lines using 2PEF microscopy [1], or even in unstained embryos using THG microscopy [3].

The transparent combination of femtosecond pulse-induced ablation and multiphoton microscopy therefore appears as a novel tool to perturb and analyze in vivo the effect of cell and tissue deformations. It provides a direct means of studying the interplay between cell deformations and molecular signaling, and should find many applications in developmental and cell biology.

References:

[1] W Supatto, D. Débarre, B. Moulia, E. Brouzés, J.-L. Martin, E. Farge & E. Beaurepaire, PNAS 102, 1047 (2005)

[2] W Supatto, D. Débarre, E. Farge & E. Beaurepaire, Med. Laser Appl., (in press)

[3] D. Débarre, W. Supatto, E. Farge, B. Moulia, M.-C. Schanne-Klein & E. Beaurepaire, Opt. Lett. 29, 2881 (2004)

6108-06, Session 2

Advances in lasers for multiphoton excitation microscopy

C. Dorman, Coherent, Inc. (United Kingdom)

Multiphoton Excitation (MPE) microscopy had become an important bioimaging technique, enabling the study of dynamic processes in living cells and tissues without causing significant damage. MPE produces high-resolution, three-dimensional images, and primarily relies on the use a tunable, ultrafast laser to excite highly specific fluorophores in order to follow specific biochemical processes. Key to future advances in MPE is the ability to work with a wider range of fluorophores, to increase data acquisition speed, and to improve data signal-to-noise ratio. In terms of laser characteristics, these requirements translate into wider tuning range, faster tuning speeds, and higher peak power delivered to the sample. This paper explores the advances in tunable ultrafast laser and amplifier technology currently under development to meet these goals and thus power the next generation of MPE instrumentation.

6108-07, Session 2

Simulation of ultrashort pulse induced plasma generation and interaction within the bulk of transparent Kerr-media

C. L. Arnold, W. Ertmer, H. Lubatschowski, Laser Zentrum Hannover e.V. (Germany)

Recent applications of ultrashort laser pulses, such as micromachining of materials, waveguide writing or modern techniques of refractive surgery, require the precise deposition of laser energy in order to manipulate material by controlled generation of localized damage or material alteration.

A theoretical understanding of the nonlinear interaction of tightly focused ultrashort laser pulses with the self-generated plasma within the focal region will be given by the work presented. Nonlinear absorption and plasma generation are limited to the direct vicinity of the focus, since the intensity required for such nonlinear effects is present only in this region.

Our model includes such nonlinear propagation effects as self-focusing and dispersion, as well as plasma defocusing due to generated free electrons. Nonlinear ionization is described using a novel multiple rate equation model recently published by Rethfeld. It combines the complexity of kinetic approaches with the simplicity of rate equations. The importance of cascade ionization versus multiphoton ionization has often been overestimated for ultrashort pulses in earlier approaches. This fact is included in our model by direct simulation of the free electron energy distribution in the plasma and by assuming a finite impact ionization probability.

Based on the above model numerical calculations are performed to understand nonlinear side-effects, such as streak formation, occurring in addition to ultrashort laser pulse induced optical breakdown. Special attention is paid to the shape and size of the generated breakdown plasmas. To push the simulations closer to reality, complex spatial shapes for the incident pulses are assumed. The diffraction pattern of focused truncated gaussian beams or focused plane waves form more realistic initial conditions than perfect gaussian beams.

The calculations presented can be performed for any transparent Kerr-medium of known optical parameters such as water or fused silica.

6108-08, Session 2

Third harmonic generation micro-spectroscopy

O. Clay, Univ. of California/San Diego; A. Millard, Univ. of Connecticut Health Ctr.; C. Schaffer, P. Tsai, Univ. of California/San Diego; J. Aus-der-Au, Spectra-Physics; J. Squier, Colorado School of Mines; D. Kleinfeld, Univ. of California/San Diego

Third harmonic generation (THG) is a useful basis for characterizing the nonlinear optical properties of materials. As a spectroscopy tool, THG has the advantages of simplicity, ubiquity, and sensitivity to two and three photon resonances. A standard nonlinear microscope with an ultra-fast pulsed laser source is easily adapted for THG micro-spectroscopy. We use THG micro-spectroscopy as a quantitative means to study the nonlinear resonances of solution phase compounds and demonstrate its ability to distinguish between oxy-, carboxy-, and deoxy-hemoglobin. An understanding of the optical properties of bio-materials is necessary in order for nonlinear microscopy to more fully realize it ability to probe and perturb biological compounds.

6108-09, Session 3

An introduction to the characterization of ultrashort laser pulses

X. Gu, Max-Planck-Institut für Quantenoptik (Germany) and Georgia Institute of Technology; S. Akturk, P. Gabolde, Q. Cao, A. P. Shreenath, R. P. Trebino, Georgia Institute of Technology

We review the state of the art of the ultrashort laser pulse measurement. The basic theoretical and experimental background of two main techniques — FROG and SPIDER — will be covered. Comparison will be made about the pros and cons of both techniques, as well as linear optical techniques such as spectral interferometry. We will also discuss some of the latest developments of ultrashort pulse measurement, including the ultrasimple commercial SHG FROG device named GRENOUILLE, the full 4D spatio-temporal measurement of an ultrashort pulse laser field using a combination of FROG and digital holography, the measurement of spatial chirp and pulse-front tilt using GRENOUILLE and FROG, the measurement of unstable, ultracomplex, and ultrabroadband laser pulses (microstructure-fiber supercontinua), and the measurement of ultraweak (aJ) light pulses, which have random absolute phase and poor spatial coherence.

6108-10, Session 3

Spectral phase measurement devices for new femtosecond laser sources

V. S. Paziouk, A. V. Konyashchenko, S. E. Egorov, A. J. Carson,

C. C. Barnes, Del Mar Photonics, Inc.

Spectral Interferometry for Direct Electric Field Reconstruction (SPIDER) is one of several methods for characterizing ultrashort optical pulses. SPIDER allows for the measure of the pulse duration, but also allows the extraction of the spectral phase from a femtosecond pulse. We present new developments of SPIDER technique stimulated by recent progress in ultrafast sources. Advances in femtosecond laser development in recent years has led to commercially available femtosecond pulsed laser systems with pulse lengths of less than 10 fs. New lasing materials and advances in fiber laser technology has allowed manufacturers to produce femtosecond pulsed laser that operate at wavelengths outside the traditional 800 nm range of Ti:sapphire. We discuss optical design and performance of SPIDER layouts developed for characterization of shorter pulse duration below 10 fs and longer IR wavelength range.

6108-11, Session 4

The MIIPS method for simultaneous phase measurement and compensation of femtosecond laser pulses and its role in two-photon microscopy and imaging

M. Dantus, Michigan State Univ.

Multiphoton intrapulse interference phase scan (MIIPS) is a relatively new method for accurately measuring the spectral phase of femtosecond pulses with better precision and reproducibility than other established methods. More importantly, MIIPS can be used to correct such distortions in order to obtain transform-limited pulses at the specimen with time-bandwidth products approaching unity. I will describe the method and demonstrate how it can be used for correcting phase distortions caused by high numerical aperture microscope objectives even when using pulses with 100 nm bandwidth and a 1.45 N.A. microscope objective. I will demonstrate that the pulse shaper used in MIIPS can be used to accurately introduce synthetic phase functions. This is tested by the agreement between the resulting second harmonic spectrum and theory. The ability to deliver accurate phase functions through high N.A. objectives allows us to exploit concepts of coherent control, such as multiphoton intrapulse interference, to cause selective two-photon activation of different chromophores. Similarly, one can use this principle to achieve functional imaging, using a chemical gradient sensitive chromophore. Our group has successfully demonstrated this concept in vitro even when the laser was transmitted through one millimeter of biological tissue. MIIPS is ideal for reproducible nonlinear biomedical imaging, and is a method that we hope will become a fully automated part of the femtosecond laser system.

6108-12, Session 4

Closed-loop control of a pulse shaper using real-time SHG FROG

D. J. Kane, Southwest Sciences, Inc.

No abstract available

6108-13, Session 4

The general theory of first-order spatio-temporal distortions of Gaussian pulses and beams

S. Akturk, X. Gu, P. Gabolde, R. P. Trebino, Georgia Institute of Technology

Ultrashort laser pulses are usually expressed in terms of the temporal and spectral dependences of their electric field. This approach disregards any couplings between the spatial coordinates and time and/or frequency. This assumption, however, often fails, as the generation and manipulation of ultrashort pulses require the introduction of spatio-temporal couplings. Furthermore, disregarding these couplings in ultrashort pulses also greatly limits the potential applications that could only be possible by exploiting the spatio-temporal behaviors. For these reasons, spatio-temporal couplings are receiving increased attention from researchers in recent years. Most of the work presented to date, however, focuses on a few particular couplings, lacking a general and rigorous analysis. We present a rigorous and mathematically simple and elegant theory of first-order spatio-temporal distortions of Gaussian pulses and beams. We write pulses in four possible domains, x-t, x-f, k-f, and k-t, including the couplings. We identify couplings in intensity profiles as: pulse-front tilt, spatial dispersion, angular dispersion, and time vs. angle. We identify four new couplings that occur in phase: “wave-front rotation,” “wave-front-tilt dispersion,” “angular temporal chirp,” and “angular frequency chirp.” While there are eight such distortions in all, only two independent distortions exist and are fundamental in each domain. So, we derive simple expressions for each distortion in terms of the others. In addition, we provide normalized, dimensionless definitions for them, which range from -1 to 1 and do not change as the beam propagates. Finally, we show that for such parameters as pulse length, bandwidth, beam spot size and divergence angle, two separate definitions are required as “local” and “global” quantities, in presence of the couplings. Our approach completely determines the explicit relations between various spatio-temporal couplings in Gaussian pulses and beams. It can be generalized to arbitrary profiles by using computational analysis instead of the analytical approach described here. We hope that our approach and definitions will provide an intuitive and useful tool for ultrafast-optics researchers to better understand the distortions that commonly occur in ultrashort pulses.

6108-14, Session 4

Using GRENOUILLE to measure spatio-temporal distortions

S. Akturk, X. Gu, Z. Wang, R. P. Trebino, Georgia Institute of Technology

The couplings between the spatial coordinates and time and/or frequency are very common in ultrashort laser pulses. This is mainly because the elements used in their generations and applications introduce massive spatio-temporal manipulations. These couplings can be residual, hence undesired or they can also be of potential use in various applications. In either case, it is crucial to be able to properly characterize the spatio-temporal distortions. We previously showed that, the ultrashort pulse intensity and phase measurement devices, single-shot FROG and its experimentally simple relative GRENOUILLE also measures some of the very common spatio-temporal distortions. Specifically, GRENOUILLE yields a sheared trace in frequency if the input pulse has spatial chirp. It also yields a trace shifted in delay, if the input pulse has pulse-front tilt. The shear and shift can also be used to measure the distortions. While this approach holds valid for relatively simple pulse, as the pulse intensity and phase gets more complicated, so does the effect of the spatio-temporal distortions. This makes it difficult to measure the spatial chirp directly from the trace shear. Therefore, we develop methods to extract the spatio-temporal distortions from GRENOUILLE traces, even for fairly complex pulses and distortions. First, we have developed a general model of GRENOUILLE for arbitrary spatio-temporal input beams. We then develop two algorithms to be run on distorted GRENOUILLE traces. The first perturbative algorithm is approximate, but is adequate for most cases where the spatio-temporal distortions are relatively small. In this case, the well-established FROG pulse retrieval code is utilized to obtain an estimate of the intensity and phase of the pulse. This retrieved pulse is then used in the retrieval of the spatio-temporal distortion parameters, which will be a simple one- or two-parameter optimization process. The advantage of this perturbative approach is that it requires very little modification to the existing FROG program, which is very fast, reliable and robust. The appended spatio-temporal distortion retrieval step takes only seconds to complete. We tested this algorithm for relatively non-complicated pulses and showed very good match between the imposed and retrieved values. The second rigorous algorithm is numerically more complicated but is capable of accurately measuring the pulse intensity and phase and the spatio-temporal distortion parameters in more general cases. It involves changing the core of the FROG algorithm. First, the expression for the electric field is

replaced by the general one that includes the spatio-temporal distortions. Then, intermediate steps are added in the algorithm, to do optimization not only on the pulse intensity and phase, but also on the spatio-temporal distortions. The intra-iteration pulse retrieval step uses a modified Newton's method, in which a direction of search is calculated using the first-order (gradient) and second-order (Hessian matrix) of the error function with respect to the pulse profile points, and an optimal step size is calculated from a polynomial. We tested this algorithm with several pulses that have various complexities and showed that this new algorithm retrieves the intensity and phase and the spatio-temporal distortions very accurately.

6108-15, Session 5

Silicon flip-chip imaging with a resolution of 325-nm using solid-immersion lenses and the optical-beam induced current method

E. Ramsay, D. Xiao, N. Pleynet, R. J. Warburton, D. T. Reid, Heriot-Watt Univ. (United Kingdom)

Using the two-photon optical beam induced current method, two- and three-dimensional imaging have been demonstrated in a silicon CMOS integrated circuit using a high peak-power femtosecond laser operating beyond the silicon band edge. This technique is particularly appropriate for the imaging of devices in flip-chip packaging, where access to the front (component) side of the chip is lost, since it allows for imaging through the backside of the chip. Recently an adaptation to confocal microscopy has been suggested and implemented which involves the use of a Weierstrass solid immersion lens (SIL), often referred to as a super-SIL. Using a super-SIL in combination with standard confocal imaging, Ippolito et al have reported optical resolutions of 20% the free-space wavelength of the imaging light. In the work that we present here we demonstrate that the combination of a solid immersion lens with two-photon absorption can give results which are equivalent to confocal imaging using a SIL. By using a 400fs Er:fibre laser operating at 1530nm we have achieved a resolution of 325nm, which is around 20% of the free space wavelength. We will present full details of this result and will also describe further strategies that should lead to improvements to this resolution figure, potentially allowing feature sizes as small as 65nm to be resolved.

6108-16, Session 5

Electrical signal probing in a silicon CMOS integrated circuit using electric-field-induced second-harmonic generation

E. Ramsay, D. Xiao, D. T. Reid, Heriot-Watt Univ. (United Kingdom); B. Offenbeck, N. Weber, Fraunhofer-Institut für Integrierte Schaltungen (Germany)

Non-invasive, non-contact probing of electrical signals in silicon integrated circuits is required for failure analysis and device-debug operations, particularly in architectures such as flip-chips where the access to the component side of the chip is obscured by multiple wiring layers. One candidate solution is based on the electric field induced second harmonic generation (EFISHG) effect which allows the strength of an externally-applied voltage to be probed by using optical second-harmonic generation. Here we present details of EFISHG electrical signal monitoring in a silicon CMOS device using femtosecond illumination at 2.2μm. The excitation source was an optical parametric oscillator and the operating wavelength allowed both the fundamental and the second-harmonic light to be below the silicon bandgap energy, therefore limiting the optical absorption and subsequent carrier generation. Previous implementations of the EFISH technique in silicon devices have relied on using excitation wavelengths with photon energies greater than or close to the bandgap energy of silicon. At these wavelengths there is a strong likelihood of carrier generation, either by the excitation beam or by the resulting second-harmonic light and consequently the EFISHG method at these wavelengths cannot be considered to be truly non-invasive. We report results showing that it is possible to use EFISHG to monitor the voltage across the device and we also show that it is possible to monitor electrical waveforms in real-time.

6108-17, Session 5

Femtosecond laser-induced lattice dynamics in semiconductors: Peierls structural transitions versus point defect formation and 'cold melting'

S. I. Kudryashov, Arkansas State Univ.

Coherent structural dynamics in highly-excited semiconductors and semimetals is described using the deformation-potential approach to characterize coherent interactions of electrons and holes with center-zone optical phonon modes, which are responsible, as precursors of corresponding soft modes, for Peierls displacive solid-solid structural transformations in crystalline semiconductor materials. This approach provides, to the first and second orders of perturbation theory, a strict description of coherent optical phonon-induced bandgap shrinkage and electronic softening of the related optical phonon mode as functions of density of electron-hole plasma produced in these materials. Characteristic values of bandgap shrinkage, coherent sub-lattice displacements and optical phonon amplitudes are calculated for different materials as a function of electron-hole plasma density and compared with experimental results obtained in this and previous studies. Moreover, thresholds for displacive "metal-insulator" transitions in various semiconductors and semimetals are calculated using this theoretical approach accounting for total bandgap renormalization and complete softening of the relevant optical modes, and are compared to experimental and theoretical asymptotic Peierls thresholds reported in this and other works. Finally, relationship of the Peierls-like coherent structural dynamics to generation of point defect and ultrafast "cold" melting in the abovementioned materials as well as their competitive and inter-related dynamics are discussed.

In conclusion, the theoretical approach presented in this work provides semi-quantitative description of ultrafast coherent structural dynamics in highly electronically excited semiconductors and semimetals, in reasonable agreement with experimental results, and further insight into the mechanism of "cold" melting in such materials.

6108-18, Session 5

The influence of input pump polarization on supercontinuum generation in photonic crystal fibers

P. Falk, Danmarks Tekniske Univ. (Denmark); M. Delgado-Pinar, Univ. de Valéncia (Spain); M. H. Frosz, Danmarks Tekniske Univ. (Denmark); L. Thrane, P. E. Andersen, Risø National Lab. (Denmark); A. O. Bjarklev, O. Bang, Danmarks Tekniske Univ. (Denmark)

Supercontinuum generation (SCG) in fibers has been studied for more than two decades. In recent years photonic crystal fibers (PCF), which allow tailoring of the dispersion profile in a way suitable for optimization of spectral broadening, have dramatically improved the SCG performance and lowered the demand on the pump laser. But, despite that the generated light is of high interest for optical coherence tomography, applications of SCG spectra have been haunted by noise. Therefore the understanding of input pulse properties and their relation to the nonlinear effects is crucial for the design of low-noise broadband light sources.

In this work we report a systematic experimental and numerical investigation of the dependence of the input pulse polarization on the generated supercontinuum in terms of intensity stability and spectral stability. A Ti:Sapphire laser, providing femtosecond pulses, is used to generate the continuum, by pumping a nonlinear PCF in the anomalous dispersion region. Particularly, the solitons generated in the infrared regime are studied and a complex dependence between polarization angle and peak wavelengths in the spectrum is observed. Furthermore, we investigate relative intensity noise (RIN) and spectral stability of the generated supercontinuum as a function of the input polarization. The supercontinuum light sources are used in an optical coherence tomogra-

phy system and the dynamic range and autocorrelation for the spectra for the spectra output from the different fibers. Experimental measurements are compared with numerical simulations.

6108-19, Session 5

Ultra-high resolution, polarization sensitive transversal optical coherence tomography for structural analysis and strain mapping

K. Wiesauer, Upper Austrian Research GmbH (Austria); M. Pircher, E. Götzinger, C. K. Hitzenberger, Medizinische Univ. Wien (Austria); R. Engelke, G. Ahrens, K. Pfeiffer, U. Ostrzinski, G. Grützner, micro resist technology GmbH (Germany); R. Oster, Eurocopter Deutschland GmbH (Germany); D. Stifter, Upper Austrian Research GmbH (Austria)

Optical Coherence tomography (OCT), originally developed for ophthalmology and so far mainly used for biomedical applications, has only recently been demonstrated as promising tool for contactless and non-destructive testing of semitransparent materials like plastics, polymers and compound materials. While by conventional OCT cross-sectional reflectivity images of the internal structure of the sample are obtained, transversal OCT provides en-face information parallel to the sample surface. An extension of OCT is polarisation-sensitive (PS-)OCT which additionally maps the internal birefringence occurring due to strain or anisotropies within a material. In this work, we combine the advantages of ultra-high resolution transversal OCT with polarization-sensitive measurements. Ultra-high depth-resolution is essential because for many applications in material research features sizes of only a few microns are of interest (e.g., the thickness of layers, the size of inclusions or the diameter of fibres within reinforced materials). Using a femtosecond Ti:Sapphire laser as broadband light source, we obtain a depth-resolution of ~ 2μm within materials. We apply transversal PS-OCT for structural investigations and for strain mapping of different types of samples, such as photoresist moulds on a wafer for the fabrication of micro electro-mechanical systems, optical waveguides consisting of different polymer layers, and glass-fibre reinforced helicopter rotor blades. Transversal PS-OCT is demonstrated to reveal, besides the structural properties, the in-plane strain distribution at different depths and in particular, at the different interfaces of the samples. Regions where excessive strain occurs are identified, and the influence of structural properties on the strain distribution can be investigated.

6108-20, Session 6

Exploiting heat-accumulation effects in high-repetition rate ultrashort laser microprocessing

P. R. Herman, S. Eaton, H. Zhang, J. Li, Univ. of Toronto (Canada)

High repetition rate femtosecond lasers are driving open new processing windows for micromachining of living cells, brittle materials, transparent glasses, and numerous other materials. This paper explores the role of thermal diffusion and heat accumulation as the pulse repetition rate surpasses hundreds of kHz. At such rates, thermal diffusion from the focal volume is insufficient to remove the absorbed laser energy prior to the arrival of the next laser pulse, leading to heat accumulation effects that expand the modification zone, reduce the thermal cycling between pulses, and present modified material properties to subsequent laser pulses. We are exploiting these effects to develop high-speed writing of low-loss optical waveguides in various transparent media. Here, heat accumulation effects mitigate micro-crack formation in brittle glasses, speed processing times, and improve control of waveguide dimension and symmetry. A variable repetition rate (0.1 to 5 MHz) femtosecond fiber laser (IMRA, μJewel) was applied to writing waveguides in various silica-based glasses. We found 300-kHz repetition rate to demark the onset of heat accumulation in borosilicate glass (AF45), as manifested by the formation of a large radius cladding zone around the ~2-μm core laser-modification zone. Thermal modeling is shown to accurately predict the radius of this cladding zone, which increases dramatically to >10 μm as repetition rate is increased from 0.3 to 2 MHz for identical laser fluence exposure. In our second approach, 40-fs pulses from a 1 kHz ultrafast laser (Spectra Physics, Spitfire) were separated into 56 MHz bursts of 2 to ~12 pulses per train and applied to waveguide writing in the same materials. The number of pulses in each burst as well as the shape of the burst-train envelope were found to dramatically affect the processing window for writing low-loss optical waveguides. Heat accumulation effects are seen to play a role during the 56-MHz bursts presented at 1-kHz repetition rate. However, thermal cycling is much more extreme than in the continuous ~1-MHz case, providing insightful contrasts to help elucidate the prominent role that thermal diffusion and heat accumulation physics plays out during the ultrafast laser interactions. By understanding these effects, one can better control this new domain of high repetition rate ultrafast laser material interaction and explore its broad application in material processing.

6108-21, Session 6

Investigation of femtosecond laser irradiation on fused silica etching selectivity

Y. Bellouard, Technische Univ. Eindhoven (Netherlands); C. D. Depeursinge,École Polytechnique Fédérale de Lausanne (Switzerland); A. A. Said, M. A. Dugan, P. Bado, Translume

Femtosecond laser irradiation has various noticeable effects on fused silica. It can locally increase the index of refraction or modify the material chemical selectivity. Regions that have been exposed to the laser are etched several times faster than unexposed regions. These effects are of practical importance from an application point-of-view and open new opportunities for the development of integrated photonics devices that combine structural and optical functions.

Various observations reported in the literature seem to show that those effects are possibly related to a combination of structural changes and the presence of internal stress.

In this paper, we present further investigations on the effect of femtosecond laser irradiation on fused silica substrate (a-SiO2). In particular, we use various experimental techniques like nano-indentation and holography-based birefringence measurements coupled with direct SEM observations on chemically etched specimens to characterize the effect of various laser parameters like power, scanning speed and irradiation pattern. We show further evidence of an interface between two different etching regimes that seems to be related to the presence of two different material phases induced by the laser irradiation.

6108-22, Session 6

Unified model of femtosecond laser ionization in bulk dielectrics

S. I. Kudryashov, Arkansas State Univ.

Dynamic interplay between multi-photon, tunnel and avalanche ionization mechanisms in bulk dielectrics is revealed by comprehensive consideration of microscopic interactions between electronic sub-system and strong transient electric fields of ultrashort (femtosecond) laser pulses. Dominating ionization mechanisms in bulk dielectrics irradiated by UV, IR and mid-IR fs-laser pulses are predicted using the proposed theoretical model, and basic scaling and governing parameters for ionization processes are derived. The proposed and previous theoretical models of ionization in bulk dielectrics are discussed.

6108-23, Session 7

Time resolved studies of femtosecond laser ablation of silicon (100) with thermal oxide films via pump-probe imaging

S. M. Yalisove, J. P. McDonald, Y. P. Picard, Univ. of Michigan

Focusing high intensity femtosecond (fs) laser pulses, just above the ablation threshold, onto the surface of a material results in energetic matter with velocity on the order 1000's of meters per second. By using pump-probe imaging techniques, a magnified and time resolved view of this fs laser pulse-material interaction can be obtained. For this work, fs laser ablation and damage of Si(100) with native and thermally grown oxide films (2 -1200 nm) was studied. Atomic force microscopy analysis of the fs laser induced damage to Si(100) samples with thin (2-1200 nm) thermally grown oxide films showed that the film could be removed in a discrete fashion, with minimal damage to the substrate, while for laser pulses of less energy, the oxide film was found to delaminate from the substrate forming a blister or bubble. Using the pump probe imaging technique, the ablation dynamics were studied as a function of film thickness and incident laser pulse energy with the overall goal of further understanding the explosive nature of the interaction of the fs laser pulse with the Si(100) substrate. The oxide films are transparent to the incident laser pulse, such that the substrate absorbs the bulk of the laser energy and is left in a molten state. The excited material was initially confined to the substrate-film interface by the intact oxide film. The subsequent expansion of excited material from the surface was observed by imaging the reflection of a probe laser pulse (reflected from the laser excited region) onto a CCD camera over a range of time delays from 0 to 12.3 ns after the arrival of the pump laser pulse. The temporal evolution of Newton's Rings (an interference phenomenon) in these images provided the expansion rate of the ablated material from the substrate. As the oxide thickness increased, the expansion rate decreased accordingly. Additionally, the time at which the expansion begins (after the arrival of the pump laser pulse) was also found to increase with oxide thickness. Finally, for a given oxide thickness, the expansion rate was found to be directly proportional to the incident laser pulse energy. Time-lapse movies of the collected images showing the dynamics of material ablation produced by femtosecond laser pulses will be presented. Molecular dynamics and hydrodynamics simulations of the experiments described above will also be discussed in order to enhance understanding of the observed phenomenon. This method, coupled with velocity determination of the ablated material, may be used for determining the expansion rates of a variety of materials post irradiation with intense fs laser pulses. Time permitting; a new technique that provides the spatial temperature profile surrounding ablation craters produced by single femtosecond laser pulses will be presented. These techniques all provide insight into the complex near threshold interaction of fs laser pulses with materials.

6108-24, Session 8

Waveguide writing in silica glass with a femtosecond fiber laser at the wavelength of 1560-nm

W. Watanabe, T. Tamaki, K. Itoh, Osaka Univ. (Japan); H. Nagai, M. Yoshida, AISIN SEIKI CO., LTD. (Japan)

Focusing femtosecond laser pulses induces refractive-index change in a wide variety of glasses. This technique has been applied to fabricate three-dimensional waveguide devices. In this paper we report on the waveguide writing in silica glass using a novel femtosecond fiber laser system (IMRA, FCPA microJEWEL, B-250) at a wavelength of 1560 nm and at a repetition rate of 258.5 kHz.

6108-25, Session 8

Optimized precision micromachining using commercially-available, high-repetition rate, microjoule, femtosecond fiber lasers

M. L. Stock, G. D. Sucha, A. Y. Arai, IMRA America, Inc.

Fiber lasers offer an excellent technology base for production of an industrial-quality tool for precision microfabrication, answering the need to expand the capabilities of laser material proc-essing beyond traditional welding, cutting, and other industrial processes. IMRA's FCPA uJewelTM femtosecond fiber laser has been developed to address the particular need for direct-write lasers for creation of clean and high-quality micron and sub-micron features in materials of commercial interest. This flexible Yb:fiber chirped-pulse amplification architecture, capable of operating at rep-rates between 100 kHz and 5 MHz, balances the need for higher-repetition rate with that of sufficient pulse energy to work at or near ablation threshold, while meeting industrial standards for temperature, shock and vibration.

Demonstration of the need for higher-repetition rates for direct write processes will be provided in this paper. Further, results of laser-processing of materials typically used in flat panel dis-plays, photomasks, and waveguide production using the FCPA uJewel laser will be presented, along with initial results of tests obtained using the most recent upgrades to the laser system.

6108-26, Session 8

Waveguide writing in bulk PMMA by femtosecond laser pulses

W. Watanabe, S. Sowa, K. Itoh, Osaka Univ. (Japan)

When femtosecond laser pulses are focused inside the bulk of transparent materials, the intensity in a focal volume becomes high enough to produce permanent structural modifications. This technique has been applied to fabricate three-dimensional photonic structure. In this paper we present the fabrication of waveguides inside the bulk PMMA.

6108-27, Session 9

Crossed beam irradiation for femtosecond laser micro and nanomachining with three-dimensionally isotropic spatial resolution

K. Sugioka, K. Midorikawa, The Institute of Physical and Chemical Research (Japan)

In laser microprocessing, resolution is always of paramount importance. The achievement of high resolution is more difficult in three-dimensional (3D) laser microprocessing compared to its two-dimensional (2D) counterpart, due to mismatch between the focal radius and Rayleigh length. A straightforward way of improving the axial resolution is to use an objective lens with a high numerical aperture (NA), as has been demonstrated in two-photon polymerization [1]. However, even for an objective lens with NA=1.4, the attainable axial resolution is approximately 500nm, which is fourfold worse than the lateral resolution of ~120nm obtained with the same objective lens [2]. The ratio of axial resolution to lateral resolution relatively increases with the reduction of NA, resulting in undesirable, elliptical cross-sectional shapes in many 3D microprocessing applications using femtosecond (fs) lasers, such as 3D photopolymerization [2], laser direct writing of optical waveguides [3] and laser micromachining of 3D microfluidic hollow channels [4]. For the fabrication of 3D microstructures, two crossed beams of a continuous wave (CW) argon ion laser have been used in laser chemical vapor deposition (LCVD) [5]. This irradiation method would be very attractive for confining the reaction region three-dimensionally to a very small area.

In this paper, we show that the use of crossed-beam irradation geometry is useful for tackling the axial resolution issue in 3D fs laser microprocessing. The developed crossed-beam system is composed of two orthogonal objective lenses which are confocally aligned (i.e., they share the same focal point) to produce an isotropic 3D illumination volume near the focal point.

To ensure an isotropic illumination volume, the foci of the two beams in the crossed-beam system must spatiotemporally overlap throughout the entire period of laser scanning. This requirement is impossible to fulfill if we scan the glass in air, because of the refractive index mismatch between the sample and air. To overcome this issue, we design a special XYZ stage which translates the glass sample in a refractive matching liquid. Since translating the glass sample in a fixed glass cell containing the refractive index matching liquid does not change the optical paths of the two orthogonal beams, the initially aligned two foci could maintain spatiotemporal overlap even during the entire scanning step. Before we starte scanning the sample, the alignment of the two objective lenses and the adjustment of the time delay between the two beams are realized by observing the fs-laser-induced fluorescence in the glass sample.

We demonstrate that 3D microfluidic channels and optical waveguides with substantially circular cross-sectional shapes can be directly fabricated inside glass by using the developed system.

(References)

[1] S. Kawata, et. al., Nature 412, 697 (2001).

[2] H. -B. Sun, et. al., Appl. Phys. Lett. 83, 819 (2003).

[3] K. M. Davis, et. al., Opt. Lett. 21, 1729 (1996).

[4] M. Masuda, K. Sugioka, et. al., Appl. Phys. A76, 857 (2003).

[5] O. Lehmanin and M. Stuke, Mater. Lett. 21, 131 (1994).

6108-28, Session 9

Femtosecond-laser microstructuring of silicon for novel photovoltaic devices

B. R. Tull, J. E. Carey III, M. T. Winkler, E. Mazur, Harvard Univ.

Photovoltaics research has recently focused on photovoltaic materials made by cheaper processes with minimal waste such as thin-films grown by chemical vapor deposition. Because silicon is the most common semiconductor material and the second most abundant element in the earth, silicon-based thin films are an excellent choice for photovoltaics. The drawback to crystalline silicon thin films is low absorption due to silicon's indirect band gap. Thicker films increase processing costs and sacrifice efficiency due to defects inherent in the thin-films.

We report the creation of a thin, highly absorbing layer on silicon surfaces using the intense conditions at the focus of a high-intensity, femtosecond laser pulse. Irradiation of a silicon surface with 100-femtosecond laser pulses in the presence of sulfur containing gases creates a highly doped layer of nanocrystalline silicon in the top several hundred nanometers. The incorporation of this thin layer results in near unity absorption of light from the near-ultraviolet (250 nm) to the near-infrared (2500 nm), including wavelengths normally invisible to silicon (> 1100 nm). After thermal annealing, a photovoltaic responsive junction is formed between the nanocrystalline silicon layer and the underlying silicon.

The high absorptance of a wide range of wavelengths of light in an extremely thin surface layer makes our process ideal for modifying and enhancing crystalline silicon thin film solar cells. Preliminary results on irradiation of a 1.5-μm thick silicon film resulted in a change of absorptance from 60% to 90% in the visible and from 10% to 40% in the near-infrared.

6108-29, Session 9

Laser-based fabrication of a displacement sensor with an integrated high-accuracy position sensor

P. Bado, M. A. Dugan, A. A. Said, Translume; Y. Bellouard, Technische Univ. Eindhoven (Netherlands)

We present a high-accuracy force or displacement sensor made only of glass. We present a high-accuracy force or displacement sensor made only of glass. This device merges integrated optics and micro-mechanics in a monolithic substrate. It differs from previous micro force sensor works in that the measured variable is optically rather than electrically acquired.

The device was manufactured using a combination of femtosecond laser pulses and chemical etching. A single manufacturing step was used to define both the optical and the mechanical features. This approach dramatically simplifies the overall fabrication and eliminates alignment issues associated with sequential fabrication processes.

Our displacement sensor is composed of a mobile platform and a fixed frame. These components are linked together through high-aspect ratio double-compound flexures. This design firmly restrains the motion of the platform along a single axis. The range of the motion exceeds 1 millimeter. Integrated waveguides are used to measure the displacement of the mobile platform using a mechanism similar to a traditional large-scale optical encoder. Using this approach, we measure highly repeatable submicron motions. Methods to improve accuracy into the 10-nanometer range will be discussed

6108-30, Session 9

Discrete spatial soliton formation in a two-dimensional fs laser written waveguide array in fused silica

A. Szameit, D. Blömer, J. Burghoff, T. Pertsch, S. Nolte, A. Tünnermann, Friedrich-Schiller-Univ. Jena (Germany)

During the past years nonlinear light propagation in waveguide arrays has been an active research topic. In these systems the formation of so-called discrete spatial solitons is a central issue. While one-dimensional discrete spatial solitons have already been observed in permanent and temporally induced systems, two-dimensional discrete solitons have been generated so far only in temporally induced waveguide systems in photorefractives. However, since such lattices are highly symmetric it is problematic to study the influence of irregularities or boundary effects.

In this work we investigate the formation of a two-dimensional discrete soliton in a fs written 5x5 cubic and 75 mm long waveguide array for the first time to the best of our knowledge. For the writing process we used a Ti:Sapphire CPA laser system with a repetition rate of 1 kHz, 50 fs pulse duration and pulse energies of 0.15 - 0.3 μJ at a wavelength of 800 nm. The writing velocity was 1250 μm/s, and the focal depth inside the sample was between 100 - 300 μm. For the investigation of the propagation properties a waveguide next to the center was excited with 200 fs laser pulses. At low peak power discrete diffraction with asymmetric coupling and strong boundary effects was obtained. When the peak power was increased a discrete spatial soliton formed.

Since femtosecond written waveguides are permanent modifications and sequentially written this approach offers the possibility to study the influence of defects, asymmetric coupling conditions and strong boundary effects at the array's border.

6108-31, Session 9

3D photonic devices at telecom wavelengths fabricated by a femtosecond oscillator

V. A. Maselli, R. Osellame, N. Chiodo, G. Cerullo, P. Laporta, Politecnico di Milano (Italy); P. Ferraro II, S. M. De Nicola, A. Finizio, Consiglio Nazionale delle Ricerche (Italy)

Optical waveguide writing with femtosecond laser pulses represents a good alternative to traditional fabrication methods thanks to its simplicity, flexibility and possibility to realize 3D structures. The direct use of a laser oscillator allows a simpler setup, without amplification stages, greater processing speed, up to 1 cm/s, and intrinsically symmetric waveguide cross-sections due to isotropic heat diffusion.

In this work we report on the fabrication and optical characterization of waveguides at telecom wavelengths by a stretched-cavity (26 MHz repetition rate) Ti:Sapphire oscillator. The best results have been obtained on Corning 0211 and the previously unexplored Schott IOG10. Operation at 1.55-micron has been demonstrated and a comparison between optical properties of the waveguides on the two glasses has been made. The refractive index profiles have been measured with two different techniques: the innovative Digital Holography Microscopy (DHM), applied for the first time to optical waveguides, and the commercial near-field refractive index profilometry (RNF). The shape of the refractive index profile was found to depend strongly on the glass type.

We demonstrate passive photonic devices at 1.55-micron, exploiting the unique 3D capabilities of the technique. These devices include: (i) a 1x2 splitter, obtained by writing two straight waveguides at an angle and separated by a depth displacement; (ii) a 1x4 splitter, realized by combining 1x2 splitters on different planes in the depth; (iii) a WDM coupler, with a good rejection of the 980-nm signal with respect to the 1550-nm one. Perspectives of the technique will also be addressed.

6108-32, Session 10

Pulse shortening utilizing acceptor dye as saturable absorber in energy transfer distributed feedback dye laser

P. Palanisamy, Anna Univ. (India); M. B. Ahamed, Crescent Engineering College (India)

In this paper a simple method of pulse narrowing by double Q-switching is presented. In energy transfer distributed feedback dye laser (ETDFDL) when acceptor dye acts as a saturable absorber, pulse narrowing is observed in both donor and acceptor emission regions. In prism-dye cell configuration using second harmonic of Nd-YAG laser as pump source, the ETDFDL output is obtained from dyes Rhodamine 6G as donor and Acid Blue 7/Thionine as acceptors. In Rhodamine 6G and Acid Blue 7 combination pulse narrowing is observed only in the acceptor region whereas in the other combination namely Rhodamine 6G and Thionine, it is observed in both donor and acceptor regions. This is because of good overlap of the emission spectra of donor with the absorption spectra of acceptor. The detailed study is presented in this paper.

6108-33, Session 10

Development of diode-pumped high average power continuous-wave and ultrashort pulse Yb:KGW lasers for nonlinear microscopy

A. Major, V. Barzda, Univ. of Toronto at Mississauga (Canada)

Diode-pumped solid-state ultrafast laser sources are widely used for applications such as nonlinear frequency conversion, high-resolution spectroscopy, and nonlinear (two-photon excitation fluorescence, second- and third-harmonic generation, etc.) microscopy. Direct diode-pumping of solid-state active media offers high efficiency and reliability at reduced manufacturing costs. Two of the most promising Yb-ion doped laser materials are double tungstates Yb:KGd(WO4)2 and Yb:KY(WO4)2. Yb-ion based laser materials are characterized by low quantum defect, broad absorption and emission bands, allowing for direct diode pumping and ultrashort pulse generation. Operation around 1000nm instead of commonly used 800nm (Ti:sapphire) is particularly suitable for applications in nonlinear microscopy, since at longer wavelengths scattering losses are lower, autofluorescence is largely reduced, and generated harmonics fall into the visible range (rather than UV) resulting in higher throughput and more simple detection.

Previously, Yb:KGW lasers were shown to operate in continuous-wave and mode-locked regimes at ~1W output power level. In this presentation we report on development of 5W continuous-wave Yb:KGW laser using single 25W fiber-coupled laser diode at 980nm and simple spherical pump optics. The pump diode radiation was focused into a 300um spot in the 4-mm-long Yb:KGW crystal. A three-mirror cavity was used in this case providing a good overlap between the pump and laser mode to ensure operation in the fundamental transverse mode. Using this laser as a platform for ultrashort pulse generation, we also achieved 2W output power in mode-locked regime with ~200 fs pulses centered around 1045 nm at a repetition rate of 100 MHz. This corresponds to 20 nJ pulse energy and 100 kW peak power. The laser used conventional delta-cavity with two SF10 prisms for dispersion compensation. This laser is intended for use in high-resolution third- and second-harmonic generation microscopy.

6108-34, Session 10

New compressed Ti:sapphire femtosecond amplifier layout

S. Y. Tenyakov, A. V. Konyashchenko, S. E. Egorov, A. J. Carson, C. C. Barnes, Del Mar Photonics, Inc.

A novel new design for an 8-pass multipass Titanium doped sapphire femtosecond amplifier (MPA) is studied. Ultrafast amplifiers based on the chirped pulse amplification (CPA) technique have been widely used to amplify the output pulses of Kerr lens mode locked (KLM) Ti:sapphire lasers from the nanojoule to the millijoule level. The system presented here also takes advantage of CPA to reduce the peak power and thus the potential damage to optical components from self-focusing. The amplifier scheme is based on a single curved mirror and a Brewster cut Ti:sapphire laser rod. Optical excitation of the Ti:sapphire gain medium is achieved by pumping with a Q-switched and frequency doubled Nd:YLF laser at 527 nm. The rear face of the gain crystal is coated to form a high reflector for both the pumping wavelength (490-550 nm) and the amplified seed pulse (740-860 nm). In this configuration the gain crystal itself acts as a second mirror, reducing the size of the amplifier and allowing for the most effective use of the pumping energy. By employing a Brewster cut lasing crystal the amount of active gain material can be adjusted for maximum gain. The advantages of this approach, compared to traditional two curved mirror MPA designs, are the reduced foot print and the ability to easily adjust the amount of gain material. At the same time the system retains the low amplified spontaneous emission (ASE) and temporally clean output pulse characteristic of MPA systems.

6108-35, Session 10

351-nm femtosecond with Nd:glass regenerative amplifier for thin films ablation

K. Mukaihara, Y. Suzuki, S. Ito, M. Yoshioka, Laserfront Technologies, Inc. (Japan)

Recently, ultra-fast pulse lasers have been attractive in the field of fine processing applications, such as three-dimensional optical waveguides, photonic crystals and ablation.:Because femotosecond lasers have the superior characteristics of a short pulse width and high peak power, we can reduce thermal influence that causes splashed, roll up of the edge and damages of glass substrate. Due to this non-thermal ablation process, a control of the stable and fine process can be available.:LFT (Laserfront Technologies, Inc., former NEC Laser Solution Division) manufactures systems repair opaque defects of photo mask and TFT-Liquid Crystal Display (LCD) substrate by using nanosecond or sub-nanosecond pulse lasers. Recently the integration of wiring patterns on the substrate advances, requirements of much more fine and accurate processing technology are increasing. Femtosecond lasers can offer advantages of the quality and the accuracy for ablation process compared to ns/ subns pulse lasers.:In this letter, we have developed a femtosecond laser system. It consists of a mode-locked fiber oscillator, a regenerative amplifier, a pulse compressor and a third harmonic generator. The gain media of the regenerative amplifier is Nd: glass. The output energy of the regenerative amplifier is 2mJ at 7 Hz repetition rate. The final THG (351 nm) output energy is 200μJ, 10% conversion efficiency was obtained. Using above femtosecond laser, we conducted ablation processing of thin films such as Cr on the glass substrate. The results of fine processing are reported.

6108-36, Session 10

Tunable ultrashort pulse energy transfer distributed feedback dye laser

M. B. Ahamed, Crescent Engineering College (India); P. Palanisamy, Anna Univ. (India)

Distributed feedback dye lasers (DFDLs) have been extensively studied since 1971. In distributed feedback dye lasers pumped with a laser of

nanosecond-pulse width, a train of picosecond pulses is generated by relaxation oscillation. Unlike the other conventional laser oscillators, DFDLs possess no external optical elements to provide feedback. Periodic variation in the refractive index/gain created within the medium provides required feedback by Bragg scattering. DFDLs have higher efficiency, broader tuning range and lower amplified spontaneous emission (ASE) background level than other dye lasers. Using nanosecond and/or subnanosecond pulses as pump source, DFDLs generate 20 to 100 times shorter pulses. This significant pulse shortening is caused by self Q-switching which is due to spatial gain modulation dependence of the feedback.

The concept of energy transfer in laser dye mixtures improves the efficiency of dye lasers and broadens their tunable spectral range. The energy transfer dye lasers (ETDLs) are more efficient because of high gain and low pump power requirements. For a particular donor-acceptor (D-A) pair, it is possible to make both donor and acceptor to lase at their respective gain regions due to energy transfer mechanism. If such a dye mixture is taken as active medium in DFDLs, ultra-short pulses tunable over the entire gain spectrum of donor and acceptor dyes are generated.

This paper presents the characteristics of energy transfer distributed feedback dye laser (ETDFDL) in a mixture of Rhodamine B (RhB) and Thionine (Th) dyes pumped by 532 nm Nd:YAG laser both theoretically and experimentally. The characteristics of donor DFDL, the acceptor DFDL, the dependence of their pulse widths and output powers on donor-acceptor concentrations and pump power are studied. Experimentally the output energy of DFDL is measured at the emission peaks of donor and acceptor dyes for different pump powers, donor-acceptor concentrations and the tunability is observed from 565 nm to 665 nm using prism dye cell arrangement.

6108-37, Session 10

Generation of tailored picosecond-pulse-trains for micro-machining

A. Nebel, T. Herrmann, B. Henrich, R. Knappe, Lumera Laser GmbH (Germany)

Novel solid-state picosecond lasers provide a strong benefit for high precision micro-machining. Pulse repetition rates as high as > 500 kHz with pulse energies of > 4 μJ enable fast machining with the precision of low fluence ablation.

In addition, new potentials for these lasers are given by advanced modulators with digital timing control that allow the user to generate sequences or groups of pulses:

E.g. a sequence of two pulses can be generated and repeated up to 300 kHz. The amplitude of these two pulses can be adjusted independently and the delay is selectable in 20 ns steps. This kind of pulse-strategies with picosecond lasers can support higher ablation rates, similar to the machining results that were demonstrated with double ns-pulses, recently.

In another application, groups of > 20 pulses were repeated with > 50 kHz for ultra-precise machining. The distribution of the energy yields a few hundred nJ per pulse and results in an ablation depth per pulse in the range of several nm. Therefore the ablation depth formed by a group can be digitally controlled by the number of pulses in group.

Samples for high quality drilling, cutting and structuring of several materials will be presented and the new potentials of this kind of picosecond laser processing with improved precision and speed will be discussed.

6108-38, Session 11

Generation of terahertz radiation using a compact ultrashort pulse parabolic fiber laser amplifier at 1064-nm

G. Matthaeus, Friedrich-Schiller-Univ. Jena (Germany); S. Haeffelin, Embry-Riddle Aeronautical Univ.; T. Schreiber, B. Ortac, J. Limpert, S. Nolte, A. Tünnermann, Friedrich-Schiller-Univ. Jena (Germany)

The terahertz region of the electromagnatic spectrum (1011 - 1013 Hz) has potential applications in many fields of science and technology, ranging from semiconductor physics and chemical spectroscopy through medical imaging. However, exploitation of this potential has been limited by the lack of high-power coherent sources. The solution to this problem has been the development of pulsed generation methods. A semiconductor surface or heterostructure illuminated with a femtosecond near-infrared laser pulse emits coherent broadband single-cycle pulses of THz radiation. They can be time resolved with femtosecond precision. Until now a Ti:Sapphire laser at 800 nm was commonly used as a source for the femtosecond laser pulses. Nevertheless the power of today's sources is still not sufficient for high-throughput inspection or security applications. In order to scale the achievable power we used a fiber laser amplifier working at 1064 nm as a seed source for the first time to the best of our knowledge. Recently, we demonstrated a high average power ytterbium-doped fiber CPA System, delivering 131 W in 220 fs pulse duration at a repetition rate of 73 MHz working at 1060 nm. This is an increase of approximately two orders of magnitude compared to ordinary Ti:Sapphire systems. Consequently, a much more powerful THz generation should be possible.

In our first experiments we used an ultrashort pulse fiber laser amplifier delivering 100 fs pulses at a repetition rate of 75 MHz with an average power of 10 W. We achieved a 2 THz broad spectrum at a center wavelength of 1 THz. The radiation was generated at a surface emitting InAs crystal. It propagated in free space and was finally focused by a Si lens onto the receiver. For detection we used a photoconducting dipole antenna. It was fabricated upon low-temperature grown GaAs with subpicosecond carrier lifetime.

We have shown, that high power fiber lasers working at 1 μm are a new promising power scalable laser source for more powerful THz generation.

6108-39, Poster Session

Method for fiber Bragg grating control during the fabrication process

N. K. Berger, B. Levit, B. Fischer, Technion - Israel Institute of Technology (Israel)

Clusters of consecutive uniform fiber Bragg gratings with different amplitude and phase reflectivity for each grating can be made to have tailored spectral responses. They can be very useful for designing complex filters for uses such as ultrashort optical pulse shaping. Such devices however need careful fabrication procedure because of their interferometric nature. In this work, we propose and experimentally demonstrate a method for a real-time control and fabrication procedure during the writing of such Bragg gratings by UV laser light radiation. The method is based on measuring and analyzing the spectrum of the reflection during the gratings fabrication, and applying a refractive index trimming process. We give an experimental demonstration of the method using an array of six fiber gratings and show its use for optical pulse shaping.

In the gratings writing process we analyzed the grating reflectivity of a broadband light source provided by the spontaneous emission of an erbium-doped fiber amplifier. The reflection spectrum contains the interference of the reflections from each fiber grating and the fiber end. A fast Fourier transform was performed in real time on the reflection spectrum, measured by an optical spectrum analyzer. The Fourier transform comprises two sets of bands: the first that includes the central band, corresponds to the interference between the gratings themselves, and the second sidebands set results from the interference between the gratings and the fiber end. Selection in the processing of only the central band and its inverse Fourier transform gives the sum of the reflection spectra of all of the gratings. In the process, when writing the successive gratings, we control the reflectivity of a currently written grating by subtracting the spectra of the previously written gratings. Selection of the corresponding sideband from the second set, getting its inverse Fourier transform and finding its absolute value provide the measurement of the reflection phase for the currently writing grating. The desired phase was is then obtained by refractive index trimming of the spacing before that grating and the former one by UV irradiation

We experimentally demonstrate optical pulse shaping using the fiber Bragg gratings written by the described method.

6108-40, Poster Session

Femtosecond laser processing of subwavelength-sized voids for compact optical devices

E. Toratani, M. Kamata, M. Obara, Keio Univ. (Japan)

We demonstrate fabrication of 200-300 nm size voids in fused silica using an amplified 1-kpps, 800 nm Ti:sapphire femtosecond (fs) laser. The effects of numerical aperture, laser energy, and pulse number on the shape of the fabricated void were investigated. The void has a linearly drawn shape in the direction of the laser irradiation when a single pulse is irradiated. Increasing number of the incident pulses resulted in breakup of the long void into multiple spherical ones, leading to a periodically-ordered void array.

Waveguide fabrication in dielectric materials is one of the attractive applications of fs laser processing, based on 3D scanning of a focal point. However, the refractive index change of the waveguide induced by this method is the order of 10-4 -10-3. This means confinement of the propagating light in such a waveguide is too weak to change the propagation direction in a small radius of curvature without a leak of the propagation beam. In other words, the waveguide cannot be sharply curved. Meanwhile, voids fabricated in transparent materials have a large refractive index change, because the fabricated voids consist of gas phase. The refractive index difference is about 0.5 in fused silica. If periodically aligned voids are attached to such optical waveguides, it is possible to manipulate light on a microscopic scale, for example, bending at a right angle using the voids as a photonic crystal reflector. The application requires high accuracy of the fabrication, because structural distortion of the voids has much influence for light propagation. However, dependence of the void shape on the incident laser parameters still remains unsolved. We investigated the void formation including self-organization of the void array.

We have tightly focused fs laser inside a fused silica to create voids. In our experiment, we used 100 fs, 0.2-3 μJ pulses generated by the amplified Ti:sapphire laser system. The fs pulse was focused inside the fused silica sample using a 0.90 NA objective lens. When a single pulse laser is irradiated, the void has a linearly drawn shape in the direction of the laser focusing. Increasing the number of the incident pulses causes the breakup of the single void to multiple ones which results in a periodically-ordered void array. The void shape is also varied with the focal depth beneath the fused silica surface, because self-focusing has a significant effect on the generation of the voids. Due to this effect, the void fabricated by a single pulse had narrower and longer shape when the laser pulse was focused in the deeper position in the fused silica. We investigated detailed mechanisms of the void formation such as breakup process from a linearly drawn void to multiple ones. Fabrication of compact optical devices was also demonstrated, for example, a void-array-type photonic crystal reflector attached to a 90 degree bend waveguide.

6108-41, Poster Session

Double pulse femtosecond laser micromachining of dielectric materials, semiconductor, and metal

T. Nagata, M. Obara, Keio Univ. (Japan)

Femtosecond (fs) laser ablation is one of the most promising technologies among the fs laser applications because ablation characteristics are drastically different from those of nanosecond and longer pulse laser ablation. The advantage of fs laser ablation processing is to minimize the heat affected zone, and hence high precision processing is demonstrated to preserve the chemical properties of the ablated area. The electron-lattice energy relaxation time of materials is theoretically ranging from 1 to 100 ps. Thermal ablation occurs when the laser pulse width is longer than the electron-lattice relaxation time. Recent studies on double pulse fs lasers have an interesting effect on the ablation processing of dielectric materials. Temporally shaped fs laser processing results in the cleaner structures and less residual stress accumulation.

We demonstrate double pulse fs laser ablation micromachining of stainless steel, silicon, sapphire and fused silica, in order to figure out the conditions for cleaner structure processing from the viewpoint of material science. In our experiment, we used a pulse width controllable Ti:sapphire fs laser system operating at a 1-kpps repetition rate and 820 nm center wavelength. Pulse width was chosen to be 100 fs for this experiment. Mach-Zehnder interferometer was employed to produce the double pulse sequence of fs laser. Pulse separation time between the double pulses can be varied from 0.25 to 200 ps.

We investigated the effect of the double pulse fs laser parameters of relative pulse energy, pulse separation time, and laser polarization on the shape of the ablated area and the ablated depth. The double pulse fs laser was focused onto the surface of the fused silica. Because fused silica has very large electron-phonon coupling strength, high electron energy is efficiently transferred to the lattice on the time scale of order of 100 fs. When the first pulse energy of the double pulses was smaller than the ablation threshold, the ablated depth was not influenced by either material removal or laser induced plasma. Meanwhile, when the first pulse energy of the double pulse was higher than the ablation threshold, the plasma generated by the first pulse prevented the second pulse from reaching the target surface, leading to a decrease in the ablated depth. This plasma effect was also observed in the ablation of crystalline silicon and stainless steel. The appearance time of the plasma effect on each material was found to be dependent upon the materials: fused silica (3 ps), sapphire (20 ps), and stainless steel (1 ps).

6108-42, Poster Session

Nanohole fabrication on silicon substrate surface by femtosecond laser pulses with gold-particles and nanorods

H. Takada, M. Obara, Keio Univ. (Japan)

In recent years near-field pattering on the substrate surface induced by laser irradiation at a spatial resolution below the diffraction limit has been paid much attention and widely studied for diagnostics, optical memory, and catalysis applications. Regarding nanofabrication methods with near-field optics, illuminating spherical particles on the substrate has been applied. Particle-enhanced field locally induced between particle and substrate is believed to be responsible for nanohole formation. The optical field enhancement mechanism is due to lens effect or Mie scattering by spherical transparent particles depending on the particle size. The formation of nanohole array on silicon substrate with particles of 450 and 820 nm was reported. The nanohole array was fabricated by 820-nm femtosecond laser irradiation to hexagonally arrayed polystyrene particles with diameter of 450 or 820 nm. On the other hand, the surface plasmon polariton resonance is responsible for particle enhancement effect using metal particles. In particular, Au, Ag and Cu particles are well applied to the field enhancement experiment due to the presence of resonance absorption and scattering, and an enhanced local electromagnetic field in the visible wavelength of the spectrum. Nanopits formation on the silicon substrate surface at various random locations below aggregated gold nanoparticles by the backside irradiation of infrared CO2 laser was reported. Recently rod-like gold nanoparticles are found to show several interesting light absorption spectra and scattering properties. Gold nanorods exhibit a remarkable spectral shift of their surface plasmon resonances as a function of the particle's aspect ratio of major and minor axes lengths, and the surface plasmon resonance is adjustable to the laser wavelength.

We have demonstrated nanohole fabrication on the silicon substrate by femtosecond laser pulses. Gold spheres or gold nanorods are placed on the substrate by a spin-coating method or vertical deposition method, and 820-nm femtosecond laser pulses are irradiated to the substrate. Using 200-nm diam. spherical gold particles, we fabricated nanoholes with diameters smaller than 100 nm, which were observed by scanning electron microscope (SEM) and atomic force microscope (AFM). Laser fluence was near the ablation threshold fluence of the silicon substrate without gold particles. We also investigated morphological changes of the laser-irradiated area in terms of particle diameter, shape, laser fluence, and pulse number. The ablated surface morphologies were found to drastically be changed as the irradiated laser fluence was increased. We also calculated absorption and scattering cross-section of the gold particles, and nanorods in order to estimate optical intensity between the particle and substrate. We also compared the theoretical results to the electromagnetic field enhancement factor achieved from the experiment to explain the machining physics.

6108-43, Poster Session

Ultrasimple alignment-free ultrashort pulse measurement devices

S. Akturk, D. Lee, A. P. Shreenath, P. Gabolde, Q. Cao, X. Gu, R. P. Trebino, Georgia Institute of Technology

We describe two novel, practical ultrashort laser pulse measurement devices. Both devices are experimentally ultrasimple. The first one is an “ultra-broadband” pulse characterization device. Most common pulse measurement devices, including FROG use second harmonic generation (SHG), which is inherently a narrowband process. It requires changing the SHG crystal several times as the pulse center wavelength is tuned from UV to IR. Worse, SHG cannot be used to characterize UV pulse. Like most nonlinear processes, SHG also requires phase-matching, another strong constraint. To overcome these issues, we describe an ultrashort pulse measurement device that is based on FROG, but uses transient grating (TG) process. TG FROG involves forming an induced grating (intensity fringe pattern) in a piece of glass by crossing two pulses in space and time and then diffracting a third pulse off it to create a fourth diffracted pulse. The fourth pulse carries the pulse length information, and spectrally resolving it yields a FROG measurement of the input pulse. The TG process is inherently very broadband and automatically phasematched. TG FROG was previously demonstrated but is rarely used in practice, since its setup was far too complex: three separate beams must be generated and overlapped in space and time. We have implemented an ultrasimple TG FROG device, which can also operate single-shot. First, three beams are created using a simple mask. Then, a cylindrical beams line-focuses the beams horizontally, where the induced grating is generated. The variation of the relative delay is achieved by crossing the two grating-creation beams at an angle using a Fresnel biprism, which maps the delay onto transverse position. Then, by detecting the diffracted pulse with spatial resolution, the TG FROG trace is captured. The standard FROG algorithm can then be used to retrieve the pulse intensity and phase. The second device that we present aims to measure ultrashort pulses with complex spectral and temporal structure, typically generated by pulse-shapers. A linear optical technique called spectral interferometry (SI) works perfectly for this purpose. SI simply involves measuring the spectrum of the sum of the unknown (shaped) and known (reference) light waves. Unfortunately, SI is very difficult to align and maintain aligned, as it requires that the two beams be nearly perfectly collinear. This problem can be solved by using a pinhole as the entrance aperture into the spectrometer. Even if two beams interfere on the pinhole at a large angle, after the pinhole, both beams will diffract and overlap in space, and a collimating lens can then easily make them collinear. A simple optical fiber can also be used for this purpose. Another important issue in SI is that, the pulses need to not overlap in time in order to yield spectral fringes. This requires significantly more spectral resolution. Fortunately, by collecting and spectrally resolving, not just one of the outputs of the beam splitter, but the also the other, it is possible to extract the intensity and phase even when the pulses overlap in time (presented earlier as Differential Spectral Interferometry (DSI)). The simple extension of the fiber-coupling idea can yield the DSI spectra, as well as the individual pulse spectra easily. Specifically, a fiber splitters split off pieces of the two input pulses, so that their spectra may be measured separately. The 50/50 coupler yields two outputs, the sum and difference of the two input pulses. The inversion algorithm, then, yields the intensity and phase of the complex pulse.

6108-44, Poster Session

Reduction of sliding surface friction by nano-dimples fabricated using femtosecond laser pulses

T. Sakai, M. Obara, Keio Univ. (Japan)

Surface structuring using laser micro-machining is widely studied. As a micro-tribology application of the material surface processing, there is an improvement of friction and wear. Actually, a material itself or a surface structure of the material has been investigated. The significant improvement by this processing includes a load capacity, wear resistance, friction coefficient, lifetimes of surface structure, etc. For these processing there are laser processing, abrasive jet machining, reactive ion etching, lithography and anisotropic etching. The laser processing takes advantage of easily controlling the surface structure size and depth of the surface profile over them. Surface structures fabricated by this method are micro-holes or micro-grooves. Ablation-specific ripple structures are also studied, and a large number of micro-holes called micro-dimples are studied mainly in the field of micro-tribology. These micro-dimples act as oil-reservoirs to supply lubricant or micro-trap to capture wear debris. Such an action decreases the friction coefficient and lengthens the life-time of the surface structure. Although micro-dimples are already fabricated by nanosecond UV excimer lasers and Nd:YAG lasers, however, some burrs due to its thermal effects are generated on the edge of the laser machined are. In addition, these nanosecond laser methods need to polish the surface after the laser irradiation.

In this study, we demonstrate how the friction coefficient is reduced by fabricating nano-dimples on aluminum surface using femtosecond lasers from the viewpoint of nano-tribology. Nano-dimples are anticipated to provide with a much lower friction coefficient and much smoother lubrication than micro-dimples do. The diameters of the nano-dimples in our experiment are ranging from a few tens nm to a few hundreds nm. The spatial period of nano-dimples is a few nm. In our experiment with femtosecond laser, there exists no burr after the nano-dimple formation. The diameter and period of the nano-dimples are much smaller than the micro-dimples. Hence we use the processing by a near-field femtosecond laser with nano-particle template on the Al surface. The merit of this processing is that the Al surface is ablated selectively and locally at the nano-contact point between the particle and the Al surface. The dependence of the dimple diameter and depth on the friction coefficient will be presented from the viewpoint of nano-tribology.

6108-45, Poster Session

Nonlinear frequency chirp measurement of frequency sweeping lasers for FD-OCT applications

T. Ahn, D. Kim, Gwangju Institute of Science and Technology (South Korea)

A noble measurement method by using a simple homodyne interferometer and Hilbert transform has been proposed and demonstrated for characterizing frequency sweeping light sources used in traditional optical frequency domain reflectometer (OFDR) and optical frequency domain imaging (OFDI). A Michelson interferometer with a tunable laser generates a sinusoidal beating signal. A phase of measured beating signal as a function of time is approximately proportional to optical frequency of the swept light source during frequency tuning and can be obtained by the Hilbert transformation. Thus, optical frequency chirp can be determined by a simple equation related with the phase of the beating signal from the interferometer. We have demonstrated the effectiveness and the simplicity of our proposed method by testing a temperature-tuned frequency sweeping DFB-LD and a commercial external cavity tunable laser source as practical examples. In the case of DFB-LD, the frequency sweep becomes more linear while the amount of frequency sweep saturates as the amplitude of the control voltage applied to a TEC driver increases, and the frequency tuning rate increases as the repetition rate decreases. We also found that a commercial frequency sweeping laser has a feed back

control to adjust its frequency sweeping rate such that the tuning rate oscillates around an intended value as a function of time. We have demonstrated the possibility of using a self-homodyne interferometer as a powerful tool for characterizing frequency sweeping laser sources. We expect this method will be useful for improving the performance of many optical frequency domain measurement techniques such as OFDR, OCT or OFDI.

6108-46, Poster Session

Multiphoton microscopy for cell surgery

J. Baumgart, A. Heisterkamp, Laser Zentrum Hannover e.V. (Germany); W. Ertmer, Univ. Hannover (Germany); H. Lubatschowski, Laser Zentrum Hannover e.V. (Germany)

Multiphoton microscopy is a very promising method for 3D imaging of living cells. The fluorochromes are solely excited in the laser focus by multiphoton absorption due to near- infrared femtosecond laser pulses. The arising fluorescence allows a pixel-to-pixel imaging with a resolution in the sub-micron region. The laser beam enters the microscope through the fluorescence port of the inverse microscope and passes the objective towards the sample. The detector, a photomultiplier, is placed inside the microscope tubus. Probe scanning is achieved by a combination of a two galvanometer-scanners and a positioner. An objective with a high numerical aperture offers a small focal volume of the laser beam which allows precise imaging at low energies and a cutting effect at high energies inside the probe due to plasma-mediated ablation.

This combination offers the possibility of simultaneous manipulation and analysis of living cells or cell organelles. The manipulation is realized at energies of only a few nJ. With the obtained resolution, it is possible to cut single cell organelles without influencing the surrounding tissue. Thus, the implementation is excellent suited for cell surgery. Ablation of tissue inside living cells was performed at different pulse energies in various cells organelles, like mitochondria. The consequences of the interference of the cell were observed with special interest in possible cell death. First results will be presented.

6108-47, Poster Session

Controlled nonlinearity in femtosecond laser written waveguides

A. Szameit, D. Blömer, J. Burghoff, T. Pertsch, S. Nolte, A. Tünnermann, Friedrich-Schiller-Univ. Jena (Germany)

In recent years, ultrashort laser pulses have drawn increasing interest for the direct writing of photonic structures in different materials. Various optical devices have already been demonstrated, e.g. optical waveguides, waveguide amplifiers and lasers, beam splitters, couplers, stacked waveguides and three-dimensional waveguide arrays and gratings.

While the linear propagation features have been explored in great detail, almost no attention was paid to nonlinear effects in these devices. Here, we present a detailed characterization of the nonlinear refractive index of femtosecond written waveguides in fused silica based on an analysis of self phase modulation. Compared to the unstructured material the nonlinear refractive index is significantly reduced. The influence of the writing parameters on the change of the linear and nonlinear refractive index is evaluated.

We will demonstrate that the value of the nonlinear refractive index can be adapted using the appropriate processing parameters. This offers an important additional degree of freedom in nonlinear integrated optical devices, like e.g. arrays of coupled waveguides or soliton couplers.

6108-48, Poster Session

Structural modification in silica glass by a femtosecond fiber laser at 1556.9-nm and 258.5 kHz repetition rate

T. Tamaki, W. Watanabe, K. Itoh, Osaka Univ. (Japan); H. Nagai, M. Yoshida, AISIN SEIKI CO., LTD. (Japan)

When femtosecond laser pulses are focused inside the bulk of glass, a permanent refractive-index change is induced. In this paper, we report on the structural modification in fused silica and borosilicate glass by a commercial femtosecond fiber laser system (IMRA America, FCPA μ-Jewel B-250) at the fundamental wavelength of 1556.9 nm, the pulse duration of 894 fs and the repetition rate of 258.5 kHz. Notably, a permanent refractive-index change was induced inside these glasses using this femtosecond fiber laser system.

6108-50, Poster Session

Reality of superposition principle and the coherence function for short pulses

C. Roychoudhuri, Univ. of Connecticut and Femto Macro Continuum

Introduction: This paper will discuss the consequences of re-casting the coherence function for short pulses in terms of the real dipole undulation of the detecting atoms and molecules induced by the superposed E-fields. This is because the superposition effects become manifest only through the measuring dipoles [1] and we believe that our theory should attempt to map actual measurement processes.

A paradox: The timeliness of the paper can be appreciated by the fact that Glauber is sharing the 2005 Physics Nobel Prize for developing the theory of quantum coherence. The engineering importance of the paper derives from our belief that innovative ideas for new applications of ultra short light pulses may be generated if we can bring the conceptual congruence between the engineering and physics definitions of the same photons that constitute our light pulses. The many engineers tacitly assume the photons to be contained within the volume of the pulse and hence they are “local” in space and time because the measurability of the energy of the pulses is determined by the classical optical arrangements (including laser cavities and optical modulators), which define all the spatial and temporal characteristics of these pulse-volumes unambiguously. In contrast, the physicists define photons as the Fourier monochromatic modes of the vacuum[2,3], which, by virtue of the time-frequency Fourier theorem, are necessarily “non-local”. We now add to this physics model the traditional hypothesis that single photo-electron “clicks’ are exclusively due to the absorption of “one at a time”, indivisible, single photons. This enforces one, specifically while carrying out interference and diffraction experiments at extremely low light levels, to assign several uncanny properties to the photons, like (i) “self-interference”, (ii) “delayed choice”, (iii) “teleportation”, etc.[3]. Thus, we have some paradoxically divergent concepts apparently held by many engineers and physicists.

Theory maps measurement process: Let us come back to one of our beginning assertions that theories should attempt to map actual processes in nature. The most important property of light pulses, the coherence function *947;(τ), is normally measured through the Michelson’s visibility V(τ)of the two-beam superposition fringes. The other important property relevant to atomic and molecular spectroscopy is the spectral content (density function(v)) of the pulses. This is usually measured by classical spectrometers using prisms (refractive dispersion), gratings (diffractive dispersion) and Fabry-Perot interferometers (dispersion by superposition). For the purpose of this paper, we will stay focused on y(τ) since we can derive s(v) the same measured fringe visibility V(τ)=|y(τ)|, using the Wiener-Khintchine theorem, which states that s(v) is simply the Fourier transform of y(τ)[4].

EM fields do not operate on each other: We now come back to the other beginning assertion that the effect of superposition becomes manifest only through the responses of the detectors to the superposed fields on

them. If light beams were to operate on each other while crossing through, then the entire visual world would have been a dazzling sight of spatial and temporal speckle patterns. It is not the EM fields that display the effects of superposition by summing themselves. It is the detecting dipoles that sum the effects of superposition on them as their resultant dipole undulations, when allowed by the quantum mechanical rules. Thus, all of our measurements are differentially “colored” by the differing QM properties of the detectors for the same set of superposed EM fields [1]. So, we propose that the coherence functions should be defined using the dipole undulation amplitudes rather than the fields themselves $y_d(\tau) = [\bar{a}(t+\tau)\cdot \bar{a}(t)]$ where $\bar{a}(t) = \chi_1 \bar{e}(t)\cos 2\pi\nu t$, $\bar{e}(t)$ being the EM field amplitude envelope and being the carrier frequency under the envelope. We are considering only the linear polarizability of the detecting molecule χ_1 and neglecting all the higher order polarizabilities $\chi_n [\bar{e}(t)\cdot \bar{e}(t)\cdot \bar{e}(t)\cdots \bar{e}(t)]_{n\text{-terms}}$, which may not always be negligible. The immediate consequence of this approach is that it gives an operational meaning to the absence of the fringes when orthogonally polarized light beams are superposed. The superposition (“interference”) cross-term for the dipole amplitudes $\bar{a}_1(t+\tau)\cdot \bar{a}_2(t)$ is zero when the inducing EM fields are orthogonal, which is derived from the intensity recording process $|\bar{a}_1(t+\tau)\exp i2\pi\nu(t+\tau)+ \bar{a}_2(t)\exp i2\pi\nu t^2|$. This implies that the same detector molecule does not undulate in two orthogonal directions simultaneously and fails to sum the effects of the two fields[1,5]. Since light does not interfere with light any way, it is operationally meaningless to say that the orthogonally polarized lights do not interfere with each other.

The paper will present and discuss more cases of the dipole-based coherence functions and the paradoxes arising out of the fact that EM fields do not operate on each other. Our presentation will be based on easy, semi-classical formalism since Sudarshan has already established (“Optical Theorem”) that Glauber’s quantum coherence functions are equivalent to Wolf’s classical coherence functions[4].

REFERENCES

1] “Measuring properties of superposed light beams carrying different frequencies”, Optics Express 11(8), 944-51, (2003); DongIk Lee and C. Roychoudhuri. [http://www.opticsexpress.org/abstract.cfm?URI=OPEX-11-8-944]

2] Quantum Optics, M. O. Scully and M. S. Zubairy, Cambridge U. Press (1999); and The Quantum Theory of Light, R. Loudon, Oxford U. Press (2000).

3] “The Nature of Light: What is a Photon?”, OPN Trends; Guest Editors - C. Roychoudhuri & R. Roy; special issue of Optics and Photonics News, October 2003.

[http://www.osa-opn.org/abstract.cfm?URI=OPN-14-10-49]

4. Optical Coherence and Quantum Optics, L. Mandel and E. Wolf, Cambridge U. Press (1995).

5. “If superposed light beams do not re-distribute each others energy in the absence of detectors (material dipoles), can an indivisible single photon interfere by/with itself?”, pp.26-35, and “What are the processes behind energy re-direction and re-distribution in interference and diffraction?”, pp.135-146, both by C. Roychoudhuri, in “The Nature of Light: What is a Photon?”, SPIE-Proc. Vol. 5866 (2005), Editors C. Roychoudhuri, K. Creath and A. F. Kracklauer.